KU Leuven
Biomedical Sciences Group
Department of Cardiovascular Sciences
Faculty of Medicine

THE ROLE OF PEAR1 IN PLATELETS AND ENDOTHELIAL CELL BIOLOGY

Christophe VANDENBRIELE

Promotor: Prof. dr. P. Verhamme
Co-promotor: Prof. dr. MF. Hoylaerts and Prof. dr. S. Janssens
Jury members:

- Prof. dr. Jean-Daniel Chiche, Université Paris Descartes, Sorbonne, Paris, France
- Prof. dr. Paul Harrison, University of Birmingham, UK
- Prof. dr. M. Delcroix, University of Leuven
- Prof. dr. M. Dewerchin, University of Leuven

Dissertation presented in partial fulfilment of the requirements for the degree of Doctor in Biomedical Sciences.

CENTER FOR MOLECULAR AND VASCULAR BIOLOGY

Opening new horizons

TABLE OF CONTENTS

LIST OF ABBREVIATIONS

Ab	Antibody
ACVRL1/Alk1	Activin receptor-like kinase 1
Ang-2	Angiopoietin-2
AVEXIS	AVidity based EXtracellular Interaction Screen
BMPR2	Bone morphogenetic protein receptor type II
BOEC	Blood Outgrowth Endothelial Cells
CD	Cluster of Differentiation
cDNA	Copy deoxyribonucleic acid
CFU	Colony Forming Unit
CLEC-2	C-type lectinlike receptor 2
Dll4	Delta like ligand 4
DxS	Dextran Sulphate
EC	Endothelial Cell
ECM	Extra Cellular Matrix
EGF	Epidermal Growth Factor
Eng	Endoglin
eNOS	Endothelial Nitric Oxide Syntase
GAPDH	Glyceraldehyde 3-phosphate dehydrogenase
GFP	Green Fluorescent Protein
HHT	Hereditary hemorrhagic telangiectasia
HUVEC	Human Umbilical Vein Endothelial Cell
IF	Immunofluorescence
Ig	Immunoglobulin
IHC	Immunohistochemistry
MEGF	Multiple epidermal growth factor-like domains
MK	Megakaryocyte
MO	Morpholino
NO	Nitric Oxide
PAHT	Pulmonary Arterial Hypertension
PEAR1	Platelet Endothelial Aggregation Receptor 1
PI3K	Phosphoinositide 3-kinase
PTEN	Phosphatase and Tensin Homolog
RNA	Ribonucleic Acid
RT-PCR	Real Time – Polymerase Chain Reaction
SFK	Src Family of Kinases
SGC	Satellite Glial Cell
Sh	Short hairpin
SMC	Smooth Muscle Cell
SNP	Single Nucleotide Polymorphism
VEGF	Vascular Endothelial Growth Factor
VWF	Von Willebrand
WB	Western blot
WT	Wildtype

Introduction

INTRODUCTION

A) THE CARDIOVASCULAR SYSTEM: A GENERAL OVERVIEW

The vascular system is the transportation network within the human body and consists of two separate circulating systems: 1) the **blood circulation** and 2) the **lymphatic system**.

1) Blood is a fluid that constantly circulates through the complex network of blood vessels (arteries and veins). It provides the body with essential nutrition and oxygen (O_2), and removes waste products. Plasma makes up about half of the blood volume. It has a broad variety of functions but importantly it contains proteins that help the blood to clot and transports substances such as glucose and other dissolved nutrients. The other half of the blood volume consists of blood cells (Figure 1):[2]

- **Red blood cells**, carry O_2 to the different tissues in the body.
- **White blood cells**, control or combat infections.
- **Platelets**, are small cells crucial for haemostasis.

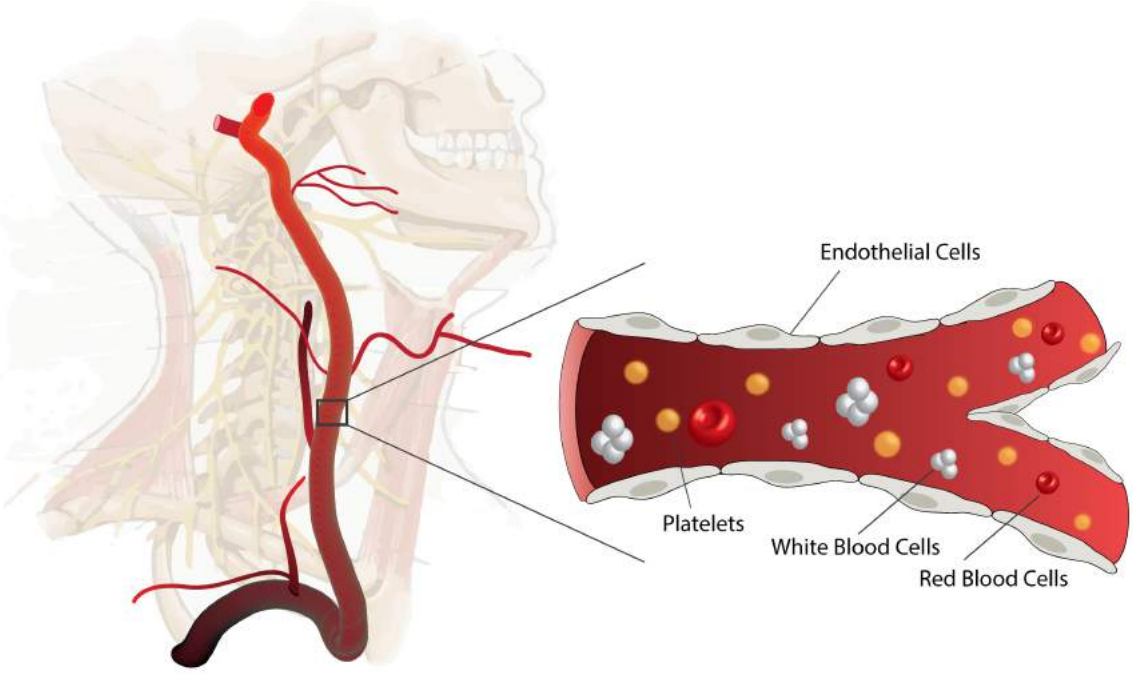

Figure 1 – Blood vessels transport plasma and blood cells to the tissues/organs of the body. The innermost layer of blood vessels consists of endothelial cells.

2) Extracellular liquid from the various bodily tissues drains into the lymphatic system which then organises the recirculation of this back to the blood circulation via lymph nodes.

B) Structure of a Normal Blood Vessel

The anatomical structure of normal arteries consists of a well-designed, trilaminar structure. The innermost layer (**tunica intima)** is made up of an endothelial cell (EC) monolayer (Figure 1), which resides on a basement membrane.[2] This membrane is built from nonfibrillar collagen such as type IV collagen, as well as laminin, fibronectin and other extracellular matrix molecules.[2] The second layer, the **tunica media**, lies beneath the intima. The media of elastic arteries (such as the aorta) are built from thick and concentric layers of smooth muscle cells (SMCs) enriched with layers of elastin-rich extracellular matrix.[2] This structure is well-adapted to withstand the kinetic energy generated by systolic tension in the walls of the great arteries.[2] The third outermost layer of arteries, the **adventitia**, is built from a loose network of collagen fibrils and contains a small network of vessels supplying the artery wall (the vasa vasorum) and various nerve endings.[2]

C) Atherothrombotic Disease: Where Platelets and ECs Meet

"During the last decades, cardiovascular disease (CVD) has become the single largest cause of death worldwide. In 2012, CVD caused an estimated 16,7 million deaths (about 29% of all deaths).More than 3 million of these deaths occurred before the age of 60 and could have largely been prevented".[3]

Atherosclerosis is a condition where the arteries become narrowed and hardened due to an excessive build-up of cholesterol plaques in the artery wall.[2] It is a slow, progressive process that only results in clinical symptoms at an advanced stage. The first step in human atherosclerosis is the accumulation and aggregation of small lipoprotein particles in the intima.[4] Predilected lesion sites in arteries are proximal to branching points or bifurcations.[5] This results in the local adhesion of leucocytes to the endothelium and their penetration into the intima (transcytosis), where they accumulate lipids and become lipid-laden macrophages, or foam cells.[6] The accumulation of foam cells/macrophages results in an ensemble of inflammatory mediators and the promotion of inflammation within the plaque which contributes to the development of the atherosclerotic lesions.[7] Whereas the early stages of atheroma plaque initiation primarily involve altered endothelial function and the recruitment and accumulation of leucocytes, the subsequent evolution of atheroma into more complex plaques requires the migration of SMC from the tunica media into the intima layer. These intimal SMCs proliferate and facilitate the development of an extracellular matrix (mainly consisting of type I and III collagen, proteoglycans and decorin), ultimately leading to the calcification of areas and a stable atherosclerotic plaque.[8, 9]

The conventional risk factors for atherosclerosis are listed in Figure 2.[10-14] The main risk of atherosclerosis is the development of a critical arterial stenosis and/or plaque rupture with atherothrombosis (Figure 2), the latter being the predominant reason for acute cardiovascular events.[15] Atherothrombosis is the formation of a thrombus within an artery resulting from an atherosclerotic plaque rupture. It can no longer be considered a disease of the developed world since myocardial infarction and stroke are increasingly prevalent worldwide and occur across all socioeconomic strata. By 2025, cardiovascular mortality on a worldwide scale will likely surpass that of every major disease group, including infection, cancer and trauma.[16, 17]

Atherotic plaque rupture usually occurs at the weakest point (the "shoulder" of the plaque), where the cap is often very thin and most heavily infiltrated with inflammatory cells.[17] Once this plaque is disrupted, the highly thrombogenic lipid-rich core is exposed to the bloodstream. This core has an abundance of tissue factor, and triggers platelet activation, aggregation and the formation of a superimposed thrombus, leading to (sub)total vessel occlusion and subsequent ischaemic symptoms distal to it.[18, 19] Depending on the localisation and degree of occlusion, this may lead to stroke, myocardial infarction, intestinal ischemia, etc.

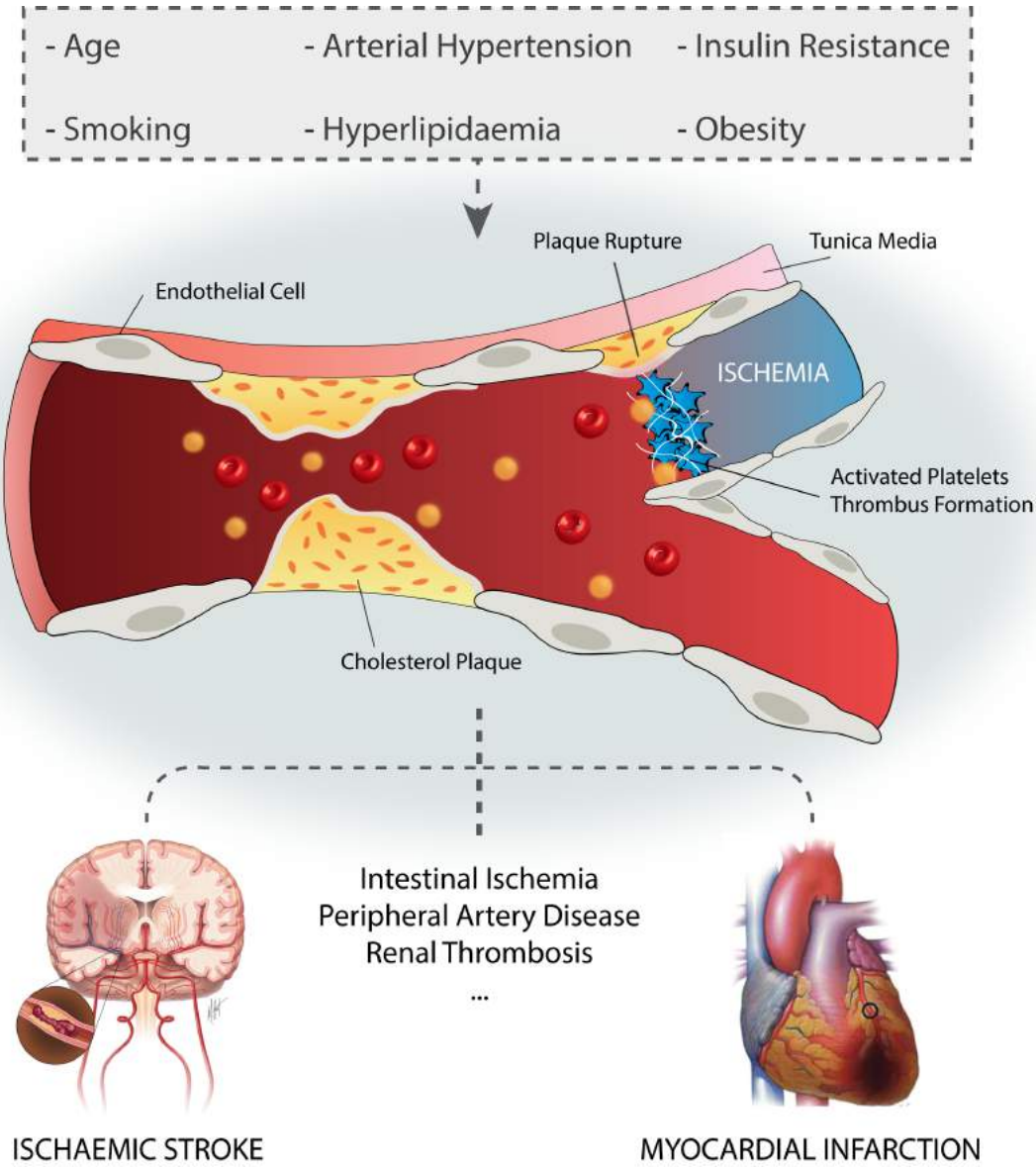

Figure 2 – Overview of atherosclerosis risk factors. Atherosclerosis involves the development of stable and/or unstable cholesterol plaques which can eventually rupture, leading to atherothrombosis and (sub)total vessel obstruction.

The most critical processes in the formation of (unstable) plaques and subsequent intraluminal thrombus formation are endothelial dysfunction and platelet aggregation, resulting in (sub)total vessel occlusion. Given the focus of this thesis, I will now further elaborate on the role and function of endothelial cells (including angiogenesis) and platelets under (patho)physiological conditions.

D) Endothelial Cells

The total human endothelial cell (EC) surface is composed of approximately 1 to 6×10^{13} cells. Its calculated weight is approximately 0,1 kg and it covers a surface area of 1 to 7.000 m^2.[20] ECs line the vessels of every organ system and are essential for regulating blood cells and controlling the flow of nutrient substances, which are diverse biologically-active molecules. This gate-keeper role of the endothelium is effected through: a) the presence of various membrane-bound receptors, that bind a variety of molecules e.g., growth factors, coagulant and anticoagulant proteins, low-density lipoprotein [LDL], serotonin, endothelin-1 etc.; and b) through specific junctional proteins and receptors that organise cell-cell and cell-matrix interactions.[21]

The endothelium also plays a pivotal role in the regulation of blood flow.[2] This is partly due to the capacity of quiescent ECs for generating an active antithrombotic surface, responsible for facilitating the transit of plasma and cellular constituents through the vasculature. Disruptions to this cellular homeostasis, such as those seen at sites of inflammation or high hydrodynamic shear stress, alter these activities and switch ECs in favour of a prothrombotic and antifibrinolytic micro-environment.[21] Blood flow is also partly regulated by ECs in a paracrine manner through the secretion and uptake of vasoactive substances by the endothelium, triggering the constriction and dilatation of specific vascular beds in response to stimuli such as endotoxin.[21]

Arteries supply tissues with oxygen and nutrients, whereas the broad network of lymphatic vessels absorb and filter interstitial fluids from these same tissues.[22] Although blood vessels mostly remain quiescent throughout life, they retain the capacity to rapidly form new vessels (sprouting) in response to local injuries or under pathological conditions such as cancer. The pivotal players in this process of neo vessel formation are ECs. In this neovascularization process (also called angiogenesis) there are three different EC subtypes which each carry out a highly specific role and are crucial for neo-capillary formation, itself an essential component of angiogenesis[23]. Tip cells are ECs with a highly migratory/non-proliferative phenotype. Their function is to guide and pull the new sprout in the correct direction. In addition, stalk cells elongate the newly formed sprout through their highly proliferative phenotype (Figure 3). Finally, quiescent phalanx cells mark the more mature part of the vessel and are typically cobblestone shaped.[24]
The differentiation of ECs into one of these subtypes is mainly driven by vascular endothelial growth factor (VEGF) whose production is triggered via hypoxic tissues and macrophages that are trying to regain an oxygen and nutrient supply via stimulating the formation of new vessels. This has been thoroughly studied in retinal angiogenesis where a continuous rise in VEGF concentration eventually reaches the existing vascular front and allows VEGF to bind to the VEGF receptor 2 (VEGFR2) in ECs, directing these ECs towards a tip cell phenotype. The newly-differentiated tip cells then force their neighbouring ECs to adopt a stalk cell phenotype via the

Notch ligand delta-like 4. This Notch ligand binds to Notch receptors in adjacent ECs, forcing the release of the Notch intracellular domain (NICD) that initiates the reprogramming of the cell to express the decoy VEGFR1-receptor at the expense of VEGFR2, a process that triggers reduced VEGF sensitivity and stimulates stalk cell behavior.[25] Tip/stalk specification is a very dynamic process in which, through continuous cell shuffling, ECs with the highest VEGFR2/VEGFR1 expression ratio (and thus the highest VEGF responsiveness) are continuously at the tip of the new vessel sprout.[26] If a tip cell encounters another tip cell or a pre-existing vessel, both will fuse together to form a lumenised, perfused vessel (a process called anastomosis). The newly-formed vessel sprout then matures, and the ECs adopt a more quiescent, non-proliferative and non-migratory, cobblestone-like phalanx cell phenotype.[27] These cells are marked with high VEGFR1 levels and low VEGF responsiveness, therefore they are able to stay quiescent for years.[27]

These EC-driven roles are important in many body processes, but particularly in wound closure, neo-angiogenesis, tumour metastasis and organ rejection.[27]

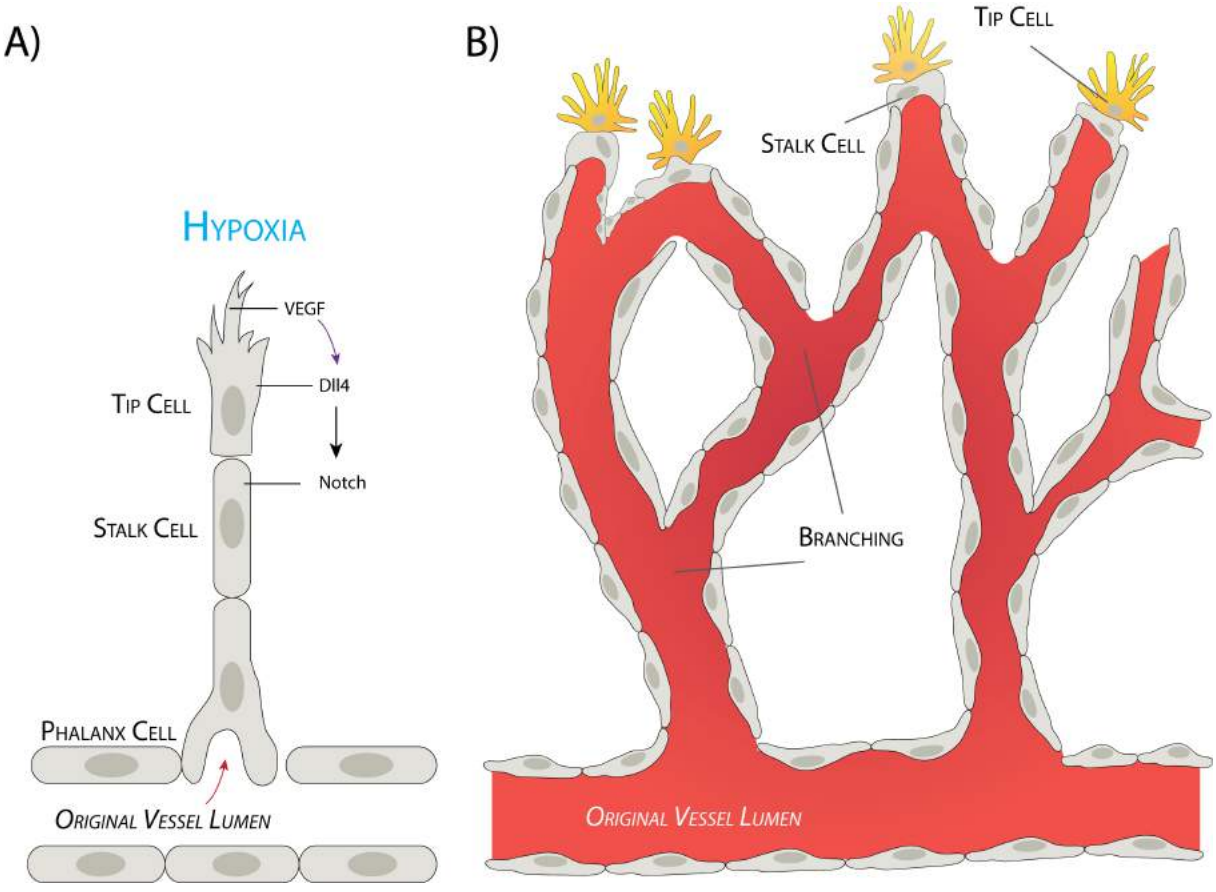

Figure 3 – A) Endothelial tip cells migrate towards an angiogenic stimulus, and are followed by a column of proliferating stalk cells. B) This process results in the formation of new vessels via branching and anastomosis to produce a new (collateral) vascular network.

E) PLATELETS

GENERAL OVERVIEW

Platelets have attracted a growing interest among scientists and clinicians as their role has extended beyond haemostasis to many physiological and/or pathophysiological conditions such as wound healing, inflammation, infectious diseases, maintenance of endothelial barrier function, angiogenesis and tumour metastasis. In the last few decades, enormous progress has been made in our understanding of the role of platelets in haemostasis and other processes. Platelets circulate in the blood in a resting state but they are able to react immediately following injury to the vessel wall by adhering to the exposed collagen and then forming a plug by platelet-platelet interaction to effectively seal the injured vessel wall and prevent excessive blood loss. Similar events take place at a rupturing atherosclerotic plaque, resulting in the formation of a platelet-rich thrombus.[28]

PLATELET AGGREGATION

Platelet aggregation is mediated by signalling events that are induced by various primary platelet agonists (e.g. thrombin, ADP and collagen). These agonists induce a conformational change in the platelet integrin $\alpha_{IIb}\beta_3$ receptor which allow it to bind to soluble fibrinogen and von Willebrand factor (VWF), thereby inducing platelet cross-linking.[29] These platelet-platelet interactions that occur during the process of aggregation then initiate multiple secondary signalling events to further activate the platelet, e.g., calcium mobilisation, protein tyrosine phosphorylation, cytoskeletal rearrangements and the release of platelet dense bodies or α-granules. The released dense body contents include ADP which, alongside the platelet activation-induced generation of thromboxane A2 (TXA_2), further adds to platelet stimulation.[29]

Following initial platelet aggregation, the formation of a stable platelet aggregate involves many factors, such as the generation of stabilising fibrin, however there are three mechanisms that appear to predominate in this process (adapted from Nanda *et al.*)[30]:

1. Shear. Platelet thrombi partially occlude arteries, which increases the shear rate within these arteries and induces further platelet stimulation.
2. The generation of autocrine loops. Platelet activation induces the release of four platelet stimuli: ADP, TXA2, sCD40L and Gas6.
3. Platelet-platelet contacts (a type of "outside-in signalling"). Platelet-platelet contacts within the aggregate further induce platelet stimulation by the activation of various surface receptors, the so-called "aggregation-induced aggregation receptors". Although the mechanisms underlying this process are not fully understood, they are clearly of fundamental importance to platelet thrombus formation as the release of the four autocrine stimuli is aggregation-dependent. Aggregation-induced signalling is the cornerstone to the formation of stable aggregates, especially when aggregation is induced by low concentrations of one or more primary agonists.

PLATELET RECEPTORS

Platelet receptor–ligand interactions are essential for a) the mobilisation and adhesion of circulating platelets at sites of damaged ECs, b) the subsequent activation of those platelets, and c) platelet aggregation and thrombus formation. The initial trigger for platelet aggregate formation is specific sequences on exposed collagen fibrils that are recognised by the GPVI (collagen) receptor. This process induces potent platelet activation and complements the (minor) activation brought about by the GPIb–VWF interaction. Together these result in the activation of intracellular signalling and induce the high-affinity state of the β-integrins at the platelet surface, allowing firm platelet adhesion to collagen via the $\alpha_2\beta_1$ integrin.[31] Platelet aggregation then occurs via platelet spreading and platelet–fibrinogen interactions through the $\alpha_{IIb}\beta_3$–receptor.[32]To maintain haemostasis, this process requires additional fine-tuning via many more receptors, all synergising to control platelet activation and arrest blood loss.[33] The most important platelet receptors involved in platelet adhesion and aggregation are listed below:

- **Collagen Receptors**. Collagen is essential for platelet adherence and platelet plug formation. Integrin $\alpha_2\beta_1$ and the CD148–GPVI–FcRγ–complex are considered the major receptors for collagen binding and platelet activation.[34]

- **Integrins**. These receptors are crucial for the metabolism and adhesion/aggregation of platelets. The most important platelet integrins are: $\alpha_5\beta_1$, the principal platelet receptor for fibronectin; $\alpha_6\beta_1$, the laminin receptor; $\alpha_{IIb}\beta_3$, the fibrinogen-induced platelet aggregation receptor that is considered to be the principal receptor for platelet adhesion *in vivo*; and $\alpha_v\beta_3$, the vitronectin receptor.[35, 36]

- **Receptors involved in the amplification phase**. TXA_2 is synthesised by activated platelets and ADP/ATP are released by damaged red blood cells and platelet dense granules. These all amplify the development of the platelet aggregate. The major receptors involved are the ADP-controlled receptors $P2Y_1$ and $P2Y_{12}$, the ATP-controlled ion channel $P2X_1$, the TXA_2/prostaglandin H_2 receptor, the thrombin protease-activated receptors (PAR1–4), the prostaglandin E_2 receptors EP1, EP3 and EP4 and the prostacyclin (PGI_2) receptor.[37, 38]

- **Receptors involved in the stabilisation phase**. See below.

- **Receptors involved in the negative regulation of platelet activation**. The essential role of NO and PGI_2 in platelets in preventing uncontrolled thrombosis is well-established.[33] The major players involved in attenuating platelet thrombus formation are PECAM-1/CD36, the immunoglobulin superfamily member G6b-B and the pituitary adenylate cyclase-activating polypeptide (PACAP).[39–41]

Given the subject of this thesis and the role of PEAR1 in sustained platelet aggregation (discussed below), platelet stabilisation receptors will be discussed in more detail (Figure 4).

PLATELET STABILISATION RECEPTORS

The stabilisation of platelet aggregates is a dynamic process that requires contact-dependent signalling via various receptors and outside-in signalling through integrins, particularly the $\alpha_{IIb}\beta_3$ receptor. Once ligand binding has occurred, $\alpha_{IIb}\beta_3$ signalling triggers essential events for thrombus stabilisation, namely cytoskeletal reorganization, enlargement of platelet aggregates, clot retraction, platelet degranulation and the development of a procoagulant surface.[42]

The major receptors involved in platelet stabilisation are:

1. **The ephrin-binding Eph-kinase receptors**

Blocking the interactions between the Eph receptors and ephrin attenuates clot retraction via the reduced phosphorylation of β_3. This inhibits platelet aggregation at lower agonist concentrations and results in a reduced size of collagen-induced thrombi under arterial flow conditions, causing premature thrombus disaggregation.

2. **Gas-6**

Gas-6 organises $\alpha_{IIb}\beta_3$-triggered outside-in signalling via PI3K/Akt, and stimulates the phosphorylation of β_3 and the subsequent retraction of the clot.[43] These effects result in an enhancement and perpetuation of the thrombus-stabilising role of ADP.[44]

3. **The tetraspanin superfamily**

The tetraspanin superfamily member CD151 is known to regulate fibrinogen-binding proteins such as the $\alpha_{IIb}\beta_3$ integrin receptor. Platelets lacking CD151 are reported to form smaller and unstable thrombi *in vivo*.[45] The absence of platelet TSSC6 (Tumour-suppressing subchromosomal transferable fragment cDNA 6), another member of the tetraspaning superfamily, is also reported to affect the secondary stability of arterial thrombi upon vascular injury *in vivo*, by regulating integrin $\alpha_{IIb}\beta_3$ "outside-in" signalling events.[46]

4. **TLT-1**

TREM-like transcript-1 (TLT-1) facilitates platelet aggregation through its interaction with a ligand or ligands exposed on activated platelets. It is assumed that TLT-1 interacts with $\alpha_{IIb}\beta_3$ to facilitate the interaction between platelets and fibrinogen and thus platelet aggregation.[47, 48]

5. **P-Selectin/PSGL-1 Couple**

PSGL-1 (P-selectin glycoprotein ligand-1) is the primary ligand for the P-selectin receptor and is constitutively found on all leukocytes. The capacity of leukocytes and activated platelets to roll along the venous endothelium is orchestrated via transient interactions between P-selectin and PSGL-1.
The formation of a fibrin network upon activation of the coagulation cascade is a critical event that contributes to thrombus stability. Recent laser injury-induced thrombosis studies in tissue factor (TF)-deficient mice have revealed that this fibrin formation depends on monocyte-derived

TF carried by microvesicles with only a minimal contribution of vessel wall TF. The TF-containing microvesicles can be captured by the thrombus via the interaction between (activated) platelet surface expressed P-selectin and the PSGL-1 present on the microvesicles, thus delivering TF to the growing thrombus. Mice lacking either PSGL-1 or P-selectin display thrombi with little TF and a reduced thrombin generation, resulting in smaller sized thrombi.[49, 50]

6. PEAR1

Although the presence and function of various surface receptors on platelets and ECs has been clarified, it is thought that not all the platelet receptors and their downstream signalling cascades have been discovered. In 2005, Nanda *et al.* identified a novel platelet stabilisation receptor that is mainly expressed on platelets and ECs and called it PEAR1 (Platelet Endothelial Aggregation Receptor 1).[29] In the next part of this introduction, I will give an overview of the existing literature on PEAR1.

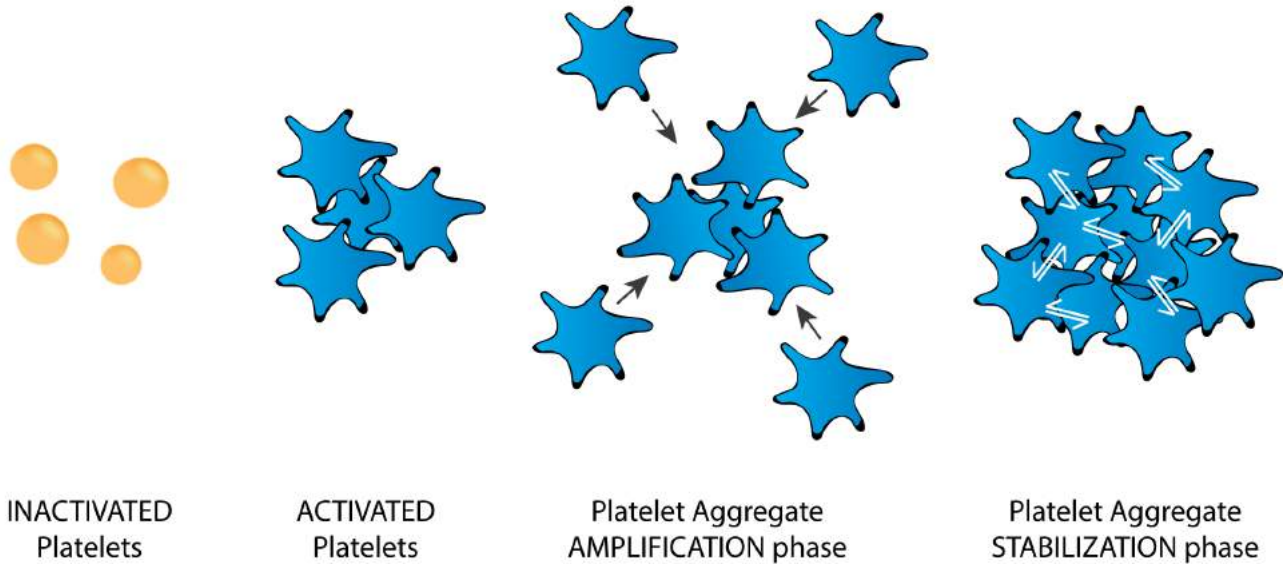

Figure 4 – Overview of the different stages of thrombus formation ranging from inactivated, circulating platelets to the aggregation of activated platelets and the formation of stable thrombi.

F) Platelet Endothelial Aggregation Receptor 1

In 2005 Nanda *et al.*[29] designed a study to identify novel platelet proteins involved in platelet proximity-induced activation. They sought not only to identify novel receptors on platelets but to specifically identify those that become phosphorylated upon platelet-platelet interactions, irrespective of the activation state of the platelet. This was performed firstly via a proteomics approach (they identified aggregation-induced aggregation receptors that became tyrosine-phosphorylated upon platelet aggregation), and secondly via a bioinformatics approach (profiling the RNA of platelets using oligonucleotide-based microarrays in order to identify novel signalling membrane proteins during platelet aggregation). They found that both techniques converged on two different groups of proteins that had not yet been described in platelets, the SLAM family of proteins (which had been thoroughly studied in immune cells) and a novel protein they termed PEAR1 (Platelet Endothelial Aggregation Receptor 1).[29, 30]

PEAR1 (also known as JEDI-1 or MEGF-12) is a 1034-amino acid type 1 membrane protein consisting of fifteen epidermal growth factor (EGF)-like repeats in its extracellular domain.[29] The intracellular domain contains five proline-rich domains, which can interact with Src homology 3 (Sh3)-domain-containing proteins, as well as four potential tyrosine phosphorylation sites (Tyr-804, Tyr-925, Tyr-943 and Tyr-979).[29] The highest levels of PEAR1 expression are found in platelets, megakaryocytes and ECs.[29] Nanda *et al.* demonstrated that platelet PEAR1 is a surface-expressed protein that, upon aggregation, becomes tyrosine phosphorylated. This phosphorylation was found to be an oligomerisation-dependent event and could be inhibited by the $\alpha_{IIb}\beta_3$-antagonist eptifibatide. This indicated that PEAR1 tyrosine phosphorylation was dependent on platelet-platelet surface contacts between activated platelets. Interestingly, they also showed that platelet-platelet contacts (induced by the centrifugation of washed platelets) also resulted in PEAR1 tyrosine phosphorylation. This is in contrast to other secondary signalling molecules that require platelet activation to signal. Finally, Nanda *et al.* demonstrated that this contact-induced PEAR1 phosphorylation was not inhibited by eptifibatide, implying that platelet-platelet contact can induce PEAR1 phosphorylation independent of previous platelet activation.[29]

PEAR1 mRNA expression has also been previously observed in early hematopoietic progenitor cells and in cells known to support haematopoiesis, more specifically in bone marrow stromal and osteogenic cells.[51] This implies that PEAR1 may have a controlling function during haematopoiesis. Krivtsov *et al.*[51] reported a role for PEAR1 in the fine-tuning of haematopoiesis by exerting negative effects on the stem/progenitor cell compartment. They provided convincing evidence in favour of a potentiating role for PEAR1 in the negative regulation of Notch-signalling and thus in the regulation of haematopoiesis.[51] However, a role for PEAR1 in processes such as megakaryopoiesis or white blood cell differentiation remains to be elucidated.

G) The Role of Genetic Variation in Platelet PEAR1

Aspirin is widely used for the inhibition of platelets and the prevention of arterial thrombosis through inhibition of cyclo-oxygenase 1 (COX1), which produces TXA_2 in platelets. Nevertheless, acute coronary artery disease (CAD) events still incidentally occur in the presence of aspirin if platelet aggregation is not sufficiently suppressed.[52] It is known that considerable heterogeneity exists both in native platelet aggregation and in the magnitude of platelet suppression by

aspirin.[53-56] Although well-described, the reason for this phenotypic heterogeneity is not completely known. Genetic factors are thought to play an important role in this heterogeneity. Genetic variants in COX1 itself are uncommon, accounting for only a small portion of platelet responsiveness to aspirin.[57] Therefore many studies have investigated whether genetic variations in signalling pathways proximal to the COX1/thromboxane A_2-pathway could be responsible for the residual platelet function during aspirin treatment.[58] Like the well-known heterogeneity in platelet response to aspirin, the overall platelet responsiveness to various agonists seems to vary between individuals, even though it has been shown that platelet responsiveness is inherited[39] and remains constant within an individual.[59, 60]

As previously discussed, PEAR1 is known to be activated by platelet-platelet contact.[29] Several studies have investigated whether inherited variations in PEAR1 are responsible for modified agonist-induced aggregation in native platelets and alter the expression and/or function of this platelet receptor. **Table 1** provides a literature overview of the identified single nucleotide polymorphisms (SNPs) in *PEAR1* and their reported effects on platelet function. These data (especially SNP rs12041331) illustrate that genetic variants in *PEAR1* are associated with altered platelet function.

SNP	PEAR1-expression	Functional phenotype	Reference
rs2768759	Expression ↑ (?)	↑ Agonist-induced platelet aggregation ↑ Response of platelets to aspirin (A > C)	Galeano et al.[58]
rs41299597	Expression ↑	↑ Platelet activation	Jones et al.[39]
rs3737224	?	↑ Platelet activation Role in Prasugrel pharmacodynamics?	Jones et al.[39] Xiang et al.[61]
rs412773215	?	↑ Platelet activation	Jones et al.[39]
rs822442	?	↑ Platelet activation Role in Prasugrel pharmacodynamics?	Jones et al.[39] Xiang et al.[61]
rs11264579	?	↑ Platelet activation	Jones et al.[39]
rs12566888	?	↓ Platelet activation (G > T) Role in Prasugrel pharmacodynamics? T/T: Protective against foetal loss	Johnson et al.[62] Xiang et al.[61] Sokol et al.[63]
rs12041331	Expression ↑ Dose response between G-allele number and PEAR1 expression	Role in Prasugrel pharmacodynamics? A-allele carriers: ↓ Platelet aggregation (collagen pathway) ↓ Response of platelets to aspirin (G > A) ↑ Risk of AMI*, ** ↑ Risk of death ↑ Risk of spontaneous abortion	Johnson et al.[62] Faraday et al.[64] Kim et al.[65] Lewis et al.[66] Würtz et al.[67] Xiang et al.[61] Sokol et al.[63] Qayyum et al.[68]

A = Adenine; C = Cytosine; G = Guanine; T = Thymine

* AMI = Acute Myocardial Infarction

** A paradoxical effect of rs12041331 on cardiovascular phenotypes has been observed; the A-allele is associated with a better aspirin response but is also associated with a higher cardiovascular event rate

H) PEAR1 Signalling in Platelets

The genetic studies conducted on PEAR1 have all pointed towards an important regulatory role for this protein in human platelet activation. In 2012, Kauskot *et al*. were the first to provide evidence of a role for PEAR1 during platelet activation and platelet aggregation.[1] Their study showed that "*PEAR1, already present in the membrane of resting platelets, was also released from α-granules during platelet activation, further raising its membrane expression. Platelet contacts between the PEAR1 EMI domain and an unidentified surface ligand (itself equally exposed during platelet activation) triggers rapid PEAR1 phosphorylation, thus initiating a signalling cascade that culminates in PI3K/Akt activation, reinforcing αIIbβ3 activation and, consequently, platelet aggregation*." They concluded that PEAR1 phosphorylation results in the persistent activation of Akt and amplified $\alpha_{IIb}\beta_3$ activation, hence it stabilises platelet aggregates.

Activation of PEAR1 results in the recruitment of c-Src, p85/PI3K, Fyn and Lyn (but not Syk), ultimately leading to progressive and long-lasting Src-dependent PI3K/Akt/$\alpha_{IIb}\beta_3$ signalling, confirming that PEAR1 is a functional platelet contact receptor (Figure 1). c-Src-dependent tyrosine phosphorylation of PEAR1 appears to be sufficient to initiate downstream signalling events. Activation of PEAR1 requires clustering of at least two membrane-PEAR1-receptors, as done by divalent PEAR1- antibodies or (unknown) PEAR1 ligand(s).

Although Kauskot *et al.* have unravelled the downstream signalling pathways of PEAR1 engagement in platelets, the ligand involved in PEAR1 activation during platelet aggregation is yet to be identified and could hold the key to fully understanding the mechanism and function of this receptor.

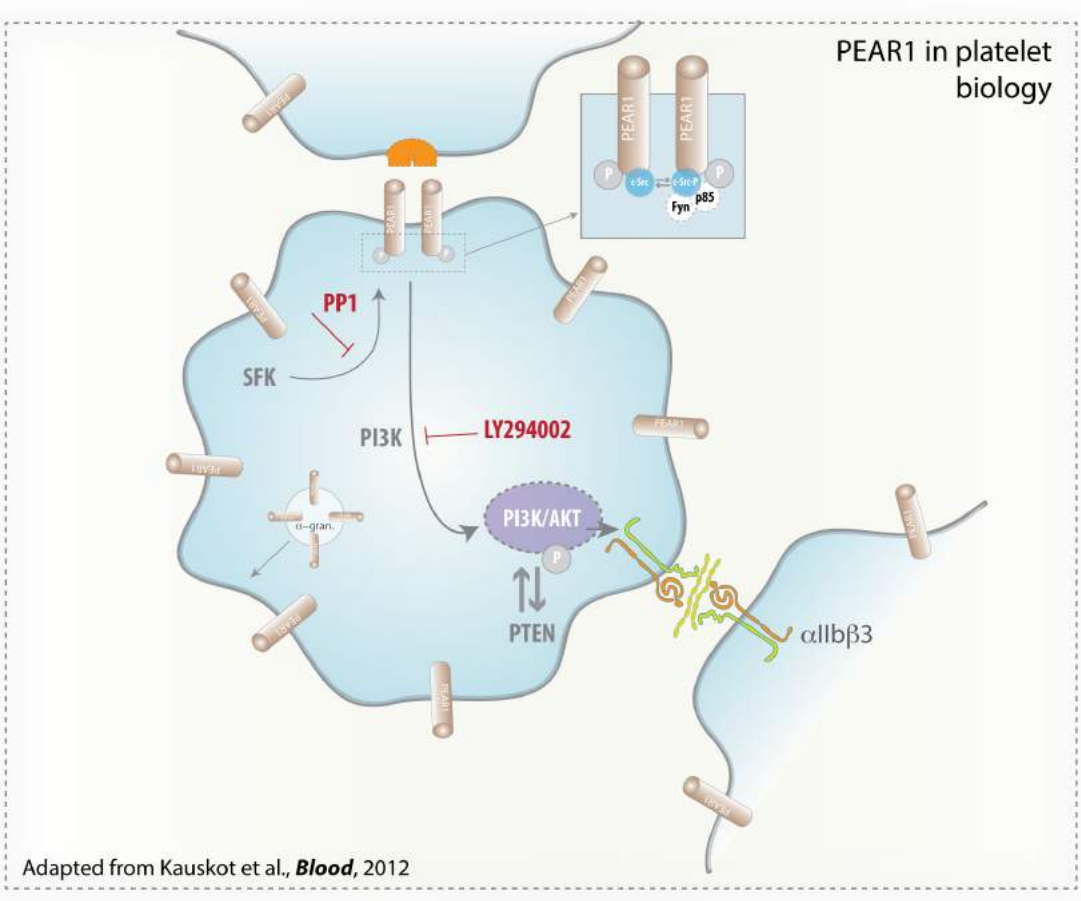

Figure 5 – Scheme for the PEAR1 signalling pathway. In resting platelets, low amounts of PEAR1 are found on the platelet surface. During platelet activation with various platelet agonists, the expression of both PEAR1 and its ligand increase at the surface.[1] Interactions between PEAR1 and its ligand on adjacent platelets induce the formation of a complex comprising at least two PEAR1 receptors. Dimeric (or oligomeric) PEAR1 complexes are rapidly tyrosine phosphorylated in a SFK-dependent manner (they are inhibited by the SFK inhibitor PP1), and transiently recruit additional c-Src and Fyn. Phosphorylated PEAR1 avidly binds to p85-PI3K, leading to strong and sustained activation of Akt at Ser^{473} via PI3K (which is inhibited by the PI3K-inhibitor LY294002 and by PP1). PI3K activation amplifies $\alpha_{IIb}\beta_3$ activation, thus sustaining platelet aggregation.

I) ENDOTHELIAL PEAR1

Nanda *et al.*[29] found that PEAR1 was highly expressed in human umbilical vein ECs (HUVECs). Experimental studies identified PEAR1 as a candidate gene that may be linked to kidney injury in the salt-sensitive Dahl rat,[69] rats developing a kidney injury that became more severe as blood pressure rose in response to salt loading. Renal biopsies in this study revealed a significantly lower nephron number in the salt-sensitive Dahl rat compared to controls,[69] suggesting a possible link between kidney damage and the development of hypertension. In a separate study in humans, Olivi and Vandenbriele *et al.* randomly recruited 1973 people and genotyped their *PEAR1* gene. They looked for associations between changes in blood pressure or incidence of hypertension with genetic variation in *PEAR1*. They found no significant association between systolic and diastolic blood pressure changes and nine SNPs in *PEAR1* (rs2768762, rs2644620, rs1256688, rs2768744, rs6671392, rs822441, rs11264581, rs12137505 and rs749256).[70] However, the most potent SNP in PEAR1 (rs12041331) was not analysed in this association study.

Although PEAR1 has be linked to both kidney injury in the salt-sensitive Dahl rat[70] and cardiovascular outcome,[66] the function of endothelial PEAR1 and its underlying signalling pathways are completely unknown despite the high expression of PEAR1 reported in HUVECs.

J) PEAR1/JEDI1: AN ENGULFMENT RECEPTOR OF SENSORY NEURON CORPSES

In the developing mammalian central nervous system, extensive neuronal cell death (around 50% of the neurons generated[71]) occurs during the ontogenesis of the sensory ganglia.[72] Programmed cell death and phagocytosis are essential for the development and maintenance of a functional nervous system.[72] Although the regulation of this naturally-occurring cell death is well-known, very little is known about the process of removal of the dead neurons from the nervous system.[73] Glial cells and microglia (which result from the differentiation of invaded macrophages) are known to be implicated in the clearance of these apoptotic neurons.[74, 75] The engulfment process used by these specific phagocytic cells, including macrophages and dendritic cells (microglia), is known to be a complex interaction between an array of receptors on these phagocytes that are able to register *'find me'* and *'eat me'* signals exposed by neighbouring dying cells and *'don't eat me'* cues from healthy cells.[76, 77] However, the function of glial cells in engulfment and the underlying molecular mechanisms involved in this process are still to be explored.

In 2009, Wu *et al.* [78] reported that satellite glial cell (SGC) precursors were the primary cell type responsible for dead neuron clearance. They identified two receptors responsible for this engulfment process on SGCs: MEGF-10 and PEAR1. They found that the extracellular domain of PEAR1 was able to recognise a signal on the surface of a dying neuron and showed that overexpression of PEAR1 and MEGF-10 significantly increased the binding of SGCs to neuronal corpses, thus enhancing the glial cell-mediated engulfment of dead neurons. They also showed that knocking down *PEAR1* in glial cells (via a short hairpin RNA construct; *shRNA*) resulted in a decreased capacity of SGCs to engulf apoptotic bodies, further indicating that endogenous PEAR1 is necessary for neuronal corpse clearance during the development of the embryonic dorsal root ganglia.

How PEAR1 transduces its signals in SGCs remained unknown until 2012 when Scheib *et al.* [73] reported that activation of PEAR1 by an unknown ligand in SGCs resulted in the recruitment of Syk. This association was enhanced by Src family kinase-mediated phosphorylation of PEAR1. Interaction with Syk was necessary to mediate phagocytosis. Syk inhibition in glial cells reduced their engulfment capacity and Syk was therefore identified as a crucial mediator for PEAR1 signalling in glial cells.[73] This is in contrast to platelets, where Kauskot *et al.* reported that platelet activation leads to an interaction between PEAR1 and Fyn or Src, but not Syk.[1] In 2014, Sullivan *et al.* [79] reported that, in SGCs, PEAR1 mediates engulfment through the recruitment of GULP (the mammalian homologue of CED-6, an important adaptor protein for the regulation of engulfment in *Drosophila*), which then associates with clathrin to facilitate phagocytosis. They showed that GULP and clathrin associate with PEAR1 and that this is essential for PEAR1-mediated engulfment of apoptotic neurons.

This introduction has provided a background on the general function of platelets and endothelial cells. In addition to describing the limited literature available on PEAR1, it highlights some important questions that exist concerning the role of PEAR1. Based on this information, I will now delineate the aims of this thesis.

REFERENCES

1. Kauskot A, Di Michele M, Loyen S, Freson K, Verhamme P, Hoylaerts MF. A novel mechanism of sustained platelet alphaIIbbeta3 activation via PEAR1. *Blood* 2012;**119**:4056-4065.
2. Bonow M, Zipes, Libby. Braunwald's Heart Disease. 2012.
3. World Health Organization: The Global Burden of Disease: 2004 Update. . World Health Organization, 2008.
4. Kruth HS. Sequestration of aggregated low-density lipoproteins by macrophages. *Curr Opin Lipidol* 2002;**13**:483-488.
5. Majesky MW. Developmental basis of vascular smooth muscle diversity. *Arterioscler Thromb Vasc Biol* 2007;**27**:1248-1258.
6. Muller WA. Mechanisms of transendothelial migration of leukocytes. *Circ Res* 2009;**105**:223-230.
7. Hartvigsen K, Chou MY, Hansen LF, Shaw PX, Tsimikas S, Binder CJ, Witztum JL. The role of innate immunity in atherogenesis. *J Lipid Res* 2009;**50 Suppl**:S388-393.
8. Dollery CM, Libby P. Atherosclerosis and proteinase activation. *Cardiovasc Res* 2006;**69**:625-635.
9. Manabe I, Nagai R. Regulation of smooth muscle phenotype. *Curr Atheroscler Rep* 2003;**5**:214-222.
10. Booth GL, Kapral MK, Fung K, Tu JV. Relation between age and cardiovascular disease in men and women with diabetes compared with non-diabetic people: a population-based retrospective cohort study. *Lancet* 2006;**368**:29-36.
11. Centers for Disease C, Prevention. Smoking-attributable mortality, years of potential life lost, and productivity losses--United States, 2000-2004. *MMWR Morb Mortal Wkly Rep* 2008;**57**:1226-1228.
12. Collins R, Armitage J, Parish S, Sleight P, Peto R, Heart Protection Study Collaborative G. Effects of cholesterol-lowering with simvastatin on stroke and other major vascular events in 20536 people with cerebrovascular disease or other high-risk conditions. *Lancet* 2004;**363**:757-767.
13. Lawes CM, Vander Hoorn S, Rodgers A, International Society of H. Global burden of blood-pressure-related disease, 2001. *Lancet* 2008;**371**:1513-1518.
14. Manson JE, Greenland P, LaCroix AZ, Stefanick ML, Mouton CP, Oberman A, Perri MG, Sheps DS, Pettinger MB, Siscovick DS. Walking compared with vigorous exercise for the prevention of cardiovascular events in women. *N Engl J Med* 2002;**347**:716-725.
15. Libby P, Theroux P. Pathophysiology of coronary artery disease. *Circulation* 2005;**111**:3481-3488.
16. Bhatt DL, Steg PG, Ohman EM, Hirsch AT, Ikeda Y, Mas JL, Goto S, Liau CS, Richard AJ, Rother J, Wilson PW, Investigators RR. International prevalence, recognition, and treatment of cardiovascular risk factors in outpatients with atherothrombosis. *JAMA* 2006;**295**:180-189.
17. He J, Gu D, Wu X, Reynolds K, Duan X, Yao C, Wang J, Chen CS, Chen J, Wildman RP, Klag MJ, Whelton PK. Major causes of death among men and women in China. *N Engl J Med* 2005;**353**:1124-1134.
18. van der Wal AC, Becker AE, van der Loos CM, Das PK. Site of intimal rupture or erosion of thrombosed coronary atherosclerotic plaques is characterized by an inflammatory process irrespective of the dominant plaque morphology. *Circulation* 1994;**89**:36-44.
19. Viles-Gonzalez JF, Fuster V, Badimon JJ. Atherothrombosis: a widespread disease with unpredictable and life-threatening consequences. *Eur Heart J* 2004;**25**:1197-1207.
20. Augustin HG, Kozian DH, Johnson RC. Differentiation of endothelial cells: analysis of the constitutive and activated endothelial cell phenotypes. *Bioessays* 1994;**16**:901-906.
21. Cines DB, Pollak ES, Buck CA, Loscalzo J, Zimmerman GA, McEver RP, Pober JS, Wick TM, Konkle BA, Schwartz BS, Barnathan ES, McCrae KR, Hug BA, Schmidt AM, Stern DM. Endothelial cells in physiology and in the pathophysiology of vascular disorders. *Blood* 1998;**91**:3527-3561.
22. Carmeliet P, Jain RK. Molecular mechanisms and clinical applications of angiogenesis. *Nature* 2011;**473**:298-307.
23. Potente M, Gerhardt H, Carmeliet P. Basic and therapeutic aspects of angiogenesis. *Cell* 2011;**146**:873-887.
24. Mazzone M, Dettori D, Leite de Oliveira R, Loges S, Schmidt T, Jonckx B, Tian YM, Lanahan AA, Pollard P, Ruiz de Almodovar C, De Smet F, Vinckier S, Aragones J, Debackere K, Luttun A, Wyns S, Jordan B, Pisacane A, Gallez B, Lampugnani MG, Dejana E, Simons M, Ratcliffe P, Maxwell P, Carmeliet P. Heterozygous deficiency of PHD2 restores tumor oxygenation and inhibits metastasis via endothelial normalization. *Cell* 2009;**136**:839-851.
25. Phng LK, Gerhardt H. Angiogenesis: a team effort coordinated by notch. *Dev Cell* 2009;**16**:196-208.

26. Jakobsson L, Franco CA, Bentley K, Collins RT, Ponsioen B, Aspalter IM, Rosewell I, Busse M, Thurston G, Medvinsky A, Schulte-Merker S, Gerhardt H. Endothelial cells dynamically compete for the tip cell position during angiogenic sprouting. *Nat Cell Biol* 2010;**12**:943-953.
27. Eelen G, de Zeeuw P, Simons M, Carmeliet P. Endothelial cell metabolism in normal and diseased vasculature. *Circ Res* 2015;**116**:1231-1244.
28. de Groot PG, Urbanus RT, Roest M. Platelet interaction with the vessel wall. *Handb Exp Pharmacol* 2012:87-110.
29. Nanda N, Bao M, Lin H, Clauser K, Komuves L, Quertermous T, Conley PB, Phillips DR, Hart MJ. Platelet endothelial aggregation receptor 1 (PEAR1), a novel epidermal growth factor repeat-containing transmembrane receptor, participates in platelet contact-induced activation. *J Biol Chem* 2005;**280**:24680-24689.
30. Nanda N, Phillips DR. Novel targets for antithrombotic drug discovery. *Blood Cells Mol Dis* 2006;**36**:228-231.
31. Savage B, Almus-Jacobs F, Ruggeri ZM. Specific synergy of multiple substrate-receptor interactions in platelet thrombus formation under flow. *Cell* 1998;**94**:657-666.
32. Varga-Szabo D, Pleines I, Nieswandt B. Cell adhesion mechanisms in platelets. *Arterioscler Thromb Vasc Biol* 2008;**28**:403-412.
33. Kauskot A, Hoylaerts MF. Platelet receptors. *Handb Exp Pharmacol* 2012:23-57.
34. Nuyttens BP, Thijs T, Deckmyn H, Broos K. Platelet adhesion to collagen. *Thromb Res* 2011;**127 Suppl 2**:S26-29.
35. Kasirer-Friede A, Ware J, Leng L, Marchese P, Ruggeri ZM, Shattil SJ. Lateral clustering of platelet GP Ib-IX complexes leads to up-regulation of the adhesive function of integrin alpha IIbbeta 3. *J Biol Chem* 2002;**277**:11949-11956.
36. Salsmann A, Schaffner-Reckinger E, Kieffer N. RGD, the Rho'd to cell spreading. *Eur J Cell Biol* 2006;**85**:249-254.
37. Gachet C. P2 receptors, platelet function and pharmacological implications. *Thromb Haemost* 2008;**99**:466-472.
38. Patrono C, Garcia Rodriguez LA, Landolfi R, Baigent C. Low-dose aspirin for the prevention of atherothrombosis. *N Engl J Med* 2005;**353**:2373-2383.
39. Jones CI, Bray S, Garner SF, Stephens J, de Bono B, Angenent WG, Bentley D, Burns P, Coffey A, Deloukas P, Earthrowl M, Farndale RW, Hoylaerts MF, Koch K, Rankin A, Rice CM, Rogers J, Samani NJ, Steward M, Walker A, Watkins NA, Akkerman JW, Dudbridge F, Goodall AH, Ouwehand WH, Bloodomics C. A functional genomics approach reveals novel quantitative trait loci associated with platelet signaling pathways. *Blood* 2009;**114**:1405-1416.
40. Mori J, Pearce AC, Spalton JC, Grygielska B, Eble JA, Tomlinson MG, Senis YA, Watson SP. G6b-B inhibits constitutive and agonist-induced signaling by glycoprotein VI and CLEC-2. *J Biol Chem* 2008;**283**:35419-35427.
41. Freson K, Hashimoto H, Thys C, Wittevrongel C, Danloy S, Morita Y, Shintani N, Tomiyama Y, Vermylen J, Hoylaerts MF, Baba A, Van Geet C. The pituitary adenylate cyclase-activating polypeptide is a physiological inhibitor of platelet activation. *J Clin Invest* 2004;**113**:905-912.
42. Rivera J, Lozano ML, Navarro-Nunez L, Vicente V. Platelet receptors and signaling in the dynamics of thrombus formation. *Haematologica* 2009;**94**:700-711.
43. Angelillo-Scherrer A, Burnier L, Flores N, Savi P, DeMol M, Schaeffer P, Herbert JM, Lemke G, Goff SP, Matsushima GK, Earp HS, Vesin C, Hoylaerts MF, Plaisance S, Collen D, Conway EM, Wehrle-Haller B, Carmeliet P. Role of Gas6 receptors in platelet signaling during thrombus stabilization and implications for antithrombotic therapy. *J Clin Invest* 2005;**115**:237-246.
44. Cosemans JM, Van Kruchten R, Olieslagers S, Schurgers LJ, Verheyen FK, Munnix IC, Waltenberger J, Angelillo-Scherrer A, Hoylaerts MF, Carmeliet P, Heemskerk JW. Potentiating role of Gas6 and Tyro3, Axl and Mer (TAM) receptors in human and murine platelet activation and thrombus stabilization. *J Thromb Haemost* 2010;**8**:1797-1808.
45. Orlowski E, Chand R, Yip J, Wong C, Goschnick MW, Wright MD, Ashman LK, Jackson DE. A platelet tetraspanin superfamily member, CD151, is required for regulation of thrombus growth and stability in vivo. *J Thromb Haemost* 2009;**7**:2074-2084.
46. Goschnick MW, Lau LM, Wee JL, Liu YS, Hogarth PM, Robb LM, Hickey MJ, Wright MD, Jackson DE. Impaired "outside-in" integrin alphaIIbbeta3 signaling and thrombus stability in TSSC6-deficient mice. *Blood* 2006;**108**:1911-1918.

47. Giomarelli B, Washington VA, Chisholm MM, Quigley L, McMahon JB, Mori T, McVicar DW. Inhibition of thrombin-induced platelet aggregation using human single-chain Fv antibodies specific for TREM-like transcript-1. *Thromb Haemost* 2007;**97**:955-963.
48. Washington AV, Gibot S, Acevedo I, Gattis J, Quigley L, Feltz R, De La Mota A, Schubert RL, Gomez-Rodriguez J, Cheng J, Dutra A, Pak E, Chertov O, Rivera L, Morales J, Lubkowski J, Hunter R, Schwartzberg PL, McVicar DW. TREM-like transcript-1 protects against inflammation-associated hemorrhage by facilitating platelet aggregation in mice and humans. *J Clin Invest* 2009;**119**:1489-1501.
49. Abdullah NM, Kachman M, Walker A, Hawley AE, Wrobleski SK, Myers DD, Strahler JR, Andrews PC, Michailidis GC, Ramacciotti E, Henke PK, Wakefield TW. Microparticle surface protein are associated with experimental venous thrombosis: a preliminary study. *Clin Appl Thromb Hemost* 2009;**15**:201-208.
50. Ramacciotti E, Blackburn S, Hawley AE, Vandy F, Ballard-Lipka N, Stabler C, Baker N, Guire KE, Rectenwald JE, Henke PK, Myers DD, Jr., Wakefield TW. Evaluation of soluble P-selectin as a marker for the diagnosis of deep venous thrombosis. *Clin Appl Thromb Hemost* 2011;**17**:425-431.
51. Krivtsov AV, Rozov FN, Zinovyeva MV, Hendrikx PJ, Jiang Y, Visser JW, Belyavsky AV. Jedi--a novel transmembrane protein expressed in early hematopoietic cells. *J Cell Biochem* 2007;**101**:767-784.
52. Mason PJ, Jacobs AK, Freedman JE. Aspirin resistance and atherothrombotic disease. *J Am Coll Cardiol* 2005;**46**:986-993.
53. Faraday N, Becker DM, Yanek LR, Herrera-Galeano JE, Segal JB, Moy TF, Bray PF, Becker LC. Relation between atherosclerosis risk factors and aspirin resistance in a primary prevention population. *Am J Cardiol* 2006;**98**:774-779.
54. Faraday N, Yanek LR, Mathias R, Herrera-Galeano JE, Vaidya D, Moy TF, Fallin MD, Wilson AF, Bray PF, Becker LC, Becker DM. Heritability of platelet responsiveness to aspirin in activation pathways directly and indirectly related to cyclooxygenase-1. *Circulation* 2007;**115**:2490-2496.
55. Freedman JE. The aspirin resistance controversy: clinical entity or platelet heterogeneity? *Circulation* 2006;**113**:2865-2867.
56. Gum PA, Kottke-Marchant K, Poggio ED, Gurm H, Welsh PA, Brooks L, Sapp SK, Topol EJ. Profile and prevalence of aspirin resistance in patients with cardiovascular disease. *Am J Cardiol* 2001;**88**:230-235.
57. Halushka MK, Walker LP, Halushka PV. Genetic variation in cyclooxygenase 1: effects on response to aspirin. *Clin Pharmacol Ther* 2003;**73**:122-130.
58. Herrera-Galeano JE, Becker DM, Wilson AF, Yanek LR, Bray P, Vaidya D, Faraday N, Becker LC. A novel variant in the platelet endothelial aggregation receptor-1 gene is associated with increased platelet aggregability. *Arterioscler Thromb Vasc Biol* 2008;**28**:1484-1490.
59. Fontana P, Dupont A, Gandrille S, Bachelot-Loza C, Reny JL, Aiach M, Gaussem P. Adenosine diphosphate-induced platelet aggregation is associated with P2Y12 gene sequence variations in healthy subjects. *Circulation* 2003;**108**:989-995.
60. Hetherington SL, Singh RK, Lodwick D, Thompson JR, Goodall AH, Samani NJ. Dimorphism in the P2Y1 ADP receptor gene is associated with increased platelet activation response to ADP. *Arterioscler Thromb Vasc Biol* 2005;**25**:252-257.
61. Xiang Q, Cui Y, Zhao X, Zhao N. Identification of PEAR1 SNPs and their influences on the variation in prasugrel pharmacodynamics. *Pharmacogenomics* 2013;**14**:1179-1189.
62. Johnson AD, Yanek LR, Chen MH, Faraday N, Larson MG, Tofler G, Lin SJ, Kraja AT, Province MA, Yang Q, Becker DM, O'Donnell CJ, Becker LC. Genome-wide meta-analyses identifies seven loci associated with platelet aggregation in response to agonists. *Nat Genet* 2010;**42**:608-613.
63. Sokol J, Biringer K, Skerenova M, Stasko J, Kubisz P, Danko J. Different models of inheritance in selected genes in patients with sticky platelet syndrome and fetal loss. *Semin Thromb Hemost* 2015;**41**:330-335.
64. Faraday N, Yanek LR, Yang XP, Mathias R, Herrera-Galeano JE, Suktitipat B, Qayyum R, Johnson AD, Chen MH, Tofler GH, Ruczinski I, Friedman AD, Gylfason A, Thorsteinsdottir U, Bray PF, O'Donnell CJ, Becker DM, Becker LC. Identification of a specific intronic PEAR1 gene variant associated with greater platelet aggregability and protein expression. *Blood* 2011;**118**:3367-3375.
65. Kim Y, Suktitipat B, Yanek LR, Faraday N, Wilson AF, Becker DM, Becker LC, Mathias RA. Targeted deep resequencing identifies coding variants in the PEAR1 gene that play a role in platelet aggregation. *PLoS One* 2013;**8**:e64179.
66. Lewis JP, Ryan K, O'Connell JR, Horenstein RB, Damcott CM, Gibson Q, Pollin TI, Mitchell BD, Beitelshees AL, Pakzy R, Tanner K, Parsa A, Tantry US, Bliden KP, Post WS, Faraday N, Herzog W, Gong

Y, Pepine CJ, Johnson JA, Gurbel PA, Shuldiner AR. Genetic variation in PEAR1 is associated with platelet aggregation and cardiovascular outcomes. *Circ Cardiovasc Genet* 2013;**6**:184-192.

67. Wurtz M, Nissen PH, Grove EL, Kristensen SD, Hvas AM. Genetic determinants of on-aspirin platelet reactivity: focus on the influence of PEAR1. *PLoS One* 2014;**9**:e111816.
68. Qayyum R, Becker LC, Becker DM, Faraday N, Yanek LR, Leal SM, Shaw C, Mathias R, Suktitipat B, Bray PF. Genome-wide association study of platelet aggregation in African Americans. *BMC Genet* 2015;**16**:58.
69. Williams JM, Johnson AC, Stelloh C, Dreisbach AW, Franceschini N, Regner KR, Townsend RR, Roman RJ, Garrett MR. Genetic variants in Arhgef11 are associated with kidney injury in the Dahl salt-sensitive rat. *Hypertension* 2012;**60**:1157-1168.
70. Olivi L, Vandenbriele C, Gu YM, Salvi E, Carpini SD, Liu YP, Jacobs L, Jin Y, Thijs L, Citterio L, Cusi D, Verhamme P, Staessen JA. PEAR1 is not a human hypertension-susceptibility gene. *Blood Press* 2015;**24**:61-64.
71. Buss RR, Sun W, Oppenheim RW. Adaptive roles of programmed cell death during nervous system development. *Annu Rev Neurosci* 2006;**29**:1-35.
72. Hamburger V, Levi-Montalcini R. Proliferation, differentiation and degeneration in the spinal ganglia of the chick embryo under normal and experimental conditions. *J Exp Zool* 1949;**111**:457-501.
73. Scheib JL, Sullivan CS, Carter BD. Jedi-1 and MEGF10 signal engulfment of apoptotic neurons through the tyrosine kinase Syk. *J Neurosci* 2012;**32**:13022-13031.
74. Hume DA, Perry VH, Gordon S. Immunohistochemical localization of a macrophage-specific antigen in developing mouse retina: phagocytosis of dying neurons and differentiation of microglial cells to form a regular array in the plexiform layers. *J Cell Biol* 1983;**97**:253-257.
75. Perry VH, Hume DA, Gordon S. Immunohistochemical localization of macrophages and microglia in the adult and developing mouse brain. *Neuroscience* 1985;**15**:313-326.
76. Grimsley C, Ravichandran KS. Cues for apoptotic cell engulfment: eat-me, don't eat-me and come-get-me signals. *Trends Cell Biol* 2003;**13**:648-656.
77. Henson PM, Hume DA. Apoptotic cell removal in development and tissue homeostasis. *Trends Immunol* 2006;**27**:244-250.
78. Wu HH, Bellmunt E, Scheib JL, Venegas V, Burkert C, Reichardt LF, Zhou Z, Farinas I, Carter BD. Glial precursors clear sensory neuron corpses during development via Jedi-1, an engulfment receptor. *Nat Neurosci* 2009;**12**:1534-1541.
79. Sullivan CS, Scheib JL, Ma Z, Dang RP, Schafer JM, Hickman FE, Brodsky FM, Ravichandran KS, Carter BD. The adaptor protein GULP promotes Jedi-1-mediated phagocytosis through a clathrin-dependent mechanism. *Mol Biol Cell* 2014;**25**:1925-1936.

Aims of the Study

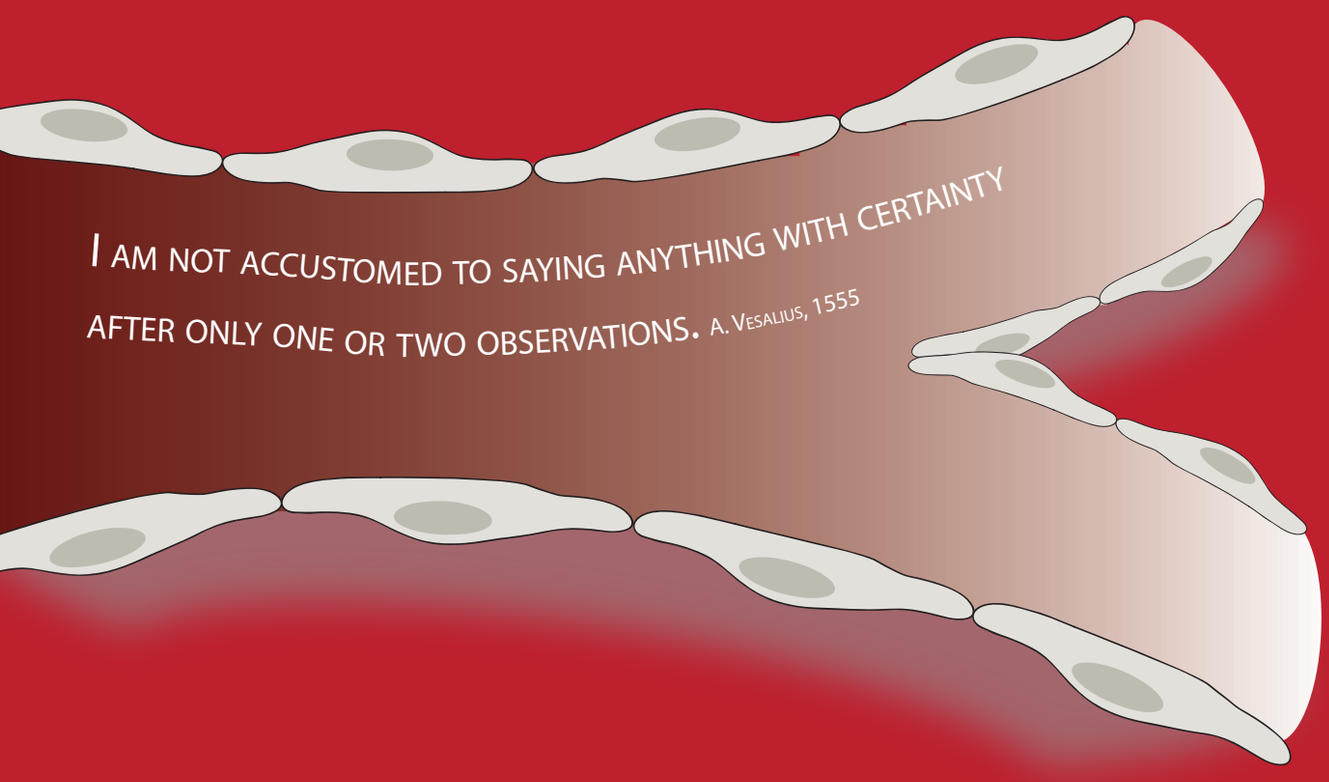

I am not accustomed to saying anything with certainty after only one or two observations. A. Vesalius, 1555

AIMS OF THE STUDY

In this thesis, we aim to study the contribution of PEAR1-signalling to the (patho)physiologic role of megakaryocytes/platelets and endothelial cells (ECs):

This was studied via:

- A short hairpin based knockdown strategy of PEAR1 in megakaryocytes and ECs,
- Activation of platelet PEAR1 with a physiological and various non-physiological ligands,
- Unravelling the role of PEAR1 in platelets and ECs in a *Pear1*$^{-/-}$ mouse model

Our results can be grouped under four different chapters (summarized in Figure 1):

1 IDENTIFICATION OF A ROLE FOR PEAR1 IN ATTENUATING MEGAKARYOPOIESIS - *CHAPTER I*

In Chapter I, we studied the role of PEAR1 in differentiating CD34+ human hematopoietic stem cells via lentiviral knockdown of PEAR1 and we confirmed our findings via a morpholino knockout strategy in zebra fish *in vivo*.

2 IDENTIFICATION OF FCER1A AS A PHYSIOLOGICAL LIGAND FOR PEAR1 ON HUMAN PLATELETS - *CHAPTER II*

In Chapter II, we sought to identify the extracellular physiological ligand for PEAR1 on human platelets by creating a protein microarray representing the secretome and receptor repertoire of the human platelet.

3 IDENTIFICATION OF DXS AS A NON-PHYSIOLOGICAL LIGAND FOR PEAR1 ON HUMAN AND MURINE PLATELETS - *CHAPTER III*

In Chapter III, we studied whether PEAR1-signalling mediates Dextran Sulphate induced human and murine platelet aggregation. This hypothesis was validated via aggregation experiments using *Pear1*$^{-/-}$ platelets.

4 IDENTIFICATION OF PEAR1 AS A NOVEL MODIFIER OF NEO-ANGIOGENESIS - *CHAPTER IV*

In Chapter IV, we studied the role for PEAR1 in EC biology. We sought whether PEAR1 plays a role in EC proliferation, migration and tube formation *in vitro* and whether it plays a role in (neo)angiogenesis *in vivo* using a *Pear1*$^{-/-}$ mouse model.

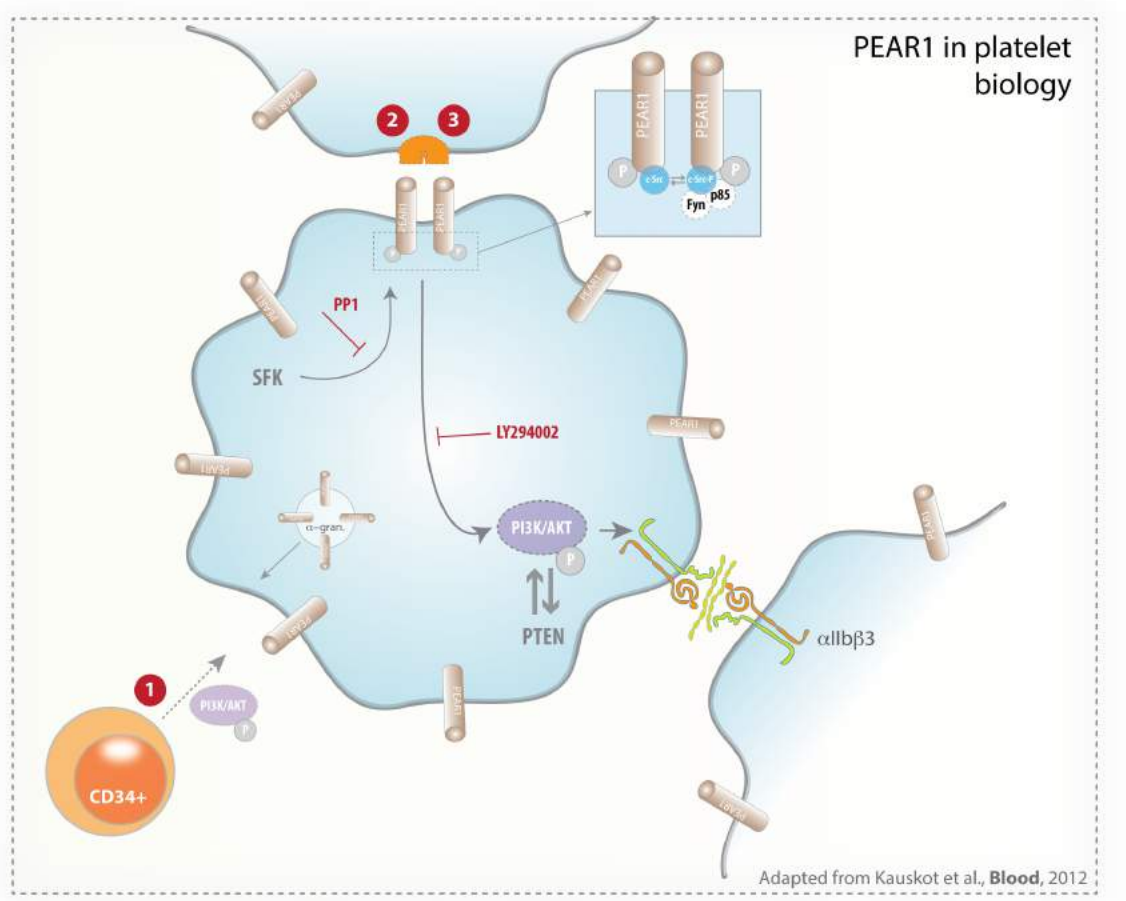

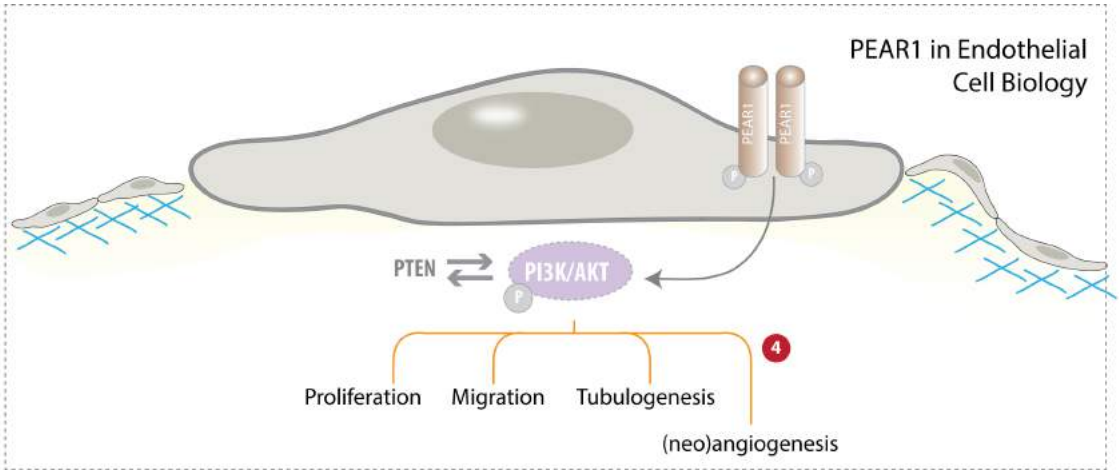

Figure 1 - Aims of the study - In this thesis we will study the role of PEAR1 in megakaryopoiesis (1), we will identify both a physiological (2) and non-physiological (3) ligand for platelet PEAR1 and we will study the role for PEAR1 in EC proliferation, migration and tubulogenesis and study its role in (neo)angiogenesis (4).

Chapter I - Illustration from "Prima musculorum Tabula - de humanum corporis fabrica libri septem" - A. Vesalius, 1543

ABSTRACT

Platelet Endothelial Aggregation Receptor-1 (PEAR1) participates in platelet aggregation via sustaining $\alpha_{IIb}\beta_3$ activation. To investigate the role of PEAR1 in platelet formation, we monitored and manipulated PEAR1 expression *in vitro* in differentiating human $CD34^+$ hematopoietic stem cells and *in vivo* in zebrafish embryos. PEAR1 expression rose during $CD34^+$ cell differentiation up to megakaryocyte maturation. Two different lentiviral short hairpin knockdowns of PEAR1 increased CFU-MK cell numbers 2-fold *vs.* control in clonogenic assays, without substantially modifying MK maturation. Knockdown of *PEAR1* resulted in a 2-fold reduction of the *PTEN* expression and modulated gene expression of several PI3K-Akt and Notch pathway genes. In zebrafish, *Pear1* expression increased progressively during the first 3 days of embryo development. Both ATG and splice-blocking PEAR1 morpholino enhanced thrombopoiesis, without affecting erythropoiesis. Western blots of 3-day-old *Pear1* knockdown zebrafish revealed elevated Akt phosphorylation, coupled to transcriptional downregulation of the PTEN isoform *Ptena*. Neutralization by morpholinos of *Ptena,* but not of *Ptenb,* phenocopied the *Pear1* zebrafish knockdown and triggered enhanced Akt phosphorylation and thrombocyte formation. In summary, this is the first demonstration that PEAR1 influences the PI3K/PTEN pathway, a critical determinant of Akt phosphorylation, itself controlling megakaryopoiesis and thrombopoiesis.

INTRODUCTION

PEAR1 is a type-1 membrane protein with an EMI domain, epidermal growth factor-like repeats (EGF-like repeats) and multiple cytoplasmic tyrosines and prolines.[1, 2] We recently reported that interactions between PEAR1, Src family kinases (C-src and Fyn) and the p85/Phosphoinosite 3-kinase (PI3K) subunit constitute a signalling complex, causing sustained $\alpha_{IIb}\beta_3$ activation via Akt phosphorylation.[1] In addition to its role in platelet function, a potential role for PEAR1 in hematopoietic cell regulation has been proposed.[3] The stable overexpression of PEAR1 in mouse bone marrow cells, using retroviral vectors decreased the number of myeloid progenitors during *in vitro* clonogenic assays, suggesting that PEAR1 regulates the early stages of hematopoietic differentiation.[3] Whether PEAR1 is also a determinant of megakaryocyte (MK) differentiation is presently unclear.

Thrombopoiesis generates approximately 10^{11} platelets daily via cytoplasmic fragmentation of MKs matured from bone marrow precursor cells. Megakaryopoiesis and MK differentiation are complex processes controlled by a series of transcription factors and regulated by a variety of cytokines and chemokines.[4, 5] Differentiation requires a dynamic endomitotic spindle formation, the maturation of a demarcation membrane system, mechanically controlled organelle transport and microtubule assembly in MKs.[6, 7]

PI3K and Phosphatase and TENsin homologue (PTEN) are both tightly linked to Akt signalling, critically controlling proliferation, survival and migration in hematopoietic cells.[8, 9] PTEN is a dual specificity protein phosphatase and an inositol phospholipid phosphatase that dephosphorylates phosphatidylinositol 3,4,5-trisphosphate (PIP3), thus producing phosphatidylinositol 4,5-bisphosphate (PIP2) and thereby negatively regulating oncogenic and non-oncogenic PI3K/Akt signaling.[10] Indeed, the constitutive activation of PI3K/Akt signalling promotes the uncontrolled growth of hematopoietic cells in commonly detected myeloproliferative disorders (MPDs) and lymphomas.[9] *PTEN* inactivation appears to be one of the major causes of the constitutive activation of PI3K/Akt. Reduced PTEN expression and/or activity in myeloid and lymphocytic leukaemia have been linked to mutations, epigenetic repression or post-translational inhibition.[10] *Pten* deletion in mouse

hematopoietic stem cells (HSCs) predisposes to MPD. Furthermore, increased megakaryopoiesis is a characteristic of *Pten*-deficient mice, which have 25% more platelets.[11]

In view of the tight link between PEAR1 and PI3K activation,[1] we have presently investigated the role of PEAR1-triggered Akt phosphorylation in MK differentiation and thrombopoiesis. Using PEAR1 knockdown strategies *in vitro* in cell cultures and *in vivo* in the zebrafish, we demonstrate a role for PEAR1 in MK precursor proliferation and thrombocyte formation via regulation of the PI3K/PTEN pathway.

MATERIALS AND METHODS

Human CD34$^+$ differentiation *in vitro*

Human CD34$^+$ HSCs were separated by magnetic cell sorting from buffy coats, and isolated from healthy donor peripheral blood (Miltenyi Biotec, Auburn, CA, USA). Isolated CD34$^+$ cells were cultured in StemSpan SFEM medium (Stem cell technologies, Vancouver, BC, Canada), supplemented with 20 ng/ml thrombopoietin (TPO), 10 ng/ml stem cell factor (SCF), 10 ng/ml interleukin (IL)-6 and 10 ng/ml FMS-like tyrosine kinase 3 (FLT-3), all from Peprotech (London, UK). On day 6 of the culture, the following cytokines were re-supplemented: 10 ng/ml TPO, 10 ng/ml IL-6 and 10 ng/ml IL-1β.

Inhibition of PEAR1 expression by siRNA

Two silencing RNA (siRNA) sequences for human PEAR1, GCACGCTGCTCATGTGAAA (referred to below as shPEAR1-1461) and GCAGCTACATGGAGATGAA (shPEAR1-2938), were developed using siSearch software (http://www.dharmacon.com/DesignCenter/ DesignCenterPage.aspx) and validated via quantitative PCR measurements (see below) for their potency to suppress mRNA expression of PEAR1 on endothelial EAhy926 cells. Their number refers to the respective positions in the reference human PEAR1 mRNA (NM_001080471.1) that are recognized by the siRNA.

Generation of lentiviral transfer plasmids

Lentiviral vectors encoding miR30-based knockdown hairpins derived from the aforementioned siRNAs were generated for stable knockdown as previously described[12] (referred to as miR_PEAR1_1461 and miR_PEAR1_2938) together with control hairpins directed against the monomeric red fluorescent protein from *Discosoma corallimorpharian*, DsRed (miR_DsRed). All constructs (pGAE-SFFV-BsdR-miR_PEAR1_1461-WPRE; pGAE-SFFV-BsdR-miR_PEAR1_2938-WPRE and pGAE-SFFV-BsdR-miR_DsRed-WPRE) contain a blasticidine

resistance cassette (BsdR) driven from a SFFV-LTR promoter, followed by the respective miRs. All cloning steps were sequence verified.

Lentiviral vector production and transduction

Lentiviral vector production was performed essentially as described earlier.[13] Briefly, vesicular stomatitis virus glycoprotein (VSV-G) pseudotyped lentiviral vector particles were produced by triple transient PEI transfection in HEK293T cells using pMDG.2, that encodes the VSV-G envelope, pAD_SIV3+, packaging plasmid, and transfer plasmids pGAE-SFFV-BsdR-miR_PEAR1_1461-WPRE and pGAE-SFFV-BsdR-miR_PEAR1_2938 -WPRE, to generate LV_miR_PEAR1_1461 and LV_miR_PEAR1_2938, respectively. Likewise controls with miR-based hairpins that target the mRNA of DsRed, were generated, resulting in LV_miR_DsRed, respectively. The latter vector will be referred to as "control" throughout the text. Stable PEAR1 knockdown cells and controls were generated following lentiviral transduction. Typically, $CD34^+$ cells (5×10^5) were transduced twice in 96-well plates (on the day of isolation and the day after).

Cell proliferation and CFU-assays

Colony-forming unit (CFU)–MK (megakaryocytic colonies) and CFU-E (erythrocyte colonies) potential was assessed as previously described. Human $CD34^+$ cells (5×10^3) were cultured in Megacult-C 04973, supplemented with recombinant cytokines according to the manufacturer's instructions. The number of CFU-MK and CFU-E was determined in a semisolid culture system using a commercially available kit (StemCell Technologies). The total number of colonies was counted at 6 and 10 days, using a light microscope (Leica DM RBE; Wetzlar, Germany) during cell culture. All rxperiments were carried out in triplicate.

PCR and real-time quantitative RT-PCR (qRT-PCR)

Total mRNA was extracted with TRIzol (Invitrogen, Carlsbad, CA, USA) for zebrafish embryos or using the Qiagen kit (RNeasy mini kit) for cultured cells. cDNAs were synthesized using M-MLV reverse transcriptase (Invitrogen).

Human gene expression was measured using FAM-labeled TaqMan assay products (Applied Biosystems, Life Technologies, Gent, Belgium) or via regular SYBR Green RT-PCR (IDT, Leuven, Belgium). Zebrafish gene expression was measured using a SYBR Green assay developed for zebrafish. All genes were normalized to the housekeeping genes human glyceraldehyde-3-phosphate dehydrogenase (*GAPDH*) or β-actin (*ACTB*), zebrafish β-actin (*Actb*) or elfa. Quantitative PCR (qRT-PCR) reactions were analysed using the ABI 7000 real-time PCR machine (Life Technologies). Expression was quantified via the $\Delta\Delta$Ct method[14] and expressed in arbitrary units (defined in figure legends) or in percentage compared to control. Expression of genes included in the PI3K/Akt (reference PAHS-058A) and Notch (reference PAHS-059A) RT^2 Profiler signaling were analyzed by qRT-PCR (SABioscience, Qiagen). Cell populations transduced by control lentivirus were used as a reference for LV_miR_PEAR1-transduced cells.

Western blot analysis

Western blot analyses were performed as previously reported.[1] The following antibodies were used: anti-PEAR1-EC (1/1000) (R&D), anti-Histone deacetylase-1 (HDAC-1) (1/1000; H-51, Santa Cruz Biotechnology), anti-Akt-P (1/500), anti-Akt (1/1000) (Cell signalling), anti-GFP (Green fluorescent protein; 1/1000) (Rockland, Gilbertsville, PA, USA) and anti-PTEN (1/500, Heidelberg, Germany). Mature red blood cell lysates were isolated as described.[15] Peripheral blood mononuclear cells (PBMC) were isolated via Ficoll-paque (BD) density centrifugation, after which residual platelets and platelet-leukocyte conjugates were eliminated via magnetic cell sorting, using a home-made anti-β3 monoclonal antibody, to capture platelet αIIbβ3. The use of flow cytometry and immunohistochemical staining are detailed in the online data supplement (www.bloodjournal.org).

Zebrafish whole-mount in situ hybridization (WISH)

Whole-mount RNA in situ hybridization for PEAR1 was performed with digoxigenin-labeled antisense riboprobes as previously described.[16] We used as primers: forward $^{5'}$GGCGTCTCTGCGAGTGCCAG$^{3'}$ and reverse $^{5'}$GCGGTGGTCACAGCGAGGAC$^{3'}$. The primers used for the in situ hybridization of GATA-1 were a kind gift of Dr. C. Verfaillie, Stem Cell Institute, KU Leuven. The microinjection of morpholino antisense oligonucleotides (MOs) is detailed in the online data supplement (www.bloodjournal.org).

O-Dianisidine staining of zebrafish red blood cells

Staining of hemoglobin by o-Dianisidine and quantification of staining intensity was performed as recently described.[17, 18]

Flow cytometry

Protein expression levels of CD41 (α_{IIb} integrin) and CD42b ($GP_{Ib\alpha}$) were measured by flow cytometry using specific antibodies from BD Biosciences (Erembodegem, Belgium). Polyploidy was analysed after anti-CD41 labelling and DNA staining with 0.01 mg/mL propidium iodide (Sigma Aldrich, Bornem, Belgium) and the DNA content was measured in CD41-positive cells. Incorporation of Pacific Blue-A labelled 5-Ethynyl-2'-deoxyuridine (EDU, Invitrogen, Molecular Probes, Ghent, Belgium) in maturing $CD34^+$ cells was determined after CD61 (β_3 integrin) labelling, using a PE-conjugated antibody from BD Biosciences. Samples were analysed on a FACSCantoII flow cytometer (BD Biosciences).

Immunohistochemical staining

Normal human bone marrow sections were stained with the anti-PEAR1 antibodies (1.25 μg/ml) and analysed on a Zeiss Oberver.D1 microscope. Use of human tissue for histological purposes was authorized by the Ethical Committee of the Academic Hospital of the KU Leuven.

Validation of the PEAR1 ATG morpholino *in vitro*

A linker containing 40 base pairs before and behind the site of the PEAR1 MO sequence was cloned in frame with luciferase in the pGL4.10-T7-Luc2 vector. Sense (and antisense) oligonucleotide sequences used for the PEAR1 MO *in vitro* test (bold: sequence targeted by the PEAR1 MO) were

$^{5'}$agcttTAGTTGAGTCCAATGCCACTTCATC**AGTAAGGATGAAGACGGCGGAGATCT**GTGTGGTCCTGTTTGTCTTGGGCT G$^{3'}$ and

$^{5'}$catgCAGCCCAAGACAAACAGGACAACACA**GATCTCCGCCGTCTTCATCCTTACT**GATGAAGTGGCATTGGACTCAACTA$^{3'}$

A TNT Lysate reaction was performed (Promega, Leiden, The Netherlands) to transcribe and translate the fusion protein in one reaction, in the presence of different concentrations of control or PEAR1 MO (100 nM-100 μM). Luciferase activity was then measured with a luminometer.

Microinjection of morpholino antisense oligonucleotides (MOs)

The transgenic zebrafish lines CD41:eGFP, a kind gift from dr. L. Zon (Hematology Division, Brigham and Women's Hospital's, Boston, MA, USA) and GATA1:dsred, a kind gift from dr. A. Luttun at our centre, were used. Zebrafish embryos were injected with a start codon (ATG) or splice-blocking MO *vs.* a control MO into 1- to 2-cell-stage embryos. All MOs were designed by Gene-Tools LLC (Philomath, OR, USA). Embryos were screened at 1, 2, and 3 days post fertilization (dpf) using a Zeiss Lumar V12 microscope, and images were captured with a Zeiss Axiocam MRc camera using AxioVision software (Carl Zeiss, Jena, Germany). All animal protocols were approved by the Ethical Committee of the KU Leuven.

Statistics analysis

Results are expressed as mean values ± SEM. Statistical significance was evaluated with unpaired Student's t-tests. (*: $p<0.05$; **: $p<0.01$; ***:$p<0.001$).

RESULTS

PEAR1 expression during human megakaryocyte differentiation

Immunohistochemical staining of normal human bone marrow showed PEAR1 positivity in MKs and revealed that granulocyte precursors, but not mature granulocytes were PEAR1 positive (Fig. 1A). Also PEAR1 positive osteoblasts and endothelial cells were observed (not shown); platelets were strongly positive, whereas erythrocyte precursors were PEAR1 negative (Fig. 1A). Western blots of isolated blood cells confirmed the presence of PEAR1 in platelets and its absence in red blood cells and PBMCs (Fig. 1B). During in vitro differentiation of $CD34^+$ cells, more detailed RT-PCR and qRT-PCR measurements showed that both PEAR1 and ITGA2B (CD41) were very low at day 0, but that their GAPDH normalized expression increased in parallel from day 6 to 12, in contrast to expression of a more stable reference, such as hypoxanthine guanine phosphoribosyl transferase (HPRT) (Fig. 1C). Similar results were seen for both genes, when tested in RT-PCR *vs.* ACTB (β-actin) (Fig. 1C). Flow cytometry and western blot analysis evidenced membrane PEAR1 protein expression in differentiated $CD34^+$ cells after 6 and 10 days of maturation initiation (Fig. 1D). Anti-PEAR1-antibodies triggered Akt phosphorylation in matured MKs, acting as a pseudo-ligand for PEAR1 as recently reported for platelets[1] (not shown). Or, PEAR1 is progressively expressed during megakaryopoiesis and appears transiently in granulocyte precursors in the bone marrow. In the circulation, PEAR1 is only present in platelets.

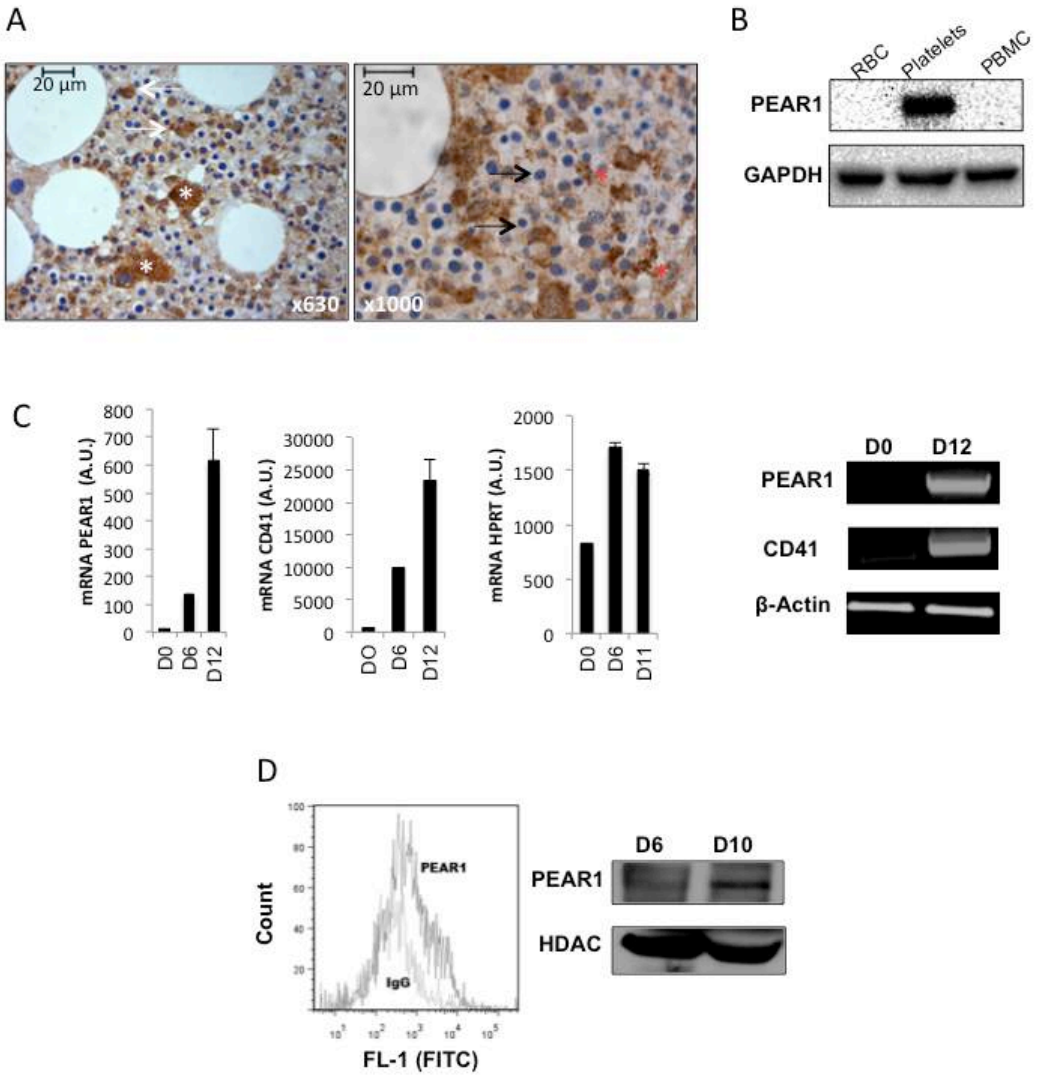

Figure 1: PEAR1 expression in differentiating human CD34$^+$ cells. A) Immunohistochemical staining of PEAR1 in human bone marrow sections, at 630 and 1000-fold magnification; megakaryocytes (*), myeloid precursors (white arrows) and erythroid precursors (black arrows) are indicated. B) Western blot for PEAR1 in red blood cell lysates (RBC), platelets and peripheral blood mononuclear cells (PBMC) *vs.* GAPDH control. C) *PEAR1*, *ITGA2B* (CD41) and *HPRT* expression on day 0, day 6 and day 12 in CD34$^+$ cells by qRT-PCR *vs. GAPDH* control and by RT-PCR *vs. ACTB* (β-actin) control. D) Flow cytometric measurement of PEAR1 on the membrane in 10-day-old CD34$^+$ cell cultures, after staining with IgG control (MFI 562) and PEAR1-Ab (MFI 1287), as indicated (representative for n=3); western blot for PEAR1 in CD34$^+$ cell lysates, at day 6 and 10, with HDAC-1 as loading control. 1 A.U. represents 1 copy for 10^5 copies of housekeeping gene.

PEAR1 in megakaryocyte differentiation: proliferation *vs*. maturation

Transduction of freshly isolated human CD34$^+$ cells with LV_miR_PEAR1_1461 decreased PEAR1 mRNA levels by 90%, compared to LV_miR_DsRed transduction (Fig. 2A). Correspondingly, protein synthesis at day 10 had dropped strongly upon transduction with LV_miR_PEAR1_1461, when investigated via western blots (Fig. 2A). Calculation of the

degree of protein expression suppression for transduction with both viral *vs.* the control vectors yielded up to 84-94% expression inhibition (Fig. 2A, single experiment comparison). During $CD34^+$ cell differentiation, proliferating cell numbers reach a plateau between day 10 and 14.[19] Trypan blue counting of the cells, 10 days after transduction with LV_miR_PEAR1_1461 or LV_miR_PEAR1_2938 detected >95% cell viability and uncovered 2.4-2.8-fold higher cell numbers of differentiating MKs following PEAR1 mRNA knockdown, compared to control ($p<0.01$ *vs.* control; $p<0.05$ between both vectors) (Fig. 2B). More stringent clonogenic assay cultures with separate counting of CFU–MK and CFU-E colonies on day 6 and 10, confirmed that LV_miR_PEAR1_1461 transduction doubled CFU-MK colony numbers, compared to control; without affecting CFU–E colony formation (Fig. 2C). These findings indicate a specific role for PEAR1 in human MK progenitor proliferation, absent in the erythroid lineage.

To further delineate how PEAR1 knockdown would affect MK maturation, first, cultured cells were analysed at day 10 for expression of the typical MK and platelet markers CD41 and CD42b, as well as for their ploidy. Fig. 2D shows a fractional shift towards positivity at day 10 for both markers and shows that, in addition to megakaryoblasts, a more mature cell subset was present, strongly positive for CD41 and CD42b. The proportion of all CD41+CD42+ positive cells at day 10 was not modified by the LV_miR_PEAR1 vector treatment (79 vs. 77%, Fig. 2D). Also the percentages of strongly positive $CD41^+CD42^+$ subpopulations were not different (15.7 *vs.* 14%, Fig. 2D, upper right population in Q2). Correspondingly, no major effect was observed on the histogram during propidium iodide staining of the matured cells, suggesting the mature subset to largely be the 4N MK precursor population (Fig. 2E). A non-significant trend for a higher ploidy was observed for the 8N fraction in the absence of PEAR1. Therefore, to specifically investigate the proliferation rate in the late differentiation phase, LV_miR_PEAR1_1461 treated $CD34^+$ cell cultures were incubated on day 10 with the fluorescently labeled BrdU analogue EDU. The CD61 positive cell fraction in these cultures varied from 4-24% in different cultures; paired comparisons revealed identical CD61 positivity for LV_miR_PEAR1_1461 *vs.* control treatment, with a mean ratio of 1.08 ± 0.13. EDU incorporation in the CD61 positive cell fraction varied from 28 to 42%, but paired comparison revealed no difference, with a mean ratio of 1.06 ± 0.045. Collectively, these

results illustrate that PEAR1 primarily controls progenitor cell proliferation and not the later stages of MK maturation.

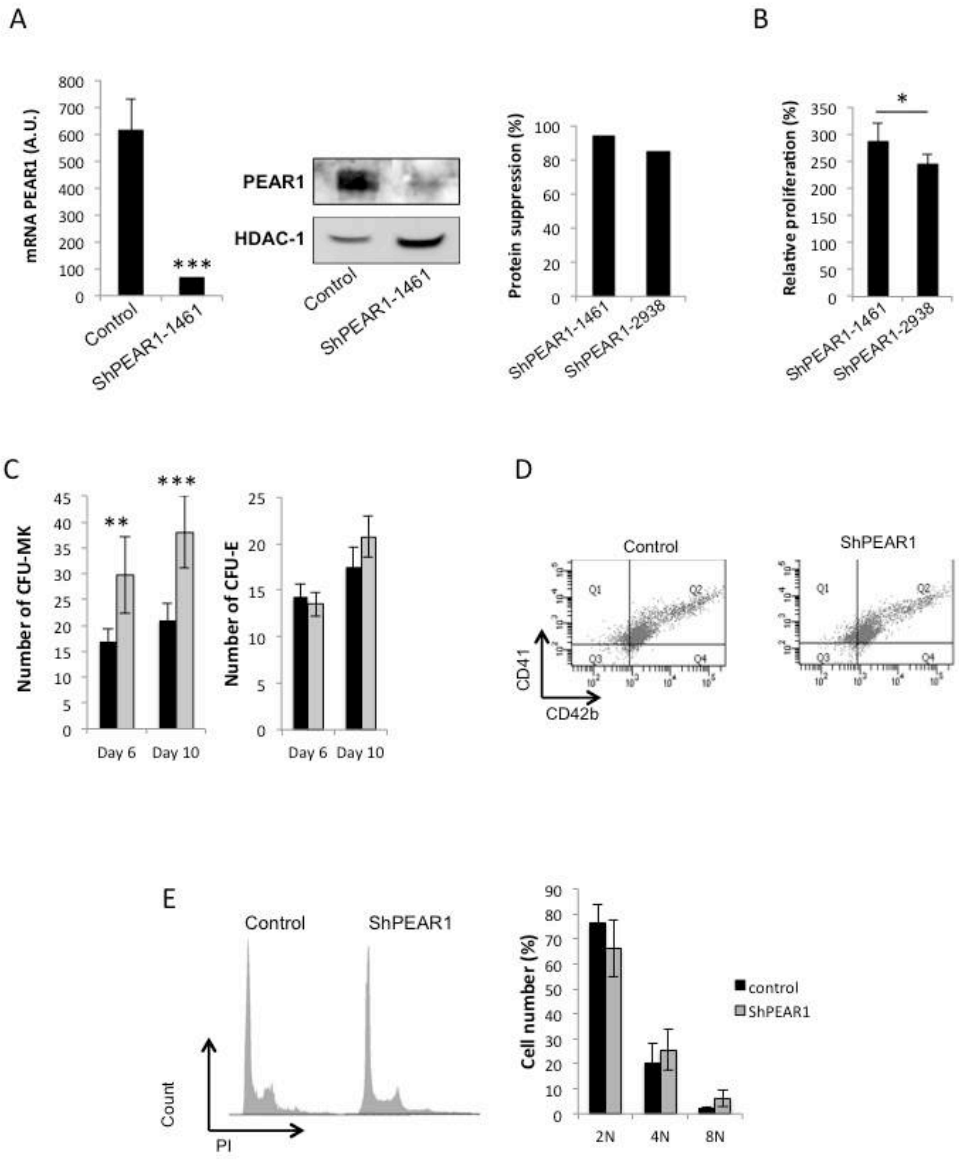

Figure 2: PEAR1 knockdown via lentiviral vector transduction. A) *PEAR1* expression at day 10, after transduction of human $CD34^+$ with control (LV_miR_DsRed) or LV_miR_PEAR1_1461 vector, analysed via qRT-PCR (left panel) and western blotting with PEAR1-EC Ab, using HDAC-1 as loading control (middle panel). Relative suppression of the GAPDH-normalized PEAR1 protein expression at day 11, following transduction of both LV_miR_PEAR1 vectors *vs.* control (right panel). B) Relative cell proliferation at day 10, after treatment with both LV_miR_PEAR1 vectors *vs.* control. C) Numbers of CFU-MK and CFU-E colonies at day 6 and 10, after transduction of human $CD34^+$ with control (black) or LV_miR_PEAR1_1461 (grey) vectors. D) Co-expression of CD41 and CD42b during $CD34^+$ cell differentiation, analysed by flow cytometry at day 12, after transduction of human $CD34^+$ with control or LV_miR_PEAR1_1461 vectors, as indicated. E) Polyploidy profiles (left panel) on day 10, representative of 3 experiments, after anti-CD41 labelling and DNA staining with propidium iodide (PI), after transduction of human $CD34^+$ with control or LV_miR_PEAR1_1461 (n=3); Ploidy histogram for control and LV_miR_PEAR1_1461 treated $CD34^+$ cells on day 12 (n=3). 1 A.U. represents 1 copy for 10^5 copies of housekeeping gene.

Gene (de)regulation by PEAR1 knockdown in megakaryocyte progenitors

Several transcription factors have been implicated in megakaryopoiesis.[20, 21] Therefore, we measured the expression of GATA-1, PU-1, RUNX1, FLI-1 and NF-E2 during MK maturation in $CD34^+$ cells (Fig. 3). The expression of GATA-1 and NF-E2 increased progressively until day 12. In contrast, RUNX1 already dropped on day 6. PU-1 expression dropped and FLI-1 mRNA levels rose during the late differentiation (n=3, at least). Comparison of the expression levels at day 12 showed that PEAR1 depletion did not affect the expression of GATA-1 and PU-1 (Fig. 3A) and had a mild effect on the expression of FLI-1 and NF-E2. In contrast, the drop in RUNX1 expression was tampered following PEAR1 knockdown, preserving 3-fold higher RUNX1 mRNA levels (Fig. 3A), i.e. RUNX1 drops more in control than in LV_miR_PEAR1_1461 treated cells.

Next, to characterize PEAR1 target genes in MKs grown from cytapheresis isolates, we compared control and LV_miR_PEAR1_1461 transduced $CD34^+$ cell cultures on day 12 by profiler qRT-PCR analysis. The Notch and the PI3K/Akt pathway have been coupled to PEAR1 signalling during myeloid progenitor proliferation in mouse bone marrow cells and in platelet activation, respectively. We, therefore, analysed a series of genes involved in both pathways, using RT^2 profiler PCR arrays, analysing 84 genes in each case (Fig. 4).

The signal from 12 probe sets in the Notch profiler and 9 probe sets in the PI3K/Akt pathway were significantly altered following PEAR1 knockdown in differentiated $CD34^+$ cells. Genes over- and underexpressed in the PEAR1 depleted cells *vs.* control cells are listed according to the fold change (Fig. 3B and Fig. 4). Interestingly, we found that a target of the Notch pathway, HES1, was upregulated without expression modification of the Notch receptors (Fig. 3B and Fig. 4). PTEN, a phosphatase regulating the PI3K pathway, and CCND1 (cyclin D1) were both downregulated (Fig. 3B). Recently, 2 different authors described how HES1, a target of the Notch pathway, negatively regulates the transcription of PTEN during megakaryopoiesis and in mouse thymocytes.[22, 23] Therefore, we choose to confirm such regulation, using a separate set of primers. Fig. 3C and 3D show for this set of primers that PEAR1 knockdown upregulated the Notch target HES1, in parallel with the downregulation of PTEN. Western blots for PTEN confirmed lower protein expression for the PEAR1 knockdown, both in LV_miR_PEAR1_1461 and LV_miR_PEAR1_2938 treated $CD34^+$ cells (Fig. 3D). Since PTEN regulates the PI3K/Akt pathway by dephosphorylating PIP3 into PIP2, we analysed the phosphorylation of Akt in LV_miR_PEAR1_1461 treated CD34+ cells. At day 10,

the PEAR1 knockdown displayed a more intense Akt-P Ser473 band (Fig. 3E), in agreement with lower PTEN activity in LV_miR_PEAR1 treated CD34+ cells, responsible for diminished Akt dephosphorylation. The absence of PEAR1 did not affect TPO signalling, since phosphorylation of ERK1/2, a target of the c-mpl/TPO pathway was not altered (Fig. 3E).

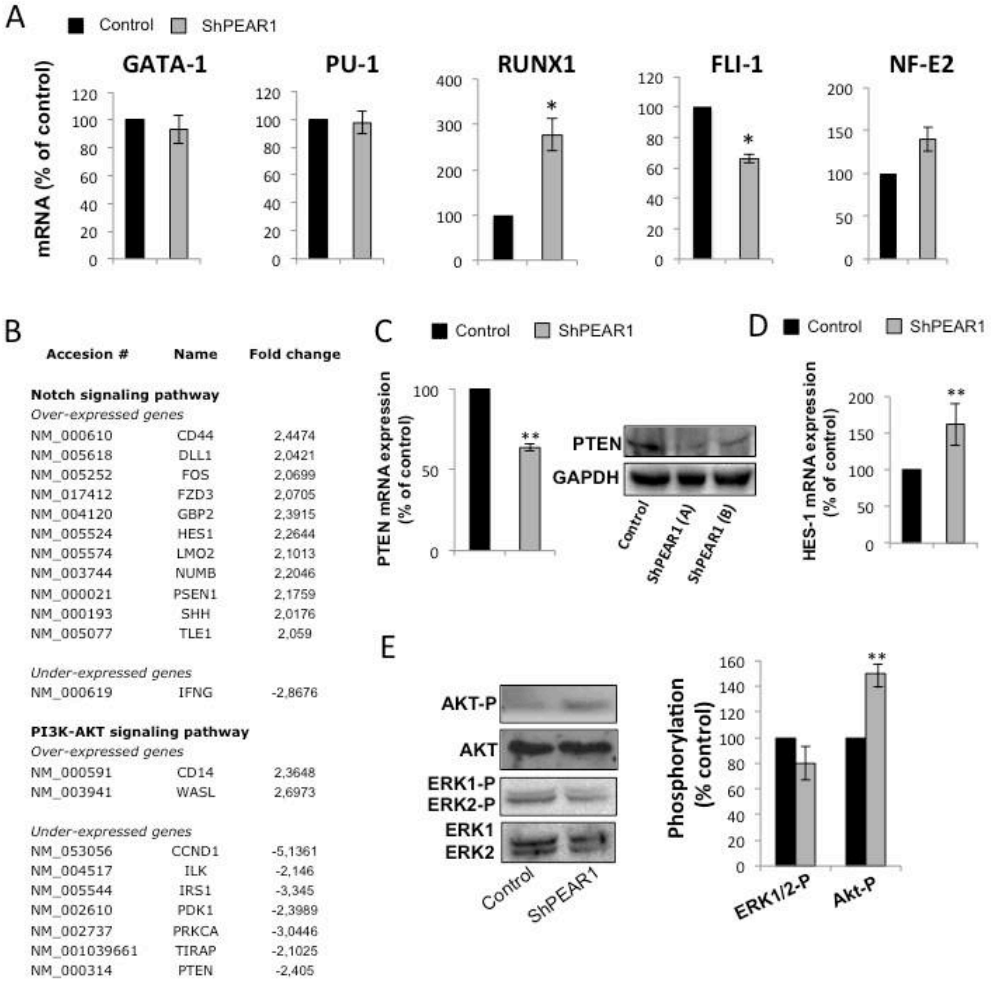

Accesion #	Name	Fold change
Notch signaling pathway		
Over-expressed genes		
NM_000610	CD44	2,4474
NM_005618	DLL1	2,0421
NM_005252	FOS	2,0699
NM_017412	FZD3	2,0705
NM_004120	GBP2	2,3915
NM_005524	HES1	2,2644
NM_005574	LMO2	2,1013
NM_003744	NUMB	2,2046
NM_000021	PSEN1	2,1759
NM_000193	SHH	2,0176
NM_005077	TLE1	2,059
Under-expressed genes		
NM_000619	IFNG	-2,8676
PI3K-AKT signaling pathway		
Over-expressed genes		
NM_000591	CD14	2,3648
NM_003941	WASL	2,6973
Under-expressed genes		
NM_053056	CCND1	-5,1361
NM_004517	ILK	-2,146
NM_005544	IRS1	-3,345
NM_002610	PDK1	-2,3989
NM_002737	PRKCA	-3,0446
NM_001039661	TIRAP	-2,1025
NM_000314	PTEN	-2,405

Figure 3: Transcriptional regulation and PI3K-Akt/Notch pathways after PEAR1 knockdown. A) Proportional mRNA expression of the indicated transcription factors on day 11 in $CD34^+$ cells transduced with control or LV_miR_PEAR1_1461 vectors *vs. GAPDH*. B) List of genes involved in the Notch and PI3K/Akt pathways under- or overexpressed in RT^2 profiler analysis in the shPEAR1 knockdown, expressed in fold change. C) qRT-PCR for *PTEN* mRNA in $CD34^+$ cells 10 days after transduction with control and LV_miR_PEAR1_1461, relative to *GAPDH*; western blot for PTEN at day 10 after transduction with control and LV_miR_PEAR1_2938, relative to GAPDH in two separate analyses (A and B). D) qRT-PCR for *HES1* mRNA in $CD34^+$ cells at day 10 after transduction with control and LV_miR_PEAR1_1461, relative to *GAPDH*. E) Western blots for AKT-P, Akt, ERK1/2-P and ERK1/2 in control and LV_miR_PEAR1_1461 treated $CD34^+$ cells at day 10. Phosphorylation was quantified with ImageJ and is shown in the right histogram.

shPEAR1 group vs. control group

Human Notch signalling pathway

Gene Symbol	Fold Difference
ADAM10	1,17
ADAM17	1,93
AES	1,83
AXIN1	1,77
CBL	1,43
CCNE1	1,96
CD44	2,45
CDC16	1,47
CDKN1A	0,7
CFLAR	1,57
CHUK	1,65
CTNNB1	1,73
DLL1	2,04
DTX1	1,17
EP300	1,24
ERBB2	1,07
FIGF	1,06
FOS	2,07
FOSL1	1,13
FZD1	1,36
FZD2	1,45
FZD3	2,07
FZD4	1,37
FZD6	1,79
FZD7	1,78
GBP2	2,39
GLI1	1,22
GSK3B	1,32
HDAC1	1,49
HES1	2,26
HEY1	1,38
HEYL	0,91
HOXB4	1,54
HR	1,03
IFNG	-2,87
IL17B	1,21
IL2RA	1,3
JAG1	1,39
JAG2	1,07
KRT1	1,19
LFNG	1,44
LMO2	2,1
LOR	1,11
LRP5	1,18
MAP2K7	1,86
MFNG	1,19

Human PI3K/AKT signalling pathway

Gene Symbol	Fold Difference
ADAR	0,83
AKT1	0,91
AKT2	0,61
AKT3	0,51
APC	0,55
BTK	ND
CASP9	0,54
CCND1	-5,14
CD14	2,36
CDC42	0,63
CDKN1B	0,71
CHUK	0,83
CSNK2A1	0,69
CTNNB1	0,52
EIF2AK2	0,61
EIF4B	0,99
EIF4E	0,77
EIF4EBP1	1,05
EIF4G1	0,71
ELK1	0,81
FASLG	0,52
FKBP1A	0,77
FOS	2,07
FOXO1	0,76
FOXO3	0,56
MTOR	0,82
GJA1	0,74
GRB10	0,88
GRB2	0,86
GSK3B	0,81
HRAS	ND
HSPB1	ND
IGF1	0,68
IGF1R	0,67
ILK	-2,15
IRAK1	0,78
IRS1	-3,35
ITGB1	0,67
JUN	ND
MAP2K1	0,78
MAPK1	0,62
MAPK14	0,74
MAPK3	ND
MAPK8	0,62
MTCP1	0,83
MYD88	1,07

MMP7	1,49	NFKB1	1,01
MYCL1	0,83	NFKBIA	0,85
NCOR2	0,67	PABPC1	0,88
NEURL	1,17	PAK1	0,62
NFKB1	1,7	PDGFRA	0,59
NFKB2	1,32	PDK1	-2,4
NOTCH1	1,4	PDK2	0,68
NOTCH2	1,58	PDPK1	0,77
NOTCH2NL	1,59	PIK3CA	0,95
NOTCH3	1,47	PIK3CG	0,69
NOTCH4	1,27	PIK3R1	0,82
NR4A2	1,64	PIK3R2	1,15
NUMB	2,2	PRKCA	-3,05
PAX5	1,06	PRKCB	0,71
KAT2B	1,73	PRKCZ	0,65
PDPK1	1,71	PTEN	-2,405
POFUT1	1,51	PTK2	0,62
PPARG	1,47	PTPN11	0,68
PSEN1	2,18	RAC1	1,45
PSEN2	1,27	RAF1	0,98
PSENEN	1,31	RASA1	0,84
PTCRA	0,57	RBL2	0,97
RFNG	1,22	RHEB	0,88
RUNX1	1,14	RHOA	ND
SEL1L	1,15	RPS6KA1	0,82
SH2D1A	1,71	RPS6KB1	0,97
SHH	2,02	SHC1	0,57
STIL	1,83	SOS1	0,84
SNW1	1,99	SRF	ND
SMO	1,21	TCL1A	1,09
STAT6	1,86	TIRAP	-2,1
SUFU	1,42	TLR4	0,94
TEAD1	1,88	TOLLIP	ND
TLE1	2,06	TSC1	1,01
WISP1	1,33	TSC2	ND
WNT11	0,88	WASL	2,7
ZIC2	1,41	YWHAH	0,92

Figure 4. PI3K/Akt and Notch signalling pathway analysis, expressed as fold-difference.

PEAR1 silencing in zebrafish boosts thrombocyte production

First, Pear1 expression was studied by semi-quantitative RT-PCR during the early development of zebrafish. Pear1 mRNA appeared at 24 hours post fertilization (hpf), progressively rising till day 4 (Fig. 5A). It was also detected in adult zebrafish blood (Fig. 5B), and was abundantly present in the nervous system (Fig. 5C, F, G), in somites (Fig. 5D) and in a putative yolk sac gland (Fig. 5E), as demonstrated by *in situ* staining for Pear1 mRNA. Staining with the sense probe was negative (Fig. 5H), but Pear1 mRNA was barely detected

in the caudal region (Fig. 5I). To confirm this region to be the site where haematopoiesis (erythropoiesis) occurs, *in situ* hybridization for Gata-1 was performed (Fig. 5J).

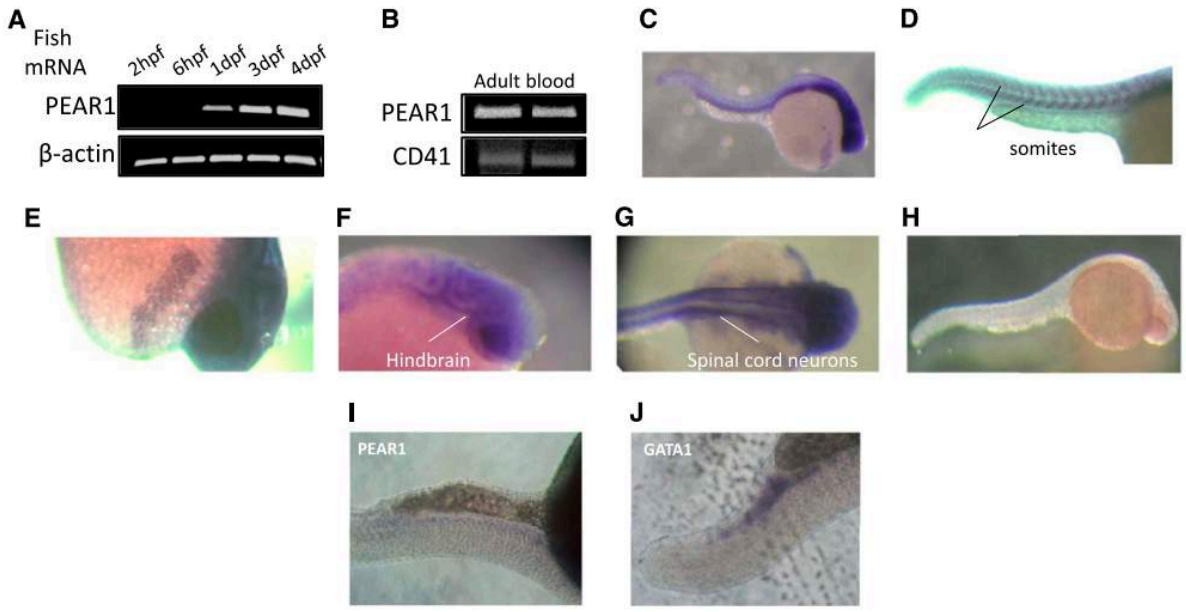

Figure 5: Pear1 expression in the zebrafish. A) mRNA *Pear1* expression during fish development, measured by RT-PCR (hpf: hours post fertilization, dpf: days post fertilization). B) RT-PCR of *Pear1* and *CD41* in adult blood in two different samples. C) Whole-mount in situ hybridization (WISH) of Pear1 at 24 hpf with a Pear1 anti-sense probe; D) Expression in somites; E) Expression in a putative yolk sac gland; F-G) Expression in the nervous system: midbrain-hindbrain boundary (F) and spinal cord neurons (G). H) Control WISH of Pear1 at 24hpf with a Pear1 sense probe; I-J) Faint Pear1 (I) and clear Gata-1 (J) expression in the caudal region.

Next, we investigated the function of PEAR1 in CD41:eGFP zebrafish, which express GFP under control of the CD41 promoter. First, the potency of the PEAR1 MOs was tested on Pear1 gene expression in an *in vitro* luciferase assay and by RT-PCR (Figure 6) and on Pear1 protein expression in fish. The PEAR1 ATG MO dose-dependently inhibited the luciferase activity and the splice PEAR1 MO inhibited the PEAR1 amplification (Fig. 6A-B), as well as the appearance of Pear1 in 3-day-old fish (Fig. 7A). Therefore, the role of Pear1 was determined during fish development and thrombocyte production. Injection of PEAR1 MO affected the development of the zebrafish in a dose-dependent manner (Fig. 6C). At low concentrations (up to 50 μM), no effects were observed. However, at a concentration equivalent to 100 μM, 42% of the fish presented a mild (23%) to severe (19%) phenotype, whereas treatment with a control MO had no effect on fish development. Defective development of the nervous system was observed (absence of eyes and head). Increasing concentrations of Pear1 MO

lead to severe phenotypic abnormalities (Fig. 6C), lethality at 500 μM (not shown) and motility limitations, reflected by a higher percentage of zebrafish residing inside the chorion after 3 days, compared to control zebrafish (Fig 6D). A low concentration of PEAR1 MO (50 μM) triggered an increase in the number of circulating GFP^+ hematopoietic cells at day 2 (Fig. 7B). Since expression of CD41 is detectable at 48 hpf in hematopoietic cells[24], the strong GFP staining (Fig. 7C) further suggested these cells to be mature thrombocytes.[24] Western blots confirmed elevated GFP expression in the fish (Fig. 7D). To study the effect of Pear1 depletion on the development of hematopoietic stem cells and erythrocytes, qRT-PCR was carried out for Scl and Gata-1, on 24-hpf embryos. No expression differences were observed for these lineage markers, with only a partial specificity in zebrafish, compared to human HSC (Fig. 7E).

At higher MO concentrations, the thrombocyte count dropped, related to developmental problems (Fig. 6E). Correspondingly, when GATA1:dsred fish embryos were injected with the PEAR1 MO (50 μM), no differences were observed in the development of red blood cells (Fig. 7F). Erythrocyte cell maturation was also studied by direct staining of red blood cells in the zebrafish yolk sac. O-dianisidine staining of whole fish embryos at 48 hpf stained red blood cells equally in control and PEAR1 MO injected embryos (Fig. 7F, G). Together, these results demonstrate that mild PEAR1 suppression, compatible with normal development of zebrafish suffices to raise thrombocyte, but not erythrocyte production.

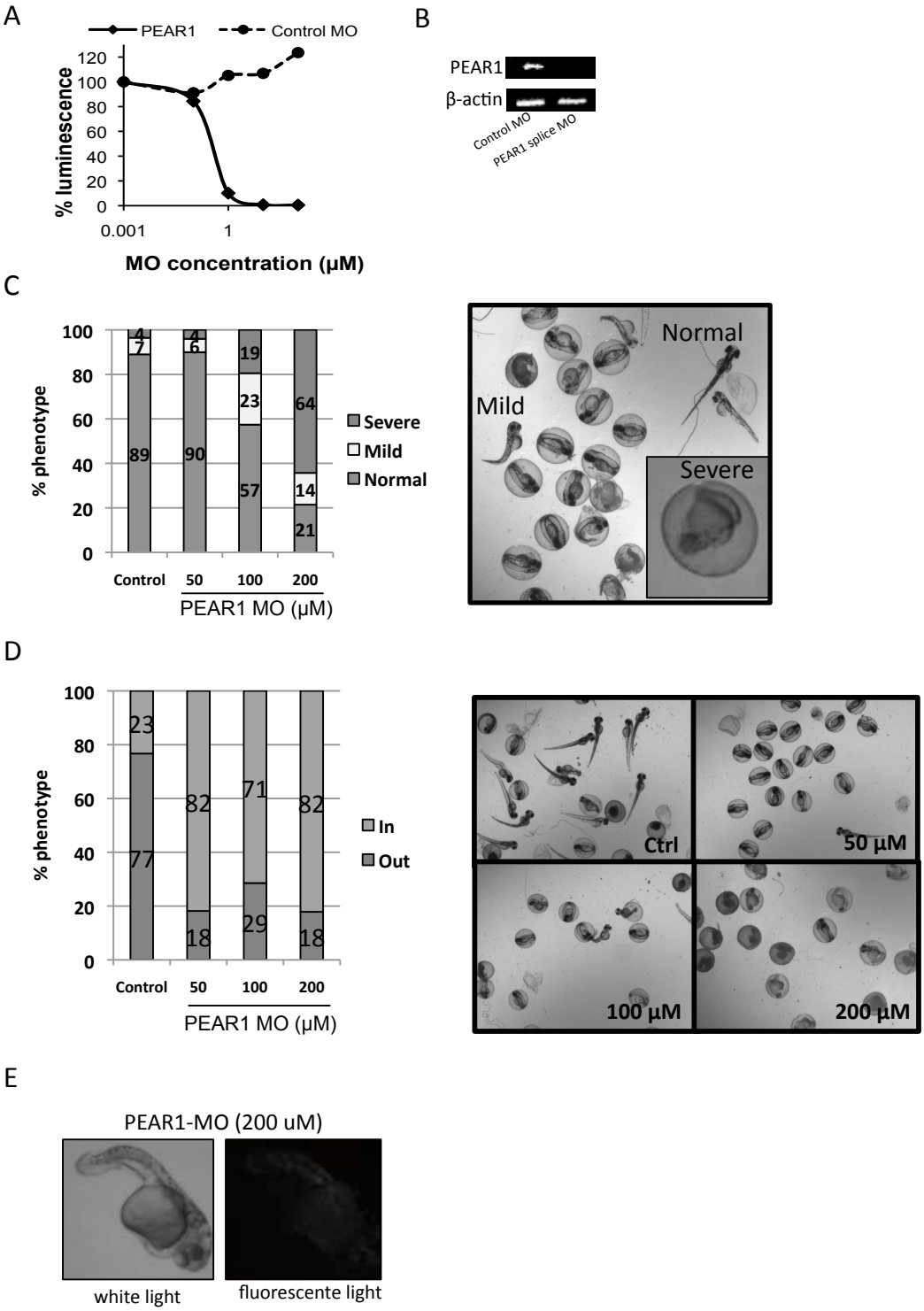

Figure 6. A) *In vitro* luciferase testing efficiency of the PEAR1 ATG MO for zebrafish *Pear1*. B) PCR testing efficiency of the PEAR1 splice MO. Embryos were injected with control or splice-blocking PEAR1 MO. The phenotype was analysed for developmental problems. A mild phenotype was defined by a curly tail, a severe phenotype by nervous system developmental defects. C) left panel: distribution of phenotypes for different MO concentrations. Right panel: pictures illustrating all phenotypes. D) left panel: distribution of phenotypes illustrating motility limitation (fish **in** or **out** of the chorion) for different splice-blocking MO concentrations. Right panel: pictures illustrating phenotype. E) Effect of PEAR1 splice-blocking MO on thrombocyte production in a severely affected zebrafish (PEAR1 MO equal to 200 µM).

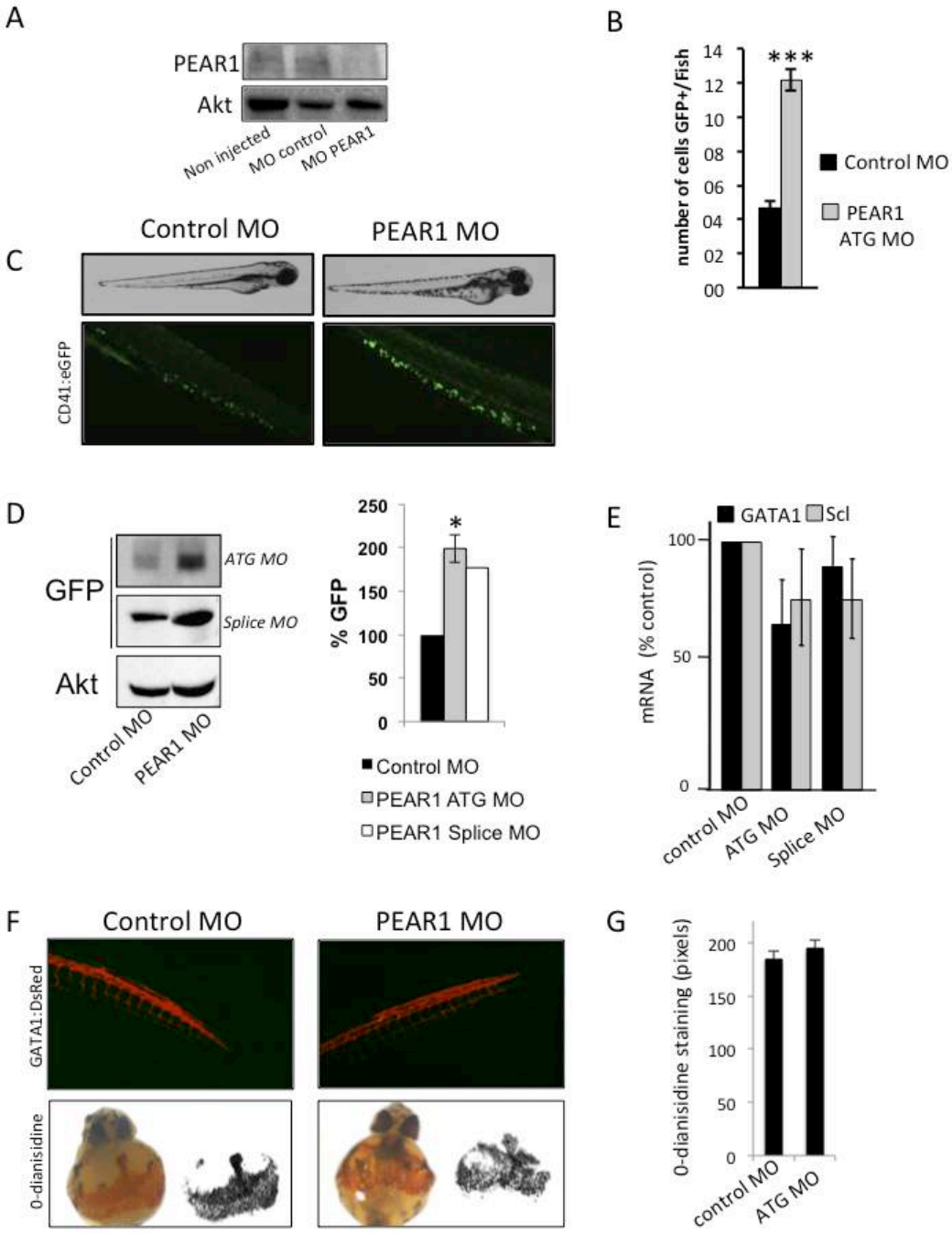

Figure 7: Pear1 in zebrafish is a negative regulator of thrombocyte production. A) Western blot for Pear1 (Pear1-EC Ab) in zebrafish, non-injected, injected with control MO or Pear1 ATG MO 3dpf; total Akt served as loading control. B) Analysis of the number of GFP-positive cells in the tail at 2 dpf after PEAR1 MO injection *vs.* control. C) Pear1 knockdown and thrombocyte production. Photography of CD41:eGFP fish at 3 dpf after injection with control or Pear1 ATG MO with white light (top panels) and with fluorescent light (bottom panels). D) Western blot of GFP expression and quantification at 3 dpf in whole fish after injection with control or Pear1 ATG or Pear1 splice MO, with Akt as loading control, E) mRNA expression of *Gata-1* and *Scl*, general markers for erythrocytes and hematopoietic stem cells, by qRT-PCR after treatment with control or Pear1 MOs. F) Pear1 knockdown in erythrocyte production: photography of GATA1:dsred fish at 3 dpf after injection with control or Pear1 ATG MO with fluorescent light (top panels); o-dianisidine staining of CD41:eGFP whole fish at 48 hpf, after injection with control or Pear1 ATG MO (lower panels). G) Analysis of area density for stained red blood cells after injection with control or Pear1 ATG MO.

PEAR1 transcriptionally regulates PTEN, modulating Akt phosphorylation

PEAR1 activates PI3K and triggers Akt phosphorylation in platelets.[1] Both PI3K and the phosphatase PTEN are necessary for platelet formation, via controlling Akt phosphorylation.[11] Therefore, Akt phosphorylation was investigated in the zebrafish Pear1 knockdown 3 dpf, after injection of Pear1 MO or control MO. Pear1 depletion induced elevated Akt phosphorylation in total zebrafish extracts (Fig. 8A). The importance of PI3K in this process is illustrated by the addition of the PI3K inhibitor LY294002, added to the water 30 hpf. Added at this time point, LY294002 was not lethal, but disrupted Akt phosphorylation and thrombocyte formation (Fig. 8B, Fig. 9). Similarly to the effect of PEAR1 neutralization in $CD34^+$ cells during MK differentiation *in vitro* (Fig. 3), Pten was downregulated in the Pear1 knockdown. Because the zebrafish genome encodes 2 *Pten* genes *Ptena* and *Ptenb*, expression of both was analysed by qRT-PCR after Pear1 MO injection. *Ptena* was potently dowregulated and *Ptenb* weakly (Fig. 8C). Therefore, the role of each phosphatase was analysed separately in thrombocyte production and Akt phosphorylation. In agreement with earlier findings,[25] the inactivation of only a single isoform did not affect fish development at 3 dpf (Fig. 9B). Also, both the injection of Ptena or Ptenb MO increased Akt phosphorylation, even though the thrombocyte count was only increased after Ptena MO treatment, as shown by the GFP western blots (Fig. 8D). Combined, these results demonstrate that Pear1 controls Ptena expression, a phosphatase regulating thrombocyte formation, via Akt dephosphorylation.

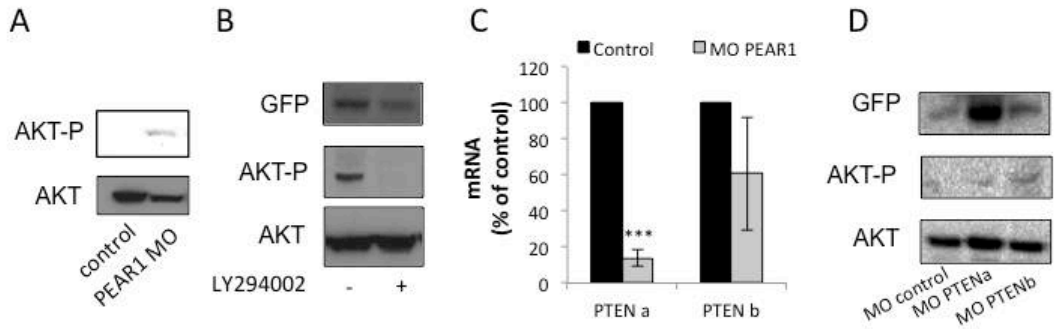

Figure 8: Pear1 controls *Ptena*, a regulator of thrombocyte production. A) Western blot of Akt-P (Ser473) at 3 dpf in zebrafish after injection of control or Pear1 splice-blocking MO. B) Western blot for GFP and Akt-P in whole fish after treatment with LY294002 or DMSO, added at 30 hpf and analysed 3dpf, with Akt as a loading control. C) mRNA expression of *Ptena* and *Ptenb* by qRT-PCR 3 dpf after injection of control or Pear1 MO, expressed as percentage of control (n=3). D) Western blot analysis of GFP, Akt-P and Akt after injection of Ptena or Ptenb MO 3 dpf after injection.

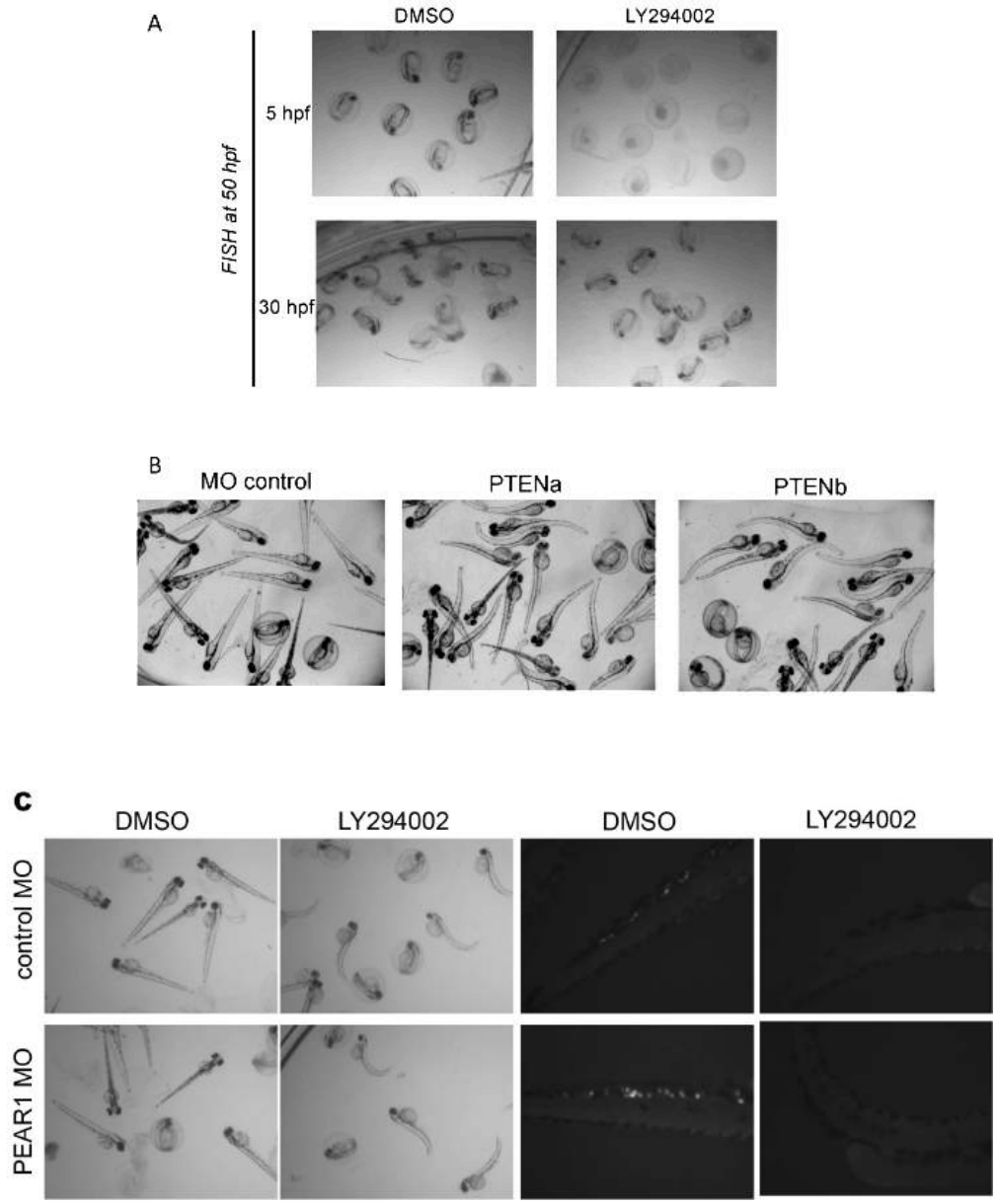

Figure 9: A) Zebrafish were treated with LY294002 (50 μM) added to the water at 5 or 30 hpf. DMSO was used as control. Phenotype was analysed at 50 hpf. B) PTENa or PTENb MO were injected at concentrations necessary to increase Akt-P (600 μM). The phenotype was analysed at 3 dpf. C) Pictures of zebrafish at 3 dpf with white light (left panels) and fluorescent light (right panels) after treatment of zebrafish with the PI3K inhibitor LY294002 (50 μM), in combination with control or PEAR1 MO. Fish were first injected with MO and then divided in two groups: control (DMSO) or LY294002. DMSO and inhibitor were added to the water at 30 hpf.

Supplemental data: Expression regulation of hematopoietic transcription factors in CD34$^+$ cells.

Figure 10 describes the expression of *GATA-1*, *PU-1*, *RUNX*, *FLI-1* and *NF-E2* in differentiating CD34$^+$ cells, treated with the control vector LV_miR_dsRed over time. GATA-1 is an important transcription factor in haematopoiesis, required in multipotent progenitors and committed precursors during erythrocyte, as well as megakaryocyte maturation[26]. A lack of GATA-1 in the MK lineage leads to decreased polyploidization and a lack of cytoplasmic maturation.[27] Interestingly, GATA-1 deficient megakaryocytes, with reduced size and polyploidization, express nearly 10-fold less cyclin D and 10-fold more p16 as their wild-type counterparts.[28] Although these authors demonstrated that cyclin D1 is a direct GATA-1 target in megakaryocytes, we found a strong reduction for *CCND1* expression in PEAR1 knockdown CD34$^+$ cells, despite similar upregulation of GATA-1 in control and LV_miR_PEAR1 treated CD34$^+$ cells, after 12 days in culture. Our findings, therefore suggest that the PEAR1-dependent downregulation of *CCND1* is GATA-1 independent.

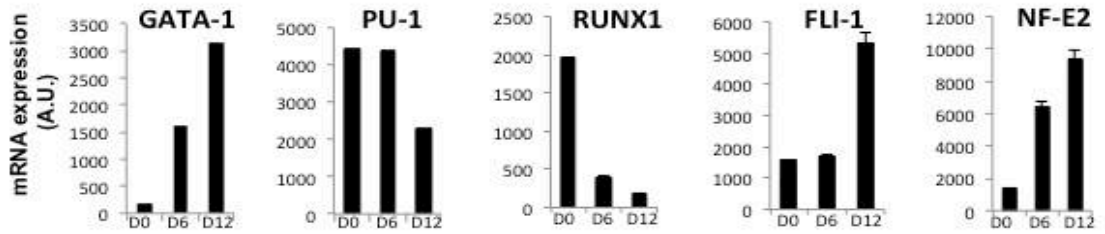

Figure 10. mRNA expression of the indicated transcription factors during human MK differentiation of CD34$^+$ cells (day 0, day 6 and day 12) relative to *GAPDH*, following treatment with the control vector LV_miR_dsRed. 1 A.U. represents 1 copy for 10^5 copies of housekeeping gene.

RUNX1 is a transcription factor, already found in pluripotent stem cells, where it is required for production, survival and self-renewal of HSCs.[26] Conditional knock-out studies also show a fundamental role for RUNX1 in megakaryopoiesis with marked decrease of polyploidization and cytoplasmic development of MKs, similarly to what is observed for GATA-1.[27] Since detailed studies via gene profiling, investigating the interrelation between polyploidization and megakaryocyte differentiation concluded that there were no marked changes during ploidization in the level of transcription factors involved in the regulation of MK-specific genes (GATA-1, FOG-1, FLI-1, SCL/TAL1 and AML1) or platelet production (NF-E2),[29] we considered this finding to be an artefact. Treatment with LV_miR_PEAR1_1461,

however, tampered the drop, in parallel analyses. Therefore, our findings seem to reflect the loss of RUNX1 in the early phases of stem cell maturation into multipotent progenitors and committed precursors, processes more pronounced in control cultures than in LV_miR_PEAR1 treated cultures with enhanced proliferation of non-committed precursors. The finding by Nagai et al. that siRNA-mediated depletion of RUNX1 in megakaryocyte-induced UT-7/GM cells resulted in up-regulation of the expression of megakaryocytic markers and polyploidization, while cell proliferation was down-regulated[30] is in agreement with the RUNX1 downregulation, which we observed during differentiation of $CD34^+$ cells, essentially to the level of 4N and 8N fractions. These authors further showed that overexpression of RUNX1 decreased the activity of megakaryocytic gene promoters in TPO-treated UT-7/GM cells. Despite the existence of a regulatory loop connecting RUNX1, GATA-1 and P-TEFb,[31] their conclusion that RUNX1 up-regulates cell-proliferation and down-regulates terminal differentiation in these cells, matches our present data.

DISCUSSION

This study reports that PEAR1 is progressively upregulated during human megakaryopoiesis and that it is a negative regulator of MK progenitor cell proliferation, but not of MK maturation. These observations were confirmed in zebrafish, where knockdown of PEAR1 enhances thrombopoiesis but not erythropoiesis. The expression of various genes, implicated in the PI3K/Akt and Notch pathways, as well as in gene transcription was mildly to moderately modified in the PEAR1 knockdowns. PTEN, a phosphatase that regulates the degree of Akt phosphorylation during megakaryopoiesis, was also downregulated. Hence, PEAR1 elimination causes chronically elevated Akt-P levels, thus enhancing MK progenitor cell proliferation.

The differentiation of cultured $CD34^+$ cells is accompanied by PEAR1 upregulation till day 12, coinciding with the expression of CD41 and GATA-1. The parallelism in the expression profiles of *PEAR1* and *GATA1* is in line with the presence of GATA-1 binding sites in the 5'-upstream sequence of the *PEAR1* promoter, identified via the TFMATRIX transcription factor binding site profile database (http://www.cbrc.jp/research/db/TFSEARCH.html) and as reported by Farnham et al.[32] Whereas progressive upregulation of NF-E2 is not surprising for a transcription factor implicated in the late stages of MK maturation and pro-platelet formation,[33] the drop in RUNX1 expression was unexpected. RUNX1 regulates constituents of the MK and platelet cytoskeleton during late megakaryopoiesis and platelet formation,[33] and shows a functional cooperation with GATA-1.[31] The earlier demonstration that depletion of RUNX1 in UT-7/GM cells caused upregulation of megakaryocyte markers and also polyploidization, accompanied by reduced cell proliferation,[30] is in line with the present findings. Correspondingly, the mildly weaker drop of RUNX1 in *shPEAR1* treated $CD34^+$ cells may reflect the higher proliferation of MK progenitors, the first few days of culture.

Overexpression of Pear1 in mouse bone marrow cells reduces myeloid progenitor proliferation. Moreover, the ectopic expression of Pear1 in NIH 3T3 fibroblasts reduced both early and late myeloid progenitors in non-adherent co-cultured bone marrow cells.[3] It is not clear whether this loss is caused by apoptosis or artificial signalling, coupled to excessive

PEAR1 phosphorylation.[1] We, therefore, investigated the role of PEAR1 in megakaryopoiesis by reducing its expression in 2 distinct models, based on expression depletion. In human $CD34^+$ cells, PEAR1 was reduced employing lentiviral vectors encoding different miRNA-based short hairpins (LV_miR_PEAR1_1461 and LV_miR_PEAR1_2938); in zebrafish embryos it was counteracted via injection of two types of morpholino. Both approaches demonstrated that PEAR1 negatively regulates the early steps of megakaryopoiesis, respectively thrombopoiesis.

Several approaches, distinguishing MK progenitor proliferation and MK maturation all pointed towards a role for PEAR1 in proliferation primarily. This is illustrated by the gradual expression of CD41 in megakaryoblasts and by the similar distribution of CD41 over smaller and larger differentiating MK precursors, after control or shPEAR1 treatment. Zebrafish CD41 positivity has been demonstrated as early as 42 hpf and it appears at 48 hpf in circulating hematopoietic cells. Since CD41-GFP zebrafish allow the identification of mature thrombocytes with high GFP positivity[24] *vs.* their precursors[34], this model was suited to study Pear1 neutralization in thrombopoiesis. This model also illustrated that the rapid stimulation of thrombopoiesis was without effect on erythropoiesis. Whereas we cannot exclude that the Pear1 knockdown affects other circulating cells (excluding red blood cells) in the zebrafish, in human blood, PEAR1 is exclusively expressed in circulating platelets. PEAR1 is also expressed in human myeloid precursors, the relevance of which remains to be elucidated.

Both in MK progenitors and zebrafish, a knockdown of PEAR1 affected the transcriptional regulation of several genes, including *PTEN*. PTEN is a tumour suppressor protein and mutations in *PTEN* have been observed in a variety of malignancies, including leukaemia. Correspondingly, the transient silencing of *PTEN* in human $CD34^+$ cells enhanced their proliferative potential and ability to engraft mice.[35] The present study shows that absence of PEAR1 also causes a partial silencing of *PTEN*, leading to a new steady state in proliferating $CD34^+$ cells, with elevated baseline levels of Akt-P, stimulating cell proliferation. Formally, this situation differs from the ligand-induced activation of PEAR1, triggering cellular signalling, which is transient and short, via reversible Akt phosphorylation.[1]

Pten$^{+/-}$ mice exhibit a predisposition to a variety of malignancies. In man, it remains to be investigated whether *PEAR1* mutations exist in oncogenic tissues where PEAR1 is expressed and whether a link exists with PTEN expression. However, several cases of breast, prostate, endometrial and liver cancers exhibited weak to moderate cytoplasmic immunoreactivity for PEAR1 (The human protein atlas at http://www.proteinatlas.org/ENSG00000187800/cancer).

The zebrafish genome encodes 2 Pten genes *Ptena* and *Ptenb*. Both have similar lipid phosphatase activity.[25] In the *Pear1* knockdown, we observed an association between elevated thrombocyte formation and downregulated *Ptena*, but not *Ptenb*. The MO-mediated knockdown of *Ptena*, but not *Ptenb*, resulted in upregulated thrombopoiesis, despite a similar increase in Akt phosphorylation in both of them. Neither PTENa nor PTENb morpholinos affected zebrafish viability, development and fertility, in agreement with similar findings in homozygous single mutant zebrafish lacking *Ptena* or *Ptenb.*[25] Hence, even when embryonic development is not affected by the PTENa MO, megakaryopoiesis and thrombocyte formation depend on Pear1, at least in part via the regulation of Ptena. Recent studies in MKs[22] and in thymocytes[23] have revealed that Hes1 is a negative regulator of Pten expression. We presently found evidence of *HES1* upregulation in the PEAR1 knockdown in CD34^{+} cells, but not in zebrafish. The regulation of PTEN expression is still unclear. Recent studies have shown that PTEN may both be positively and negatively regulated transcriptionally, as well as post-translationally by phosphorylation, oxidation and acetylation. Transcription factors known to be involved include peroxisome proliferator-activated receptor γ,[36] EGR1,[37] p53[37], etc. Several factors negatively regulate PTEN, including microRNAs,[38] 17β-estradiol,[39] MKK4,[40] JUN,[41] IGF-1,[42] and TGFβ.[43] Furthermore, the expression of PTEN appears to be dependent also on NF-κB,[39] linking MK differentiation and apoptosis.[44] Western blots confirmed that reduced mRA levels in CD34^{+} cells coincided with weaker PTEN protein bands.

Src family tyrosine kinases (SFKs) have been identified as negative regulators of thrombopoiesis. A reduced PEAR1 expression inevitably interferes with PEAR1-dependent SFK signalling. Hence, our present findings that the loss of PEAR1 increases thrombopoiesis comply with these observations that SFK inhibitors and mice deficient in Lyn enhance MK

proliferation, maturation, polyploidy and platelet release in cell culture.[45, 46] Therefore, PEAR1 may join other previously described negative regulators like SFKs, focal adhesion kinase, platelet factor 4, thrombospondin-1[47], and the pituitary adenylyl cyclase-activating peptide.[48]

In addition to the role of PEAR1 in platelet function[1], and in megakaryopoiesis and thrombocyte formation (this study), PEAR1 is abundantly present in the neuronal crest of zebrafish where it appears to be necessary for embryo development. Progressively increasing Pear1 MO concentrations caused a variety of central nervous system defects. Previously, Wu et al.[49] identified PEAR1 in glial precursor cells as an engulfment receptor, implicated in the phagocytosis of dead sensory neurons. The developmental problem in PEAR1 knockdowns is, therefore, compatible with this putative role for PEAR1 in the clearance of the sensory neuron corpse. Thus, a defective phagocytosis in Pear1 MO treated zebrafish embryos may very well be the cause of the developmental phenotypes observed, further illustrating the importance of neuronal crest PEAR1.

In conclusion, the present study shows that a reduced PEAR1 expression in MK progenitors lowers Akt dephosphorylation, secondarily to transcriptional downregulation of *PTEN*, an intervention promoting MK progenitor proliferation, indirectly enhancing megakaryopoiesis and thrombopoiesis.

REFERENCES

1. Kauskot A, Di Michele M, Loyen S, Freson K, Verhamme P, Hoylaerts MF. A novel mechanism of sustained platelet alphaIIbbeta3 activation via PEAR1. *Blood* 2012;**119**:4056-4065.
2. Nanda N, Bao M, Lin H, Clauser K, Komuves L, Quertermous T, Conley PB, Phillips DR, Hart MJ. Platelet endothelial aggregation receptor 1 (PEAR1), a novel epidermal growth factor repeat-containing transmembrane receptor, participates in platelet contact-induced activation. *J Biol Chem* 2005;**280**:24680-24689.
3. Krivtsov AV, Rozov FN, Zinovyeva MV, Hendrikx PJ, Jiang Y, Visser JW, Belyavsky AV. Jedi--a novel transmembrane protein expressed in early hematopoietic cells. *J Cell Biochem* 2007;**101**:767-784.
4. Drachman JG, Millett KM, Kaushansky K. Thrombopoietin signal transduction requires functional JAK2, not TYK2. *J Biol Chem* 1999;**274**:13480-13484.
5. Freson K, Devriendt K, Matthijs G, Van Hoof A, De Vos R, Thys C, Minner K, Hoylaerts MF, Vermylen J, Van Geet C. Platelet characteristics in patients with X-linked macrothrombocytopenia because of a novel GATA1 mutation. *Blood* 2001;**98**:85-92.
6. Hartwig JH, Italiano JE, Jr. Cytoskeletal mechanisms for platelet production. *Blood Cells Mol Dis* 2006;**36**:99-103.
7. Richardson JL, Shivdasani RA, Boers C, Hartwig JH, Italiano JE, Jr. Mechanisms of organelle transport and capture along proplatelets during platelet production. *Blood* 2005;**106**:4066-4075.
8. Buitenhuis M, Verhagen LP, van Deutekom HW, Castor A, Verploegen S, Koenderman L, Jacobsen SE, Coffer PJ. Protein kinase B (c-akt) regulates hematopoietic lineage choice decisions during myelopoiesis. *Blood* 2008;**111**:112-121.
9. Polak R, Buitenhuis M. The PI3K/PKB signaling module as key regulator of hematopoiesis: implications for therapeutic strategies in leukemia. *Blood* 2012;**119**:911-923.
10. Salmena L, Carracedo A, Pandolfi PP. Tenets of PTEN tumor suppression. *Cell* 2008;**133**:403-414.
11. Weng Z, Li D, Zhang L, Chen J, Ruan C, Chen G, Gartner TK, Liu J. PTEN regulates collagen-induced platelet activation. *Blood* 2010;**116**:2579-2581.
12. Schrijvers R, De Rijck J, Demeulemeester J, Adachi N, Vets S, Ronen K, Christ F, Bushman FD, Debyser Z, Gijsbers R. LEDGF/p75-independent HIV-1 replication demonstrates a role for HRP-2 and remains sensitive to inhibition by LEDGINs. *PLoS Pathog* 2012;**8**:e1002558.
13. Ibrahimi A, Vande Velde G, Reumers V, Toelen J, Thiry I, Vandeputte C, Vets S, Deroose C, Bormans G, Baekelandt V, Debyser Z, Gijsbers R. Highly efficient multicistronic lentiviral vectors with peptide 2A sequences. *Hum Gene Ther* 2009;**20**:845-860.
14. Livak KJ, Schmittgen TD. Analysis of relative gene expression data using real-time quantitative PCR and the 2(-Delta Delta C(T)) Method. *Methods* 2001;**25**:402-408.
15. Rinalducci S, Ferru E, Blasi B, Turrini F, Zolla L. Oxidative stress and caspase-mediated fragmentation of cytoplasmic domain of erythrocyte band 3 during blood storage. *Blood Transfus*;**10 Suppl 2**:s55-62.
16. Thisse C, Thisse B. High-resolution in situ hybridization to whole-mount zebrafish embryos. *Nat Protoc* 2008;**3**:59-69.
17. Cvejic A, Serbanovic-Canic J, Stemple DL, Ouwehand WH. The role of meis1 in primitive and definitive hematopoiesis during zebrafish development. *Haematologica*;**96**:190-198.
18. Detrich HW, 3rd, Kieran MW, Chan FY, Barone LM, Yee K, Rundstadler JA, Pratt S, Ransom D, Zon LI. Intraembryonic hematopoietic cell migration during vertebrate development. *Proc Natl Acad Sci U S A* 1995;**92**:10713-10717.
19. Lepage A, Leboeuf M, Cazenave JP, de la Salle C, Lanza F, Uzan G. The alpha(IIb)beta(3) integrin and GPIb-V-IX complex identify distinct stages in the maturation of CD34(+) cord blood cells to megakaryocytes. *Blood* 2000;**96**:4169-4177.
20. Yamaguchi Y, Zon LI, Ackerman SJ, Yamamoto M, Suda T. Forced GATA-1 expression in the murine myeloid cell line M1: induction of c-Mpl expression and megakaryocytic/erythroid differentiation. *Blood* 1998;**91**:450-457.
21. Zhang C, Gadue P, Scott E, Atchison M, Poncz M. Activation of the megakaryocyte-specific gene platelet basic protein (PBP) by the Ets family factor PU.1. *J Biol Chem* 1997;**272**:26236-26246.

22. Cornejo MG, Mabialah V, Sykes SM, Khandan T, Lo Celso C, Lopez CK, Rivera-Munoz P, Rameau P, Tothova Z, Aster JC, DePinho RA, Scadden DT, Gilliland DG, Mercher T. Crosstalk between NOTCH and AKT signaling during murine megakaryocyte lineage specification. *Blood* 2011;**118**:1264-1273.
23. Wong GW, Knowles GC, Mak TW, Ferrando AA, Zuniga-Pflucker JC. HES1 opposes a PTEN-dependent check on survival, differentiation and proliferation of TCRbeta-selected mouse thymocytes. *Blood* 2012.
24. Lin HF, Traver D, Zhu H, Dooley K, Paw BH, Zon LI, Handin RI. Analysis of thrombocyte development in CD41-GFP transgenic zebrafish. *Blood* 2005;**106**:3803-3810.
25. Faucherre A, Taylor GS, Overvoorde J, Dixon JE, Hertog J. Zebrafish pten genes have overlapping and non-redundant functions in tumorigenesis and embryonic development. *Oncogene* 2008;**27**:1079-1086.
26. Orkin SH, Zon LI. Hematopoiesis: an evolving paradigm for stem cell biology. *Cell* 2008;**132**:631-644.
27. Tijssen MR, Ghevaert C. Transcription factors in late megakaryopoiesis and related platelet disorders. *J Thromb Haemost* 2013.
28. Muntean AG, Pang L, Poncz M, Dowdy SF, Blobel GA, Crispino JD. Cyclin D-Cdk4 is regulated by GATA-1 and required for megakaryocyte growth and polyploidization. *Blood* 2007;**109**:5199-5207.
29. Raslova H, Kauffmann A, Sekkai D, Ripoche H, Larbret F, Robert T, Le Roux DT, Kroemer G, Debili N, Dessen P, Lazar V, Vainchenker W. Interrelation between polyploidization and megakaryocyte differentiation: a gene profiling approach. *Blood* 2007;**109**:3225-3234.
30. Nagai R, Matsuura E, Hoshika Y, Nakata E, Nagura H, Watanabe A, Komatsu N, Okada Y, Doi T. RUNX1 suppression induces megakaryocytic differentiation of UT-7/GM cells. *Biochem Biophys Res Commun* 2006;**345**:78-84.
31. Goldfarb AN. Megakaryocytic programming by a transcriptional regulatory loop: A circle connecting RUNX1, GATA-1, and P-TEFb. *J Cell Biochem* 2009;**107**:377-382.
32. Farnham PJ. Insights from genomic profiling of transcription factors. *Nat Rev Genet* 2009;**10**:605-616.
33. Tijssen MR, Ghevaert C. Transcription factors in late megakaryopoiesis and related platelet disorders. *J Thromb Haemost*.
34. Ma D, Zhang J, Lin HF, Italiano J, Handin RI. The identification and characterization of zebrafish hematopoietic stem cells. *Blood* 2011;**118**:289-297.
35. Kim I, Kim YJ, Metais JY, Dunbar CE, Larochelle A. Transient silencing of PTEN in human CD34(+) cells enhances their proliferative potential and ability to engraft immunodeficient mice. *Exp Hematol* 2012;**40**:84-91.
36. Farrow B, Evers BM. Activation of PPARgamma increases PTEN expression in pancreatic cancer cells. *Biochem Biophys Res Commun* 2003;**301**:50-53.
37. Wang J, Ouyang W, Li J, Wei L, Ma Q, Zhang Z, Tong Q, He J, Huang C. Loss of tumor suppressor p53 decreases PTEN expression and enhances signaling pathways leading to activation of activator protein 1 and nuclear factor kappaB induced by UV radiation. *Cancer Res* 2005;**65**:6601-6611.
38. Liu L, Jiang Y, Zhang H, Greenlee AR, Han Z. Overexpressed miR-494 down-regulates PTEN gene expression in cells transformed by anti-benzo(a)pyrene-trans-7,8-dihydrodiol-9,10-epoxide. *Life Sci* 2010;**86**:192-198.
39. Zhang H, Zhao X, Liu S, Li J, Wen Z, Li M. 17betaE2 promotes cell proliferation in endometriosis by decreasing PTEN via NFkappaB-dependent pathway. *Mol Cell Endocrinol* 2010;**317**:31-43.
40. Xia D, Srinivas H, Ahn YH, Sethi G, Sheng X, Yung WK, Xia Q, Chiao PJ, Kim H, Brown PH, Wistuba, II, Aggarwal BB, Kurie JM. Mitogen-activated protein kinase kinase-4 promotes cell survival by decreasing PTEN expression through an NF kappa B-dependent pathway. *J Biol Chem* 2007;**282**:3507-3519.
41. Hettinger K, Vikhanskaya F, Poh MK, Lee MK, de Belle I, Zhang JT, Reddy SA, Sabapathy K. c-Jun promotes cellular survival by suppression of PTEN. *Cell Death Differ* 2007;**14**:218-229.
42. Ma J, Sawai H, Matsuo Y, Ochi N, Yasuda A, Takahashi H, Wakasugi T, Funahashi H, Sato M, Takeyama H. IGF-1 mediates PTEN suppression and enhances cell invasion and proliferation via activation of the IGF-1/PI3K/Akt signaling pathway in pancreatic cancer cells. *J Surg Res* 2010;**160**:90-101.
43. Chow JY, Dong H, Quach KT, Van Nguyen PN, Chen K, Carethers JM. TGF-beta mediates PTEN suppression and cell motility through calcium-dependent PKC-alpha activation in pancreatic cancer cells. *Am J Physiol Gastrointest Liver Physiol* 2008;**294**:G899-905.
44. Di Michele M, Peeters K, Loyen S, Thys C, Waelkens E, Overbergh L, Hoylaerts M, Van Geet C, Freson K. Pituitary Adenylate Cyclase-Activating Polypeptide (PACAP) impairs the regulation of apoptosis in megakaryocytes by activating NF-kappaB: a proteomic study. *Mol Cell Proteomics* 2012;**11**:M111 007625.

45. Lannutti BJ, Drachman JG. Lyn tyrosine kinase regulates thrombopoietin-induced proliferation of hematopoietic cell lines and primary megakaryocytic progenitors. *Blood* 2004;**103**:3736-3743.
46. Lannutti BJ, Minear J, Blake N, Drachman JG. Increased megakaryocytopoiesis in Lyn-deficient mice. *Oncogene* 2006;**25**:3316-3324.
47. Yu M, Cantor AB. Megakaryopoiesis and thrombopoiesis: an update on cytokines and lineage surface markers. *Methods Mol Biol* 2012;**788**:291-303.
48. Peeters K, Loyen S, Van Kerckhoven S, Stoffels K, Hoylaerts MF, Van Geet C, Freson K. Thrombopoietic effect of VPAC1 inhibition during megakaryopoiesis. *Br J Haematol* 2010;**151**:54-61.
49. Wu HH, Bellmunt E, Scheib JL, Venegas V, Burkert C, Reichardt LF, Zhou Z, Farinas I, Carter BD. Glial precursors clear sensory neuron corpses during development via Jedi-1, an engulfment receptor. *Nat Neurosci* 2009;**12**:1534-1541.

Chapter II – Illustration from "Secunda musculorum Tabula – de humanum corporis fabrica libri septem" – A. Vesalius, 1543

ABSTRACT

Genome-wide association studies to identify loci responsible for platelet function and cardiovascular disease susceptibility have repeatedly identified polymorphisms linked to a gene encoding Platelet endothelium aggregation receptor 1 (PEAR1), an "orphan" cell surface receptor that is activated to stabilize platelet aggregates. To investigate how PEAR1 signalling is initiated, we sought to identify its extracellular ligand by creating a protein microarray representing the secretome and receptor repertoire of the human platelet. Using an avid soluble recombinant PEAR1 protein and a systematic screening assay designed to detect extracellular interactions, we identified the high-affinity immunoglobulin E (IgE)-binding subunit FcεR1α, as a PEAR1 ligand. FcεR1α and PEAR1 directly interacted through their membrane-proximal Ig-like and 13th EGF domains with a relatively strong affinity (K_D ~ 30nM). Pre-complexing FcεR1α with IgE potently inhibited the FcεR1α-PEAR1 interaction and this was relieved by the anti-IgE therapeutic, omalizumab. Oligomerised FcεR1α potentiated platelet aggregation and led to PEAR1 phosphorylation, an effect that was also inhibited by IgE. These findings demonstrate how a protein microarray resource can be used to gain important insight into the function of platelet receptors, and provide a mechanistic basis for the initiation of PEAR1 signalling in platelet aggregation.

INTRODUCTION

Platelets play a vital role in preserving blood circulation in response to vessel injury by detecting lesions, aggregating to form a haemostatic plug, and nucleating the formation of a fibrin-rich, injury-occluding clot. While necessary to prevent blood loss at sites of tissue trauma, clot formation must also be attenuated to prevent blockage of the vasculature serving vital organs that would cause life-threatening ischemia and infarction. Inappropriate platelet aggregation and vessel occlusion - often triggered by atherosclerotic plaque rupture - is a major pathological process that is a major contributor to cardiovascular disease which is the leading cause of mortality worldwide.[1] With the eventual aim of guiding the development of new treatments and diagnostic assays, genome-wide association studies using large patient cohorts have identified several genetic loci that are associated with cardiovascular disease susceptibility and platelet function.[2, 3] Amongst the candidate genes identified, polymorphisms linked to *PEAR1* have been repeatedly linked to natural variation in response to platelet agonists in several independent studies.[3-7] *PEAR1* encodes platelet endothelium activation receptor 1 (PEAR1, also known as Multiple epidermal growth factor-like domains protein 12 (MEGF12) or JEDI-1), a platelet cell surface receptor that was originally identified as a protein phosphorylated in response to platelet aggregation.[8, 9] PEAR1 is expressed at low levels on the surface of circulating platelets but is significantly upregulated during platelet activation when released from cytoplasmic α-granules.[8] Consistent with polymorphisms linked to *PEAR1* being associated with cardiovascular disease and platelet function, PEAR1-mediated signalling was shown to reinforce and stabilize the interactions between platelets within a forming aggregate.[8] PEAR1 is an orphan receptor and an important unanswered question in understanding the mechanism of PEAR1 function during platelet aggregation, therefore, is the identification of its activating ligand.

Identifying interactions between membrane-embedded receptor proteins is technically challenging and many commonly-used approaches such as biochemical purifications are generally not suitable to detect them. This is largely due to the amphipathic nature of membrane-embedded proteins, making them difficult to solubilize in detergents that retain their native conformation, and the fact that their extracellular interactions are often highly transient, having half-lives of just fractions of a second.[10] To address these issues, we and others have developed assays based on detecting direct protein interactions between the

entire ectodomains of cell surface receptors expressed as soluble recombinant proteins in eukaryotic cells. [11-14] Using this approach, binding avidity can be increased by the purposeful inclusion of oligomerising tags to overcome the fleeting nature of these interactions. In our assay, termed AVEXIS (for AVidity-based EXtracellular Interaction Screen), arrays of monomeric biotinylated "bait" proteins are screened against multimerised, enzyme-tagged, highly avid "preys" [11, 15]; a schematic of the assay is shown in Fig. 1. The likelihood that the extracellular binding functions of receptors are preserved is increased by expressing whole ectodomains in mammalian cells so that structurally critical posttranslational modifications such as disulfide bonds are faithfully added. Consequently, this method has identified interactions that have subsequently been demonstrated to be essential for cellular recognition processes *in vivo.* [16-18]

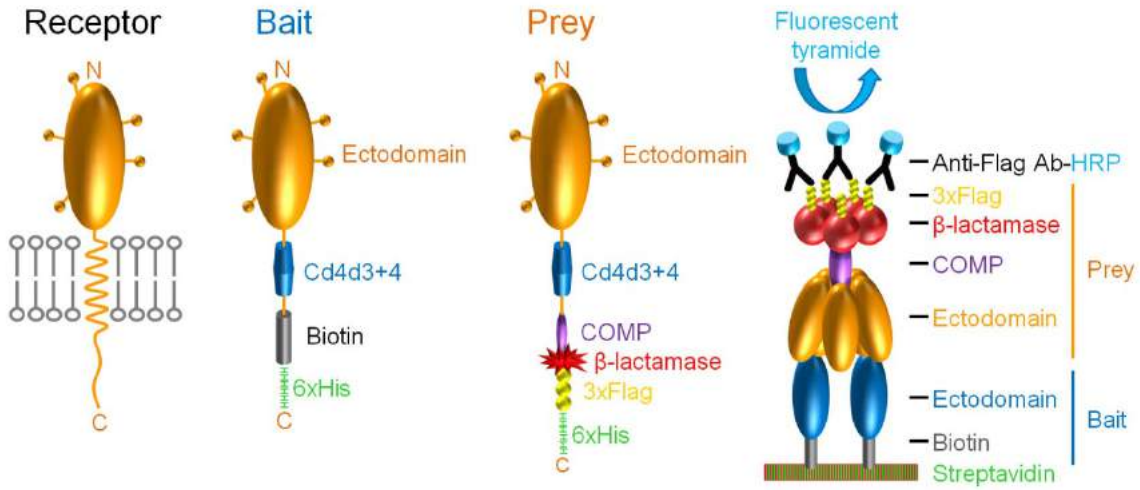

Figure 1: Schematics showing design of bait and prey constructs and the AVEXIS interaction assay. A typical type I cell surface receptor is shown embedded within a membrane with the entire ectodomain shown as an orange oval, and filled lollipops representing potential N-linked glycosylation sites. The design of both monomeric biotinylated "bait" and pentameric β-lactamase-tagged "prey" containing the entire ectodomain of the receptor are shown (prey is shown as a monomer for clarity); both contain the rat Cd4 domain 3 and 4 (Cd4d3+4) and 6 His tags. The AVEXIS assay is shown with a biotinylated bait captured on streptavidin-coated slide interacting with a pentameric FLAG-tagged prey and interactions detected with an anti-FLAG HRP-conjugated secondary antibody and fluorescent tyramide HRP-substrate deposition.

In this study, we have compiled a protein resource representing the cell surface receptor repertoire and secretome of the human platelet that will be useful to identify intercellular interactions important for platelet biology. As an example, we identify the activating ligand

for PEAR1 as the high affinity IgE receptor subunit, FcεR1α and show that multimerised FcεR1α potentiated platelet aggregation and led to PEAR1 phosphorylation, an effect that was specifically inhibited by IgE.

MATERIALS AND METHODS

Human platelet protein selection and expression plasmid construction

After compiling a list of platelet receptor proteins and classifying them into structural categories, the extent of each ectodomain was identified by careful manual examination of its structural features such as signal peptides, transmembrane regions and GPI anchors; for secreted proteins, the entire protein was used. The ectodomain regions were codon-optimized for human expression and chemically synthesized with unique flanking NotI (5') and AscI (3') restriction sites (GeneArt AG) and subcloned into bait expression plasmids according to its structural class. While we have previously expressed typeI/GPI-anchored and secreted proteins for interaction screening,[11] we designed new expression vectors to express the ectodomains of type II and multi-span transmembrane proteins, in a way that would most appropriately preserve their structure when presented at the cell surface *in vivo*. Similarly, for multimeric protein complexes such as integrins, Glycoprotein1bαβ, and fibrinogen, care was taken to design the constructs that would promote correct and active complex formation. The truncated fragments of PEAR1 and FcεR1α were designed based on their domain structures, amplified by PCR from the full length constructs and cloned into an expression vector containing an exogenous signal peptide and C-terminal 6-His and biotinylatable peptide sequence. The 218- and 325- amino-acid fragments encoding the Cε3-4 and Cε2-4 domains of the IgE constant heavy chain were amplified from plasmid pFUSE-CHIg-hE (Invivogen) and cloned into a vector containing an exogenous signal peptide and C-terminal 6-His tag. IgE fragments were expressed and purified as described below. All plasmid constructs are openly available from Addgene.

Recombinant protein expression

All proteins were produced by transient transfection using HEK293E cells as described[11] to ensure posttranslational modifications such as disulfide bonds and glycans were added. Proteins were purified using their 6His tag using a bespoke supernatant loading rig and 96-well Ni^{2+}-NTA filter plates.[15] Heat-labile immunoreactivity to demonstrate folding was confirmed by heat denaturing the proteins for 10 minutes at 90°C before capture on a streptavidin-coated plate via their biotin tag and determination of immunoreactivity by ELISA as described. [19]

Construction of the human platelet receptor protein microarray

Normalized bait proteins were diluted in phosphate-buffered saline (PBS) supplemented with 50% glycerol, 0.02% Tween and 0.5% bovine serum albumin (BSA) prior to printing. Bait proteins were printed on streptavidin-coated slides that also contained an inert hydrogel coating (XanTec) using a Marathon arrayer

(Arrayjet) at 60% relative humidity according to the manufacturer's instructions. Printed slides were incubated for 1 hour at 60% relative humidity and blocked with PBS containing 1% BSA and 10 mM D-biotin for 45 min. Slides were then incubated with normalized prey proteins for 1 hour, before being incubated with an anti-FLAG HRP antibody (Sigma, 1:1000) for 1 hour and finally detected by TSA Alexa 555 substrate (Invitrogen) for 1 hour. Between different incubation steps, slides were washed three times in PBS buffer containing 0.1% Tween with gentle rocking. Arraying, incubations and washing steps were performed at 22°C. Positive interactions were identified and quantified by scanning slides with a ScanArray Express Microarray Scanner (PerkinElmer) at 550 nm.

AVEXIS interaction screening

To determine the effect of IgE/omalizumab and map the interacting domains of the FcεR1α-PEAR1 interaction, we used the AVEXIS method formatted on streptavidin-coated 96-well microtitre plates as described. [11, 17] Briefly, bait and prey proteins were first normalized to activities suitable for the AVEXIS assay. [20] Biotinylated baits that had been either purified or dialysed against HBS were immobilised in streptavidin-coated 96-well microtitre plates (NUNC). Preys were incubated for two hours, washed three times with PBS/0.1 % Tween-20, once in PBS and 125 µg/mL of nitrocefin added, and absorbance values measured at 485 nm on a Pherastar plus (BMG laboratories). A protein consisting of the Cd4d3+4 tag alone was used as a negative control bait and a biotinylated anti-Cd4 monoclonal antibody (anti-prey) used as a positive control as required.

Surface plasmon resonance (SPR) studies

All SPR studies were performed on a Biacore T100 instrument essentially as described.[17] Purified analyte proteins were resolved by gel filtration just prior to use in SPR experiments. Increasing concentrations of proteins were injected at 10 µl/min for equilibrium analysis or high flow rates (100 µl/min) for kinetic studies to minimise the confounding effects of analyte rebinding. Both kinetic and equilibrium binding data were analysed in the manufacturer's Biacore T100 evaluation software (Biacore).

Platelet aggregometry assays

Venous blood was collected from normal donors following guidelines from ethical committee of the Leuven University Hospital number B322201111373/S53239. Platelet-rich plasma (PRP) was prepared and platelet aggregation monitored as described.[8] Platelets ($4x10^5$ per µL) were preincubated with either soluble recombinant purified pentameric proteins extensively dialyzed into PBS: PEAR1 (s5-PEAR1), FcεR1α (s5-FcεR1α), and control rat Cd200 all used at 10 µg/mL; or commercially available antibodies: human IgE (10 µg/mL (53 nM); Abcam, UK), anti-PEAR1 (3 µg/mL; R&D systems), and omalizumab (10 µg/mL (67 nM), Xolair ®, Novartis, Belgium) at 37°C, as appropriate. The IgE fragments were used at an equimolar concentration of 67 nM. Platelet aggregation was triggered by collagen with the concentration adjusted to reach 40 to 70% platelet aggregation for each donor and measured as the percentage of change in light transmission relative to a blank (buffer without platelets) set to 100%.

Western blotting

Western blotting was performed essentially as described[8] using the primary antibodies: PEAR1-EC Ab (R&D Systems), PEAR1-EC Ab (Santa Cruz), FcεR1α Ab (LifeSpan Biosciences), anti-PLCγ2 (Sigma), anti-PLCγ2-P (Cell Signaling), anti–Akt-P (Cell Signaling), anti-phosphoprotein (P-Tyr) 4G10 platinum (Millipore). After adding HRP–conjugated secondary antibodies (Dako), immunoreactive bands were visualized by ECL (Amersham Biosciences). PEAR1 phosphorylation on Tyr residues, referred to as PEAR1-P, was evaluated after immunoprecipitation with PEAR1-EC Ab and detection of P-Tyr by 4G10 platinum as previously described. [8]

Platelet immunocytochemistry

Platelets were stained essentially as described[8] using the primary antibodies: anti-human IgE, 5 µg/ml, BD Pharmingen; anti-human FcεRI, 5 µg/ml, eBioscience; anti-human PEAR1, 2 µg/ml, R&D systems, washed and detected using an appropriate Alexa-488-conjugated secondary antibody (1/200; Invitrogen) for 60 minutes at 37°C. Coverslips were mounted with DAPI prolong gold (Invitrogen, Ghent, Belgium), sealed on glass slides and analyzed on a Zeiss ELYRA Superresolution Microscope and Zen 2011 Image software (Carl Zeiss).

RESULTS

A protein resource representing the secretome and receptor repertoire of the human platelet.

To identify an activating ligand for PEAR1, we first created a protein library that represented the cell surface receptor repertoire and secretome of the human platelet expressed as secreted recombinant proteins. We and others have previously only expressed typeI/GPI-anchored and secreted proteins for large scale extracellular interaction screening [11-14], but because platelets also express cell surface proteins from other structural classes, we designed new expression plasmids. We constructed these new expression plasmids with the goal of preserving the structure of the receptor when displayed at the platelet surface (Fig. 2A). In the case of multimeric protein complexes such as integrins, Glycoprotein1bαβ, and fibrinogen, care was taken to design the constructs such that they would promote correct and active complex formation; for example, secretion of integrin α chains can be dependent on the presence of the β chain,[21] and so tags were only added to the α-chain, ensuring the expression of a tagged α/β complex in an active conformation (Fig. 2A). [22] We next compiled a list of secreted and membrane proteins expressed by human platelets from 18 proteomic datasets and the literature (not shown; see online supplement). To increase the chances of identifying functionally relevant interactions, each protein was classified into one of six

structural categories. The entire extent of the ectodomain region was then determined, and an expression construct manually designed by pairing it with an appropriate expression vector. The final library contained 173 proteins and complexes (76 type I, 7 GPI-anchored, 14 type II, 57 secreted, 7 heterodimeric complexes, and 12 multi-span transmembrane proteins) represented by a total of 178 plasmids (not shown, see online supplement). The proteins were expressed and purified as monomeric biotinylated "baits" in mammalian cells so that structurally-important posttranslational modifications such as disulfide bonds and glycans were added. Similar to other secreted recombinant protein libraries that we [11, 17, 23, 24] and others [13, 25, 26] have made, expression levels varied widely, but averaged ~3 µg/mL (not shown, see online supplement). After purification, 126 proteins were expressed at sufficient levels for our interaction screens. As expected, Western blots of the protein library showed that the vast majority (113/121 – 93%) of proteins exhibited mass heterogeneity centered on their expected size suggesting the presence of different glycoforms (Fig. 2B). The recombinant proteins were antigenically active as assessed by demonstrating heat labile immunoreactivity to a panel of monoclonal antibodies (mAbs) recognizing at least one protein from each structural category (Fig. 3A). The library of biotinylated bait proteins was serially diluted, and arrayed on streptavidin-coated glass slides (Figure not shown). Proteins immobilized on the slides retained their immunoreactivity to mAbs known to stain native proteins at the cell surface (Fig. 3B). These plasmids and recombinant protein library represent a valuable resource for the investigation of human platelet biology, particularly in regard to the role of these proteins in thrombosis.

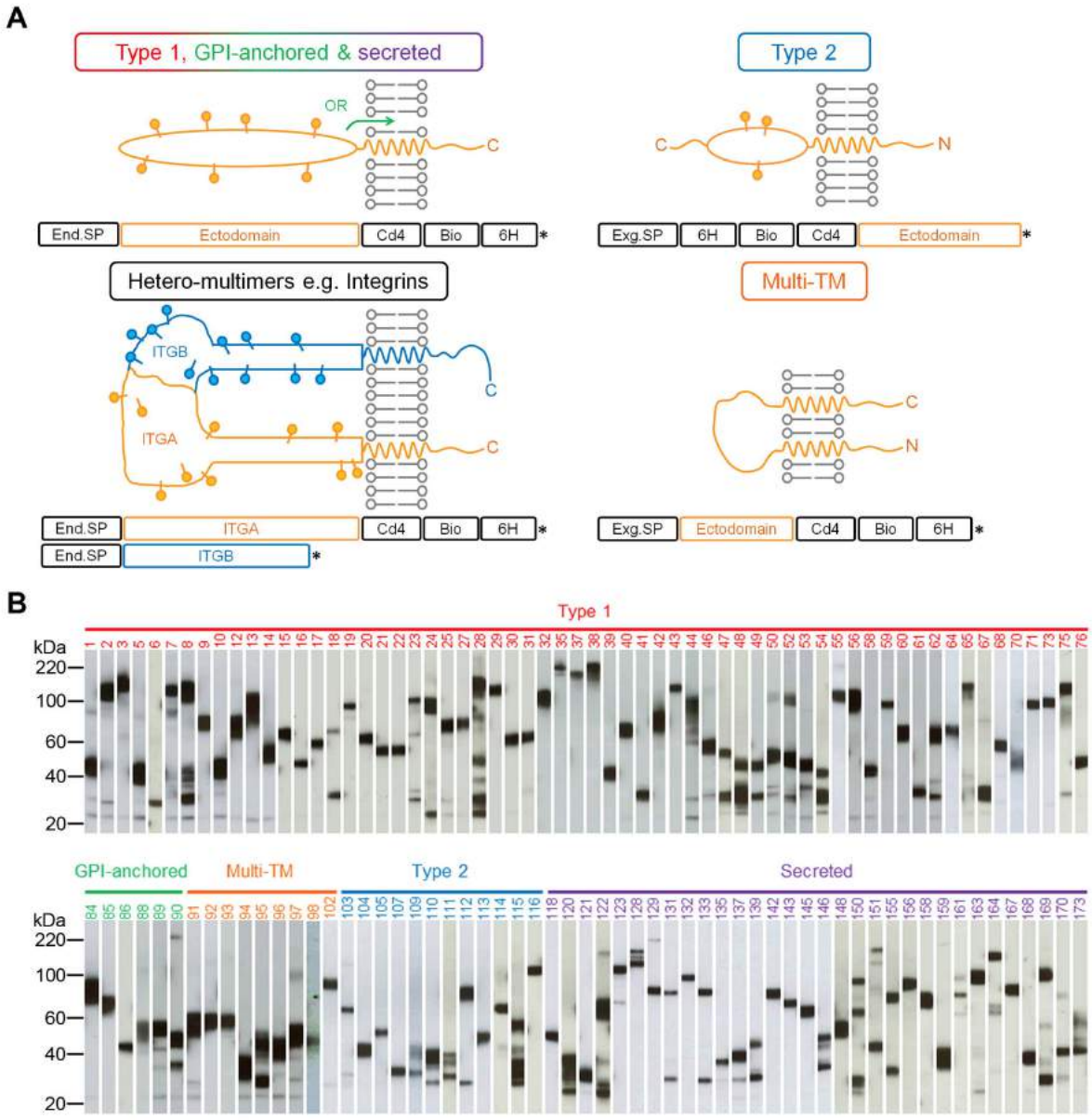

Figure 2: Design and expression of a human platelet receptor library for common structural classes of cell surface and secreted proteins for AVEXIS. A) Cartoons schematically show the design of ectodomain expression constructs. Type II and multispan proteins contained an exogenous signal peptide (Exg.SP) while the others retain their endogenous signal peptide (End.SP). Heteromeric complexes, such as the integrins shown here, were tagged on only one chain to ensure expression of only tagged complexes. * = stop codon. B) An anti-biotin Western blot of the 121 bait proteins organized into their structural categories. The majority of proteins were expressed at the expected size with little processing. Numbering is according to Supplemental Table S2 (not shown, see online supplement) note that the five expressed heteromeric complexes are not included since only one chain would have been detected.

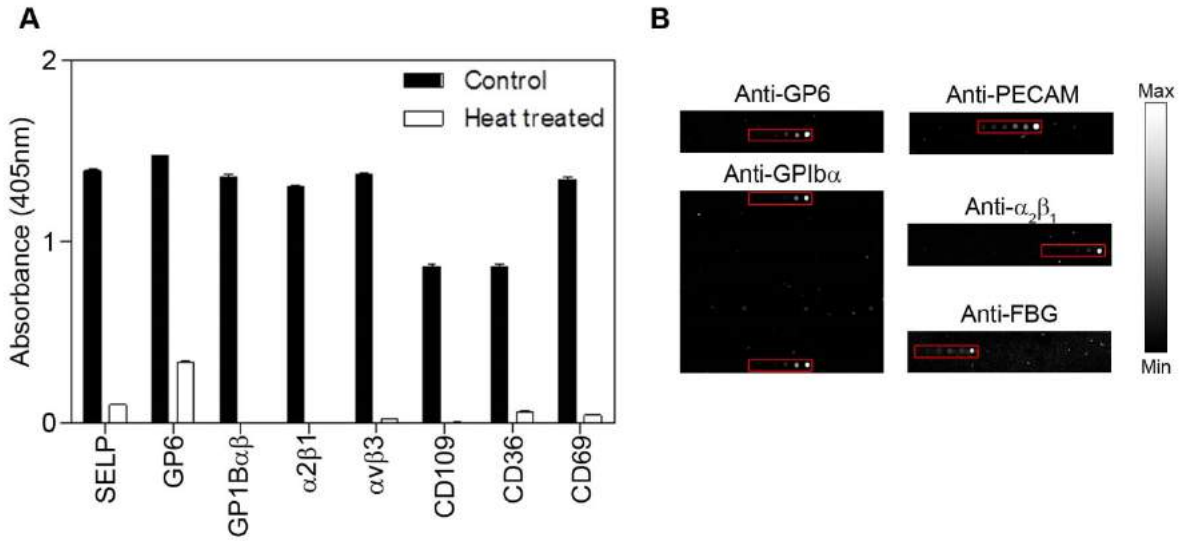

Figure 3: Proteins in the human platelet receptor library are antigenically active. A) The biochemical activity of selected recombinant proteins representing each structural class was confirmed by demonstrating heat-labile immunoreactivity of monoclonal antibodies which are known to stain the native protein on the platelet surface. The heat-treated and control proteins were probed with monoclonal antibodies (SELP: Thromb6; GP6: HY101; GP1Bαβ: PAB-5; α2β1: P1E6; αvβ3: BV3; CD109: B-E47; CD36: CB38; CD69: FN50) and detected by ELISA. Bars represent mean ± SEM; *n* ≥ 3. B) Immunoreactivity to mAbs recognizing the individual named platelet receptors that are known to bind native proteins on platelets is preserved when arrayed on streptavidin-coated glass slides; note that anti-GP1bα identifies both the GP1bα monomer (bait 75) and GP1bαβ complex (bait 77).

Systematic interaction screening of the platelet receptor microarray identified FcεR1α as a ligand for PEAR1

To identify an activating ligand for PEAR1 during platelet aggregation, we systematically screened the human platelet receptor microarray using the AVEXIS assay which required expressing the entire ectodomain of PEAR1 as a recombinant pentameric, FLAG-tagged soluble "prey". Probing the array with a control pentameric FLAG-tagged prey protein labelled the high affinity IgG receptor Fcγ2α (which directly bound the anti-FLAG antibody) and P4HB, a bait that presumably interacted with the tags on the control prey (Fig. 4A). Screening the receptor microarray with the PEAR1 prey identified the high affinity IgE-binding subunit, FcεR1α, as a PEAR1 ligand (Fig. 4B, Fig. 5). Since PEAR1 was presented as a bait on the microarray, and to rule out any possible artifacts, we expressed the entire ectodomain of FcεR1α as a prey protein and rescreened the array. As expected, we observed that the FcεR1α prey interacted with the PEAR1 bait, showing that we could detect the same interaction, but in the reciprocal bait:prey orientation (Fig. 4C).

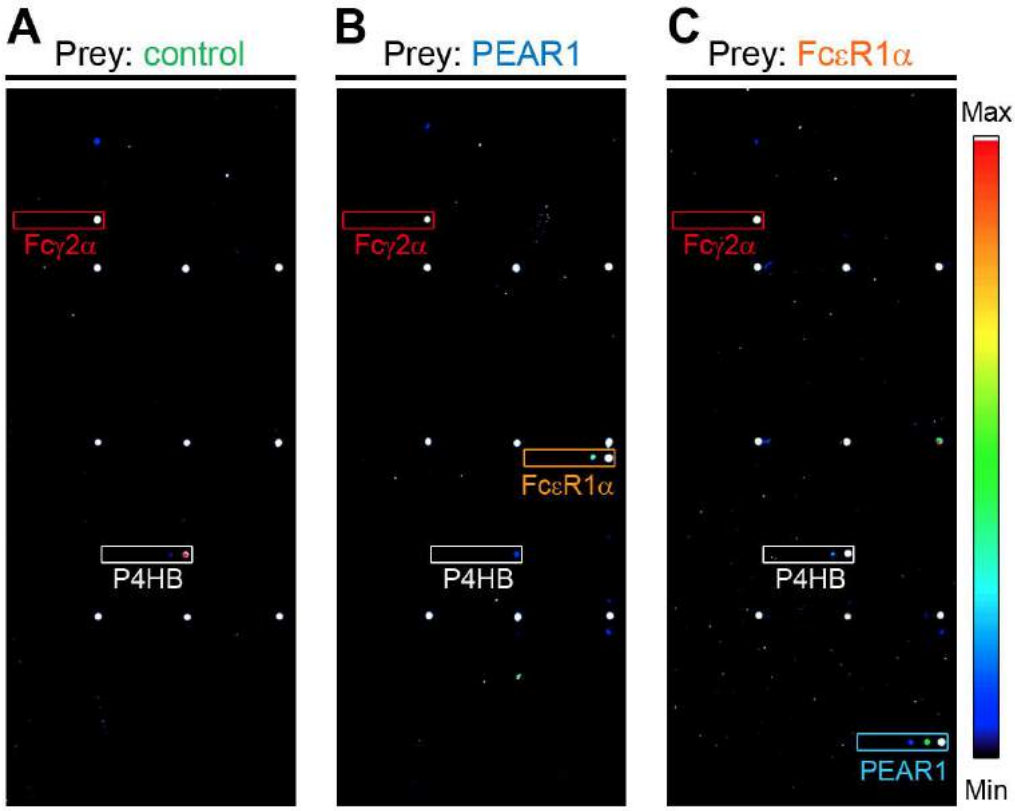

Figure 4: A human platelet secretome and receptor protein microarray identifies FcεR1α as a ligand for PEAR1. Soluble recombinant biotinylated proteins representing the secretome and receptor repertoire of the human platelet were purified and arrayed in six three-fold dilutions on streptavidin-coated slides. A) The array was screened with a control (rat Cd200) pentamerized FLAG-tagged prey which bound the background baits FcγR2α (red box) and P4HB (white box). B) PEAR1 prey additionally interacted with the FcεR1α bait (orange box) when compared to the control in A; fluorescence intensities are quantified in Figure 5. C) FcεR1α prey additionally interacted with the PEAR1 bait (blue box) in comparison to the control. Note that the nine regularly spaced markers are orientation markers and that the boxed areas marked on the array enclose the location of the six spots containing the dilutions of the named immobilized baits.

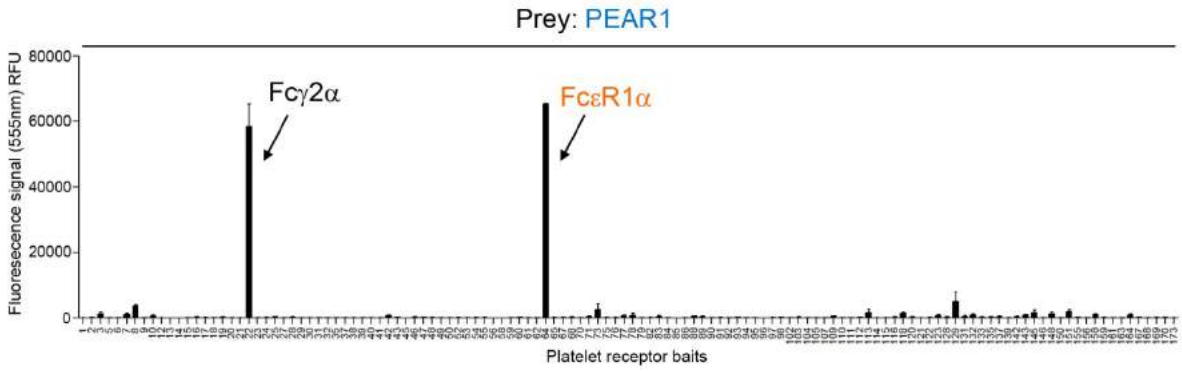

Figure 5: Systematic screening of a human platelet receptor protein microarray identified FcεR1α as a ligand for PEAR1: quantification of fluorescence signals. Quantification of the florescence at 555 nm associated with each bait on a human platelet receptor protein microarray probed with FLAG-tagged PEAR1 prey protein identifying FcεR1α (bait 64) as a ligand for PEAR1. The IgG receptor, Fcγ2α (bait 22) directly interacted with the HRP-conjugated secondary antibody; bars represent mean florescence signals ± SEM; *n* = 3.

PEAR1 and FcεR1α directly interact through their membrane-proximal domains.

To validate and quantify the interaction, we used surface plasmon resonance (SPR) and observed clear saturable binding between PEAR1 and FcεR1α with an equilibrium binding constant (K_D) of 27.4 ± 1.3 nM (Fig. 6A). The saturable binding behavior demonstrated the specificity of the interaction which had a remarkably high affinity when compared with similar receptor-ligand interactions, which are usually in the micromolar range when measured using the same approach.[10] An independent kinetic analysis confirmed this, and revealed that the higher affinity was largely due to a comparatively slow dissociation rate constant (Fig. 6B). By using the AVEXIS assay and a series of structure-guided truncations in both PEAR1 and FcεR1α, we showed that the minimal FcεR1α binding unit on PEAR1 was contained solely within the 45 amino acids comprising the 13th EGF domain (Fig. 7A, C). Similarly, the PEAR1 binding site was located within the membrane proximal Ig-like domain of the FcεR1α ectodomain, the same domain bound by IgE [27] (Fig. 7B, C), raising the possibility that IgE may prevent PEAR1 binding when complexed with its receptor. Indeed, IgE, when bound to FcεR1α, could potently inhibit the FcεR1α-PEAR1 interaction at low concentrations, consistent with the high affinity of IgE for FcεR1α (Fig. 7D). To show that this inhibitory effect was due to blocking of the FcεR1α-PEAR1 interaction, and not steric interference with the large (190 kDa) IgE molecule, we demonstrated that smaller subfragments of the IgE heavy chain which bound FcεR1α, and blocked the FcεR1α-PEAR1 interaction (Fig. 7E). To demonstrate the specificity of this effect, we showed that addition of an anti-IgE monoclonal antibody that prevents IgE binding to FcεR1α (omalizumab) could relieve the inhibitory effect of IgE on both the FcεR1α-PEAR1 interaction (Fig. 7F).

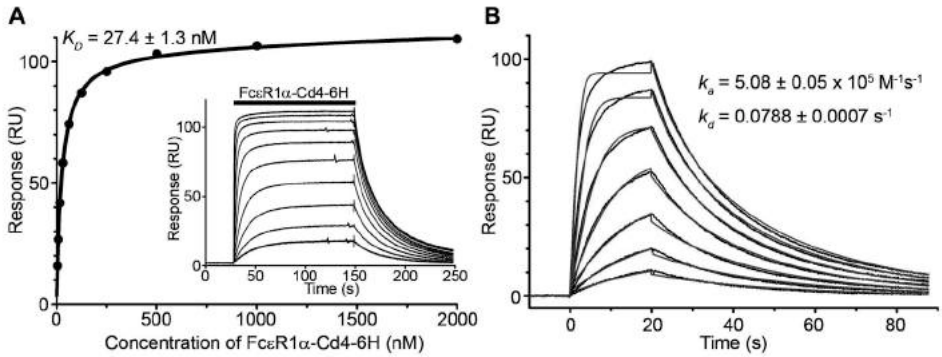

Figure 6: FcεR1α and PEAR1 directly and specifically interact with a relatively high affinity. A) Purified monomeric FcεR1α-Cd4-6His was serially diluted and injected over immobilized PEAR1 until equilibrium was achieved (inset). Binding data that had been reference subtracted were plotted as a binding curve and a K_D of 27.4 ± 1.3 nM was calculated. B) Association and dissociation rate constants derived from an independent kinetic analysis of the FcεR1α-PEAR1 interaction were consistent with the equilibrium analysis. Seven serial dilutions of purified, soluble FcεR1α-Cd4-6His were injected over immobilized PEAR1 (black lines), and kinetic parameters for the interaction derived from a 1:1 binding model fitted to the family of sensorgrams.

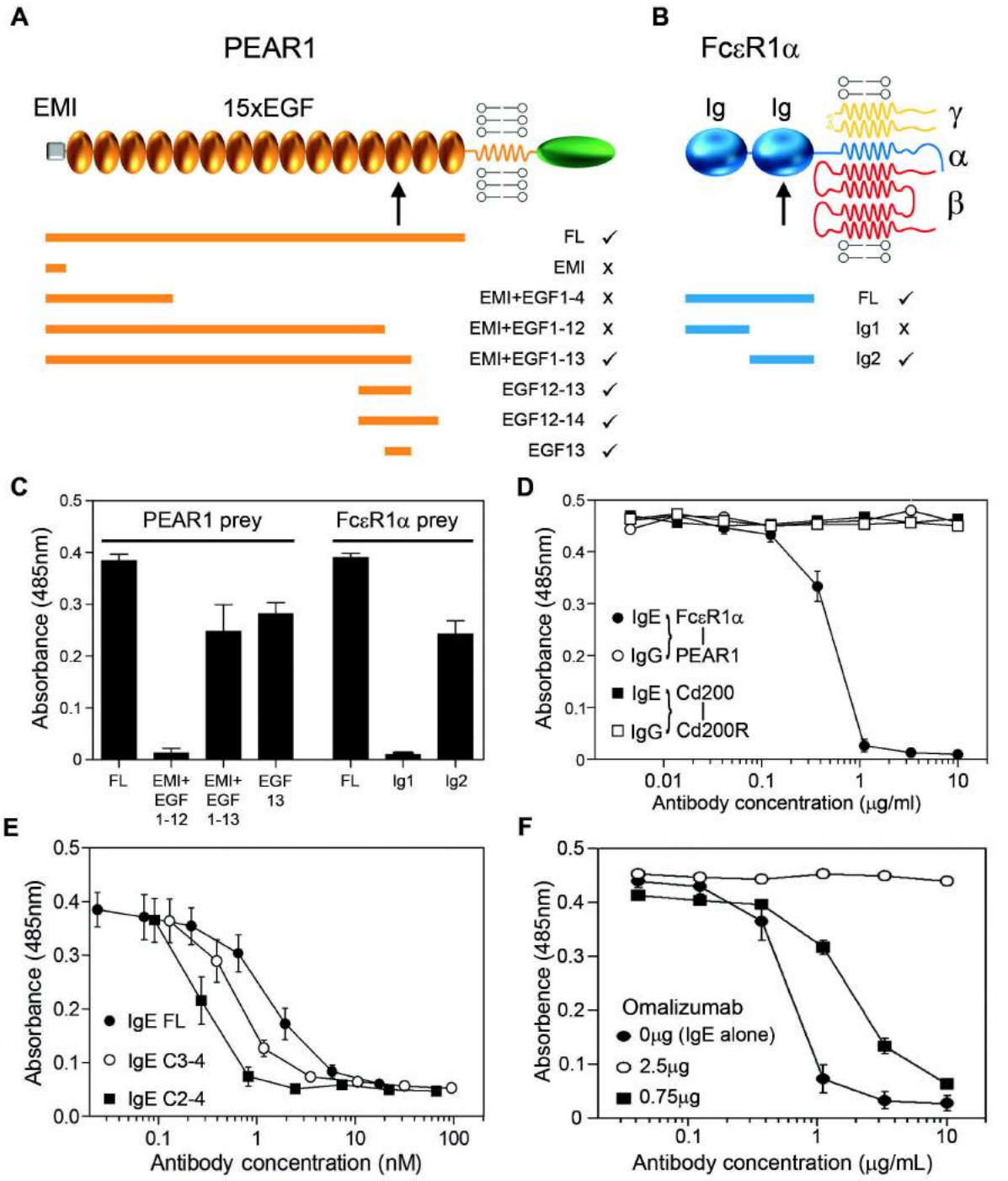

Figure 7: The FcεR1α-PEAR1 interaction is mediated by membrane proximal domains and can be specifically inhibited by IgE. A) A schematic illustrating the domain organization of the PEAR1 receptor in the membrane. Expressed fragments of the PEAR1 protein are represented by orange bars and the ticks and crosses indicate the ability of the fragments to bind the full-length (FL) ectodomain of FcεR1α as determined by AVEXIS; a similar summary for FcεR1α, but tested for binding to PEAR1 is shown in B. C) Binding data using AVEXIS showing the 13th EGF domain of PEAR1 and the 2nd-Ig-like domain of FcεR1α are necessary and sufficient for binding. Bars represent means ± SEM, $n \geq 3$. D) The FcεR1α-PEAR1 interaction detected by AVEXIS using PEAR1 as a plate-immobilized bait, was completely inhibited by low (IC_{50} ~ 0.5 ng/ml) concentrations of IgE (filled circles) but not control IgG (open circles). A control interaction, rat Cd200-Cd200R (squares), was not inhibited by either antibody. E) The indicated concentrations of purified full-length (FL) and both smaller fragments of the IgE constant heavy chain (C2-4) and (C2-3) were preincubated with the FcεR1α prey before being added to the PEAR1 bait and the interaction detected using AVEXIS. Data points are mean ± SEM; $n = 3$. F) The FcεR1α-PEAR1 interaction was detected using AVEXIS, and the inhibition by IgE (IgE alone, filled circles) could be relieved by the addition of 2.5 μg of omalizumab (open circles). Data points are mean ± SEM, $n \geq 3$.

Oligomerised FcεR1α specifically potentiates platelet aggregation via phosphorylation of PEAR1

To investigate the role of the FcεR1α-PEAR1 interaction in platelet activation, we confirmed cell surface expression of PEAR1 [8, 9] and FcεR1α [28, 29] by platelets using both Western blotting and immunocytochemistry (Fig. 8). Unlike PEAR1, [8] we did not observe any increase in the cell surface expression of FcεR1α after platelet activation. We next added clustered soluble oligomers (pentamers) of PEAR1 and FcεR1α to platelet aggregation assays and showed that they did not, by themselves, trigger platelet aggregation (data not shown). Preincubating unactivated platelets with FcεR1α oligomers followed by collagen stimulation, however, potentiated platelet aggregation (Fig. 9A). The specificity of this effect was demonstrated by pre-complexing the FcεR1α pentamers with IgE to completely block FcεR1α-mediated PEAR1 signaling, and suggested the possibility that IgE could act as an endogenous plasma-borne restrictive regulator of thrombus formation (Fig. 9B). PEAR1 oligomers modestly inhibited platelet aggregation (Fig. 9A), and did not trigger known FcεR1α signalling effectors such as the phosphorylation of PLCγ (data not shown), suggesting that they competed with membrane-tethered PEAR1 for FcεR1α binding. Finally, oligomerised FcεR1α, but not a control, was able to trigger PEAR1 phosphorylation with similar potency to an activating anti-PEAR1 antibody (Fig. 9C), and led to clear AKT phosphorylation, a known mediator of PEAR1 signalling [8] (Fig. 9D).

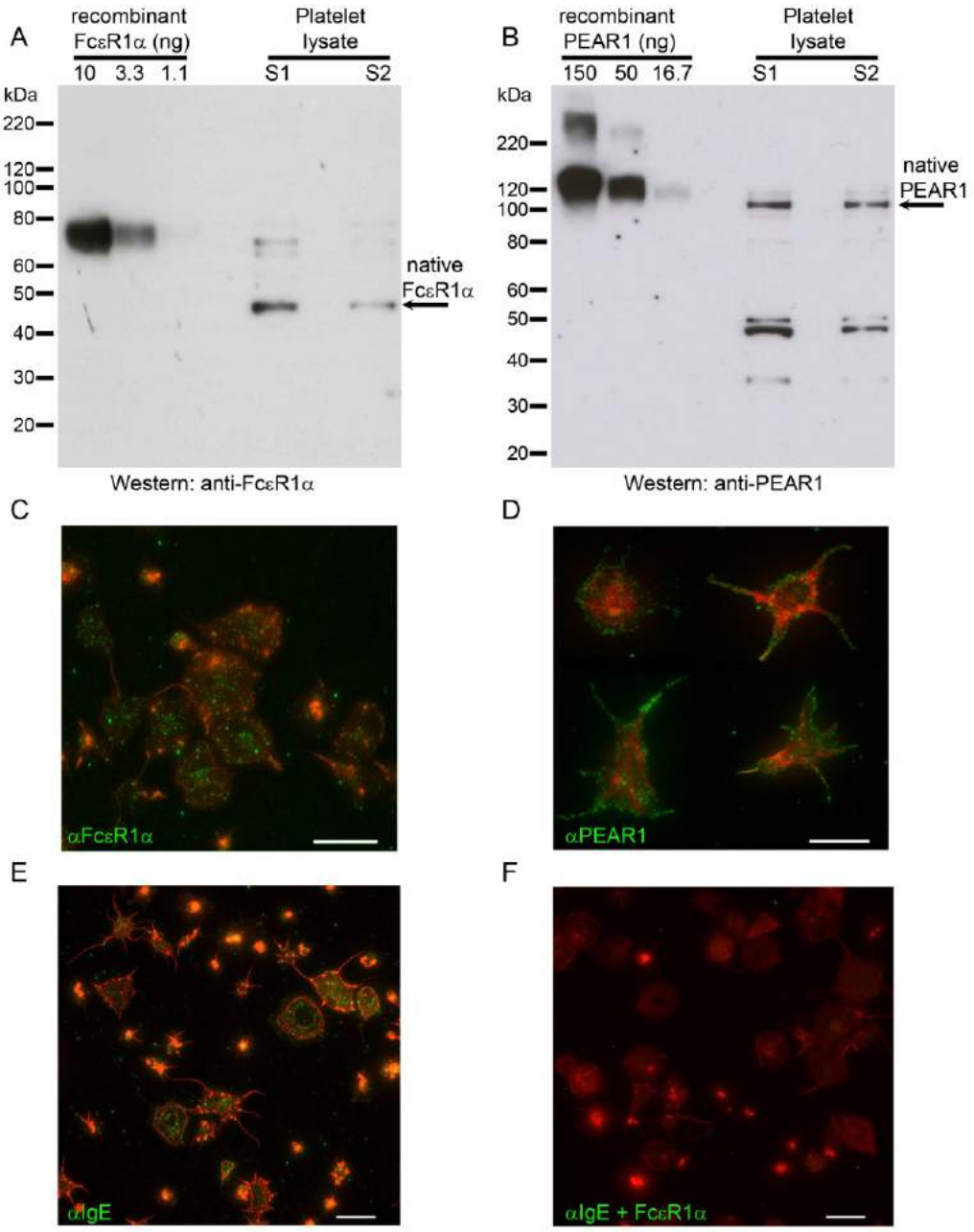

Figure 8: FcεR1α and PEAR1 are both expressed by human platelets. A and B) Western blot analysis showing gels loaded with the indicated amount of recombinant monomeric FcεR1α (A) and PEAR1 (B) and platelet lysate samples from two individuals (S1 and S2, at $1.95x10^7$ platelet equivalents per lane) probed with antibodies raised against the extracellular regions of human FcεR1α and PEAR1. Surface expression of both PEAR1 and FcεR1α was confirmed by immunofluorescence antibody staining on platelets (data not shown). Note that the molecular mass difference between the recombinant FcεR1α and PEAR1 proteins versus the native proteins is due to the tags present in the recombinant proteins. Blots shown are representative of three independent experiments. C and F) Staining of platelets spread over a fibrinogen matrix and stained with either anti-FcεR1α (C) or anti-PEAR1 (D) in green and counter-stained with phalloidin (red). E and F) Platelets were spread over a fibrinogen matrix and stained with anti-IgE (green). The IgE staining pattern was punctate (E) and shown to be both specific and extracellular since it could be abolished by incubating the platelets with an excess of soluble recombinant FcεR1α (F). Unlike PEAR1, cell surface FcεR1α is not increased upon platelet activation and using densitometry and the recombinant protein standards, we estimate that FcεR1α is expressed at ~10-fold lower levels than PEAR1 in platelets. Scale bars represent 5 µm.

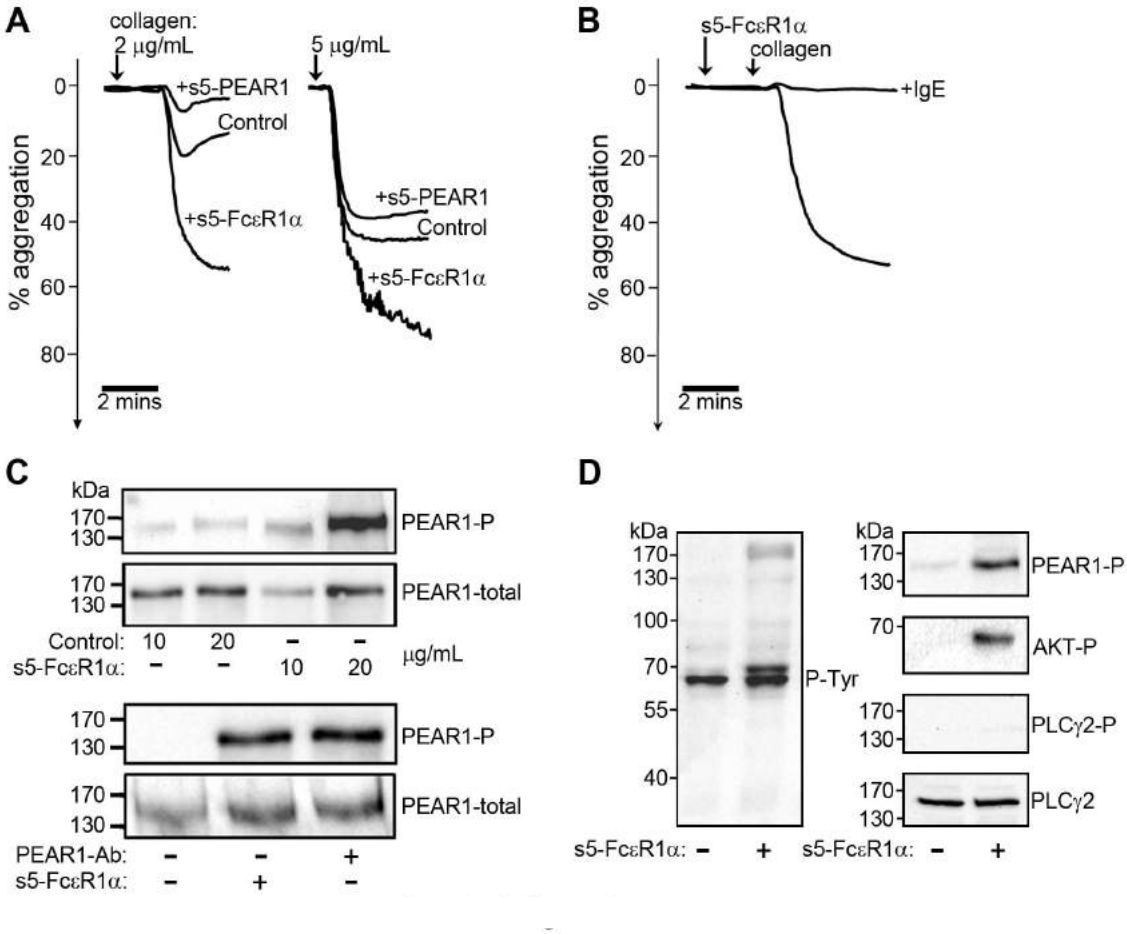

Figure 9: Oligomerised FcεR1α promotes platelet aggregation via phosphorylation of PEAR1. A) Soluble recombinant pentamerised (s5) PEAR1 ectodomains modestly inhibited, whereas a similar s5-FcεR1α protein strongly promoted platelet aggregation relative to a control (rat s5-Cd200) when added prior to collagen-induced platelet aggregation. B) Precomplexing s5-FcεR1α with IgE completely inhibited s5-FcεR1α-potentiated aggregation of collagen-activated platelets. C) Oligomeric FcεR1α, but not a control protein, triggered the phosphorylation of PEAR1 (top panel) in human platelets with similar potency to an anti-PEAR1 antibody (lower panel); total PEAR1 protein was detected as a loading control. D) Oligomeric FcεR1α induced tyrosine phosphorylation in human platelets as shown by anti-phosphotyrosine (P-Tyr) Western blotting of lysates. Phosphorylation of PEAR1 and AKT but not PLCγ2 (a mediator of FcεR1α signalling) was observed. Total PLCγ2 protein was used as a loading control. Aggregation data are representative from at least ten independent experiments.

DISCUSSION

Platelets perform a delicately-balanced role in haemostasis because they must detect and seal vascular breaches to restrict bleeding whilst ensuring a proportionate response to avoid vascular occlusion and maintain circulation. Interactions between receptor proteins displayed on the surface of platelets are a major class of thrombogenic regulator, and we report here a large recombinant protein library representing the secretome and receptor repertoire of the human platelet in a format suitable for systematic extracellular interaction screening using the AVEXIS assay. Importantly, we have expanded the utility of this assay to include receptor proteins from a greater range of structural classes as we work towards achieving a cell-type rather than the protein-family orientated screening approach; only the latter has been possible in the past.[11-14, 24] Central to this approach is the use of a mammalian expression system to promote the correct folding of the receptor ectodomains which we have previously shown can identify interactions that are functionally relevant *in vivo.* [16-18] The human platelet protein library will be a useful resource in further defining the role of platelet receptors and their interactions in cardiovascular disease, particularly since all the expression plasmids have been made openly available through the Addgene repository. [30] We have demonstrated the usefulness of this resource by identifying the ligand for PEAR1, an "orphan" platelet receptor that is of topical interest because it has been identified in several recent independent genome-wide association studies linking it with variation in patients' responses to thrombogenic agonists in both health and disease.[3-7] Because both FcεR1α and PEAR1 are expressed on the same cell, this raises the possibility that the two proteins might interact either in '*cis*' within the same membrane, or in '*trans*', between neighbouring cells. Although these need not be mutually exclusive, PEAR1 phosphorylation is known to be dependent upon platelet contact [8, 9] within forming aggregates suggesting that the interaction is likely to occur in trans. The kinetic analysis of the interaction between the soluble monomeric proteins suggest that the two proteins interact with a 1:1 stoichiometry, although both proteins are likely to form signalling-competent clusters within the membrane, consistent with previous findings that bivalent, but not monovalent, anti-PEAR1 antibodies trigger PEAR1 phosphorylation.[8] Soluble oligomers of FcεR1α, but not PEAR1, triggered known signalling effectors which is consistent with a unidirectional signal triggered by the FcεR1α ligand through the PEAR1 receptor.

The function of the high affinity IgE receptor on platelets is poorly characterized, but previous work is consistent with the established role of IgE in immunity to parasitic infections since cross-linking FcεR1α on the platelet surface triggered platelet cytotoxicity to a parasitic worm, *Schistosoma mansoni.* [29] Why FcεR1α has been adopted in the regulation of platelet biology is currently unclear, but perhaps the ability to block the interaction with endogenous plasma-borne IgE provides a clue. In healthy individuals, the concentration of circulating IgE is very low at approximately 0.5 nM. [31] Because the affinity of FcεR1α for IgE is within the same range (K_D ~ sub nM [32], and about two orders of magnitude higher than the affinity for PEAR1), this would suggest that in normal circulation, a significant fraction - but not all - (as shown in Hasegawa *et al*. [28]) of any FcεR1α on the surface of resting platelets will be bound by IgE, and unable to interact with PEAR1. Where circulating levels of IgE are increased, for example in atopic patients [31], this would significantly decrease the amount of IgE-free FcεR1α on the platelet surface available for PEAR1 binding. This is consistent with reports of a systemic lack of secondary platelet responsiveness in atopic patients, an observation that, in one study, was correlated with elevated IgE levels.[33-36] Others, however, have not replicated these findings [37, 38] suggesting a more complex relationship between circulating IgE levels and platelet function.

The controlled reduction of circulating IgE can be achieved in humans in the treatment of allergy with a humanised anti-IgE monoclonal antibody (omalizumab) that is currently licensed for the treatment of severe persistent allergic asthma.[39] It is a systemic anti-IgE agent which prevents the interaction of IgE with its receptors, reducing plasma IgE levels by 99% and downregulating FcεR1 on mast cells and basophils. [40, 41] We have shown here that omalizumab is able to relieve the IgE-mediated inhibition of the FcεR1α-PEAR1 interaction suggesting that omalizumab treatment could lead to alterations in the regulation of PEAR1 signalling. Indeed, concerns have recently been raised about an increased risk of arterial thrombotic events, particularly myocardial infarction and stroke, linked to the use of omalizumab ([42], and references therein).

In conclusion, we believe that the platelet receptor protein microarray and plasmid resource will be a valuable tool in cardiovascular disease research, and the identification of FcεR1α as a ligand for PEAR1 makes an important contribution toward understanding the mechanistic role this receptor plays in platelet function and cardiovascular disease.

REFERENCES

1. Yusuf S, Reddy S, Ounpuu S, Anand S. Global burden of cardiovascular diseases: part I: general considerations, the epidemiologic transition, risk factors, and impact of urbanization. *Circulation* 2001;**104**:2746-2753.
2. Deloukas P, Kanoni S, Willenborg C, et al. Large-scale association analysis identifies new risk loci for coronary artery disease. *Nat Genet* 2013;**45**:25-33.
3. Johnson AD, Yanek LR, Chen MH, et al.. Genome-wide meta-analyses identifies seven loci associated with platelet aggregation in response to agonists. *Nat Genet* 2010;**42**:608-613.
4. Faraday N, Yanek LR, Yang XP, Mathias R, Herrera-Galeano JE, Suktitipat B, Qayyum R, Johnson AD, Chen MH, Tofler GH, Ruczinski I, Friedman AD, Gylfason A, Thorsteinsdottir U, Bray PF, O'Donnell CJ, Becker DM, Becker LC. Identification of a specific intronic PEAR1 gene variant associated with greater platelet aggregability and protein expression. *Blood* 2011;**118**:3367-3375.
5. Herrera-Galeano JE, Becker DM, Wilson AF, Yanek LR, Bray P, Vaidya D, Faraday N, Becker LC. A novel variant in the platelet endothelial aggregation receptor-1 gene is associated with increased platelet aggregability. *Arterioscler Thromb Vasc Biol* 2008;**28**:1484-1490.
6. Jones CI, Bray S, Garner SF, Stephens J, de Bono B, Angenent WG, Bentley D, Burns P, Coffey A, Deloukas P, Earthrowl M, Farndale RW, Hoylaerts MF, Koch K, Rankin A, Rice CM, Rogers J, Samani NJ, Steward M, Walker A, Watkins NA, Akkerman JW, Dudbridge F, Goodall AH, Ouwehand WH. A functional genomics approach reveals novel quantitative trait loci associated with platelet signaling pathways. *Blood* 2009;**114**:1405-1416.
7. Lewis JP, Ryan K, O'Connell JR, Horenstein RB, Damcott CM, Gibson Q, Pollin TI, Mitchell BD, Beitelshees AL, Pakzy R, Tanner K, Parsa A, Tantry US, Bliden KP, Post WS, Faraday N, Herzog W, Gong Y, Pepine CJ, Johnson JA, Gurbel PA, Shuldiner AR. Genetic variation in PEAR1 is associated with platelet aggregation and cardiovascular outcomes. *Circ Cardiovasc Genet* 2013;**6**:184-192.
8. Kauskot A, Di Michele M, Loyen S, Freson K, Verhamme P, Hoylaerts MF. A novel mechanism of sustained platelet alphaIIbbeta3 activation via PEAR1. *Blood* 2012;**119**:4056-4065.
9. Nanda N, Bao M, Lin H, Clauser K, Komuves L, Quertermous T, Conley PB, Phillips DR, Hart MJ. Platelet endothelial aggregation receptor 1 (PEAR1), a novel epidermal growth factor repeat-containing transmembrane receptor, participates in platelet contact-induced activation. *J Biol Chem* 2005;**280**:24680-24689.
10. Wright GJ. Signal initiation in biological systems: the properties and detection of transient extracellular protein interactions. *Mol Biosyst* 2009;**5**:1405-1412.
11. Bushell KM, Sollner C, Schuster-Boeckler B, Bateman A, Wright GJ. Large-scale screening for novel low-affinity extracellular protein interactions. *Genome Res* 2008;**18**:622-630.
12. Ozkan E, Carrillo RA, Eastman CL, Weiszmann R, Waghray D, Johnson KG, Zinn K, Celniker SE, Garcia KC. An extracellular interactome of immunoglobulin and LRR proteins reveals receptor-ligand networks. *Cell* 2013;**154**:228-239.
13. Ramani SR, Tom I, Lewin-Koh N, Wranik B, Depalatis L, Zhang J, Eaton D, Gonzalez LC. A secreted protein microarray platform for extracellular protein interaction discovery. *Anal Biochem* 2012;**420**:127-138.
14. Wojtowicz WM, Wu W, Andre I, Qian B, Baker D, Zipursky SL. A vast repertoire of Dscam binding specificities arises from modular interactions of variable Ig domains. *Cell* 2007;**130**:1134-1145.
15. Sun Y, Gallagher-Jones M, Barker C, Wright GJ. A benchmarked protein microarray-based platform for the identification of novel low-affinity extracellular protein interactions. *Anal Biochem* 2012;**424**:45-53.
16. Bianchi E, Doe B, Goulding D, Wright GJ. Juno is the egg Izumo receptor and is essential for mammalian fertilization. *Nature* 2014;**508**:483-487.
17. Crosnier C, Bustamante LY, Bartholdson SJ, Bei AK, Theron M, Uchikawa M, Mboup S, Ndir O, Kwiatkowski DP, Duraisingh MT, Rayner JC, Wright GJ. Basigin is a receptor essential for erythrocyte invasion by Plasmodium falciparum. *Nature* 2011;**480**:534-537.
18. Powell GT, Wright GJ. Jamb and jamc are essential for vertebrate myocyte fusion. *PLoS Biol* 2011;**9**:e1001216.
19. Crosnier C, Wanaguru M, McDade B, Osier FH, Marsh K, Rayner JC, Wright GJ. A library of functional recombinant cell-surface and secreted P. falciparum merozoite proteins. *Mol Cell Proteomics* 2013;**12**:3976-3986.

20. Kerr JS, Wright GJ. Avidity-based extracellular interaction screening (AVEXIS) for the scalable detection of low-affinity extracellular receptor-ligand interactions. *J Vis Exp* 2012:e3881.
21. Briesewitz R, Epstein MR, Marcantonio EE. Expression of native and truncated forms of the human integrin alpha 1 subunit. *J Biol Chem* 1993;**268**:2989-2996.
22. Lane-Serff H, Sun Y, Metcalfe P, Wright GJ. Expression of recombinant ITGA2 and CD109 for the detection of human platelet antigen (HPA)-5 and -15 alloantibodies. *Br J Haematol* 2013;**161**:453-455.
23. Martin S, Sollner C, Charoensawan V, Adryan B, Thisse B, Thisse C, Teichmann S, Wright GJ. Construction of a large extracellular protein interaction network and its resolution by spatiotemporal expression profiling. *Mol Cell Proteomics* 2010;**9**:2654-2665.
24. Sollner C, Wright GJ. A cell surface interaction network of neural leucine-rich repeat receptors. *Genome Biol* 2009;**10**:R99.
25. Battle T, Antonsson B, Feger G, Besson D. A high-throughput mammalian protein expression, purification, aliquoting and storage pipeline to assemble a library of the human secretome. *Comb Chem High Throughput Screen* 2006;**9**:639-649.
26. Gonzalez R, Jennings LL, Knuth M, Orth AP, Klock HE, Ou W, Feuerhelm J, Hull MV, Koesema E, Wang Y, Zhang J, Wu C, Cho CY, Su AI, Batalov S, Chen H, Johnson K, Laffitte B, Nguyen DG, Snyder EY, Schultz PG, Harris JL, Lesley SA. Screening the mammalian extracellular proteome for regulators of embryonic human stem cell pluripotency. *Proc Natl Acad Sci U S A* 2010;**107**:3552-3557.
27. Garman SC, Wurzburg BA, Tarchevskaya SS, Kinet JP, Jardetzky TS. Structure of the Fc fragment of human IgE bound to its high-affinity receptor Fc epsilonRI alpha. *Nature* 2000;**406**:259-266.
28. Hasegawa S, Pawankar R, Suzuki K, Nakahata T, Furukawa S, Okumura K, Ra C. Functional expression of the high affinity receptor for IgE (FcepsilonRI) in human platelets and its' intracellular expression in human megakaryocytes. *Blood* 1999;**93**:2543-2551.
29. Joseph M, Gounni AS, Kusnierz JP, Vorng H, Sarfati M, Kinet JP, Tonnel AB, Capron A, Capron M. Expression and functions of the high-affinity IgE receptor on human platelets and megakaryocyte precursors. *Eur J Immunol* 1997;**27**:2212-2218.
30. Herscovitch M, Perkins E, Baltus A, Fan M. Addgene provides an open forum for plasmid sharing. *Nat Biotechnol* 2012;**30**:316-317.
31. Gould HJ, Sutton BJ. IgE in allergy and asthma today. *Nat Rev Immunol* 2008;**8**:205-217.
32. McDonnell JM, Calvert R, Beavil RL, Beavil AJ, Henry AJ, Sutton BJ, Gould HJ, Cowburn D. The structure of the IgE Cepsilon2 domain and its role in stabilizing the complex with its high-affinity receptor FcepsilonRIalpha. *Nat Struct Biol* 2001;**8**:437-441.
33. Gallagher JS, Bernstein IL, Maccia CA, Splansky GL, Glueck HI. Cyclic platelet dysfunction in IgE-mediated allergy. *J Allergy Clin Immunol* 1978;**62**:229-235.
34. Maccia CA, Gallagher JS, Ataman G, Glueck HI, Brooks SM, Bernstein IL. Platelet thrombopathy in asthmatic patients with elevated immunoglobulin e. *J Allergy Clin Immunol* 1977;**59**:101-108.
35. Palma-Carlos AG, Palma-Carlos ML, Santos MC, de Sousa JR. Platelet aggregation in allergic reactions. *Int Arch Allergy Appl Immunol* 1991;**94**:251-253.
36. Ind PW. Platelet and clotting abnormalities in asthma. *Clin Exp Allergy* 1991;**21**:395-398.
37. Harwell WB, Patterson JT, Lieberman P, Beachey E. Platelet aggregation in atopic and normal patients. *J Allergy Clin Immunol* 1973;**51**:274-284.
38. McDonald JR, Tan EM, Stevenson DD, Vaughan JH. Platelet aggregation in asthmatic and normal subjects. *J Allergy Clin Immunol* 1974;**54**:200-208.
39. Lieberman JA, Chehade M. Use of omalizumab in the treatment of food allergy and anaphylaxis. *Curr Allergy Asthma Rep* 2013;**13**:78-84.
40. Holgate S, Casale T, Wenzel S, Bousquet J, Deniz Y, Reisner C. The anti-inflammatory effects of omalizumab confirm the central role of IgE in allergic inflammation. *J Allergy Clin Immunol* 2005;**115**:459-465.
41. MacGlashan DW, Jr., Bochner BS, Adelman DC, Jardieu PM, Togias A, McKenzie-White J, Sterbinsky SA, Hamilton RG, Lichtenstein LM. Down-regulation of Fc(epsilon)RI expression on human basophils during in vivo treatment of atopic patients with anti-IgE antibody. *J Immunol* 1997;**158**:1438-1445.
42. Ali AK, Hartzema AG. Assessing the association between omalizumab and arteriothrombotic events through spontaneous adverse event reporting. *J Asthma Allergy* 2012;**5**:1-9.

Chapter III – Illustration from "Tertia musculorum Tabula – de humanum corporis fabrica libri septem" – A. Vesalius, 1543

ABSTRACT

Dextran sulphate (DxS; Mr 500kD) induces fibrinogen receptor ($\alpha_{IIb}\beta_3$)-activation via CLEC-2/Syk-signalling and via a Syk-independent SFK/PI3K/Akt-dependent tyrosine kinase pathway in human and murine platelets. The platelet surface receptor, responsible for the DxS-induced Syk-independent Akt-activation, has hitherto not been identified. We found that DxS elicited a concentration-dependent aggregation of human platelets resulting from direct PEAR1-activation by DxS. Blocking the PEAR1 receptor, in combination with a selective Syk-inhibitor completely abrogated the DxS-driven platelet aggregation. The DxS-induced Syk-phosphorylation was not affected in *Pear1*$^{-/-}$ platelets, but Akt-phosphorylation was largely abolished. As a result, the aggregation of *Pear1*$^{-/-}$ platelets was reduced and reversible, i.e. aggregates were less stable compared to wild-type platelet aggregates. Moreover, DxS-induced *Pear1*$^{-/-}$ platelet aggregation was fully abrogated by Syk-inhibition, indicating that the remaining platelet aggregation of *Pear1*$^{-/-}$ platelets was Syk-dependent. Hence, the Pear1/c-Src/PI3K/Akt- and CLEC-2/Syk-signalling pathways are independently and additively activated during platelet aggregation by DxS.

Conclusion – The DxS-induced aggregation of human and murine platelets is the result of activation of PI3K/Akt through direct PEAR1-phosphorylation and parallel Syk-signalling through CLEC-2.

INTRODUCTION

PEAR1 (platelet endothelial aggregation receptor 1), a type-1 transmembrane protein of the multiple epidermal growth factor (EGF)–like domain protein family is mainly expressed in platelets and endothelial cells.[1, 2] PEAR1 comprises an extracellular EMI domain (protein-protein interaction domain), 15 extracellular EGF-like repeats, and multiple cytoplasmic tyrosines and prolines.[1] Nanda *et al*. identified PEAR1 as a platelet-platelet contact receptor. During platelet aggregation, PEAR1 becomes phosphorylated at Tyr-925 and Ser-953/1029, which is mediated by the Src family kinases (SFK) c-Src and Fyn, but not Syk.[1] We reported that PEAR1, c-Src and Fyn, and the p85/phosphatidylinositol 3-kinase (PI3K) subunit constitute a signalling complex in platelets that sustains the activation of $\alpha_{IIb}\beta_3$ in aggregating platelets, favouring the formation of stable platelet aggregates[3], and we identified the high affinity immunoglobulin E (IgE) receptor subunit α (FcεR1α) as a platelet PEAR1 ligand.[4]

Using high Mr dextran sulphate (DxS; 500K) as an agonist of both human and murine platelet aggregation, Getz *et al.* demonstrated that DxS-induced platelet $\alpha_{IIb}\beta_3$ activation occurs via two different pathways in both human and murine platelets: a Syk-dependent pathway (activating $\alpha_{IIb}\beta_3$ via Syk/PLCγ2 activation) and a Syk-independent SFK/PI3K/Akt-dependent tyrosine kinase pathway.[5, 6] Alshehri *et al.* recently identified CLEC-2 as the major receptor for the Syk/PLCγ2 mediated $\alpha_{IIb}\beta_3$ activation via DxS.[7] However, the receptor through which DxS induces PI3K-mediated $\alpha_{IIb}\beta_3$ platelet activation, independent from Syk, still had to be identified.

Since both DxS and PEAR1 induce sustained platelet aggregation via the SFK/PI3K/Akt pathway in platelets, and since activation of PEAR1 in human platelets is independent from Syk[3], we hypothesized that the Syk-independent DxS-induced platelet aggregation involves PEAR1. The aim of this study was to investigate whether DxS-induced SFK/PI3K/Akt-signalling occurs via direct phosphorylation of PEAR1 (Figure 3) and whether the activation of CLEC-2 and PEAR1 by DxS suffices to explain DxS-induced platelet aggregation (Figure 1).

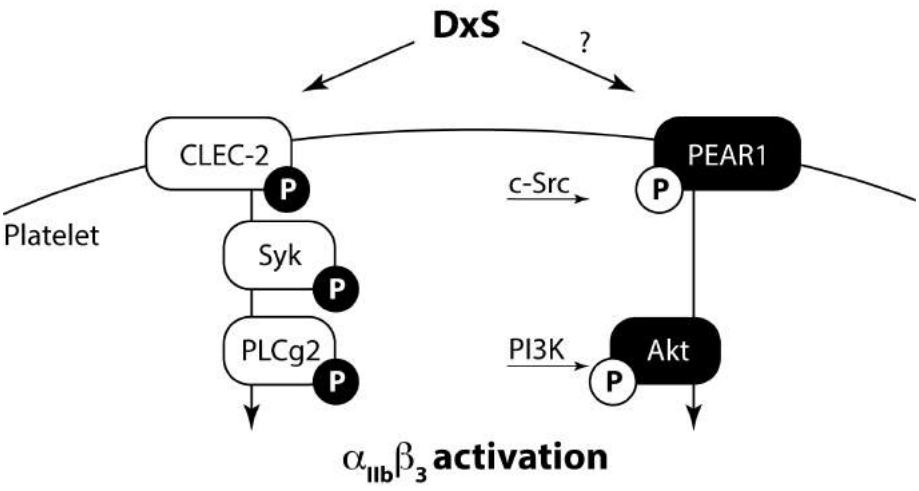

Figure 1: Hypothesis of DxS-induced human and murine platelet activation.

MATERIALS AND METHODS

Reagents

Watersoluble dextran sulphate sodium salt (Mr 500K), dimethylsulfoxide (DMSO) and anti-PLCγ2 were from Sigma-Aldrich (St. Louis, USA). The dextran polymer is the result of approximately 95% alpha-D-(166) linkages. For the longest molecules, branching up to 50 glucose units has been measured (data sheet Sigma). The human and mouse Syk-inhibitor BAY 61-3606 was from Santa Cruz (Dallas, USA). The PI3K inhibitor LY294002 was purchased from Calbiochem (California, USA) and the SFK inhibitor PP1 from Enzo Life Sciences (Antwerp, Belgium). The $\alpha_{IIb}\beta_3$-antagonist eptifibatide was from GSK (Integrilin®). The 4G10/anti-P-Tyr-antibody was from Millipore (Overijse, Belgium). Rabbit monoclonal antibodies against the phosphorylated (human and murine) form of Akt (pSer-473), Syk (pTyr-352) and PLCγ2 (pTyr-759) and polyclonal antibodies against total Akt, total β-actin and total Syk were from Cell Signaling Technology (Bioké, The Netherlands). The anti-GAPDH/Gapdh antibody was from Fitzgerald (Acton, USA). Horseradish peroxidase-conjugated secondary antibodies were from Dako (Heverlee, Belgium). A rabbit anti-human PEAR1 polyclonal antibody against the extracellular domain of PEAR1 and a rabbit anti-murine Pear1 polyclonal antibody against the extracellular domain of Pear1 were purchased from R&D Systems (Minneapolis, USA).

sFcεR1α, s5FcεR1α, sPEAR1 and s5PEAR1

Monomeric recombinant FcεR1α protein, pentameric recombinant FcεR1α protein (s5FcεR1α) and pentameric recombinant PEAR1 (s5PEAR1) constructs were designed, produced and validated as recently published by our group.[4] A human recombinant extracellular PEAR1-domain was made by cloning the corresponding mRNA-fragment, encoding amino-acids residues Met1-Ser-754 into the pSecTag2/Hygro A-vector (Life Technologies, Ghent, Belgium). The resulting construct was transfected in COS-7 cells using a jetPRIME transfection kit (Polyplus, Leuven, Belgium) according to the manufacturer's protocol. Conditioned medium containing the extracellular PEAR1 recombinant protein was collected after 48 hours. The presence of homogeneous recombinant PEAR1-protein in the medium was confirmed by western blot (Mr 125 kDa).

DxS binding to PEAR1 (ELISA)

Microtiter plates were coated (O/N, 4°C) with 20 µg/ml pentameric s5FcεR1α in 100µl TBS, washed with TBS + 0.1% BSA and blocked with 1% BSA in TBS for 1 hour at room temperature (RT). Conditioned medium (200 µl) containing the extracellular domain of PEAR1 (see below) was loaded in duplicates and incubated for 2 hours at RT, followed by the addition of 100 µl anti-PEAR1 antibody (1 µg/ml) for an additional hour at RT. Binding of DxS was investigated by co-incubation of PEAR1 with DxS during the first binding step. Bound anti-PEAR1 antibodies were detected via HRP-conjugated rabbit anti-goat IgG (1/2000, in TBS + 0.1% BSA for 1 hour, RT). Binding was visualized by the addition of 100 µl chromogenic substrate (TMB) for 30 min. The reaction was stopped with 50 µl H_2SO_4 (2M) and absorbance at 450 nm was measured using a PowerWave X-340 plate reader (Bio-Tek Instruments, Winooski, USA).

Platelet aggregation

Venous blood was collected from healthy donors. Washed platelets were prepared as previously published,[3] in the presence of 0.1 IU/ml of apyrase (Sigma-Aldrich). Platelet aggregation was monitored by measuring light transmission through the stirred suspension of washed platelets (3×10^5/µL) at 37°C with a Chronolog dual-beam aggregometer, in the absence of added fibrinogen. In some experiments, platelets were preincubated with LY294002 (5 minutes, 50 µM), PP1 (10 minutes, 10 µM), DMSO (5 minutes), eptifibatide (10 minutes, 10 µg/ml) or BAY 61-3606 (10 minutes, 10 µM) at 37°C. The DMSO concentration never exceeded 0.2% (vol/vol). Platelet aggregation was triggered by DxS after adding Ca^{2+} (2 mM) and measured and expressed as the percentage of change in light transmission, with the value for the blank sample (buffer without platelets) set at 100%. Each aggregation plot is the representative image of at least three independent experiments. Each aggregation was stopped by adding SDS denaturing buffer or ice-cold Triton lysis butter at 30% aggregation to avoid displacement of PEAR1 to the insoluble cytoskeleton fraction (as previously published [3]).

Static platelet incubation

Washed platelets were prepared as previously published.[3] In some experiments, platelets ($4 \times 10^5/\mu L$) were incubated under static conditions, (i.e. unstirred) with DxS (15 min), DxS 5K (15 min), sFcεR1α (15 min; excess concentration of 100µg/ml), s5PEAR1 (15 min; excess concentration of 100µg/ml) or the polyclonal anti-PEAR1/Pear1 antibody (15 min; NaN_3- free, reconstituted with sterile PBS), as specified. After incubation with the various reagents, platelets were lysed in SDS denaturing buffer.[3]

Western blotting

Platelets were lysed with ice-cold Triton lysis buffer (10 mM Tris-HCl pH 8, 125 mM NaCl, 2 mM EDTA, 1% Triton X-100, 10 mM NaF, 2 mM Na_3VO_4, protease inhibitor cocktail) or in SDS denaturing buffer (10 mM Tris-HCl pH 8, 125 mM NaCl, 2 mM EDTA, 1% sodium dodecyl sulfate (SDS), 10 mM NaF, 2 mM Na_3VO_4, protease inhibitor cocktail). Proteins were subjected to SDS-polyacrylamide gel electrophoresis (PAGE) and transferred to nitrocellulose. Membranes were incubated with various primary antibodies, i.e. anti-PEAR1 (1/1000), anti-Pear1 (1/1000), anti-Akt-P (1/500), anti-Akt (1/1000), anti-Syk (1/1000), anti-Syk-P (1/1000), anti-PLCγ2-P (1/1000), anti-PLCγ2 (1/1000), anti-β-actin (1/1000), anti-phosphotyrosine (P-Tyr) 4G10 (1/1000) and anti-GAPDH/Gapdh (1/10.000). After adding complementary horseradish peroxidase–conjugated secondary antibodies, immunoreactive bands were visualized by ECL (Amersham Biosciences) on a Bio-Rad Universal Hood II Imager model. Each Western blot is the representative image of at least three independent experiments.

PEAR1/Pear1-phosphorylation on Tyrosine residues, referred to as pPEAR1 or pPear1, was evaluated after immunoprecipitation with anti-PEAR1/Pear1-Ab and detection of P-Tyr by 4G10, as previously described; membranes were stripped and reprobed for total PEAR1/Pear1 detection.[3]

Isolation of *Pear1*$^{-/-}$ platelets

The *Pear1*$^{+/-}$ mouse (*Pear1*$^{tm1a(KOMP)Wtsi}$; C57BL/6N-background) was acquired through courtesy of the International Mouse Phenotype Consortium (IMPC; EPD0299_2_C05). *Pear1*$^{+/-}$ mice were mated to obtain *Pear1*$^{-/-}$ mice and WT littermate controls. Mice were genotyped by tail DNA-extraction, followed by PCR-amplification, using the following primer sequences (Table I):

Table I: *Pear1*$^{tm1a(KOMP)Wtsi}$ **-** *Genotyping primers*

PCR type	
Mutant PCR	Forward primer = $^{5'}$GTGGTGGGGTGCTACTGTCT$^{3'}$
	Reverse primer = $^{5'}$TCGTGGTATCGTTATGCGCC$^{3'}$
Wild-type PCR	Forward primer = $^{5'}$GTGGTGGGGTGCTACTGTCT$^{3'}$
	Reverse primer = $^{5'}$TAGTCAGAGCCGTGGAATGG$^{3'}$
LacZ PCR	Forward primer = $^{5'}$ATCACGACGCGCTGTATC$^{3'}$
	Reverse primer = $^{5'}$ACATCGGGCAAATAATATCG$^{3'}$

Mouse blood of 13 weeks old mice was collected in ACD (acid citrate dextrose) pH 6.5 (93mM sodium citrate; 7mM citric acid; 14mM dextrose; pH 6.8) containing 0.1 U/ml apyrase, by left ventricular heart puncture after a high dose (20 μg/ml blood volume) of intraperitoneal pentobarbital. Platelet-rich plasma (PRP) was prepared by centrifugation for 30 seconds at 3000 rpm, followed by 5 min at 800 rpm at room temperature. The PRP was diluted threefold in ACD and centrifuged for 10 minutes at 2000 rpm to collect the platelet pellet. Platelets were resuspended in Ca^{2+}-free Tyrode's buffer (137mM NaCl, 12mM NaHCO3, 2mM KCl, 0.34mM Na2HPO4, 1mM MgCl2, 5.5mM glucose, and 5mM HEPES [N-2-hydroxyethylpiperazine-N'-2-ethanesulfonic acid], pH 7.4) at a density of 4×10^5/μL and used immediately.

RESULTS

DxS induces human and murine platelet aggregation

DxS induced a concentration-dependent aggregation of stirred washed human (Figure 2A) and murine (Figure 2B) platelets in the concentration range previously shown to provoke platelet activation and ATP secretion.[5] Getz *et al.* performed murine platelet aggregations in the presence of DxS 5 nM. We did not observe substantially altered aggregation of murine platelets for DxS 0.25 nM compared to DxS 5 nM (Figure 2B). The DxS-induced human platelet aggregation was abrogated in the presence of the $\alpha_{IIb}\beta_3$-receptor blocker eptifibatide, confirming that DxS induced proper platelet aggregation and not platelet agglutination (Figure 2A).

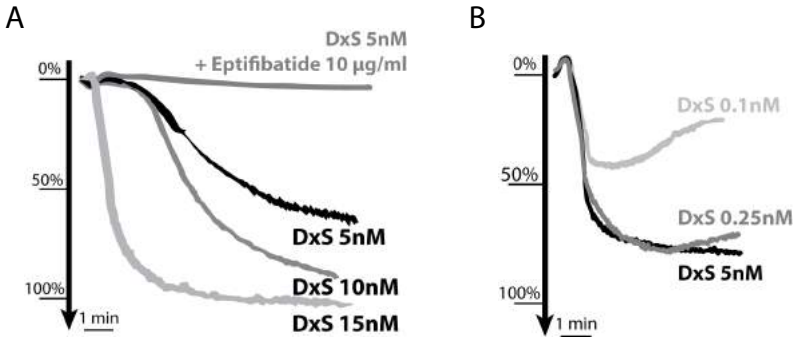

Figure 2: DxS induces human and murine platelet aggregation.
Human (A) and murine (B) platelet aggregation induced by the indicated concentrations of DxS. Murine platelet aggregation was comparable for 0.25 and 5 nM DxS. (A) DxS (5 nM) induced human platelet aggregation was abolished by eptifibatide (10 µg/ml), indicating that DxS induces platelet aggregation and not agglutination.

DxS induces direct PEAR1 activation

As previously published by our group,[3] PEAR1 phosphorylation can be the result of direct PEAR1-activation via a PEAR1-ligand interaction or it can be triggered indirectly following platelet-platelet contact as part of platelet amplification induced by various classical platelet agonists (e.g. thrombin, collagen). This is schematically shown in Figure 3; Western blots show corresponding pPEAR1 (PEAR1 immunoprecipitation and western blot for P-Tyr; Figure 3G).

Activation of platelets with a specific PEAR1 ligand (e.g. soluble recombinant pentameric FcεR1α (s5FcεR1α) or anti-PEAR1-extracellular-antibodies, Figure 3A) and activation of platelets with traditional platelet agonist (e.g. collagen or thrombin, binding to their own classical receptors; Figure 3B) result both in platelet aggregation and PEAR1-phosphorylation under stirring conditions. However, blocking the $\alpha_{IIb}\beta_3$-receptor under stirring conditions in the direct PEAR1-activation pathway (Figure 3C) preserves the phosphorylation of PEAR1, although aggregation is absent. In contrast, blocking the $\alpha_{IIb}\beta_3$-receptor in the indirect PEAR1-activation pathway (Figure 3D) results in abrogation of the PEAR1-phosphorylation.
Therefore, to illustrate that DxS binds directly to PEAR1, we analysed DxS-induced PEAR1 phosphorylation under stirring conditions in the presence of an $\alpha_{IIb}\beta_3$-receptor blocker (Figure 3C) or, alternatively, under static conditions (Figure 3E and 3F) to avoid indirect PEAR1 phosphorylation by platelet-platelet contacts. Next we performed competition experiments (ELISA and platelet aggregation) between DxS and the PEAR1 ligand FcεR1α to confirm the direct DxS-PEAR1 interaction.

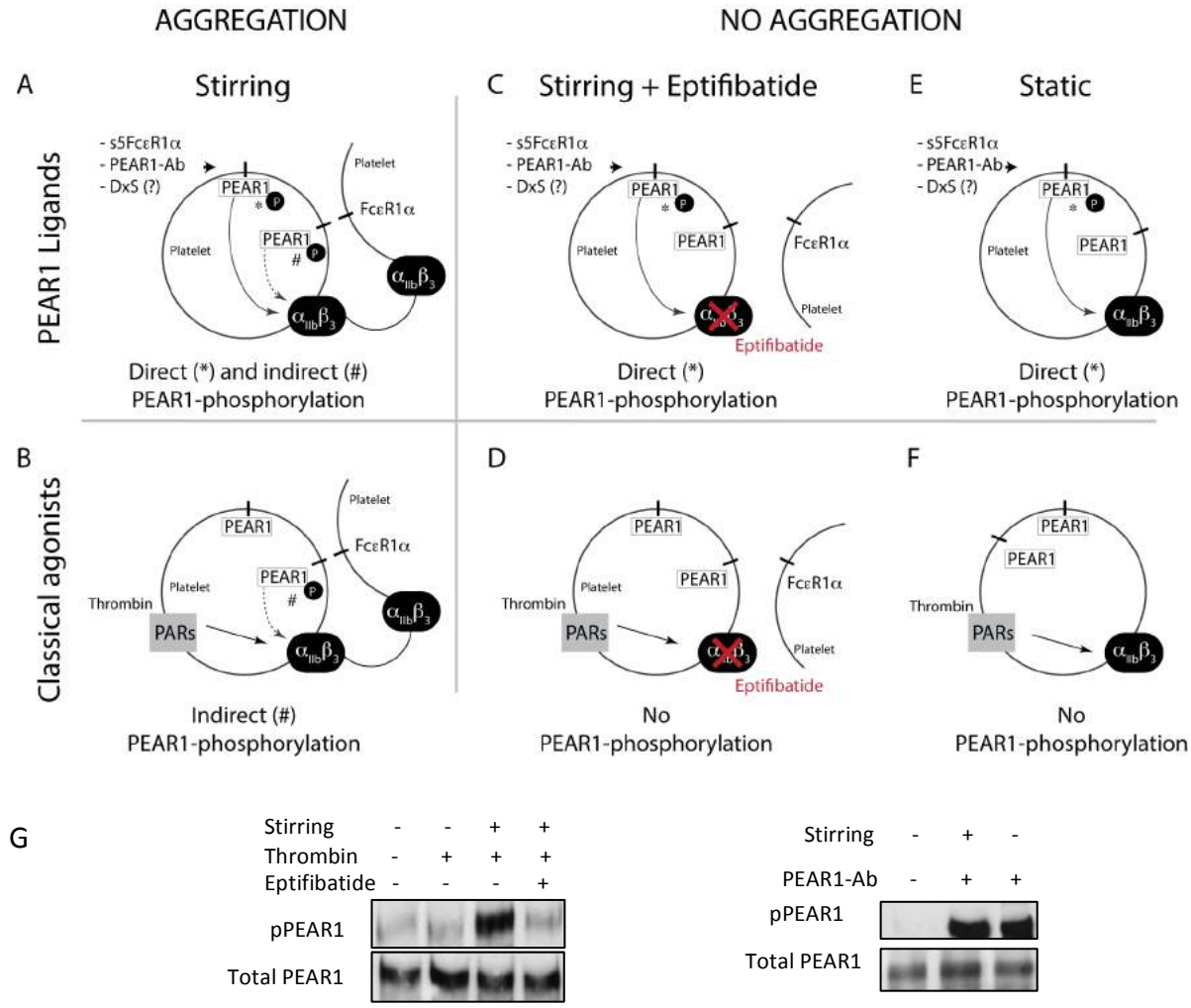

Figure 3 – Platelet PEAR1-phosphorylation can be triggered directly or indirectly

As previously published by our group,[3] PEAR1 phosphorylation can be the result of direct PEAR1-activation (* in Figure 3) via a PEAR1-ligand (e.g. soluble recombinant pentameric FcεR1α (s5FcεR1α) or anti-PEAR1-extracellular-antibodies) interaction or can be triggered indirectly (# in Figure 3) as part of platelet amplification with traditional platelet agonists (e.g. thrombin, collagen). This has been schematically shown in Figure 3 and confirmed by western blot for pPEAR1 (PEAR1 immunoprecipitation and western blot for P-Tyr; Figure 3G). Direct activation of platelets by a specific PEAR1-ligand under stirring conditions (Figure 3A) results in direct PEAR1-phosphorylation via a PEAR1-ligand interaction and indirect PEAR1-phosphorylation via platelet-platelet contact. This is in contrast with platelet activation under stirring conditions with classical platelets agonists (Figure 3B), where only indirect PEAR1-phosphorylation occurs via platelet-platelet contact. Incubation of platelets with a specific PEAR1-ligand in non-aggregating conditions (stirring conditions in the presence of eptifibatide (Figure 3C) or static conditions (Figure 3E)) results only in direct PEAR1-phosphorylation due to the lack of platelet-platelet contact. The presence of classical platelet agonists in non-aggregating conditions does not result in phosphorylation of PEAR1 due to the lack of direct PEAR1-activation and the lack of platelet-platelet contacts.

a) Static incubation of washed human platelets with DxS

Static incubation of washed human platelets with DxS (0-10 nM) for 15 min resulted in a dose-dependent PEAR1 phosphorylation comparable to that induced by anti-PEAR1-antibodies (PEAR1 immunoprecipitation and western blot for P-Tyr; Figure 4A). In agreement with Figure 3E and 3F, this phosphorylation is compatible with direct binding of DxS to PEAR1.

b) Stirring conditions in the presence of an $\alpha_{IIb}\beta_3$-receptor blocker

To further investigate a direct interaction between DxS and PEAR1, we investigated the phosphorylation state of PEAR1 in DxS-induced platelet aggregation in the presence of eptifibatide (Figure 4B; anti-PEAR1-Ab served as a positive control). The phosphorylation state of PEAR1 was unaffected by eptifibatide (Figure 4B, right panel), further supporting direct binding of DxS to PEAR1 (in agreement with Figure 3C).

c) Competition experiments

Next, we confirmed the direct binding of DxS to PEAR1 by competition experiments for PEAR1 with its physiologic ligand FcεR1α. We previously reported that phosphorylation of PEAR1 requires clustering of the PEAR1-receptor.[3, 4] As summarized in Figure 4C, static incubation of platelets with a (divalent) anti-PEAR1-extracellular-antibody or with pentameric recombinant FcεR1α (s5FcεR1α) resulted in PEAR1-activation whereas incubation with Fab-fragments of the anti-PEAR1-antibody[8] or with a monomeric form of recombinant FcεR1α (sFcεR1) prevents clustering of PEAR1,[3, 4] abrogating its phosphorylation.

As shown in Figure 4D and E, DxS-induced PEAR1 phosphorylation is blocked when platelets were pre-incubated with an excess of recombinant pentameric PEAR1 (s5PEAR1), compatible with the direct binding of pentameric s5PEAR1 to DxS and thus competing with DxS binding to platelet PEAR1. Similarly, DxS-induced PEAR1 phosphorylation is blocked when platelets were pre-incubated with an excess of monomeric sFcεR1α, shielding the

PEAR1-receptor from DxS-mediated PEAR1-clustering. Since we were interested in direct phosphorylation of PEAR1, these competition experiments were performed under static conditions.

We also confirmed the direct interaction of DxS to PEAR1 through ELISA; the binding of recombinant PEAR1 to its coated ligand, i.e. recombinant pentameric FcεR1α (s5FcεR1α), was dose-dependently inhibited by DxS (500K; 1-100 nM) with an IC_{50} = 25±3.4 nM (Figure 4F). All of these results confirmed direct phosphorylation of PEAR1 by DxS.

Figure 4 – DxS induces PEAR1 clustering and direct PEAR1 activation
(A) Static incubation of human platelets with DxS resulted in concentration-dependent phosphorylation of PEAR1. (B) DxS-induced platelet aggregation is abrogated in the presence of eptifibatide (10 μg/ml); corresponding western blot for phospho-PEAR1 showed a sustained DxS-induced PEAR1 phosphorylation in the presence of eptifibatide, compatible with direct binding of DxS to PEAR1. (C) PEAR1 activation requires PEAR1 receptor clustering (schematic overview). Divalent anti-PEAR1-Ab and soluble recombinant pentameric FcεR1α induce direct PEAR1-phosphorylation whereas direct PEAR1 activation is blocked in the presence of the PEAR1 shielding/blocking monovalent anti-PEAR1-Ab Fab or monomeric sFcεR1α, as previously shown.[3, 4] (D and E) Static incubation of washed human platelets with DxS in competition with an excess of the PEAR1 shielding/blocking monomeric sFcεR1α (D) or an excess of recombinant pentameric PEAR1 (s5PEAR1; E) resulted in reduced PEAR1-phosphorylation. These experiments were performed under static conditions in order to avoid indirect PEAR1-activation as shown in Figure 3. (F) Competitive ELISA for the binding of soluble PEAR1 to its coated ligand (pentameric s5FcεR1α) in the presence of increasing concentrations of DxS (500K; 1-100 nM). (A, B, D and E: washed human platelets; pPEAR1: P-Tyr after immunoprecipitation for PEAR1; Polyclonal anti-PEAR1-Ab served as positive control).

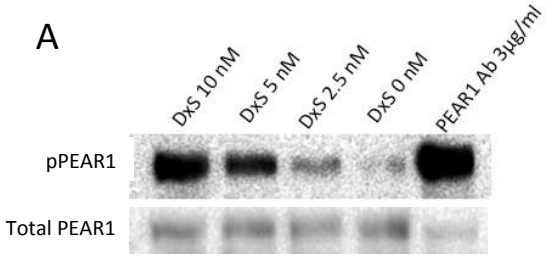
A
DxS 10 nM
DxS 5 nM
DxS 2.5 nM
DxS 0 nM
PEAR1 Ab 3µg/ml
pPEAR1
Total PEAR1

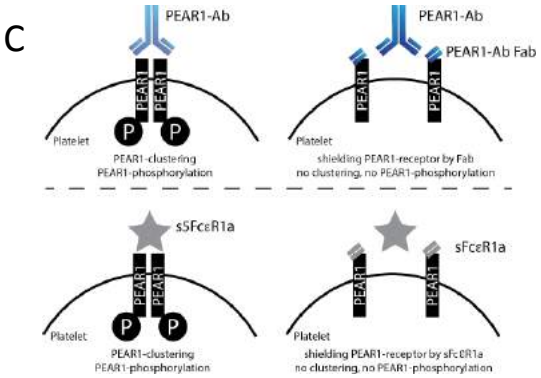
C
PEAR1-Ab
PEAR1-Ab Fab
Platelet
PEAR1-clustering
PEAR1-phosphorylation
shielding PEAR1-receptor by Fab
no clustering, no PEAR1-phosphorylation
s5FcεR1a
sFcεR1a
shielding PEAR1-receptor by sFcεR1a
no clustering, no PEAR1-phosphorylation

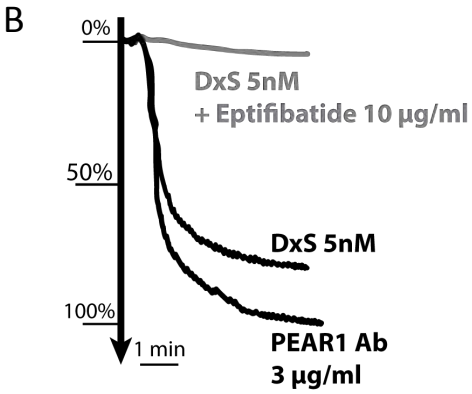
B
0%
50%
100%
1 min
DxS 5nM
+ Eptifibatide 10 µg/ml
DxS 5nM
PEAR1 Ab
3 µg/ml

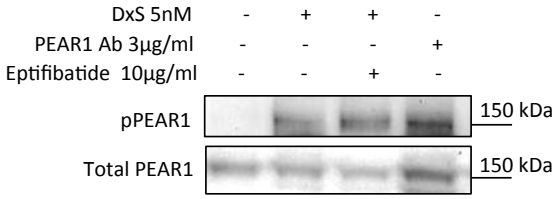
DxS 5nM - + + -
PEAR1 Ab 3µg/ml - - - +
Eptifibatide 10µg/ml - - + -
pPEAR1
150 kDa
Total PEAR1
150 kDa

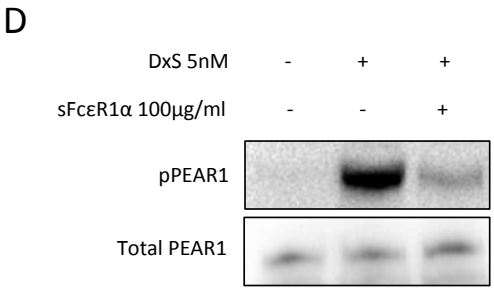
D
DxS 5nM - + +
sFcεR1α 100µg/ml - - +
pPEAR1
Total PEAR1

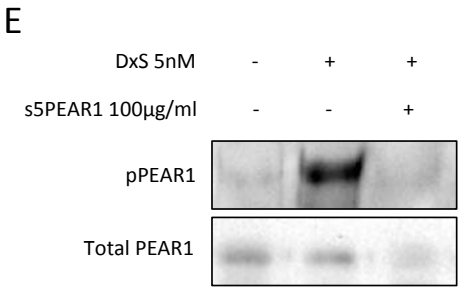
E
DxS 5nM - + +
s5PEAR1 100µg/ml - - +
pPEAR1
Total PEAR1

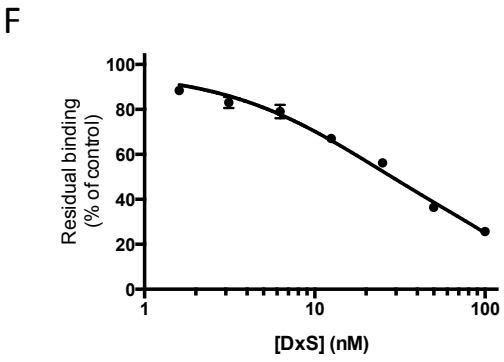
F
Residual binding
(% of control)
100
80
60
40
20
0
1
10
100
[DxS] (nM)

DxS mediates human platelet aggregation via PEAR1 and CLEC-2/Syk

Alshehri *et al.* recently identified CLEC-2 as the major receptor responsible for the Syk/PLCγ2 mediated $\alpha_{IIb}\beta_3$ activation via DxS.[7] Here, our results highlight PEAR1 as the receptor through which DxS induces PI3K/$\alpha_{IIb}\beta_3$ -mediated platelet activation. Therefore, we investigated whether Syk/PLCγ2-activation together with PEAR1/Akt-activation is sufficient to explain DxS-mediated platelet aggregation. Indeed, we showed that DxS-induced platelet aggregation (Figure 5A; left panel) could be completely blocked after pre-incubation with sFcεR1α (shielding the PEAR1 receptor) plus the Syk-inhibitor BAY 61-3606, coinciding with abrogated Akt and Syk-phosphorylation (Figure 5A, right panel, western blot).

The PEAR1 antagonist sFcεR1α alone incompletely blocked aggregation, without affecting the degree of Syk phosphorylation (Figure 5B). Correspondingly, inhibition of the Syk/PLCγ2-pathway after preincubation with the selective Syk-inhibitor BAY 61-3606 only partially reduced DxS-mediated human platelet aggregation (Figure 5C). The phosphorylation of PEAR1 and Akt remained unaffected in the presence of BAY 61-3606 (Figure 5A; right panel), because of the lack of Syk-involvement in PEAR1-signalling, as previously reported.[3]

To further support these findings in human platelets, we will extrapolate our results to murine platelets and confirm our observations in *Pear1*$^{-/-}$ platelets.

Figure 5 – DxS mediates human platelet aggregation via PEAR1 and Syk
(A) DxS-induced human platelet aggregation was completely abrogated by combined preincubation of the PEAR1-blocking ligand (sFcεR1α-monomer) and the selective Syk-inhibitor BAY 61-3606 (left panel), indicating that blocking PEAR1 together with Syk is sufficient to explain DxS-induced human platelet aggregation; corresponding western blot for phosphorylation of PEAR1, Akt and Syk (right panel) in the presence of monomeric sFcεR1α and/or BAY 61-3606. (B and C) DxS-induced platelet aggregation was partially reduced by preincubation with monomeric sFcεR1α (B) or with the selective Syk-inhibitor BAY 61-3606 (C); right panels: corresponding western blots for phosphorylation of Syk and PLCγ2 showed the effect of BAY 61-3606 and showed that shielding PEAR1 with monomeric sFcεR1α did not affect DxS-induced phosphorylation of Syk. A-C: washed human platelets; pPEAR1: P-Tyr after immunoprecipitation for PEAR1.

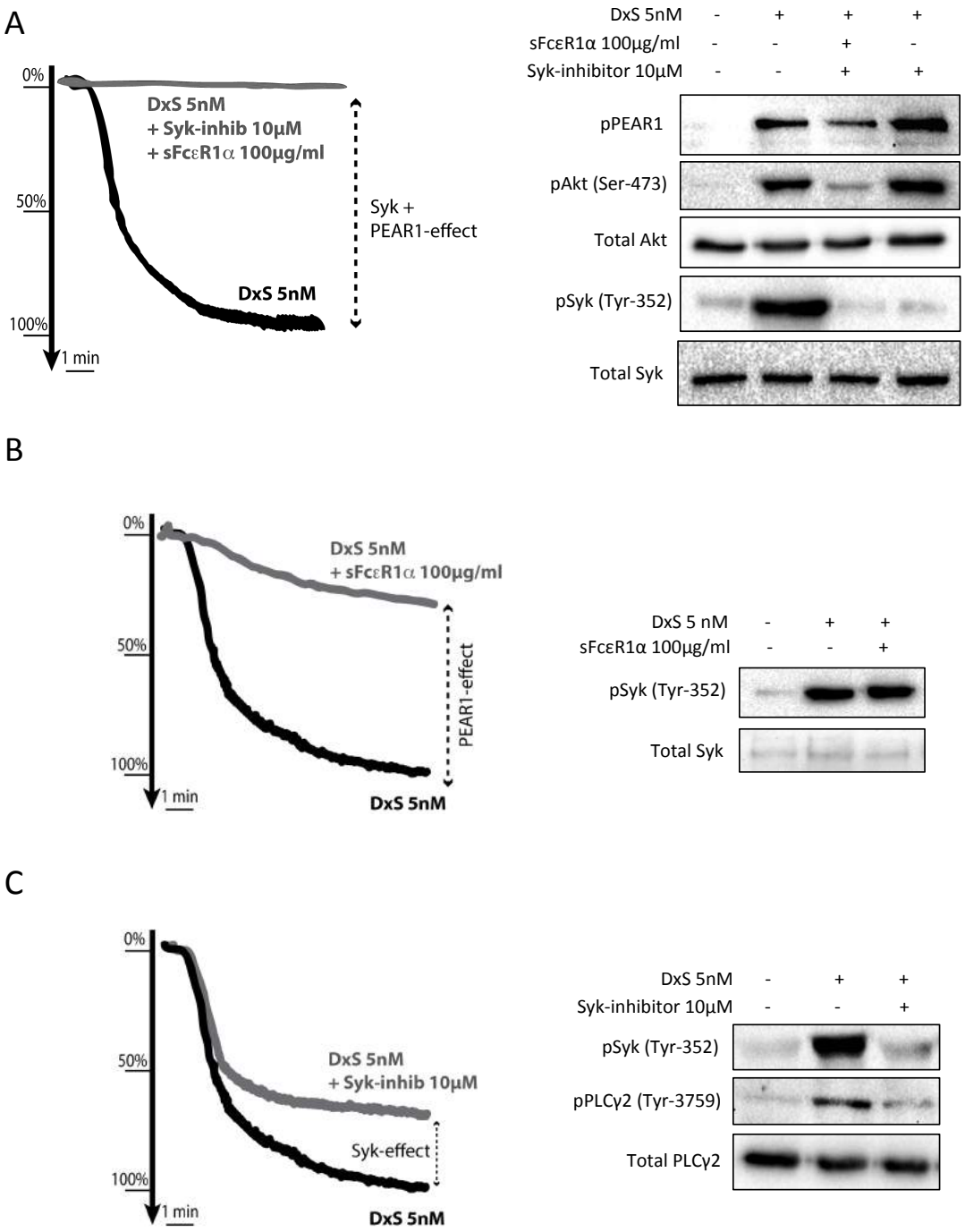

DxS and Pear1-signalling in murine platelets

This is the first manuscript using *Pear1*$^{-/-}$ platelets. Therefore, we firstly investigated whether the Pear1 signalling pathway in murine platelets is comparable to that in human platelets and confirmed the direct activation of Pear1 in murine platelets by DxS as well. Pear1 was

absent in washed *Pear1*$^{-/-}$-platelets (Figure 6A). Similar to human platelets, incubation of washed murine WT platelets with a polyclonal murine anti-Pear1-Ab resulted in phosphorylation of Pear1 and similar phosphorylation was observed after incubation with DxS 0.25 nM (Figure 6B; P-Tyr after immunoprecipitation for Pear1; western blot). Also similar to human platelets, we found that the phosphorylation of Pear1 by DxS was blocked by the SFK-inhibitor PP1 (Figure 6C; P-Tyr after immunoprecipitation for Pear1; western blot) and that DxS induced the phosphorylation of Akt downstream of Pear1, which was blocked by the PI3K-inhibitor LY294002 (Figure 6D; western blot). These findings identify a similar signalling-pathway for PEAR1 in human and murine platelets. In order to avoid indirect Pear1-activation, as previously explained, these signalling experiments were performed under static conditions, again confirming direct binding of DxS to Pear1 (see Figure 3E).

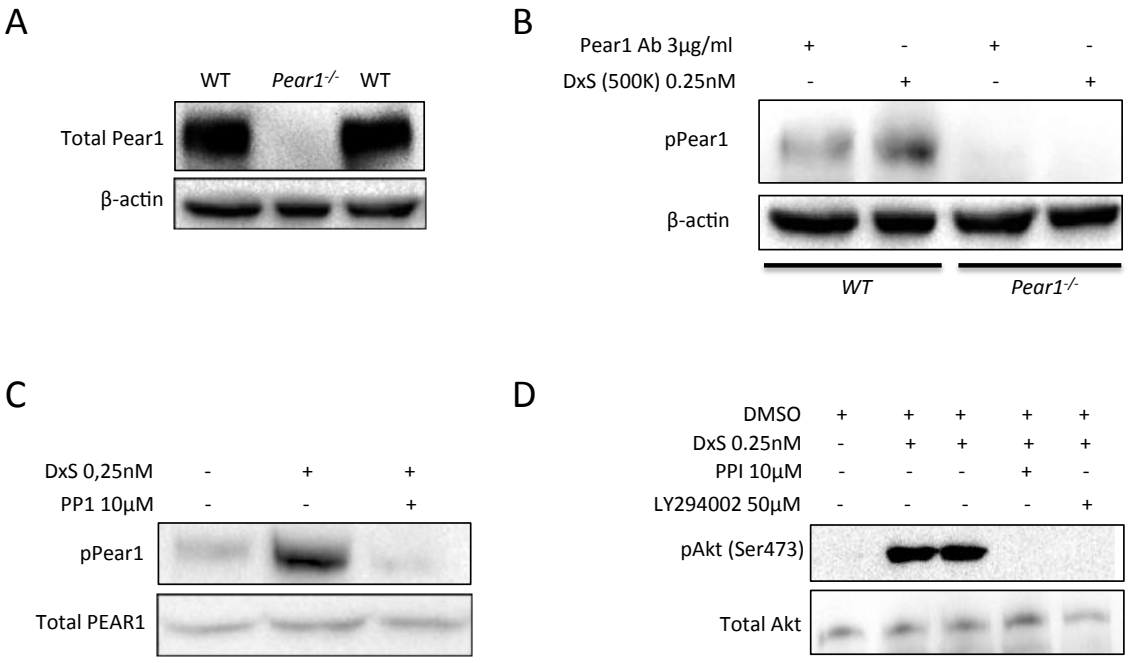

Figure 6 –*Pear1-signalling in murine platelets is mediated via SFK/PI3K, compatible to human platelet PEAR1-signalling*

(A) Confirmation of absence of Pear1-expression in *Pear1*$^{-/-}$ *vs*. WT platelets. (B) Static incubation of WT and *Pear1*$^{-/-}$ platelets with 0.25 nM DxS resulted in Pear1-phosphorylation of WT platelets (compatible with direct DxS-induced Pear1-phosphorylation in murine platelets) and its absence in *Pear1*$^{-/-}$ platelets, used as a negative control. (Western blot; pPear1: P-Tyr after immunoprecipitation for Pear1; Polyclonal Pear1-Ab serves as positive control). (C) DxS-induced Pear1-phosphorylation under static conditions was abrogated by preincubation with PP1 (inhibitor of SFK; 10 µM). (D) Static incubation of two separate murine platelet pools (lane 2 and 3) with DxS resulted in phosphorylation of Akt, which was abolished after preincubation with PP1 or LY294002 (western blot). A-D: washed murine platelets; these experiments were performed under static conditions, again to show direct Pear1/Akt-activation by DxS (Figure 3).

Pear1$^{-/-}$ platelets confirm that DxS-induced platelet aggregation is mediated via Pear1 and CLEC-2/Syk

The DxS-induced platelet aggregation in *Pear1*$^{-/-}$-platelets was reduced and reversible compared to WT platelet aggregation (Figure 7A; left panel), compatible with a weaker Pear1-induced $\alpha_{IIb}\beta_3$-integrin stabilisation and thus decreased aggregate stability. Corresponding western blots of *Pear1*$^{-/-}$ platelets compared to WT platelets resulted in strongly reduced phosphorylation of Akt in *Pear1*$^{-/-}$-platelets whereas phosphorylation of Syk and PLCγ2 was not affected (Figure 7A; right panel). Finally, we showed that the residual DxS-induced platelet aggregation of *Pear1*$^{-/-}$ platelets could be fully abrogated by the Syk-inhibitor BAY 61-3606 (compared to aggregation of WT platelets with DxS; Figure 7B), confirming that both Pear1 and Syk-coupled receptor signalling are sufficient to explain the DxS-induced platelet aggregation.

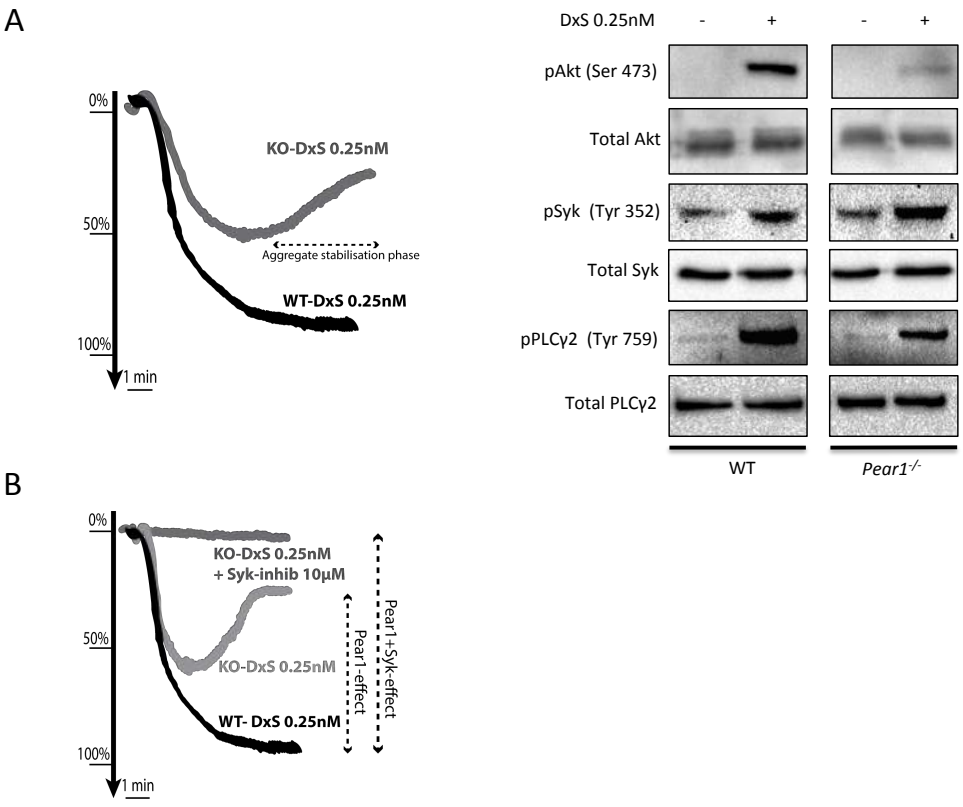

Figure 7 – *Pear1*$^{-/-}$ platelets confirmed that DxS-induced platelet aggregation is mediated via Pear1 and CLEC2/Syk

(A) DxS-induced platelet aggregation in *Pear1*$^{-/-}$ platelets was weaker and displayed decreased platelet aggregate stability compared to WT platelets, compatible with a weaker Pear1-induced $\alpha_{IIb}\beta_3$-integrin stabilisation (left panel); corresponding western blot for phosphorylation of Akt, Syk and PLCγ2 showed a strongly reduced, but not completely abrogated, phosphorylation of Akt in DxS-induced *Pear1*$^{-/-}$ platelet aggregation, whereas the Syk/PLCγ2-activation remained unaffected. (B) DxS-induced platelet aggregation was fully eliminated in *Pear1*$^{-/-}$ platelets after preincubation with a Syk-inhibitor, indicating that Pear1- and Syk-signalling are sufficient to explain DxS-induced platelet aggregation. (A-B: washed murine platelets).

DISCUSSION

DxS was originally evaluated as an anticoagulant with heparin-like properties.[9] The present study was undertaken based on recent findings that high molecular DxS initiated human and murine platelet activation both via a Syk-dependent [5, 10] and a Syk-independent pathway, the latter involving PI3K-mediated phosphorylation of Akt.[5] Alsheri *et al.* recently showed that the Syk-dependent pathway through which DxS induces platelet aggregation is predominantly mediated via CLEC-2 [7], but the platelet surface receptor(s) responsible for the DxS-induced platelet aggregation through the Syk-independent pathway remained to be identified.[5, 7]

Both DxS and PEAR1 induce sustained platelet aggregation via SFK/PI3K/Akt and share the same underlying signalling pathway in human platelets.[3, 5] Therefore, we hypothesized that PEAR1 is responsible for the activation of the Syk-independent pathway upon DxS induced platelet aggregation, compatible with our previous findings, showing that PEAR1-signalling does not recruit Syk (Figure 1). To support this hypothesis, it was crucial to show that DxS directly induced phosphorylation of PEAR1 or in other words, to show that DxS functions as an activating ligand for PEAR1. Therefore, as schematically shown in Figure 3, we analysed whether DxS induces phosphorylation of human platelet PEAR1 under static incubations and under stirring conditions in the presence of an $\alpha_{IIb}\beta_3$-receptor blocker, in order to avoid indirect PEAR1-phosphorylation induced by PEAR1- FcεR1α interactions during platelet-platelet contacts. We also performed competition experiments with an excess of the PEAR1-blocking sFcεR1α-monomer [4] (shielding the receptor and preventing PEAR1-multimerisation) and by an excess of soluble pentameric PEAR1 (s5PEAR1), inhibiting the binding of DxS to platelet PEAR1. All these results identified DxS as a direct activating ligand for PEAR1 and excluded indirect activation of PEAR1 through DxS, as seen during platelet aggregation by classical agonist, e.g. collagen and thrombin.

Next, we showed that the activation of Syk and PEAR1 by DxS suffices to explain the DxS-induced platelet aggregation. Although preincubation with monomeric sFcεR1α eliminated the DxS-induced PEAR1 activity, the remaining DxS-induced human platelet aggregation was substantial. Correspondingly, shielding the PEAR1-receptor during aggregation did not affect

the phosphorylation state of Syk or PLCγ. In counterpart, blocking the phosphorylation of Syk by a selective Syk-inhibitor [11, 12] also mildly reduced the DxS-induced human platelet aggregation, whereas it did not affect phosphorylation of PEAR1. Furthermore, the combined preincubation with selective blockers of both the PEAR1 and Syk-pathway completely abrogated DxS-induced platelet aggregation as well as PEAR1- and Syk-phosphorylation. All these results suggested that both receptors independently but additively initiate DxS $\alpha_{IIb}\beta_3$-mediated human platelet aggregation. To further support our findings, we extrapolated our analyses to murine platelets and confirmed our findings in *Pear1*$^{-/-}$ platelets.

Similarly as previously reported [5], we confirmed that DxS (5 nM) also induces murine platelet aggregation, although we observed no significant differences in aggregation intensity between low dose (0.25 nM) and high dose (5 nM) DxS. We identified the presence of Pear1 on murine platelets and showed for the first time that murine Pear1-signalling is coupled to the SFK/PI3K/Akt-pathway, similarly as for human PEAR1. We showed that murine platelet Pear1 was also directly phosphorylated by DxS under static conditions, to the same extent as reached with a polyclonal anti-mPear1-Ab (positive control). Interestingly, DxS-induced *Pear1*$^{-/-}$-platelet aggregation was reduced and reversible, compared to WT platelet aggregation, compatible with a weaker Pear1-induced $\alpha_{IIb}\beta_3$-integrin stabilisation and thus decreased aggregate stability, in line with our findings in human platelets.[3] The *Pear1*$^{-/-}$ platelet aggregation by DxS was reduced compared to WT platelets but not completely abrogated, confirming that Pear1 is not the only surface receptor on mouse platelets activated by DxS during platelet aggregation, in agreement with previous reports.[7, 10] Corresponding western blots showed that DxS only induced minimal phosphorylation of Akt in *Pear1*$^{-/-}$ platelets, whereas Syk- and PLCγ2-phosphorylation were comparable to that for WT platelets activated by DxS. Ultimately, we found that the DxS-induced platelet aggregation of *Pear1*$^{-/-}$ platelets was abrogated after preincubation with a Syk-inhibitor. This indicated that the remaining platelet aggregation of *Pear1*$^{-/-}$ platelets was fully Syk-dependent, confirming that Pear1- and Syk-signalling both are sufficient to explain DxS-induced murine platelet aggregation, as seen in human DxS-induced platelet aggregation.

The major platelet receptors that employ SFK and Syk are the platelet receptor for podoplanin CLEC-2, the major collagen receptor GPVI and the platelet receptor for von Willebrand GPIb. As mentioned above, Alsheri *et al.* recently found that DxS activates both GPVI and CLEC-2, with a clear preference for CLEC-2 over the collagen receptor. They found reduced platelet aggregation in CLEC-2-deficient and in GPVI/CLEC-2 double deficient platelets, whereas the response to DxS was not altered in GPVI deficient platelets.[7] Although the DxS-induced Akt-phosphorylation was strongly reduced during aggregation of *Pear1*$^{-/-}$ platelets, it was not completely absent. This is in agreement with the recent report of Manne *et al.* [10], who showed that the PI3K/Akt-pathway is a downstream player of CLEC-2, further supporting that CLEC-2 is the Syk coupled receptor responsible for DxS-induced platelet aggregation. However, our data show that PEAR1-activation is the major trigger for the DxS-induced Akt-signalling and that there is only a minor role for Akt in DxS-activated *Pear1*$^{-/-}$ platelets, downstream of CLEC-2.

In conclusion, DxS is a direct ligand of PEAR1, causing $\alpha_{IIb}\beta_3$-activation via the PEAR1/PI3K/Akt-pathway and via the complementary activation of Syk, both in human and murine platelets. The major effect of DxS on Akt-activation results from PEAR1-phosphorylation via c-Src through clustering of the receptor and direct activation of PEAR1, whereas DxS-induced Syk-signalling occurs independently from PEAR1-pathway activation. The direct PEAR1-signalling in human and murine platelets is similar and Pear1 stabilizes murine platelet aggregates.

Further research will have to define whether DxS-induced platelet aggregation can be of importance in certain (physio)pathologic processes and further research in *Pear1*$^{-/-}$ mice will need to address the contribution of Pear1 to thrombus stability in proper models of flow-dependent thrombosis and whether PEAR1 is activated by other negatively charged and sufficiently long biologically active polymers (e.g. dermatan, heparan sulphate, chondroitin sulphate,…).

REFERENCES

1. Nanda N, Bao M, Lin H, Clauser K, Komuves L, Quertermous T, Conley PB, Phillips DR, Hart MJ. Platelet endothelial aggregation receptor 1 (PEAR1), a novel epidermal growth factor repeat-containing transmembrane receptor, participates in platelet contact-induced activation. *J Biol Chem* 2005;**280**:24680-24689.
2. Vandenbriele C, Kauskot A, Vandersmissen I, Criel M, Geenens R, Craps S, Luttun A, Janssens S, Hoylaerts MF, Verhamme P. Platelet endothelial aggregation receptor-1: a novel modifier of neoangiogenesis. *Cardiovasc Res* 2015;**108**:124-138.
3. Kauskot A, Di Michele M, Loyen S, Freson K, Verhamme P, Hoylaerts MF. A novel mechanism of sustained platelet alphaIIbbeta3 activation via PEAR1. *Blood* 2012;**119**:4056-4065.
4. Sun Y, Vandenbriele C, Kauskot A, Verhamme P, Hoylaerts MF, Wright GJ. A human platelet receptor protein microarray identifies FcepsilonR1alpha as an activating PEAR1 ligand. *Mol Cell Proteomics* 2015.
5. Getz TM, Manne BK, Buitrago L, Mao Y, Kunapuli SP. Dextran sulphate induces fibrinogen receptor activation through a novel Syk-independent PI-3 kinase-mediated tyrosine kinase pathway in platelets. *Thromb Haemost* 2013;**109**:1131-1140.
6. Manne BK, Badolia R, Dangelmaier CA, Kunapuli SP. C-type lectin like receptor 2 (CLEC-2) signals independently of lipid raft microdomains in platelets. *Biochem Pharmacol* 2015;**93**:163-170.
7. Alshehri OM, Montague S, Watson S, Carter P, Sarker N, Manne BK, Miller JL, Herr AB, Pollitt AY, O'Callaghan CA, Kunapuli SP, Arman M, Hughes CE, Watson SP. Activation of Glycoprotein VI (GPVI) and C-type Lectin-like receptor-2 (CLEC-2) underlies platelet activation by diesel exhaust particles and other charged/hydrophobic ligands. *Biochem J* 2015.
8. Kauskot A, Vandenbriele C, Louwette S, Gijsbers R, Tousseyn T, Freson K, Verhamme P, Hoylaerts MF. PEAR1 attenuates megakaryopoiesis via control of the PI3K/PTEN pathway. *Blood* 2013;**121**:5208-5217.
9. Walton KW. The biological behaviour of a new synthetic anticoagulant (dextran sulphate) possessing heparin-like properties. *Br J Pharmacol Chemother* 1952;**7**:370-391.
10. Manne BK, Badolia R, Dangelmaier C, Eble JA, Ellmeier W, Kahn M, Kunapuli SP. Distinct pathways regulate Syk protein activation downstream of immune tyrosine activation motif (ITAM) and hemITAM receptors in platelets. *J Biol Chem* 2015;**290**:11557-11568.
11. Yamamoto N, Takeshita K, Shichijo M, Kokubo T, Sato M, Nakashima K, Ishimori M, Nagai H, Li YF, Yura T, Bacon KB. The orally available spleen tyrosine kinase inhibitor 2-[7-(3,4-dimethoxyphenyl)-imidazo[1,2-c]pyrimidin-5-ylamino]nicotinamide dihydrochloride (BAY 61-3606) blocks antigen-induced airway inflammation in rodents. *J Pharmacol Exp Ther* 2003;**306**:1174-1181.
12. Yang WS, Seo JW, Han NJ, Choi J, Lee KU, Ahn H, Lee SK, Park SK. High glucose-induced NF-kappaB activation occurs via tyrosine phosphorylation of IkappaBalpha in human glomerular endothelial cells: involvement of Syk tyrosine kinase. *Am J Physiol Renal Physiol* 2008;**294**:F1065-1075.

Chapter IV – Illustration from "Quarta musculorum Tabula – de humanum corporis fabrica libri septem" – A. Vesalius, 1543

ABSTRACT

Platelet Endothelial Aggregation Receptor 1 (PEAR1) is a cell membrane protein, expressed on platelets and endothelial cells (ECs). PEAR1 sustains $\alpha_{IIb}\beta_3$-activation in aggregating platelets and attenuates megakaryopoiesis via controlling the degree of Akt-phosphorylation. Its role in EC biology is unknown. The aim of this study was to determine the expression of PEAR1 in human endothelium of various tissues and to investigate its role in ECs *in vitro* and in angiogenesis, using *Pear1*$^{-/-}$ mice.

PEAR1 is present on the membrane and on filo- and lamellipodia of human cultured ECs and its expression coincides with CD31 in various tissues. PEAR1-expression is variable in ECs of different origin. Lentiviral knockdown of *PEAR1* in cultured ECs doubled EC proliferation and significantly stimulated EC migration, in turn enhancing *in vitro* tube formation on matrigel through the Akt/PTEN-dependent p21/CDC2-pathway. Even when physiological blood vessel formation was unaffected in *Pear1*$^{-/-}$ mice, neoangiogenesis in these mice was significantly increased both in a hind limb ischemia ligation model (4.7-fold increase in capillary density in the ligated limb of *Pear1*$^{-/-}$ mice compared to ligated limbs in WT-mice) and in a skin wound healing model, resulting in a 2-fold faster wound closure in *Pear1*$^{-/-}$ mice compared to WT-littermates.

We established an inverse correlation between endothelial PEAR1-expression and vascular assembly both *in vitro* and *in vivo*. These findings identify PEAR1 as a novel modifier of neoangiogenesis.

INTRODUCTION

Cardiovascular disease is the leading cause of death worldwide[2], in part due to various interactions between platelets and blood vessels. In response to hypoxia, ischemia, or developmental cues, new capillary sprouts are formed from pre-existing vessels in a process called angiogenesis. These newly formed blood vessels play an important role in crucial processes such as organ growth and repair of wounded tissues while an excessive or insufficient growth of blood vessels contributes to the pathogenesis of numerous disorders (cancer, inflammatory diseases, myocardial infarction, stroke, retinopathy, ...).[3-5]

The formation of vessels is a complex process, requiring a finely tuned balance between numerous stimulatory and inhibitory signals. Endothelial growth factors (*e.g.*, VEGF, FGFs, angiopoietins,…) are of particular interest because of their key role in angiogenesis, wound healing, arteriosclerosis, and inflammatory reactions.[3, 6] A major signalling event downstream of pro-angiogenic factors is the activation of Akt, which is tightly balanced by phosphatidylinositol 3-kinase (PI3K) and phosphatase-and-tensin-homolog (PTEN).[7]

Platelet Endothelial Aggregation Receptor-1 (PEAR1) is a 1034-amino acid transmembrane protein, first described in 2005 as a platelet contact activation receptor by Nanda *et al.* and mainly expressed on platelets and endothelial cells (ECs).[8, 9]

Various genome-wide association and functional genomic studies have suggested a link between common single nucleotide polymorphisms in the *PEAR1*-locus and increased platelet responses to standard platelet activation agonists, both in control populations and various cohorts of patients with cardiovascular disease.[10-13] We have identified a functional role for PEAR1 during platelet activation and demonstrated that PEAR1-signaling sustains the activation of αIIbβ3 in aggregating platelets, favouring the formation of stable platelet aggregates.[14] We also observed that PEAR1 attenuates megakaryopoiesis via controlling the activity of the PI3K/Akt/PTEN-pathway during megakaryocyte progenitor proliferation.[15] Nevertheless, the abundance of PEAR1-expression in ECs and its role in these cells remains unknown.

To understand the contribution of PEAR1 to (neo)angiogenesis, we studied the effect of *PEAR1*-deficiency on EC proliferation, migration and tube formation *in vitro* and in two revascularization models *in vivo* in *Pear1*$^{-/-}$ mice. We were able to match our *in vitro* and *in vivo* data with the phosphorylation status of Akt, a central player in vessel assembly.[16]

MATERIALS AND METHODS

EC culture and isolation

The following cultured human EC types were used: freshly isolated Blood Outgrowth Endothelial Cells (BOECs), freshly isolated Human Umbilical Vein and Artery Endothelial cells (HUVECs and HUAECs), and the immortalized HUVEC cell line EAhy926. Confluent cells were cultured to maximally passage six-seven (approximately 10-20 days), to avoid senescence. Senescence was monitored by measuring *eNOS*-mRNA by qPCR[17] in all non-immortalized cells.

All HUVECs and HUAECs used in this manuscript were freshly isolated from human umbilical veins and arteries of healthy volunteers, the day after birth, following a modification of the method of Jaffe *et al.*[18] Cells were extracted using 0.2% collagenase type 1 (Gibco, Life Technologies, Ghent, Belgium), and seeded on gelatine-coated (0.1%) culture dishes in EBM-2 containing EGM-2 BulletKit (Lonza, Walkersville, USA) and cultured (37°C, 5% CO_2) until they reached confluence. Each *in vitro* experiment, performed in this study, has been performed with HUVECs/HUAECs isolated from at least 3 different umbilical cords (n=3), with each data point being the mean value of 3-4 replicates. Formal permission was given by the ethics committee of the Leuven University Hospitals to use human umbilical cords (Ref nr. ML8663 – Approval S54528) and an informed consent was signed by each mother.

BOECs were isolated from blood of healthy volunteers, as previously reported.[19] A more detailed method description is provided in the online supplement. Informed consent was given for the isolation of the blood samples and this study was granted by the ethics committee of the Leuven University Hospitals.

The macrovascular EAhy926 cell line (a permanent, easily maintained EC line derived from the fusion of human umbilical vein endothelial cells (HUVEC) and A549 (epithelial)cells[20]; American Type Culture Collection USA) was grown in Dulbecco's Modified Eagle Medium (GIBCO, Pailey, UK), 10% fetal bovine serum (FBS), 1% glutamine, 1.5% sodium bicarbonate and 0.5% antibiotics (penicillin, 100U/ml and streptomycin, 100 µg/mL) and was purchased from the American Type Culture Collection (USA). This robust and stable cell line has most of the characteristics of primary cultured endothelial cells.[20]

Human microvascular (µ)ECs were freshly isolated from heart or liver biopsies, as described.[21] For human heart ECs, biopsies were digested with 1.5 mg/mL collagenase I; for human liver ECs, biopsies were digested with 0.08 Wunsch U/mL liberase and 39 U/mL DNAse. After a final wash in PBS, cells were resuspended in

Fluorescence Activated Cell Sorter (FACS) buffer, filtered with a 40 μm mesh and sorted directly in RLT or TRIzol® (+ 1% β-mercapto-ethanol [BME]) for RNA extraction. Sorting was done based on the Tie2+podoplanin-CD45- fraction using a FACS Aria I™ device. For murine μEC-isolation, tissues from 8-12 weeks-old *Tie2-GFP* mice were dissected out, surrounding connective tissue and visible large vessels removed and tissues enzymatically digested using optimized procedures for each organ [*i.e.*, 1.2 U/mL dispase (BD), followed by Percoll gradient centrifugation for liver; 1.5 mg/mL collagenase I for heart], as described.[21] After a final wash in PBS, cells were resuspended in a FACS buffer (PBS/EDTA, 1 mmol/L/HEPES, 25 mmol/L /1% Bovine Serum Albumin (BSA), pH7), filtered through a 40 μm mesh and the GFP-positive fraction was sorted on a FACS Aria I™ (Beckton Dickinson) directly in RLT (Qiagen) or TRIzol® (+ 1% BME) for RNA extraction. Human biopsies were obtained under informed consent. Procedures were approved by the University Hospitals Leuven. All endothelial cell studies were performed conform the declaration of Helsinki.

Isolation of BOECs

Briefly, peripheral blood samples were diluted two-fold in PBS and centrifuged on Ficoll Paque (GE Healthcare, 17-440-02). Buffy coats were pooled and centrifuged multiple times in PBS. Pellets were resuspended in Endothelial Basal Medium-2 (EBM-2; Lonza) medium and seeded on collagen type-I coated dishes (37°C, 5% CO_2) for 30 days (medium was changed daily during the first week and every 2 days thereafter) after which outgrowing colonies were pooled and passaged. After 20-30 days, typical cobble-stone-like colonies appear, showing a exceptionally high proliferative phenotype, so called BOECs. These cells are able to perform de-novo tube formation and are pro-angiogenic. BOECs express a clear endothelial morphology (cobble stone and Weibel-Palade bodies) and phenotype (positive for CD31, VEGR2, CD34, VWF, VE-Cadherin, eNOS), comparable to HUVECs.[19, 22-24] Interestingly, they have higher expression of the pro-angiogenic gene Akt (and lower PEAR1-expression) compared to HUVECs, which is compatible with the controlling function for PEAR1 on Akt/PTEN. BOECs (Figure 1D) were immediately harvested for cDNA-synthesis after isolation.

Generation of lentiviral transfer plasmids

Two short hairpin (sh)-based miRNA lentiviral vectors, previously designed and described by our group, *i.e., shPEAR1*-1461 and *shPEAR1*-2938,[15] were used to suppress *PEAR1*-expression in various EC lineages. Both constructs were equipotent in suppressing *PEAR1* in various ECs (see supplement) and are designated "*shPEAR1*" throughout the manuscript. Most experiments were performed with the *shPEAR1*-1461 lentiviral vector, unless mentioned otherwise. Control cells were transduced with a non-coding dsRed lentiviral vector[15], further referred to as control ECs. *PEAR1*-knockdown was achieved by plating ECs (HUVECs, HUAECs and EAhy926) at 500 $x10^3$ cells per well in 12-well plates and by double transduction with lentiviral particles overnight, both on day 0 and 1. After 72 hours, virally transduced cells were selected for resistance to blasticidin (50 mg/L; Invitrogen).

Real-time quantitative PCR (qRT-PCR)

Total mRNA was extracted with the Qiagen kit (RNeasy mini kit, Hilden, Germany) from cultured cells. cDNAs were synthesized using M-MLV reverse transcriptase (Invitrogen, Ghent, Belgium). Human and murine gene expression was measured using FAM-labelled TaqMan assay products (*PEAR1, CIP1/CIP1, PTEN, HIF1α*, *GAPDH*; Applied Biosystems, Life Technologies, Ghent, Belgium) or via Sybr Green PCR (*FLK1, CDH5, ENOS and GAPDH*; IDT, Leuven, Belgium). qRT-PCR reactions were analysed using an ABI 7000 real-time PCR machine (Life Technologies, Ghent, Belgium). Expression was quantified via the $\Delta\Delta$Ct method[25] and expressed in arbitrary units (1 A.U. is 1 copy for 10^5 copies of housekeeping gene) or in percentage compared to control. Control ECs were used as a reference for *shPEAR1*-transduced ECs. Primer sequences are listed in Table S1 and Table S2.

Western blotting

ECs, serum-starved for 4 hours by reducing FBS to 0.1%, were lysed with ice-cold SDS lysis buffer (10 mmol/L Tris-HCl pH 8, containing 125 mmol/L NaCl and 1% sodium dodecyl sulphate (SDS), 5 mmol/L NaF, 2 mmol/L Na_3VO_4, protease inhibitor cocktail). Proteins were subjected to SDS-polyacrylamide gel electrophoresis (SDS-PAGE) and transferred to nitrocellulose membranes in a Trans-Blot Turbo apparatus (Bio-Rad, Nazareth, Belgium). Membranes were incubated with various primary antibodies overnight: anti-PEAR1-EC (1:1.000; R&D Systems), anti-HIF1α (1:1.000; R&D Systems), anti-β-actin (1:1000; Cell Signaling), anti-Akt-P (1:500; Cell Signaling), anti-Erk1/2-P (1:1.000; Cell Signaling), anti-VEGF and VEGFR2 (1:500; Cell Signaling), anti-p21 (1:1,000; Cell Signaling), anti-CDC2/-Cdc2 (1:1,000; Cell Signaling; membranes were stripped and reprobed for GAPDH as loading control), anti-eNOS-S1177 (1:1000; BD), anti-GAPDH/-Gapdh (1:10.000; Fitzgerald), anti-PTEN/-Pten (1:500; Santa Cruz), anti-p53 (1:1000; Santa Cruz). The PI3K-inhibitor LY294002 was purchased from Calbiochem. After adding horseradish peroxidase-conjugated secondary antibodies, immunoreactive bands were visualized by ECL (Amersham Biosciences, Diegem, Belgium). The band intensity was digitally quantified using a Bio-Rad molecular imager (ChemiDoc XRS+, Nazareth, Belgium).

Immunofluorescence and immunohistochemical staining

ECs were seeded on sterile coverslips overnight (37°C, 5% CO_2). For immunofluorescence (IF), ECs were fixed with 4% paraformaldehyde in cytoskeleton buffer pH 6.9 (0.1 mmol/L PIPES, 2 mol/L glycerol, 1 mmol/L EGTA [ethylene glyco-bis(b-aminoethyl ester)-N,N,N',N'-tetra-acetic acid], 1 mmol/L $MgCl_2$) for 15 minutes at room temperature (RT). ECs were washed with PBS and permeabilised in cytoskeleton buffer, containing 0.2% Triton X-100 for 15 minutes at RT. Filamentous actin was visualized by incubation with rhodamin-labeled phalloidin. ECs were stained with Isolectin GS-IB4 (1/100; Invitrogen; conjugated with Alexa Fluor 568) or were incubated overnight at 4°C with primary antibodies (PEAR1-EC Ab 1 mg/L, p21/CIP1 (1:100; Cell Signaling #2947), F-actin (1:100; Alexa-Phalloidin 488), CD31 (2 mg/L; Dako); and with the appropriate Alexa 488– or 647–labelled secondary antibody (1:200; Invitrogen) for 45 minutes at 37°C. Coverslips were mounted with DAPI Prolong Gold (Invitrogen, Ghent, Belgium), sealed on glass slides and analysed on a Zeiss ELYRA Superresolution Microscope and Zen 2011 or Imager LSM510 Version 3.2 SP2 software (Carl Zeiss).

Immunohistochemistry (IHC) for tissue sections was performed using standard protocols with the following antibody dilutions: Pre-immune Rabbit Ig (1:5; Dako), human anti-PEAR1-EC Antibody (5 mg/L; R&D Systems), murine anti-PEAR1-EC Ab (3 mg/L; R&D Systems), human CD31 (2 mg/L; Dako), murine CD31 (2 mg/L; Dako) and PCNA (2 mg/L; Dako). Briefly, sections were deparaffinised using xylol, quenched with ethanol, and antigen retrieval was performed using Dako Target Retrieval Solution (S169984). Subsequently, we incubated tissues with primary antibodies overnight followed by incubation with secondary antibodies for 45 minutes at room temperature, 30 minutes of streptavidin-HRP (1:100; Perkin Elmer) and 8 minutes of amplification diluent (1:50; Perkin Elmer). Signals were detected using Diaminobenzidine (DAB; Sigma Aldrich). Images were taken on a Zeiss microscope with colour camera (Carl Zeiss, Jena, Germany). Negative controls were obtained for each IF and IHC staining.

Proliferation analysis

Time interval cell counting

Non serum-starved (10% FBS) and serum-starved (0.1% FBS; 4 hours) EAhy926 cells and HUVECs (control *vs. shPEAR1*) were plated in equal numbers ($100x10^3$) in 6-well plates. At fixed time intervals (22, 44 and 66 hours) cells were trypsinized and manually counted by a blinded observer.

Mitotic count

Serum-starved (0.1% FBS; 4 hours) control and *shPEAR1* EAhy926 cells were fixed with 4% paraformaldehyde in cytoskeleton buffer pH 6.9 and stained with DAPI Prolong Gold (Invitrogen, Ghent, Belgium). A blinded observer counted cellular mitoses for both conditions, using a Zeiss fluorescence microscope. These results were confirmed by automatic counting of mitotic figures, using ImageJ software.

S-phase synthesis analysis

Control and *shPEAR1* EAhy926 cells were incubated with EdU (BrdU-alternative; Invitrogen, Ghent, Belgium) following the manufacturer's protocol. Active DNA-synthesis was measured by the Click-iT® EdU Alexa Fluor® 488 Flow Cytometry Assay Kit (Invitrogen).

Scratch wound assay

HUVECs ($4×10^5$) were plated in 60-mm tissue culture dishes and allowed to reach confluence (2–3 days). After aspiration of the medium, a standardized scratch wound was created using a 200 µL micropipette tip. Plates were then rinsed with PBS and incubated (37°C, 5% CO_2) in EBM-2 medium with or without the PI3K-inhibitor LY294002 (dissolved in DMSO; 10 µmol/L) for the duration of the experiment. Wound closure was followed and photographed up to 12 hours. EC migration was determined as the total distance travelled from the initial scratch border. Experiments were analysed by a blinded observer. These experiments were repeated six times (*n*=6) with three different HUVEC isolations.

Matrigel tube formation

The capacity of control ECs and lentiviral transduced *shPEAR1* HUVECs and HUAECs to form capillary-like structures (tubes) was evaluated *in vitro* on matrigel (BD Biosciences, Erembodegem, Belgium). Ice-cold matrigel (200 µl) was added to 24-well plates and allowed to solidify at 37°C for 60 min. ECs (1.3×10^4 cells) were added in 250 µL EBM-2 medium with EGM-2 bulletkit (Lonza, Walkersville, USA) and blasticidin (50 mg/L). Cells were incubated at 37°C with humidified 95% air/5% CO_2 for 16 hours. Tubes were visualized using a Zeiss microscope and photographed. The number of branching points, total tubes and number of tubes were counted manually by a blinded observer and were confirmed using ImageJ. Images were analysed at x50 magnification.

DAF-FM measurement of nitric oxide

DAF-FM diacetate was used for quantification of NO formation in EAhy926 cells as previously reported.[26]

Pear1-knockout mouse

The *Pear1*$^{+/-}$ mouse (*Pear1*$^{tm1a(KOMP)Wtsi}$; C57BL/6N-background) was acquired through courtesy of the International Mouse Phenotype Consortium (IMPC; EPD0299_2_C05). *Pear1*$^{+/-}$ mice were mated to obtain *Pear1*$^{-/-}$ mice and wild-type (WT) littermate controls. Mouse genotyping was performed by conventional PCR. Primers are listed in Table S3. The local Ethics Committee of the KU Leuven approved all animal experimental procedures (Ref Anr. B322201111373 – Approval S53239). All animal procedures were performed conform the guidelines from Directive 2010/63/EU of the European Parliament. All *in vivo* experiments were performed and interpreted by a blinded observer.

Isometric tension measurements:

Twelve-week-old C57BL/6N-mice were sedated with an overdose of intraperitoneal pentobarbital (70 mg/kg) and distal thoracic aortic segments were prelevated and immediately incubated in cold (4°C) Krebs solution. Distal thoracic aortic segments (±2 mm) were mounted between two parallel tungsten wire hooks in 5 ml baths containing Krebs solution (37°C, 95% O_2, 5% CO_2, and pH 7.4) with 118 mM NaCl, 4.7 mM KCl, 2.5 mM $CaCl_2$, 1.2 mM KH_2PO4, 1.2 mM $MgSO_4$, 25 mM $NaHCO_3$, 0.025 mM Ca^{2+} EDTA and 11.1 mM glucose. Isometric tension was measured with force transducers (F10 force transducers type 375; Hugo Sachs Elektronic) connected to a data acquisition system (cDAQ-9171; National Instruments) and was reported in gram (g). Segments were gradually stretched until a stable loading tension of 2 g was attained. Approximately one hour after isolation of the aorta, both rings were exposed to concentrations of phenylephrine (PE, 10 µM; 20 minutes). The PE curve was immediately followed by injection of ACh (10 µM; 20 minutes). Responses to vasodilators were expressed as percentages of the initial contractions (set as 100%) for the WT mice. After three washing steps (5 minutes each) with fresh Krebs solution, rings were exposed again to 10 µM of PE during 20 minutes. The PE curve was immediately followed by injection of 300 µM Nω-nitro-L-arginine methyl ester (L-NAME), followed by 20 minutes of ACh, 10 µM. The difference in maximum responses between rings with and without L-NAME was determined as an index of basal release of NO.[27]

Hind limb ischemia model

Surgery and Isolectin staining gastrocnemius muscle

This method was adapted from Limbourg et al.[6] Briefly, eleven-week-old C57BL/6N-mice were sedated with an intraperitoneal injection of ketamine (125 mg/kg body weight)/xylazine (12,5 mg/kg body weight). The left proximal femoral artery was double ligated and cut in the middle. Laser-Doppler imaging (LDI) was performed immediately after surgery to evaluate the efficiency of flow interruption. At day 21, mice were sacrificed using an overdose of intraperitoneal pentobarbital (70 mg/kg). Gastrocnemius muscles were excised and fixed with 4% paraformaldehyde. Tissue sections were obtained using standard protocols and stained with the Alexa Fluor 568-labeled lectin (GS-IB4, Invitrogen). Micrographs were obtained using a Zeiss fluorescence microscope and isolectin-positive vessels were counted manually. Results were expressed in number of vessels per area in square millimetres.

Laser-Doppler Imaging (LDI)

The animals were placed on a preheated plate (37.4°C) to avoid vasoconstriction by anaesthetic heat loss and sedated with Isoflurane inhalation. A Laser Doppler imager (PIM II – Laser Doppler Perfusion Imager, Lisca AB, Sweden) was used to estimate relative blood flow in the paws. To correct for variables, including ambient light and temperature, calculated perfusion was expressed as a ratio of the ischemic (left) to non-ischemic (right) limb at each time point (LDPIwin-software, Perimed, Sweden). Measurements were performed at a pixel resolution of 64x64. Results per time point were calculated as the mean of 5 images per time point.

Micro-computed tomography (μCT) visualization

The vasculature in the gastrocnemius muscle was visualized 21 days after unilateral (left) femoral artery ligation in *Pear1*$^{+/+}$ (WT) and *Pear1*$^{-/-}$ mice. Therefore, mice were sedated with an intraperitoneal injection of ketamine (125 mg/kg body weight)/xylazine (12,5 mg/kg body weight) and perfused with 0.2% adenosine for vasodilatation, followed by 4% paraformaldehyde for fixation, subsequently saline to wash out the fixative and finally with a preheated solution of 30% barium sulphate (Micropaque, Guerbet) as contrast agent in 2% gelatin. Mice were stored on ice at 4°C overnight to solidify the gelatin with the contrast agent in the vessels. After overnight solidification, limbs were dissected out, stored in PBS and imaged with the SkyScan 1172 micro-CT system, using a peak tube voltage of 50 kV, a current of 200 mA, a filter of 0.5 mm aluminium and an exposure time of 590 ms. The FDK-algorithm of the manufacturer (NRecon, SkyScan, Kontich, Belgium) was applied to reconstruct the dataset into a 3D-image with isotropic voxel size of 8 μm. The dataset was downsampled by a factor two for reasons of computational feasibility and subsequently visualized using custom-made software developed in MeVisLab (MeVis Medical Solutions AG and Fraunhofer MEVIS, Bremen, Germany). Therefore, the bone was manually delineated and excluded from the volume of interest. The blood vessels were segmented using hysteresis thresholding and fragments smaller than 10 voxels were excluded to minimize the influence of noise, rendering a visualization of the vascular network in the gastrocnemius muscle. The methods used to harvest muscles tissues and the methods to extract protein and mRNA in order to determine the concentration of HIF1α, VEGF and VEGFR2 are described in the online data supplement.

Ligated muscle tissue harvest and protein/cDNA extraction:

Tissues were prepared as previously described;[28] after an intraperitoneal injection of ketamine (125 mg/kg body weight)/xylazine (12,5 mg/kg body weight), the left proximal femoral artery was twice ligated and cut in the middle as previously described. At day 4, mice were sacrificed using an overdose of intraperitoneal pentobarbital (70 mg/kg). The gastrocnemius muscles (both at the ligated and non-ligated limb) were surgically excised from tendon to tendon. The most proximal part of the muscle was used for mRNA-extraction (immediately incubated in TRIzol® and ribolyzed for cDNA-synthesis). In brief, tissue samples were homogenized in 200 µL TRIzol reagent per 50 to 20 mg tissue and incubated for 10 minutes at room temperature; afterwards, 40 µL chloroform per 200 µL of TRIzol reagent was added. After centrifugation at 13.000*g* for 20 minutes at 4°C, the RNA-containing colourless upper aqueous phase of the mixture was collected, precipitated, and washed with isopropyl alcohol and 75% ethanol. RNA concentration was determined by spectrophotometry. For protein extraction, middle and distal parts of the gastrocnemius muscle samples were weighed (300-400 mg), pulverized in liquid nitrogen, and homogenized in 3 ml of 10 mM Tris (pH 7.4) and 100 mM NaCl. The suspension was then centrifuged twice at 8.000*g* at 4°C for 15 min. The protein content of the supernatant was determined by Bradford assay[29] and the pellet was resuspended in 250 µL of SDS lysis buffer.

Total muscle VEGF concentrations:

Total VEGF protein concentrations in the muscle supernatants were determined by a solid state ELISA system with a murine Quantikine VEGF ELISA kit (R&D Systems) as previously described.[29]

Skin wound healing model

Mice were sedated with an intraperitoneal injection of ketamine (125 mg/kg body weight) / xylazine (12,5 mg/kg body weight). Full-thickness skin wounds (29 mm^2) were made on the back of *Pear1*$^{-/-}$ mice (C57BL/6N) and their littermates, using a dermal biopsy puncher. Wounds were splinted with a silicone ring (Fig. 15A), moistened with saline and covered with a Tegaderm dressing. Every other day, a digital picture of the wounds was taken (Canon digital Camera) and wound dimensions were measured under Isoflurane anaesthesia and the dressing was renewed. Mice were sacrificed at day 4 or day 8 using an overdose of intraperitoneal pentobarbital (70 mg/kg). Granuloma tissue was dissected using a Leica M650 microscope and tissues were pooled for each group in SDS-loading buffer and ribolyzed for conventional Western blotting.

Statistical analysis

For some experiments, the number of replicates is presented in the figure legend. The replicate number is the total number of analyses done to calculate an averaged value, statistically treated as 1 data point (*e.g*. *n*=3, 6 replicates represents 3x6 measurements, for which 3 averages are calculated, reported as *n*=3). Results are expressed as mean values plus or minus SEM. Statistical significance was evaluated with unpaired Student's t-tests, One-way or Two-way ANOVA with Bonferroni's post-test correction or linear regression. (*) Indicates $P<0.05$.

RESULTS

PEAR1-expression in human ECs

In this first study addressing the role of PEAR1 in ECs, we performed a detailed analysis of its expression in various human tissues (Fig. 1). IHC-staining for PEAR1 and the specific EC marker CD31 confirmed comparable expression of both proteins in human liver, lung and kidney, substantiating expression of PEAR1 in ECs primarily (Fig. 1A). Double IF staining for CD31 and PEAR1 co-localized both proteins in the endothelium of the human renal glomerulus (Fig. 1B). IF staining for PEAR1 in freshly isolated HUVECs (Fig. 1C; upper panel) and confluent immortalized HUVECs (EAhy926 cells; Fig. 1C, lower panel) revealed PEAR1 in the cell membrane and in the filo- and lamellipodia of ECs. *PEAR1* mRNA was detected in blood outgrowth endothelial cells (BOECs), in ECs from human umbilical cord (EAhy926, HUAECs and HUVECs) and in microvascular ECs (µECs) isolated from the vascular beds of human liver and heart and lysed immediately after isolation. The mRNA expression of *PEAR1* was heterogeneous with the lowest expression in less differentiated ECs (BOECs) and the highest in freshly isolated µECs from heart and liver tissue. mRNA of HUAECs and HUVECs (lysed immediately after isolation from umbilical cords) and cultured EAhy926 ECs revealed intermediate levels of *PEAR1* mRNA (Fig. 1D). Protein levels (WB) were low in BOECs and comparable for HUAECs, EAhy926 and HUVECs. Protein levels of µECs could not be determined, due to the small amount of ECs that could be isolated from the human liver- and heart biopsies only.

PEAR1-knockdown enhances EC proliferation

To investigate the role of PEAR1 in ECs, we first performed a knockdown of *PEAR1* by double miRNA-based short hairpin constructs (*shPEAR1*). This was achieved via two different *shPEAR1*-constructs, both reducing *PEAR1* mRNA-expression by approximately 70% (Fig. 2A, HUVECs and EAhy926; Fig. 3) and confirmed by the concomitant reduction of PEAR1-protein levels (Fig. 2B; cultured HUVECs and EAhy926; WB) compared to control ECs. Similar results were observed in cultured *shPEAR1* HUAECs (not shown). *PEAR1*-knockdown increased the proliferation rate in various ECs. Twenty-two hours after seeding, a two-fold higher number of HUVECs was observed in the *shPEAR1* group compared to the control group, both in non-

starved (Fig. 2C) and starved (not shown) ECs. Similar results were seen when EAhy926 cells were studied (Fig. 2C, right panel). Evaluation of serum-starved EAhy926 cell proliferation by flow cytometry showed an increased incorporation of the fluorescent BrdU-analogue EdU in the *shPEAR1* vs. control cells (Fig. 2D). The assessment of the number of mitoses (DAPI-stained control and *shPEAR1* EAhy926 cells; 22 hours after seeding) by a blinded observer confirmed a two-fold increase of ECA mitoses in *shPEAR1 vs.* control ECs (17.3±2.1% *vs.* 9.5±0.9%; $P<0.05$). Thus, in steady state, 70% knockdown of *PEAR1* results in a doubled cell count *in vitro*. This interpretation is supported by low *PEAR1*-levels in ECs with a high proliferative phenotype (*e.g.*, BOECs; Fig. 1D) and by our finding that highly proliferative ECs of a pyogenic granuloma (a fast growing endothelial skin tumour) express lower PEAR1, compared to the expression in ECs of normal skin in the same tissue section (Fig. 4).

Figure 1: PEAR1-expression in human endothelial cells
(A) Immunohistochemical staining for PEAR1 and CD31, illustrating PEAR1-protein expression in ECs of human liver, lung and kidney, as indicated (x100 left panel; x1000 middle panel; x100 right panel). (B) IFA staining (x630) for CD31 (red), PEAR1 (green) and merge (white colour represents the calculated overlap) in a human kidney glomerulus, illustrating the co-localization of PEAR1 and CD31. (C) Co-immunofluorescence staining for F-actin (red) and PEAR1 (green), localizes PEAR1 at the EC border and filo-/lamellipodia in HUVECs (x630; upper panel) and confluent EAhy926-cells (lower panel; x200). (D) A Comparative qRT-PCR (mean±SEM *vs. GAPDH*; arbitrary units (A.U.); $n=3$) for human *PEAR1* mRNA. Low expression in cultured Blood Outgrowth Endothelial Cells (BOECs), intermediate levels in cultured EAhy926 cells (immortalized HUVECs), HUVECs and HUAECs; high expression in microvascular ECs (µEC) from human liver and heart. For BOECs, HUVECs, HUAECs and EAhy926 cells, the protein expression of PEAR1 was confirmed by Western blot. Results are given as mean±SEM.

AB

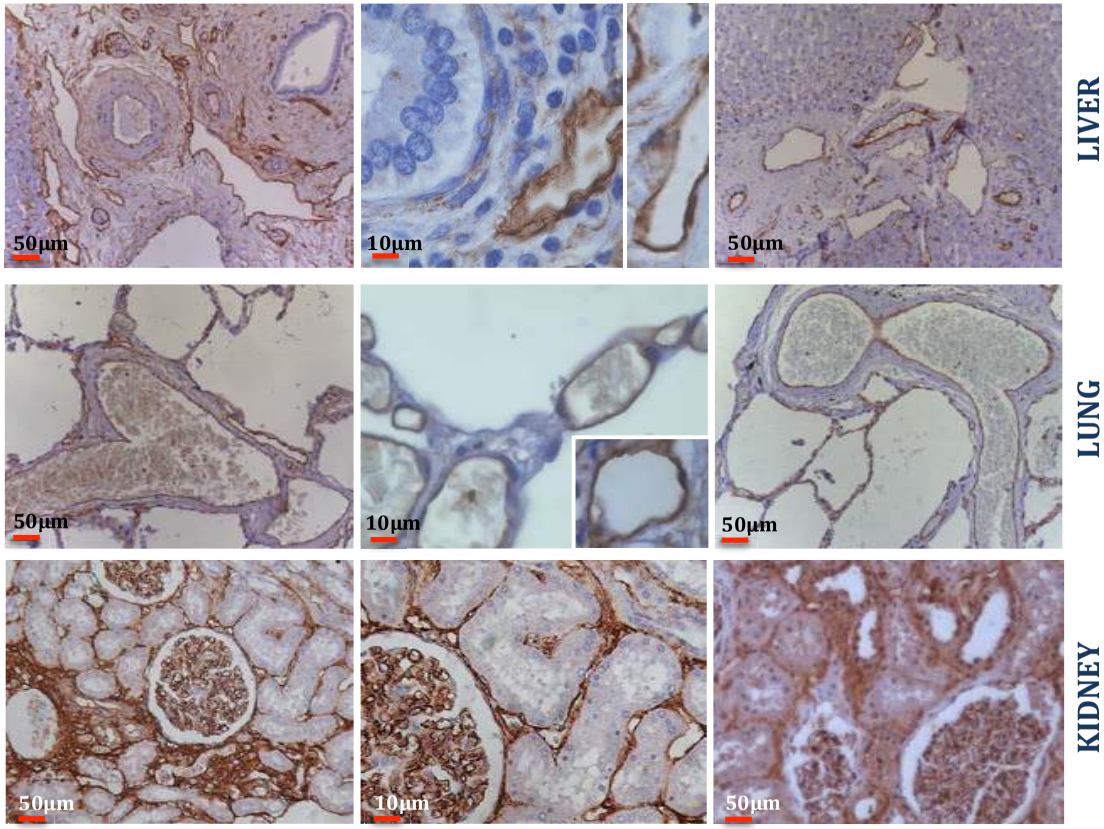
PEAR1
PEAR1
CD31
LIVER
LUNG
KIDNEY
50µm
10µm
50µm
50µm
10µm
50µm
50µm
10µm
50µm

BB

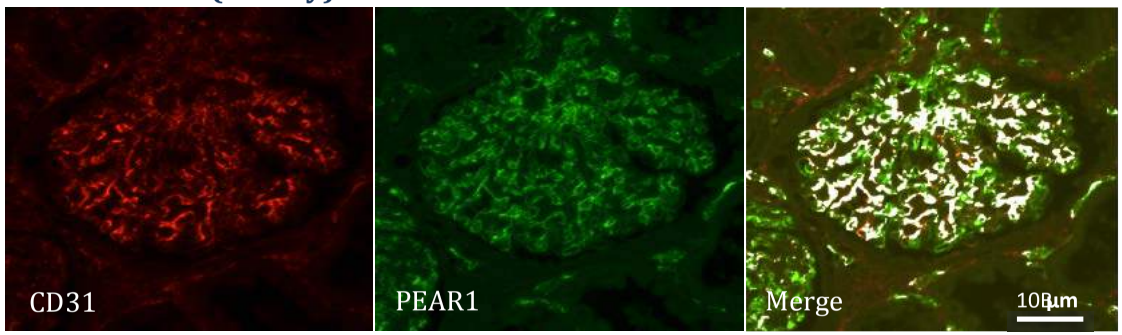
Glomerulus (kidney)
CD31
PEAR1
Merge
10µm

CB

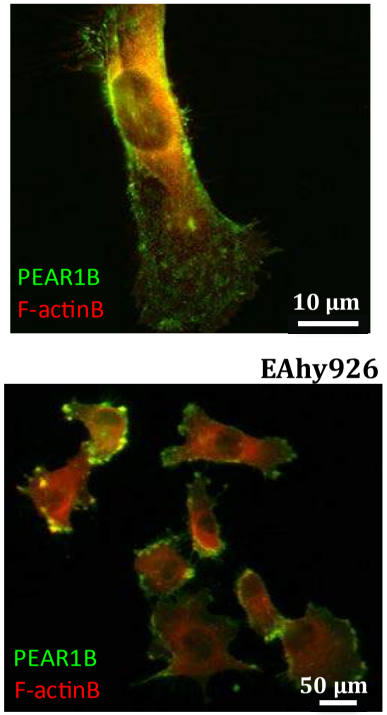
HUVEC
PEAR1B
F-actinB
10 µm
EAhy926
PEAR1B
F-actinB
50 µm

DB

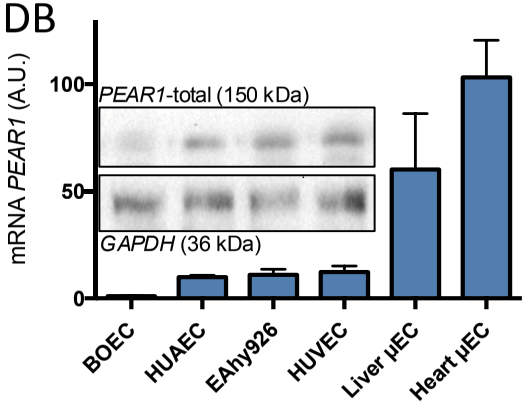
mRNA PEAR1 (A.U.)
100
50
0
PEAR1-total (150 kDa)
GAPDH (36 kDa)
BOEC
HUAEC
EAhy926
HUVEC
Liver µEC
Heart µEC

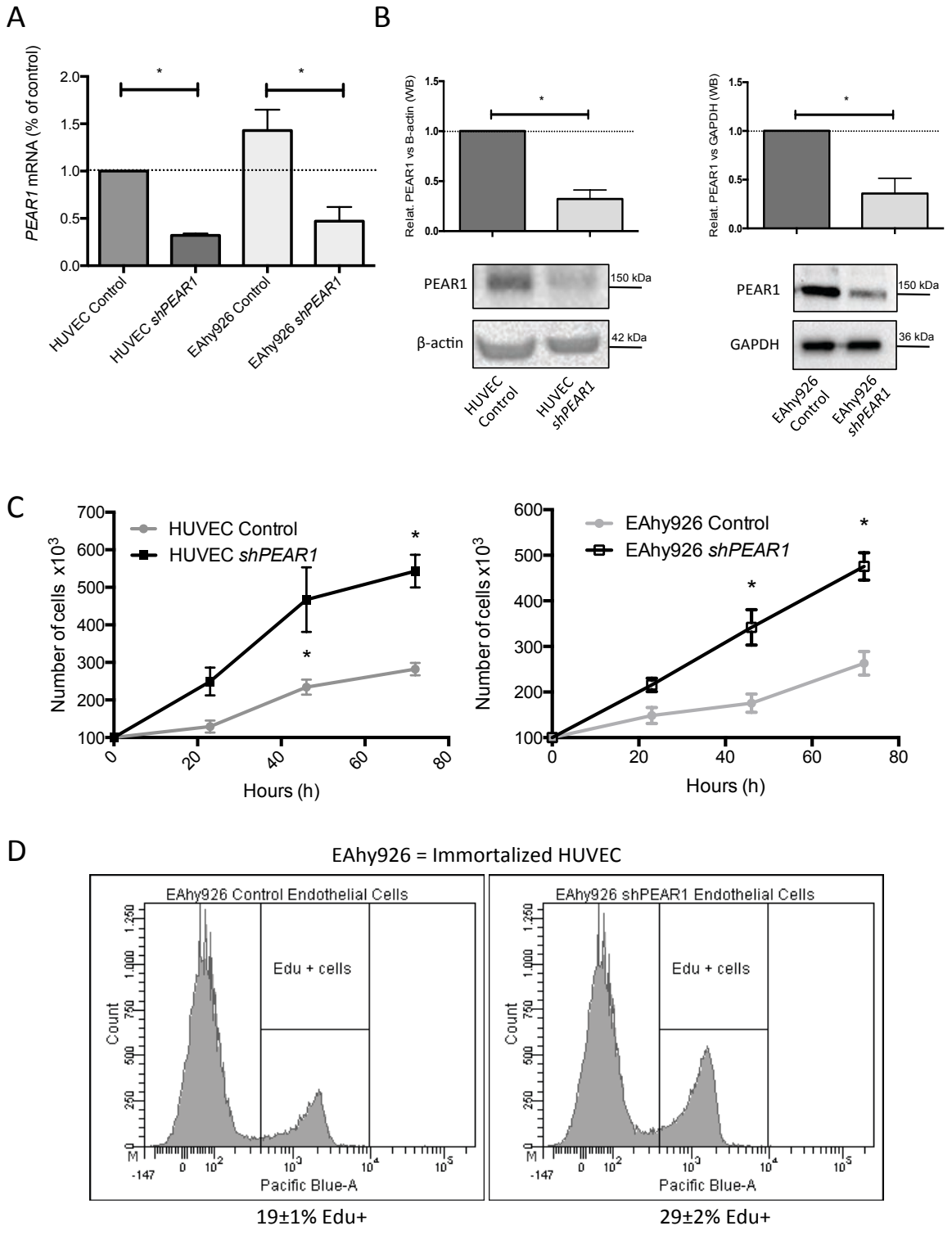

Figure 2: Lentiviral knockdown of *PEAR1* enhances EC proliferation

(A) Double *shPEAR1* lentiviral transduction of HUVECs and EAhy926 cells resulted in ± 70% reduction of human *PEAR1* mRNA compared to control ECs (*n*=5; relative *vs.* *GAPDH* housekeeping gene; unpaired t-test). (B) Corresponding suppression of PEAR1-protein in *shPEAR1* HUVECs (± 67% protein reduction) and EAhy926 cells (± 65% protein reduction) *vs.* control ECs (*n*=4; results are relative *vs.* β-actin or GAPDH; unpaired t-test). (C) ECA counts 23, 46 and 72 hours after seeding of *shPEAR1* HUVECs *vs.* control and of *shPEAR1* EAhy926 cells *vs.* control showed a two-fold higher cell number per well after *PEAR1*-knockdown (*n*=3; 6 replicates per time point; two-way ANOVA). (D) Flow cytometric measurements of DNA-synthesis via EdU incorporation for *shPEAR1* EAhy926 cells *vs.* control ECs (29±1% *vs.* 19±1% EdU positive cells; *n*=3). Results are given as mean±SEM (* $P<0.05$).

A

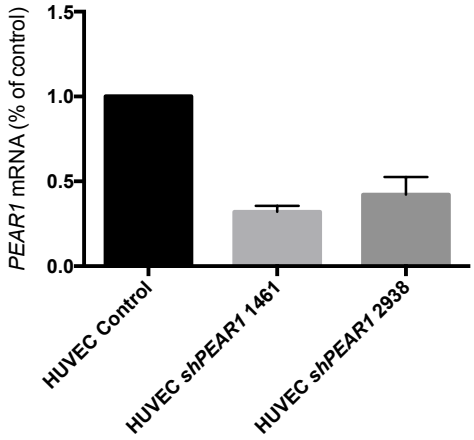

Figure 3: Two short hairpin (sh) based miRNA lentiviral vectors, i.e. *shPEAR1*-1461 and *shPEAR1*-2938 equally suppressed PEAR1-expression in HUVECs (qPCR). Control cells were transduced with a non-coding DsRed lentiviral vector (control ECs). $n=3$; results are given as mean±SEM.

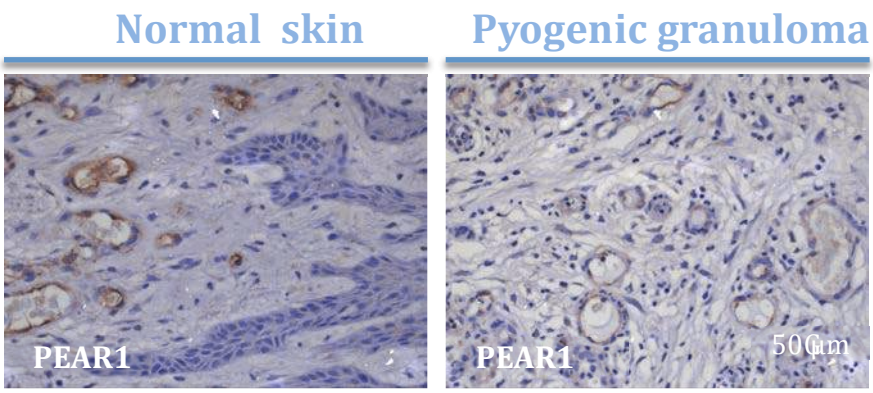

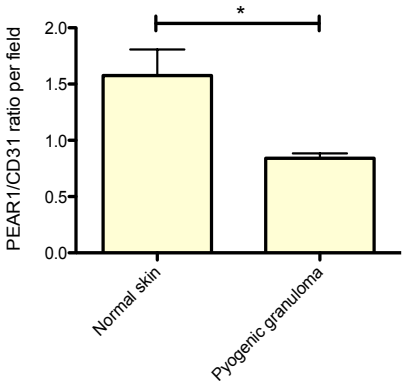

Figure 4: PEAR1 controls EC proliferation. (A) Representative PEAR1 staining of normal human skin (x400; left) and hyperproliferative skin endothelioma on the same tissue section (x400; pyogenic granuloma; right). (B) A PEAR1/CD31 intensity-ratio for normal skin compared to pyogenic granuloma (ImageJ; mean±SEM for 2 different tumors, with 6 fields per tumor analyzed for PEAR1 and CD31; unpaired *t*-test; * $P<0.05$; results are given as mean±SEM).

Knockdown of PEAR1 modulates EC proliferation via Akt/p21/CDC2

Our previous work demonstrated a tight link between PEAR1 and PI3K/Akt-activation in platelets and megakaryocytes.[14, 15] To unravel the mode of action of PEAR1 in ECs, we selected the immortalized EAhy926 cells to avoid effects of senescence throughout different cell passage numbers. Western blots revealed constitutively increased phosphorylation of Akt (Ser473) in *shPEAR1 vs.* control ECs (Fig. 5A; 5.1-fold increase) both in confluent and non-confluent cells, indicating a confluence-independent enhanced Akt-phosphorylation state. The MAPK-pathway (Erk1/2) was not affected by *PEAR1*-knockdown (Fig. 14). At the same time, we found a decrease of PTEN-expression (HUVECs and EAhy926) and p21/CIP1 (EAhy926 cells) in *shPEAR1* ECs, both at protein (WB; *n*=3) and mRNA-level (qRT-PCR; *n*=3; Fig. 5A). p21/CIP1 is an Akt-controlled nuclear suppressor of EC proliferation via p34/CDC2, a cyclin that regulates G2-to-M transition during cell division. Accordingly, we found a 4.7-fold upregulation of p34/CDC2 in the *shPEAR1* EC group (Fig. 5A). This upregulation of p34/CDC2 in *shPEAR1* ECs was reversed to basal CDC2-levels in the presence of the PI3K-inhibitor LY294002 (Fig. 5B), indicating a direct link between the phosphorylation of Akt and CDC2-expression, explaining the association between increased Akt-P and the upregulation of CDC2 in *shPEAR1* ECs. IF-staining of EAhy926 cells (*shPEAR1 vs.* control ECs) for p21 and nuclear DAPI showed a nuclear localization of p21 in control ECs and a strong shift of p21 towards the cytoplasm in *shPEAR1* ECs, consistent with increased mitosis (Fig. 6). A critical role for Akt in proliferation and angiogenesis can be mediated by the Akt-downstream effector eNOS. However, the mRNA-expression of *eNOS* and the degree of phosphorylation of eNOS (S1177) was not affected in *shPEAR1* ECs. We confirmed that *shPEAR1* ECs did not produce higher levels of NO as measured with DAF-FM diacetate (Fig. 7A; EAhy926 cells and Fig. 7B; HUVECs) and that functional relaxation experiments of WT thoracic aortic segments vs. *Pear1*$^{-/-}$ aortic segments did not show any differences in Ach-induced aortic relaxation or during PE-induced vasoconstriction in the absence of NO-production (Fig. 7C). We conclude that PEAR1 controls the expression of PTEN and that the drop of PTEN in *shPEAR1* ECs is associated with the increased phosphorylation status of Akt, leading to enhanced cell cycle progression due to an increase in CDC2-expression (Fig. 5C), in turn caused by a shift of nuclear p21/CIP1 towards the cytoplasm and a downregulation of total p21/CIP1-levels.

Knockdown of PEAR1 enhances EC migration *in vitro*

Migration of ECs is an essential process in (neo)angiogenesis[30] and is known to be mediated via phosphorylation of Akt.[30] Since PEAR1 was found to be highly expressed at filo- and lamellipodia of ECs, in EC-ruffles and at the migratory border of low confluent ECs (Fig. 8A), suggesting a role for PEAR1 in EC migration, we performed *in vitro* migration assays and demonstrated enhanced cellular migration of *shPEAR1* HUVECs *vs.* control ECs. Migration was analysed within a 12 hours time window to avoid confounding interference of effects on EC proliferation. Analysis of the migration distance in a cell migration assay revealed up to 3-fold higher migration for the *shPEAR1* ECs (Fig. 8B). Interestingly, this enhanced *shPEAR1*-induced migration was abrogated in the presence of the PI3K-inhibitor LY294006 (10 µmol/L; Fig. 8C).

PEAR1 controls *in vitro* tube formation

Since both EC proliferation and migration are important players in blood vessel formation, we further investigated whether the *PEAR1*-knockdown would affect tube formation in a matrigel assay, using control and *shPEAR1* HUVECs and HUAECs. Tubes were evaluated 16 hours after EC seeding (Fig. 9A). We observed a significant increase in the number of branching points, number of tubes and of the total tube length in *shPEAR1* HUVECs, compared to control HUVECs (Fig. 9B). Similar results were found for both *shPEAR1* constructs (Fig. 9C) and for lentiviral transduced HUAECs (not shown). The mRNA levels of 3 typical EC markers (*KDR/VEGFR2*, *CD31/PECAM1* and *VE-cadherin/CDH5*) were mildly upregulated during tubulogenesis but no significant differences between control and *shPEAR1* ECs were observed (Fig. 10), suggesting that endothelial identity was not affected by *PEAR1*-knockdown. The expression of *PEAR1* and *PTEN* was measured in control and *shPEAR1* HUVECs by qRT-PCR at the beginning and at the end of the tube formation process (Fig. 9D). *PEAR1* was upregulated in control ECs during tubulogenesis (left panel), in parallel with upregulation of *PTEN* mRNA levels (right panel). Interestingly, in *shPEAR1* ECs, *PTEN*-expression was very low, both before and during tubulogenesis (right panel). These findings suggest that PEAR1 controls the *in vitro* tube formation, leading to enhanced tubulogenesis upon its absence, compatible wit a role in EC proliferation and migration.

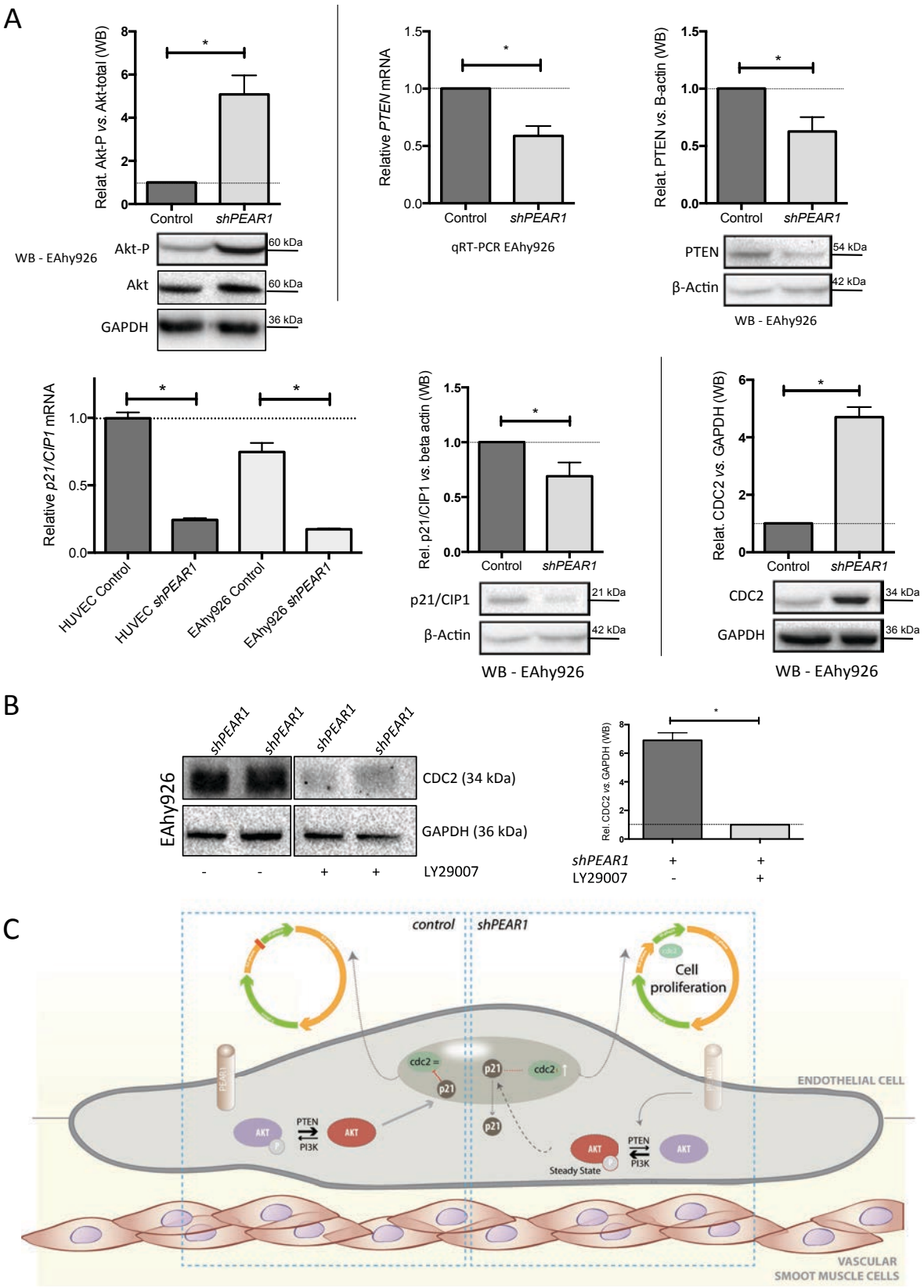

Figure 5: Knockdown of *PEAR1* modulates EC proliferation via Akt/p21/CDC2

(A) A Five-fold A increased A Akt-P A levels A in A confluent A *shPEAR1* EAhy926 A cells A *vs.* A confluent A control A ECs A and A decreased A PTEN-levels A (both A at A protein A level A (Western A blot; A reduction A by A 37±7%; A *n*=4) A and A mRNA-level A (qRT-PCR; A reduction A by A 42±8.2%; A EAhy926 A cells; A *n*=4). A Decreased A p21/CIP1-expression, A a A nuclear A suppressor A of A CDC2, A both A at A mRNA-level A (qRT-PCR; A HUVECs A (*n*=4) A and A EAhy926 A cells A (*n*=4); A reduction A by A 76±2%) A and A protein A level A (Western A blot; A EAhy926 A cells A (*n*=4); A reduction A by A 53±9%) A in A *shPEAR1* A ECs A *vs.* A control A ECs; A approximately A 5-fold A elevated A protein A expression A level A of A CDC2A (a A cyclin A that A regulates A G2-to-M A transition A in A cell A division; A Western A blot; A *n*=4) A in A *shPEAR1* A ECs. A β-actin A and A GAPDH A served A as A reference A proteins A for A Western A blot; A qRT-PCR A results A are A relative A *vs.* A *GAPDH* A housekeeping A gene. A (B) A Incubation A of A *shPEAR1* A EAhy926 A cells A with A the A PI3K-inhibitor A LY294002 A (60 A minutes; A 10 A μmol/L) A reversed A the A increased A levels A of A CDC2A in A *shPEAR1* A ECs A to A levels A of A CDC2A in A control A ECs A (*n*=4). A (C) A Schematic A overview; A Knockdown A of A *PEAR1* A in A ECs A results A in A a A steadily A increased A phosphorylation A levels A of A Akt, A resulting A in A a A downregulation A of A nuclear A p21/CIP1, A shift A of A p21/CIP1 A towards A the A cytoplasm, A reduction A of A the A nuclear A p21/CIP1-mediated A suppression A of A CDC2A and A ultimately A resulting A in A increased A EC A proliferation A due A to A an A enhanced A CDC2-driven A cell A division. A Results A are A given A as A mean±SEM; A unpaired A *t*-test A was A applied; A * *P*<0.05. A

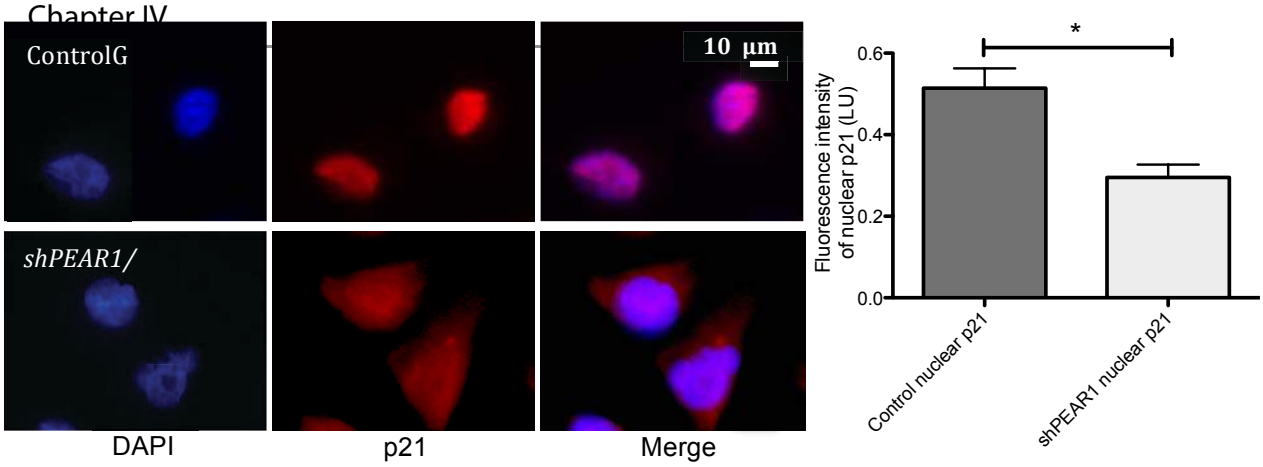

Figure 6: Immunofluorescent staining of p21/CIP1 in *shPEAR1* EAhy926 *vs.* control ECs (x100; left panel). A Quantification of fluorescence intensity of nuclear p21 (right panel). (*n*=5; Results are given as mean±SEM; unpaired t-test; **P*<0.05).

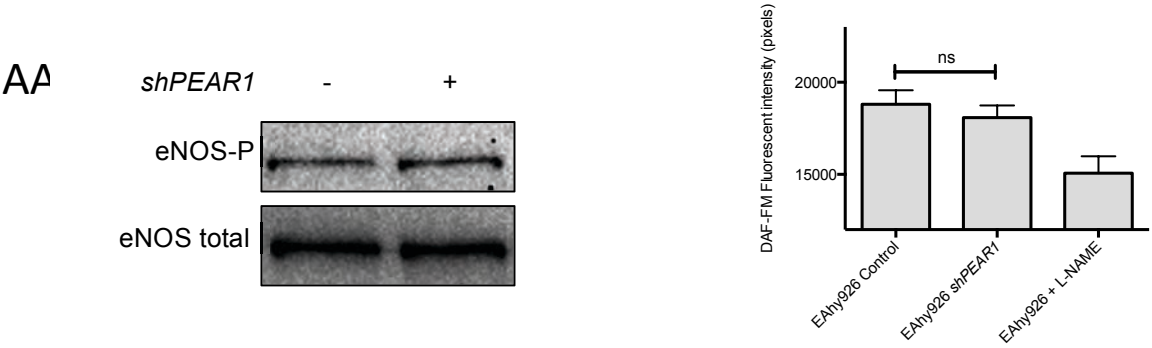

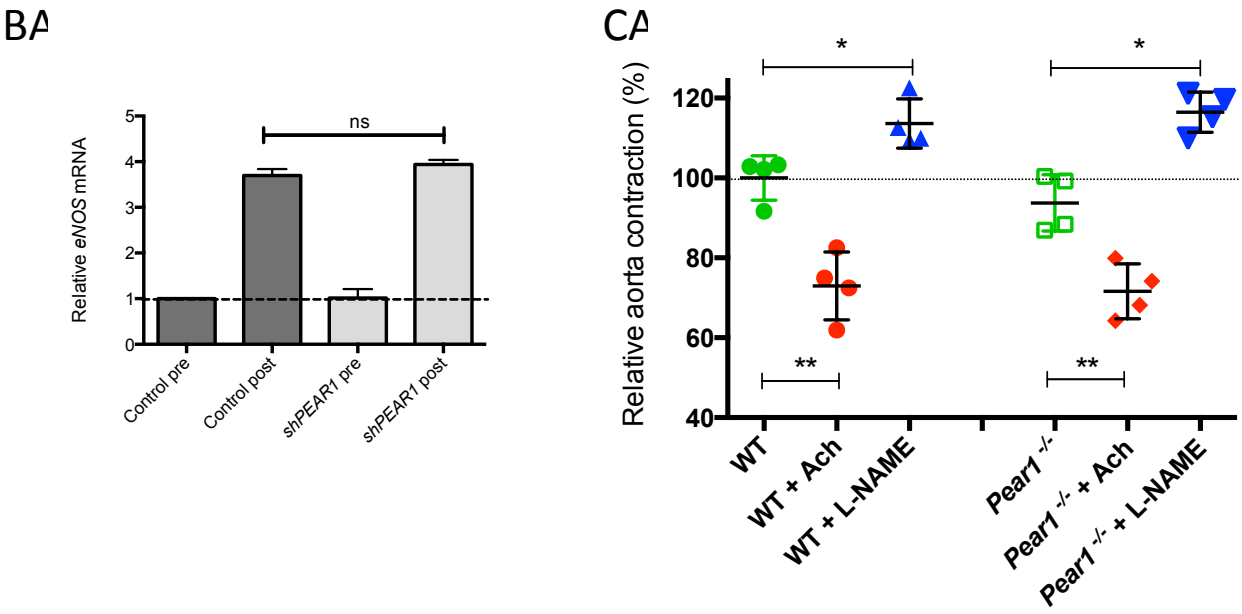

Figure 7: (A) Similar eNOS-P levels in *shPEAR1* EAhy926 ECs *vs.* control ECs (WB; left panel). Absence of effect by the PEAR1 knockdown on baseline NO-production, analysed with DAF-FM dye (right panel; *n*=10; L-NAME served as negative control). (B) Upregulation of total eNOS mRNA during tube formation of control HUVECs; similar eNOS-expression after tube formation of shPEAR1 HUVECs (*n*=3; relative vs. GAPDH-housekeeping; one-way ANOVA with Bonferroni's post hoc test). (C) Isometric tension measurements of distal thoracic aortic segments of *Pear1*$^{-/-}$ (*n*=4) vs. control (WT)-aorta's (*n*=4). Ach-induced relaxation and L-NAME induced contraction were plotted relative to the initial PE-induced aortic contraction, set to 100% for the WT-mice. No differences in Ach induced aortic relaxation or in L-NAME induced contraction were observed between WT and *Pear1*$^{-/-}$ mice (**P*<0.05; unpaired t-test; results are given as mean±SEM).

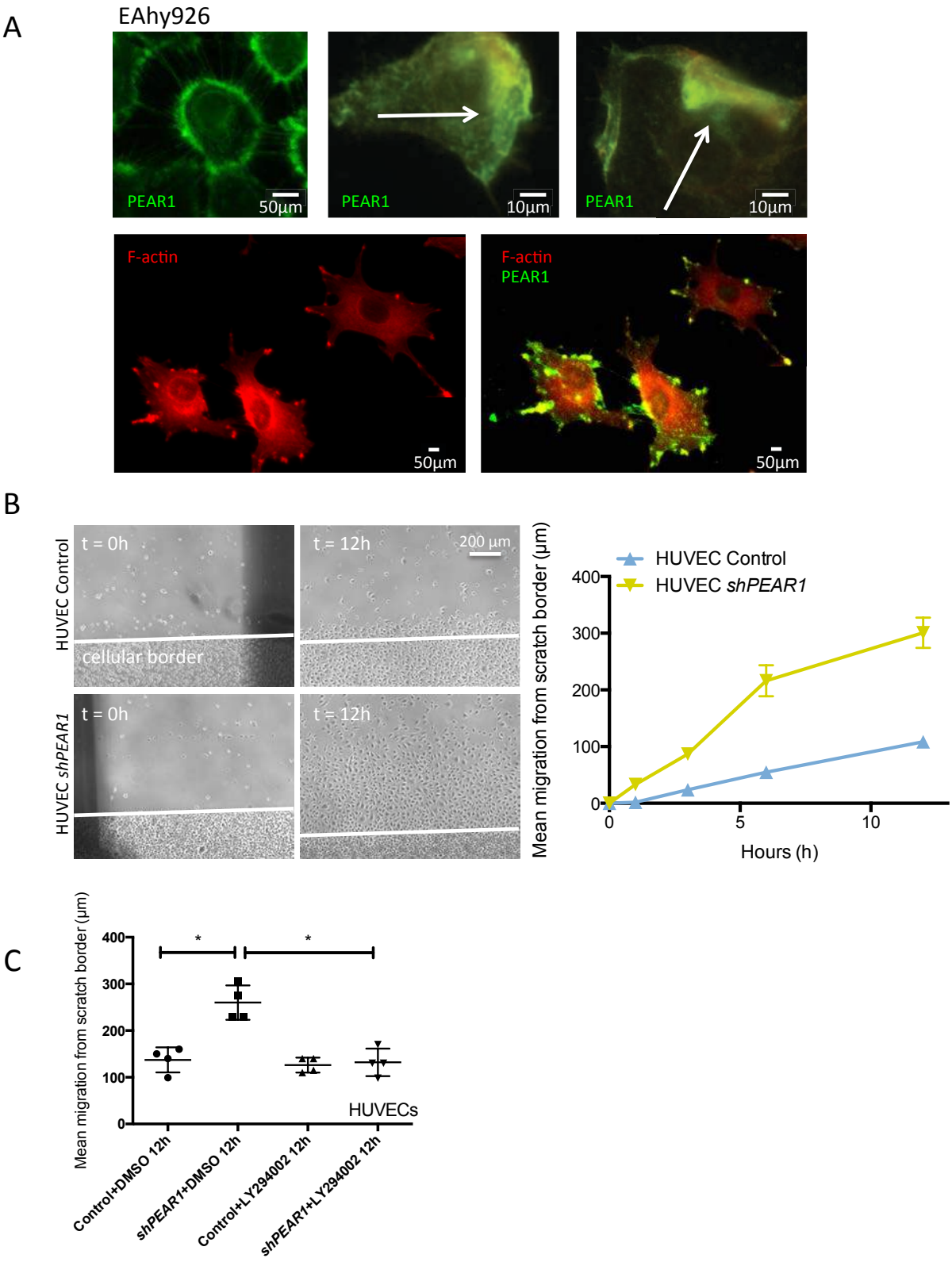

Figure 8: Knockdown of *PEAR1* stimulates EC-migration
(A) Immunofluorescent staining of EAhy926 ECs (low confluence) for PEAR1 and/or F-actin, showing high expression of PEAR1 in filo- and lamellipodia (left upper panel), at the migratory EC border (middle upper panel) and in an endothelial ruffle (right upper panel). We confirmed high expression of PEAR1 at migrating filopodia by co-staining with F-actin (lower panel). (B) Enhanced migration of the EC scratch-border of *shPEAR1* HUVECs *vs.* that of control ECs (10x; $n=6$; $^*P<0.05$; linear regression analysis). (C) Enhanced migration of *shPEAR1* HUVECs *vs.* WT ECs upon 12 hours was reversed in the presence of the PI3K-inhibitor LY294006 (10 µmol/L; 10x; $n=4$; $^*P<0.05$; one-way ANOVA with Bonferroni's post-hoc test). Results are given as mean±SEM.

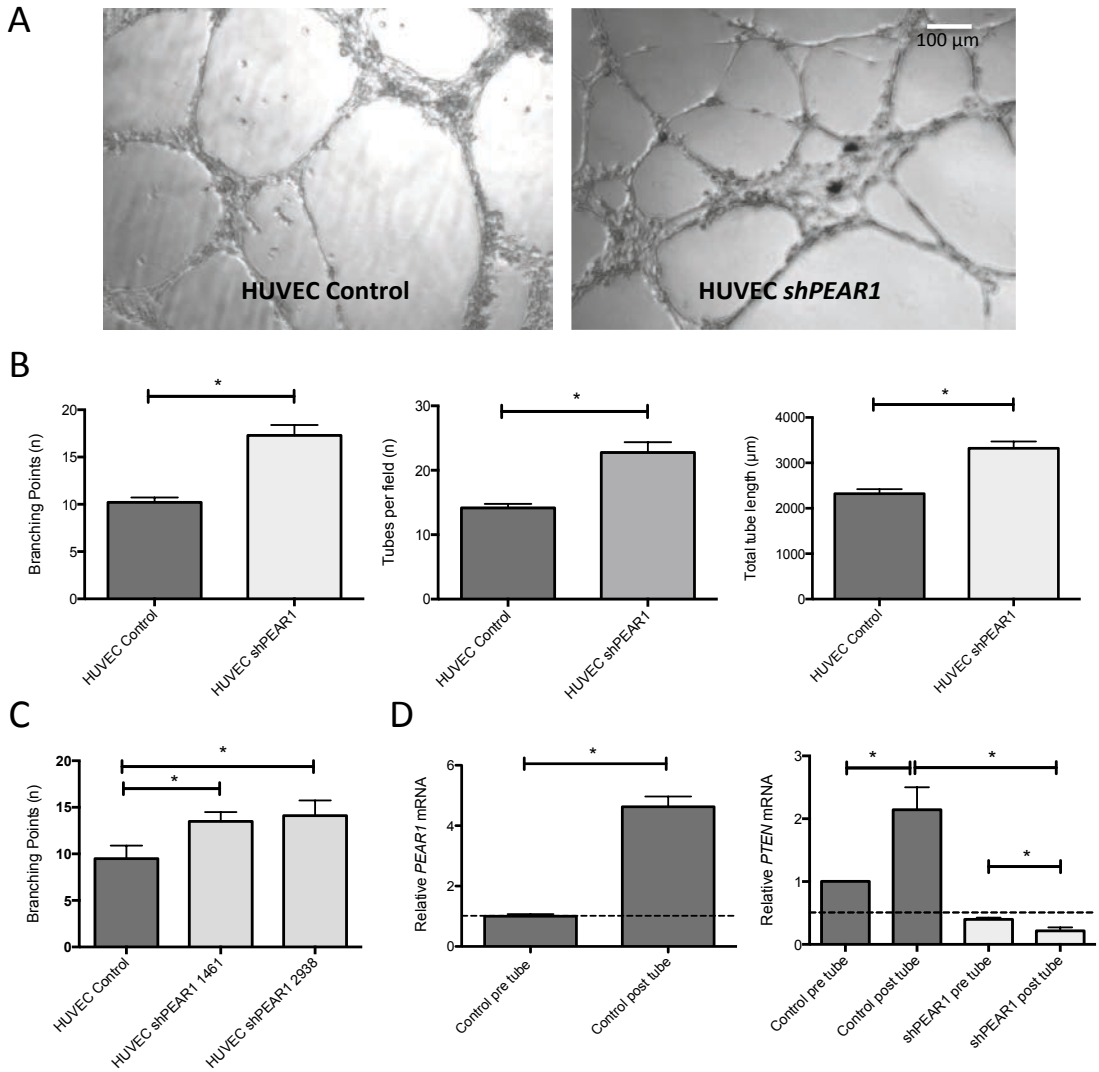

Figure 9: PEAR1 modulates *in vitro* tube formation (A) Tubes on matrigel of control HUVECs (left) and *shPEAR1* HUVECs (right) 16 hours after seeding (x200; *n*=5). (B) 1.7-Fold increase in the number of branching points, 1.6-Fold increase in the number of tubes per field and a 1.5-fold increase in total tube length following knockdown of *PEAR1* in *shPEAR1* HUVECs *vs.* control HUVECs (*n*=5; unpaired t-test). (C) Increased *in vitro* tube formation on matrigel was also achieved after double lentiviral transduction with a second *shPEAR1*-construct. Number of branching points for control HUVECs and HUVECs treated with *shPEAR1* viral constructs 1461 and 2938 (*n*=3; one-way ANOVA with Bonferroni's post-hoc test). (D) Upregulation of *PEAR1* mRNA (left panel) and *PTEN* mRNA (right panel) during tube formation of control HUVECs; in contrast, lower levels of *PTEN* mRNA in *shPEAR1* HUVECs, both prior and after tube formation of *shPEAR1* HUVECs (right panel; *n*=3; relative vs. *GAPDH*-housekeeping gene; one-way ANOVA with Bonferroni's post-hoc test). Results are given as mean±SEM (* $P<0.05$).

A

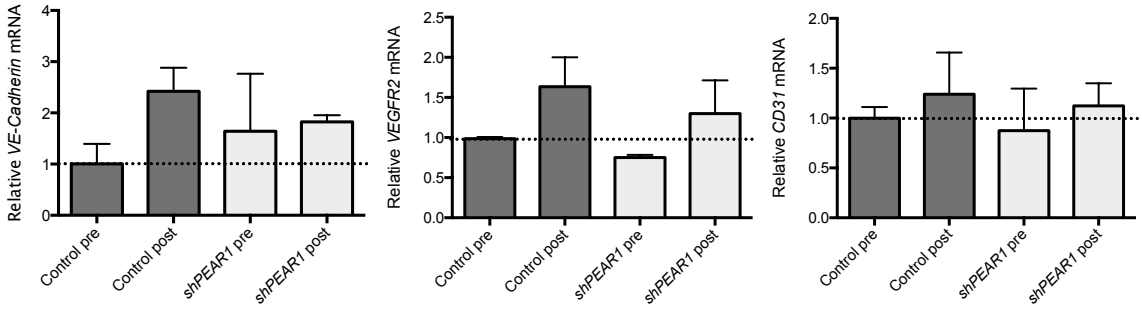

Figure 10: A mRNA A levels A of A 3A typical A ECA maturation A markers A (*KDR/VEGFR2, CD31/PECAM1 and VE-cadherin/CDH5*) A before A and A after *in vitro* A matrigel A tube A formation A of A HUVECs; A no A significant A differences A were A observed. A (*n*=4; A results A are A relative A versus A GAPDH A housekeeping A gene; A results A are A given A as A mean±SEM). A

Expression of Pear1 in different murine ECs

Subsequently, we investigated the Pear1-expression pattern in mice by qRT-PCR and immunohistochemistry (IHC) and confirmed expression of *Pear1* (*vs. Gapdh*) in freshly isolated and pure[21] µECs of murine liver and heart (qRT-PCR; Fig. 11A). Absence of Pear1 in blood vessels from *Pear1*$^{-/-}$ mice (skin) confirmed the specificity of the anti-Pear1 antibody used (IHC; not shown). Phenotyping by the International Mouse Phenotyping Consortium (IMPC) did not reveal any overt cardiovascular phenotype in unchallenged *Pear1*$^{-/-}$ mice (https://www.mousephenotype.org/data/genes/MGI:1920432). Correspondingly, CD31 staining (Fig. 11B) and H&E-staining (not shown) of murine lung, kidney and liver tissue did not reveal structural differences or fluctuations in blood vessel density between *Pear1*$^{-/-}$ mice and their WT-littermates.

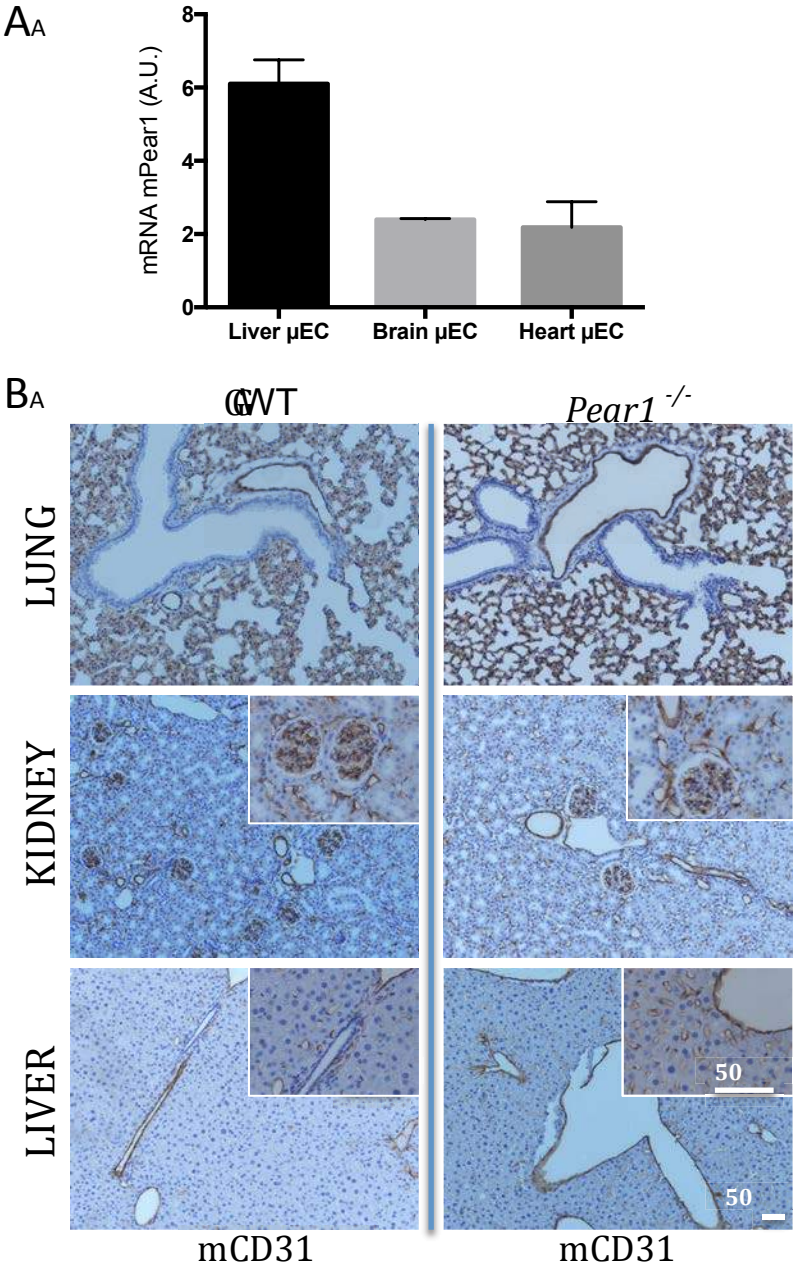

Figure 11: A) Comparative qPCR (mean±SEM *vs.* Gapdh) for murine *Pear1* (*mPear1*) mRNA in freshly isolated µECs from WT murine lung, kidney and liver. B) IHC staining for murine CD31 and lung, kidney and liver in WT vs. *Pear1*$^{-/-}$ mice.

Pear1 controls neoangiogenesis *in vivo*

Next, we examined whether the role of PEAR1 in tubulogenesis *in vitro* could be at play during angiogenesis *in vivo* in mice. Therefore, two established models of neoangiogenesis in *Pear1*$^{-/-}$ mice were studied.

Ischemia-induced angiogenesis in Pear1$^{-/-}$ *mice*

Hind limb ischemia is a pre-clinical model for peripheral arterial disease, where both arteriogenesis and angiogenesis are induced upon femoral artery ligation. After the ligation of the femoral artery, increased shear stress triggers outward collateral remodelling in the adductor muscle, while the more distal gastrocnemius becomes hypoxic, triggering an angiogenic response in the lower leg.[6, 31] Therefore, we adopted this hypoxia model to investigate angiogenesis in the gastrocnemius muscle after ligation of the femoral artery in *Pear1*$^{-/-}$ mice *vs.* littermates. We non-invasively monitored blood flow recovery in the paws by means of a Laser Doppler system over a period of 21 days (Fig. 12A; left panel; representative images). The average perfusion in each limb was calculated. Calculated perfusion was expressed as a ratio of the ligated (left) to non-ligated (right) limb. Blood flow in the ischemic limb gradually recovered with time in both WT and *Pear1*$^{-/-}$ mice. However, the blood flow recovery was significantly faster in *Pear1*$^{-/-}$ mice compared to WT from 7 to 14 days after ligation (Fig. 12A; left panel). We evaluated the level of angiogenic sprouting in the gastrocnemius muscle by IF staining for the endothelial marker isolectin GS-IB4 three weeks after the induction of ischemia.[6, 31] The density of isolectin-positive capillaries was 2.4-fold higher in *Pear1*$^{-/-}$ compared to WT-mice, which supports the enhanced angiogenesis in the gastrocnemius muscle in *Pear1*$^{-/-}$ mice after chronic hind limb ischemia (Fig. 12B). Capillary density in non-ligated limbs of *Pear1*$^{-/-}$ was comparable with that in WT-mice; supporting our findings that PEAR1 does not affect embryological vascular development (Fig. 12B). A 3D reconstruction by micro-CT (CT-angiography after barium-instillation) of the gastrocnemius at the ligated side (day 21) confirmed a stronger angiogenic response and hence denser vascular network in the *Pear1*$^{-/-}$ mice, compared to WT-littermates (representative images in Fig. 12C). Micro-CT images of non-ligated hind limbs revealed no differences in vessel density between *Pear1*$^{-/-}$ mice and WT-mice (Fig. 13); in agreement with our histological analysis. Various reports have shown a role for PTEN in modulating angiogenesis.[32-36] *E.g.* in pancreatic cancer cells, PTEN knockdown increases VEGF secretion, cell proliferation, migration of co-cultured vascular ECs and enhances tube formation by HUVECs[37]; high levels of PTEN were shown to inhibit VEGF-induced sprouting and capillary tube formation.[37, 38] The inhibitory effect of PTEN on EC proliferation and neo-angiogenesis is due to suppression of Akt-phosphorylation.[37]

Since enhanced Akt-phosphorylation can result in enhanced VEGF-activity (Fig. 14A), we assessed the concentration of these major pro-angiogenic molecules VEGF/VEGFR in enhanced neo-angiogenesis upon knockout of *Pear1*. We performed analyses for HIF1α, VEGFR2 (considered the major receptor that transduces the effects of VEGF in ECs)[39] and total-VEGF on homogenized tissues of ischemic and non-ischemic gastrocnemius muscles since muscle specific VEGF/VEGFR2 levels play a crucial role in EC proliferation and angiogenesis.[40] Tissue levels of HIF1α provide a marker of hypoxia/ischemia and are known to be elevated in the gastrocnemius muscle until 3-4 days after femoral ligation.[41] Therefore,

HIF1α levels and VEGF/VEGFR2 levels were measured at day 4 post-ligation, since this is also the starting point of enhanced neo-angiogenesis in *Pear1*$^{-/-}$ mice. Although we found a strong increase of HIF1α protein expression in the ischemic limb at day 4 post-ligation (Fig. 14B), no significant differences between WT and *Pear1*$^{-/-}$ mice could be observed. Also VEGF-levels in the non-ligated limb were comparable between WT and *Pear1*$^{-/-}$ mice (Fig. 14C). The protein expression levels for VEGFR2 were significantly upregulated after ligation, compatible with previous reports[28], but again no significant differences in VEGFR2-expression between WT and *Pear1*$^{-/-}$ mice were observed (Fig. 14E).

Since VEGF is a strong activator of Erk1/2 via VEGFR2[42] and since Erk1/2 can potentiate the activity of HIF1α[1], we investigated the phosphorylation status of p42/p44 in cultured EAhy926 ECs in the absence of VEGF in the EC medium. No differences in phosphorylation state of p42/p44 were observed when WT ECs were compared to *shPEAR1* ECs (Fig. 14D), again confirming that VEGF-production by ECs is not affected upon PEAR1-KD. It has been reported that the tumour suppressor gene p53 suppresses cell proliferation and tube formation/angiogenesis through inhibition of the PI3K/AKT/mTOR pathway and through inhibition of HIF1α, although its role in angiogenesis is not clear at this moment.[43] In view of these data, we measured the total p53 protein levels in WT ECs *vs.* shPEAR1 ECs, but observed no differences in p53 protein expression levels (Fig. 14D).

Capillary wound density and wound closure in Pear1$^{-/-}$ *mice*

Wound healing is the result of a complex interaction between keratinocytes, various growth factors and vascularization.[44, 45] We performed a standardized wound-healing assay to study EC proliferation during wound closure in *Pear1*$^{-/-}$ *vs.* WT-littermates. IHC confirmed ECs as the only Pear1-positive cells in murine skin tissues (Fig. 16; left panel) *vs.* the expected absence of Pear1 in skin of *Pear1*$^{-/-}$ mice (Fig. 16; right panel). Fig. 15A (left panel) reports wound healing up to day 8. At day 2, we observed a significantly decreased wound size in *Pear1*$^{-/-}$ compared to WT littermates. This difference in wound closure in *Pear1*$^{-/-}$ persisted until day 8 (time point of sacrifice; Fig. 15A; middle panel). In a separate set of experiments, we confirmed the accelerated wound closure in *Pear1*$^{-/-}$ mice (Fig. 15A; right panel). These mice were sacrificed at day 4 to allow for Western blot and histological analysis at an early stage of the healing process. When blood vessel density (per mm^2 wound) was measured via IHC at day 8 (CD31 staining; Fig. 15B), quantification in *Pear1*$^{-/-}$ mice *vs.* WT littermates revealed significantly larger CD31-positive areas per surface ratio (*i.e.* reflecting a higher blood vessel density) in the wounds of *Pear1*$^{-/-}$ mice. IHC showed a strong ingrowth of CD31$^+$ vessels in the granuloma tissue of the *Pear1*$^{-/-}$ wound at day 4, while the invasion of newly formed vessels in the granuloma tissue of the WT mice was still absent (Fig. 15C). The higher number of blood vessels coincided with an increased proliferative response, as shown by PCNA-staining in the wound bed of *Pear1*$^{-/-}$ mice *vs.* their WT-littermates; Fig. 17). To correlate the underlying mechanistic pathway responsible for this enhanced vascularization and proliferation in *Pear1*$^{-/-}$ mice with our *in vitro* findings, we pooled the granuloma tissue of 5 mice per group, performed Western blot analyses for mCD31, mAkt-P and mCdc2 and found a strong upregulation of these 3 key-players in *Pear1*$^{-/-}$ *vs.* WT mice (Fig. 15D). Thus, increased blood vessel formation contributes to the enhanced wound closure rate in *Pear1*$^{-/-}$ mice; ECs being the only Pear1-positive cells in the regenerating wound.

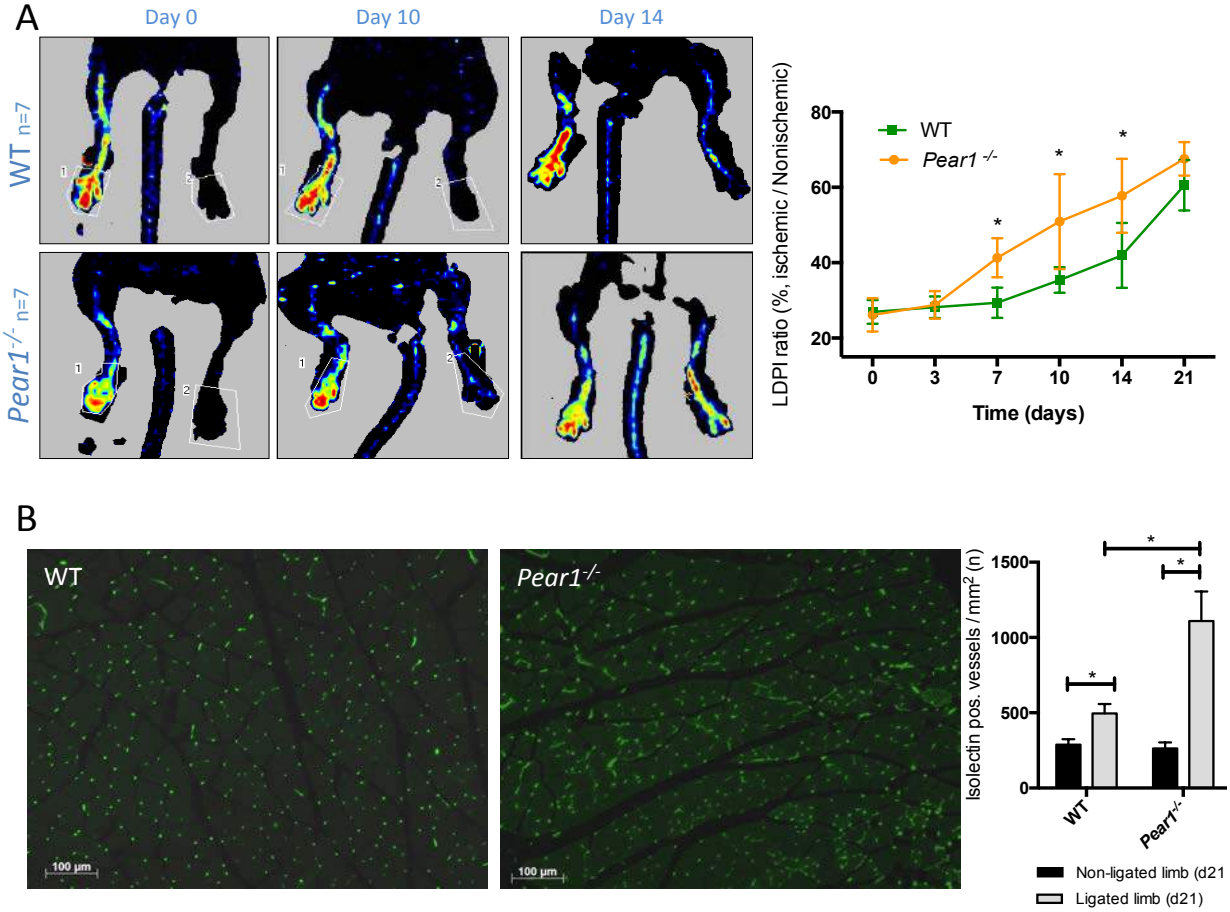

Figure 12: Enhanced ischemia-induced angiogenesis in *Pear1*$^{-/-}$ mice. A) Laser Doppler blood flow analysis of the hind limbs of WT (*n*=7) and *Pear1*$^{-/-}$ (*n*=7) mice after ligation of the left femoral artery. The recovery of blood flow was significantly accelerated in *Pear1*$^{-/-}$ limbs compared to WT from 7 to 14 days after ligation. Ligated/non-ligated hind limb blood flow ratio was measured at days 0, 3, 7, 14 and 21 after left femoral artery ligation. Results are expressed as the ratio (%) of the ligated hind limb to non-ligated limb perfusion (left panel; repeated time measurements ANOVA with Bonferroni post-hoc test; blinded observations). Representative Laser-Doppler Images (LDI) just after (day 0), at day 10 and day 14 after femoral of the ischemic (left) and non-ligated (right) limbs (left panel). Blood flow is displayed by color-coded pixels. B) Capillaries of gastrocnemius muscles in WT (*n*=4) *vs.* *Pear1*$^{-/-}$ (*n*=4) mice stained with fluorescent labeled isolectin (x100). Increased capillary density (1007±105 *vs.* 496±14 isolectin positive vessels/mm^2) in the muscle of the *Pear1*$^{-/-}$ mice, 21 days after occlusion, compared to WT mice (capillary density was calculated as the mean of 4 muscle locations (proximal, middle 1, middle 2 and distal) of which 3 adjacent sections were analysed; unpaired t-test). Results are given as mean±SEM; blinded observations; * $P<0.05$. C) Representative micro-CT angiograms of the gastrocnemius muscle 21 days after femoral artery ligation in the left limb of WT (*n*=3) and *Pear1*$^{-/-}$ (*n*=3) mice (non-ligated limbs Fig. 13).

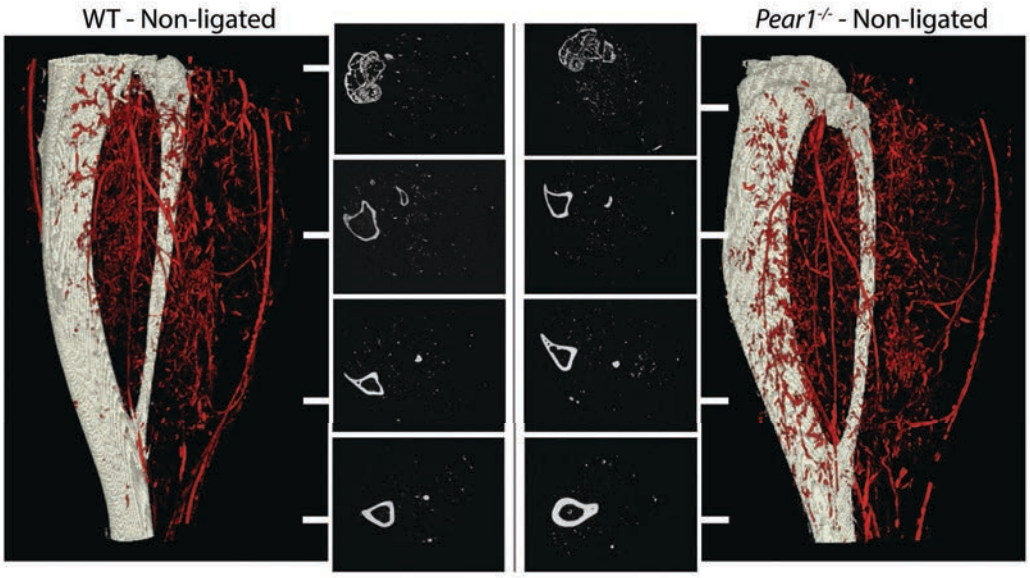

Figure 13: Representative micro-CT angiograms of the gastrocnemius muscle in the right (non-ligated) limb of WT and *Pear1*$^{-/-}$ mice.
A

A
A
A
A
A
A
A
A
A
A
A

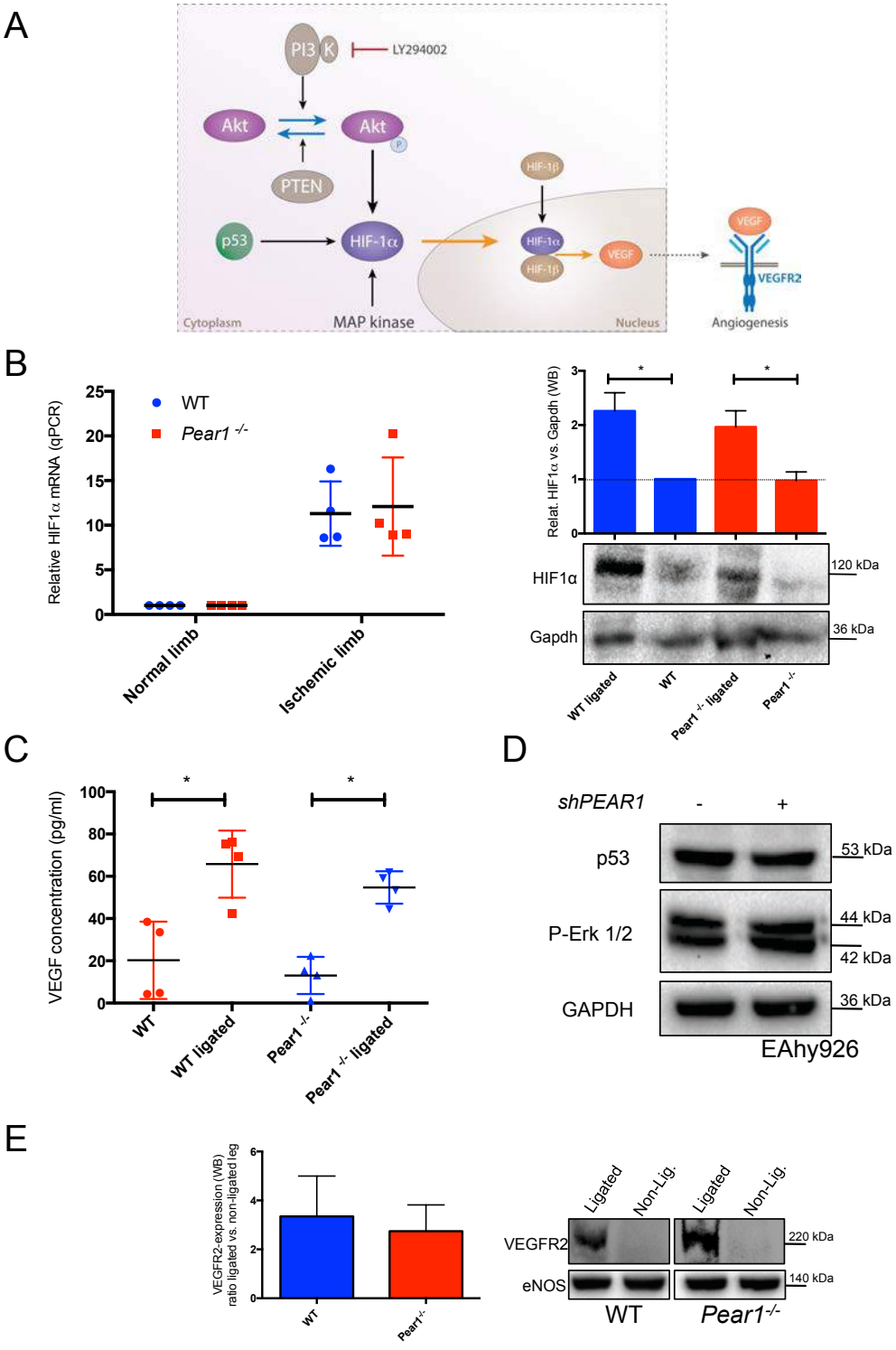

Figure 14: A) A Classical schematic overview of the PI3K/HIF1α/VEGF-pathway, adapted from [1]. B) A (left panel) A Upregulation of *HIF1α* mRNA-levels in ischemic gastrocnemius muscles in both WT (*n*=4; increase by 11±3.7) and *Pear1*$^{-/-}$ (*n*=4; increase by 12±4.9) muscles, compared to HIF1α mRNA-levels in non-ligated limbs of WT (n=4) and *Pear1*$^{-/-}$ mice (n=4). Upregulation of *HIF1α* mRNA-levels in the ischemic limb was not statistically different in WT *vs.* *Pear1*$^{-/-}$ limbs (repeated measurements ANOVA with Bonferroni post-hoc test). (right panel) Corresponding upregulation of HIF1α protein levels in the ischemic limbs of WT (*n*=4; 2.3±0.3) and *Pear1*$^{-/-}$ mice (*n*=4; 1.96±0.7). Again no statistically differences were found in ligated WT *vs.* *Pear1*$^{-/-}$ muscles. C) A VEGF-concentrations (ELISA; pg/ml) measured on supernatants of the gastrocnemius muscles. A significant upregulation of VEGF in the ligated muscle of WT (*n*=4; 4±3.3-fold increase) and *Pear1*$^{-/-}$ muscles (*n*=4; 4±3.9-fold increase) *vs.* non-ligated limbs. No statistical differences were found in VEGF-concentration between WT and *Pear1*$^{-/-}$ muscles both at baseline conditions and after ligation (one-way ANOVA with Bonferroni's post-hoc test). D) A Western blot analyses for p53 and phosphorylation of Erk1/2 (MAPK) in human WT EAhy926 ECs *vs.* shPEAR1 EAhy926 ECs. A knockdown of PEAR1 did not affect p53 expression nor phosphorylation of Erk1/2 (*n*=4). E) A Ratio of VEGFR2-protein expression in ligated *vs.* non-ligated muscles of WT (*n*=4; 3.34±1.4) *vs.* *Pear1*$^{-/-}$ (*n*=4; 2.74±1.05) muscles. (Western blot; eNOS served as loading control). A *P<0.05; results are given as mean±SEM. A

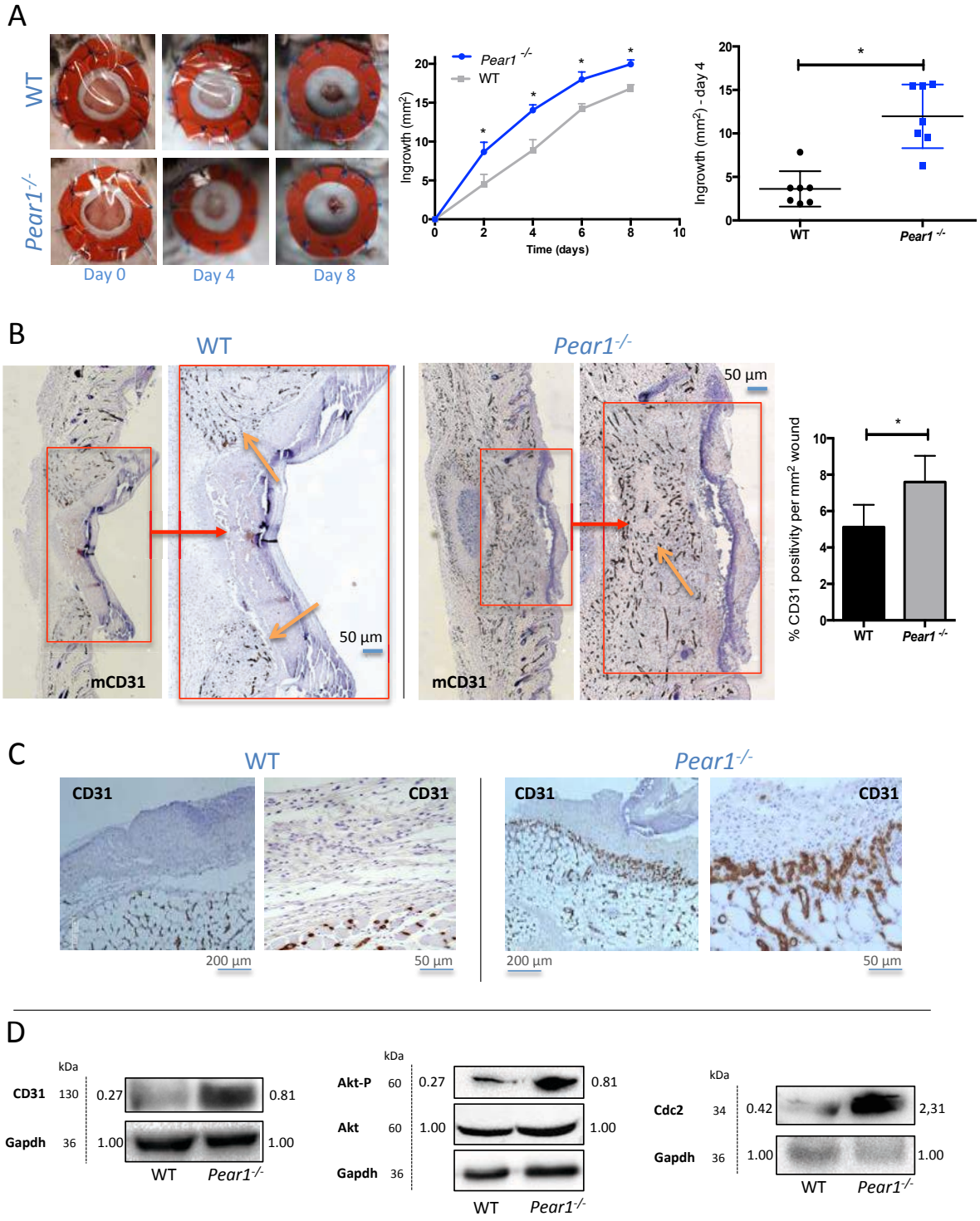

Figure 15: Higher capillary wound density and accelerated wound closure in *Pear1*$^{-/-}$ mice. A) Wound ingrowth (mm^2) after a fixed (29 mm^2) dorsal skin wound in *Pear1*$^{-/-}$ mice (n=10) *vs.* WT littermates (n=10) with follow-up until day 8 (left and middle panel; blinded observations; one-way ANOVA with Bonferroni's post-hoc test). Independent experiment of dorsal skin wound in *Pear1*$^{-/-}$ mice (n=7) *vs.* WT littermates (n=7) with follow-up until day 4 (right panel; unpaired t-test). A faster wound closure was observed from day 2 onwards, in *Pear1*$^{-/-}$ compared to WT-mice. B) Representative immunohistochemical staining for murine CD31 of the wound area (day 8; x25 and x50) of the WT-mice (n=4; left panel) and of the *Pear1*$^{-/-}$ mice (n=4; middle panel). Orange arrows show the invasion of newly formed vessels in the wound. A significant increase of CD31-positivity (vessel density per mm^2 wound area) in *Pear1*$^{-/-}$ mice *vs.* WT wound areas (right panel; x50; day 8; unpaired t-test). Results are given as mean±SEM; *P<0.05. C) CD31 staining of the wound area at day 4 showed a strong ingrowth of newly formed vessels in the granuloma tissue in the *Pear1*$^{-/-}$ wounds (n=5) while still absent in the WT granuloma (n=5). D) Western blot analysis of pooled granuloma tissues (day 4; n=5 for WT-granulomas and n=5 for *Pear1*$^{-/-}$ *granulomas*). Proportional values for the density of the protein band show increased levels of CD31 (blood vessels), Akt-P and CDC2, compatible with corresponding findings for the ECA analysis *in vitro*.

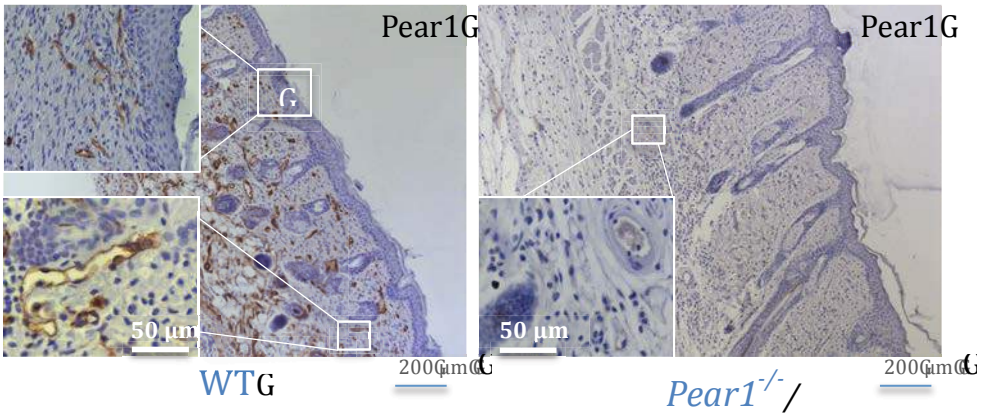

Figure 16: IHC staining (x50) for murine Pear1, showing presence and absence of Pear1 in normal skin ECs of WT (left panel) and *Pear1*$^{-/-}$ mice (right panel), respectively.

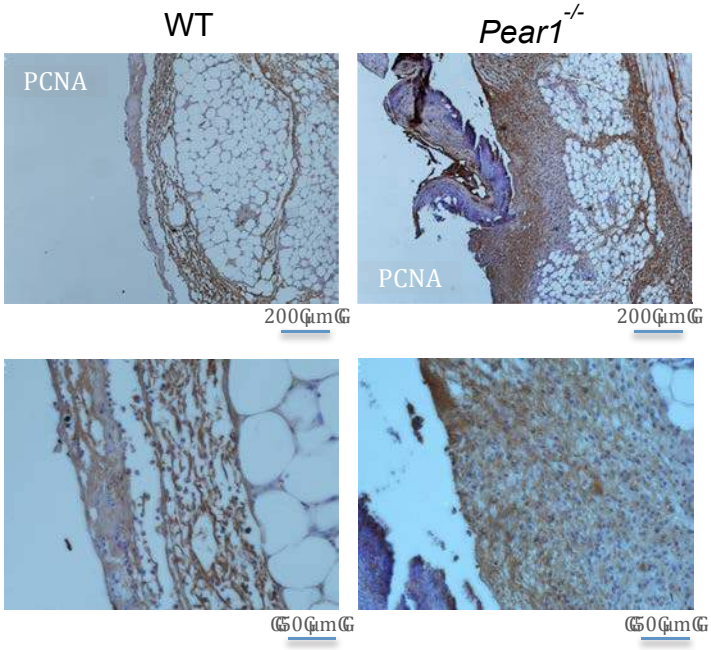

Figure 17: Representative immunohistochemical staining for murine PCNA of the wound area (day 4) (x25 A upper panel; x50 A lower panel) of the WT (left panel) and *Pear1*$^{-/-}$ wound areas (*n*=3).

DISCUSSION

PEAR1 is a transmembrane protein expressed on the cellular border and on filo- and lamellipodia of ECs. So far, the role of PEAR1-signalling in the vascular endothelium during angiogenesis has remained undefined. Herein we report that knockdown of *PEAR1* in cultured human ECs resulted in increased tube formation *in vitro* and that knockout of *Pear1* resulted in enhanced angiogenesis in two established *in vivo* mouse models.

In various human tissues, the presence of PEAR1 in ECs was demonstrated both at mRNA and protein level. We observed a lower *PEAR1*-expression in rapidly proliferating cultured ECs (BOECs, HUVECs and HUAECs) and a higher expression in slow-proliferating µECs of heart and liver. Also in rapidly proliferating ECs of a pyogenic granuloma, a hypervascularized skin tumour, an inverse association between PEAR1-expression and EC proliferation was observed. It was of particular interest that *PEAR1*-expression rose 2.3-fold during *in vitro* tube formation. All these results suggested a modifier function for PEAR1 on endothelial angiogenic behaviour leading to an increased proliferation rate and tube forming capacity upon its absence, similar to our previous findings of enhanced megakaryopoiesis in *shPEAR1* CD34+ cells.[15] This hypothesis was confirmed by lentiviral knockdown of *PEAR1*; knockdown reduced *PEAR1*-expression by approximately 70% and resulted in a doubled proliferation rate for these *shPEAR1* ECs. The augmented proliferation was documented via a manual EC counting technique, via flow cytometric assessment of EC EdU-incorporation[46] and via direct analysis of the number of cellular mitoses. This doubled proliferation rate was confirmed applying two different miRNA lentiviral vectors in different human cultured ECs.

Next, we unravelled the underlying mechanistic pathway responsible for enhanced EC proliferation in *PEAR1*-knockdown cells. Signalling of receptor tyrosine kinases through mitogen-activated protein kinases (MAPKs) and phosphatidylinositol 3-kinase (PI3K) and Akt are the two major pathways in EC proliferation.[47, 48] We observed that knockdown of *PEAR1* in ECs resulted in increased baseline Akt-phosphorylation, accompanied by a downregulation of the expression of the phosphatase PTEN, priming ECs to adopt a more proliferative phenotype. This is in line with our previous report showing that a similar PEAR1-dependent Akt-driven mechanism is operative during megakaryopoiesis.[15] Cell cycle progression in ECs is tightly regulated by the family of cyclin-dependent kinase inhibitors. The increased Akt-activity upon *PEAR1*-knockdown was associated with a decrease of nuclear $p21^{CIP1/WAF1}$ and elevated the cytosolic localization of $p21^{CIP1/WAF1}$, an important regulatory mechanism of mitosis.[49] These findings provided a molecular basis for the enhanced CDC2-driven EC proliferation. Indeed, $p21^{CIP1/WAF1}$ inhibits the activity of CDC2, a cyclin that regulates G2-to-M transition during cell division.[50] In HER-2/neu-overexpressing cells, it was established that growth inhibition is coupled to nuclear localization of $p21^{CIP1/WAF1}$. PI3K/Akt-driven phosphorylation of $p21^{CIP1/WAF1}$ resulted in cytoplasmic localization of $p21^{CIP1/WAF1}$, which is no longer effective in suppressing CDC2.[51, 52] These enhanced levels of CDC2 in *shPEAR1* ECs could be reversed by inhibition of PI3K, indicating a direct link between elevated Akt-P levels upon *PEAR1*-knockdown and enhanced proliferation. The Erk-pathway represents one of the best characterized MAPK signalling pathways in EC proliferation.[53] However, *PEAR1*-knockdown did not affect the phosphorylation of Erk1/2.

ECs will rapidly form capillary-like structures *in vitro* when plated on top of a reconstituted, VEGF-containing basement membrane extracellular matrix (Matrigel). This differentiation process, used as an *in vitro* assay of angiogenesis, involves several steps in blood vessel formation, including cell adhesion, migration, alignment and tubule formation.[54, 55] We observed an upregulation of *PEAR1* during tube formation *in vitro* and we illustrated that endothelial *PEAR1*-knockdown boosted the *in vitro* tube formation, underpinning a significant role for PEAR1-modulated EC proliferation during tube formation. A major signalling event downstream of pro-angiogenic factors such as *e.g.* VEGF is the activation of Akt, both *in vitro* and *in vivo*.[16, 56, 57] Although we were unable to measure Akt-P before and after tube formation, due to the small amount of available cells, we were able to measure it indirectly by qRT-PCR for *PTEN,* since the inverse correlation between phosphorylation levels of Akt and expression levels of *PTEN* has been well established.[58] We not only observed a lower expression of *PTEN* in *shPEAR1* ECs before tube formation as discussed above but also a lack of the physiological *PTEN*-enrichment during tubulogenesis,[42, 59] indicating a permanent lack of dephosphorylation of Akt during *shPEAR1* tube formation. Expression levels of other important markers of terminal EC differentiation (*VE-cadherin*, *VEGFR2* or *PECAM1*) were not significantly affected during tube formation upon *PEAR1*-knockdown. It has been reported that critical roles of Akt in angiogenesis can be regulated by the Akt-downstream effector eNOS.[60, 61] Enhanced nitric oxide (NO) synthesis could be the explanation for the increased EC proliferation and angiogenesis, observed upon *PEAR1*-knockdown. However we observed no differences in eNOS-phosphorylation (activating site, S1177) upon *PEAR1*-knockdown, could not detect any differences in NO-production (DAF-FM dye) of *shPEAR1* ECs compared to control cells *in vitro* and were not able to show any differences in functional aortic relaxation experiments of WT *vs. Pear1*$^{-/-}$ aortas. Therefore, it is unlikely that NO accounts for the observed phenotype.

Vascular assembly is a complex interaction between EC proliferation, migration and sprouting.[30] PEAR1 was strongly positive at the tips of endothelial filo- and lamellipodia and was found to be expressed in endothelial ruffles. Since we found enhanced tube formation at early time-points on matrigel assays upon PEAR1-knockdown and since it has been previously reported that constitutively enhanced phosphorylation levels of Akt strongly promote EC migration,[62, 63] we could confirm in an *in vitro* migration model a significantly higher migration capacity of PEAR1-knockdown ECs compared to control ECs (scratch wound assay; after 12 hours). We were able to reverse this enhanced migration phenotype in the presence of an inhibitor of PI3K, confirming the direct link between enhanced migration and constitutively enhanced phosphorylation levels of Akt upon *PEAR1*-knockdown. Several downstream mediators of Akt, responsible for enhanced migration have been suggested (*e.g.*, eNOS, G-protein-coupled receptors such as EDG-1,[41] but the relevant downstream targets have not yet been defined in literature.[7]

PEAR1-ablation not only promoted EC assembly *in vitro*, but also stimulated neoangiogenesis *in vivo*. First, we confirmed the expression of Pear1 in murine ECs of various tissues. *Pear1*$^{-/-}$ mice showed no overt vascular phenotype and detailed IHC and angiographic analyses of various murine tissues did not detect abnormalities in blood vessels in the absence of *Pear1*. However, after femoral artery occlusion in *Pear1*$^{-/-}$ mice, we observed a faster neoangiogenesis in the gastrocnemius muscle. Angiogenesis, *i.e.*, the sprouting of capillaries and proliferation of ECs from the pre-existing vasculature, is mainly initiated by hypoxia in

ischemic tissue and is different from vasculogenesis (*i.e.*, *de novo* vessel growth processes).[31, 41, 64, 65] Various reports show evidence that surgical ligation of the femoral artery leads to an angiogenic response in distal ischemic muscles.[6, 31, 64] Therefore, we focused on neoangiogenesis in the gastrocnemius muscle at day 21 and used isolectin staining, Laser Doppler imaging and angio-CT after hind limb ischemia to demonstrate an increased angiogenic response in *Pear1*$^{-/-}$ mice compared to their WT-littermates.[6]

Angiogenesis is also central to granulation tissue formation, because the ingrowth of newly formed vessels is needed to ensure the supply of oxygen and nutrients to the regenerating tissue. Wound healing is the result of a complex interaction between keratinocytes, fibroblasts and neoangiogenesis, resulting from growth factor-induced (FGF, VEGF, TGF-β,…) EC proliferation and migration.[44, 45, 66] The expression of *Pear1* in the endothelium of skin tissue was documented and we showed ECs to be the only Pear1-positive cells via IHC. At day 4 of wound healing, there was an approximately two-fold increase in the speed of wound closure ($t_{1/2}$ of full recovery was 4 days in KO-mice and 7 days in WT-mice) in *Pear1*$^{-/-}$ mice, compared to their WT littermates. This was accompanied by increased cell proliferation (by PCNA-staining) and increased angiogenesis in the wound areas of *Pear1*$^{-/-}$ mice. The difference in healing rate remained present until the time point of sacrifice on day 8. The faster wound closure in *Pear1*$^{-/-}$ mice could be explained by enhanced neo-formation of blood vessels in the wound surface and was illustrated by enhanced positivity for CD31, both by IHC and WB of the granuloma tissue of *Pear1*$^{-/-}$ mice.

Angiogenesis constitutes an important aspect of EC function and PI3K/Akt-signalling is critical in these processes.[16, 56, 67] We were able to demonstrate, in parallel with our *in vitro* findings, an enhanced Akt-P-driven Cdc2-upregulation in the pooled granuloma tissues of the *Pear1*$^{-/-}$ mice compared to littermates at day 4 of wound healing. This allowed us to extrapolate our *in vitro* signalling data to that of the *in vivo* wound healing assay and supported the controlling role for PEAR1 in Akt-driven proliferation/migration of ECs and angiogenesis via the PI3K/Akt-pathway. It remains to be shown how PEAR1 controls PI3K/PTEN, but an inverse relation between Akt-P and PTEN has been shown in many cell types.[30] We showed that the enhanced neo-angiogenesis, observed upon ligation of the femoral artery in *Pear1*$^{-/-}$ mice is not the result of increased VEGF-signalling. Several reports have shown that sustained endothelial Akt-activation and/or Akt-overexpression in hind limb ischemia models resulted in enhanced angiogenesis even when levels of VEGF were unaffected.[68] Nevertheless, several other signalling pathways are implicated in angiogenesis (*e.g.*, NOTCH, mTOR-pathway, integrins, …),[69-72] potentially contributing to further regulation of PTEN and Akt-phosphorylation and its effects on angiogenesis.

The present work reveals PEAR1 as a modulatory factor of vascular assembly. We previously showed a role for PEAR1 in mekaryocyte proliferation but also a role for PEAR1 as a contact receptor in platelet aggregation. Platelet PEAR1 is phosphorylated via c-Src upon stimulation with the high-affinity immunoglobulin E (IgE)-binding subunit FcεR1α (ligand for platelet PEAR1)[73] and with a polyclonal anti-PEAR1 antibody, acting as a pseudo-ligand.[14] So far, the physiological ligand for PEAR1 on ECs remains to be identified.

In conclusion, we identified PEAR1 as a novel modifier of neoangiogenesis. This study will trigger further research on the role of PEAR1 in pathological endothelial hyperproliferation (as seen in *e.g.* neo-intima formation after stent implantation[74] or in pulmonary hypertension[75]) and on the interaction between platelets and ECs, two major players in cardiovascular disease. Further research will also need to identify how various SNPs regulate the expression of *PEAR1* and whether PEAR1 contributes to pathologies with excessive vessel growth *e.g.* inflammatory diseases, retinopathy and cancer.[3]

REFERENCES

1. Giaccia A, Siim BG, Johnson RS. HIF-1 as a target for drug development. *Nat Rev Drug Discov* 2003;**2**:803-811.
2. World Health Organization. Fact sheet No. 317 Feb 2007, 2007.
3. Carmeliet P. Angiogenesis in life, disease and medicine. *Nature* 2005;**438**:932-936.
4. Potente M, Gerhardt H, Carmeliet P. Basic and therapeutic aspects of angiogenesis. *Cell* 2011;**146**:873-887.
5. Geudens I, Gerhardt H. Coordinating cell behaviour during blood vessel formation. *Development* 2011;**138**:4569-4583.
6. Limbourg A, Korff T, Napp LC, Schaper W, Drexler H, Limbourg FP. Evaluation of postnatal arteriogenesis and angiogenesis in a mouse model of hind-limb ischemia. *Nat Protoc* 2009;**4**:1737-1746.
7. Manning BD, Cantley LC. AKT/PKB signaling: navigating downstream. *Cell* 2007;**129**:1261-1274.
8. Nanda N, Bao M, Lin H, Clauser K, Komuves L, Quertermous T, Conley PB, Phillips DR, Hart MJ. Platelet endothelial aggregation receptor 1 (PEAR1), a novel epidermal growth factor repeat-containing transmembrane receptor, participates in platelet contact-induced activation. *J Biol Chem* 2005;**280**:24680-24689.
9. Wu HH, Bellmunt E, Scheib JL, Venegas V, Burkert C, Reichardt LF, Zhou Z, Farinas I, Carter BD. Glial precursors clear sensory neuron corpses during development via Jedi-1, an engulfment receptor. *Nat Neurosci* 2009;**12**:1534-1541.
10. Lewis JP, Ryan K, O'Connell JR, Horenstein RB, Damcott CM, Gibson Q, Pollin TI, Mitchell BD, Beitelshees AL, Pakzy R, Tanner K, Parsa A, Tantry US, Bliden KP, Post WS, Faraday N, Herzog W, Gong Y, Pepine CJ, Johnson JA, Gurbel PA, Shuldiner AR. Genetic variation in PEAR1 is associated with platelet aggregation and cardiovascular outcomes. *Circ Cardiovasc Genet* 2013;**6**:184-192.
11. Jones CI, Bray S, Garner SF, Stephens J, de Bono B, Angenent WG, Bentley D, Burns P, Coffey A, Deloukas P, Earthrowl M, Farndale RW, Hoylaerts MF, Koch K, Rankin A, Rice CM, Rogers J, Samani NJ, Steward M, Walker A, Watkins NA, Akkerman JW, Dudbridge F, Goodall AH, Ouwehand WH. A functional genomics approach reveals novel quantitative trait loci associated with platelet signaling pathways. *Blood* 2009;**114**:1405-1416.
12. Faraday N, Yanek LR, Yang XP, Mathias R, Herrera-Galeano JE, Suktitipat B, Qayyum R, Johnson AD, Chen MH, Tofler GH, Ruczinski I, Friedman AD, Gylfason A, Thorsteinsdottir U, Bray PF, O'Donnell CJ, Becker DM, Becker LC. Identification of a specific intronic PEAR1 gene variant associated with greater platelet aggregability and protein expression. *Blood* 2011;**118**:3367-3375.
13. Kim Y, Suktitipat B, Yanek LR, Faraday N, Wilson AF, Becker DM, Becker LC, Mathias RA. Targeted deep resequencing identifies coding variants in the PEAR1 gene that play a role in platelet aggregation. *PLoS One* 2013;**8**:e64179.
14. Kauskot A, Di Michele M, Loyen S, Freson K, Verhamme P, Hoylaerts MF. A novel mechanism of sustained platelet alphaIIbbeta3 activation via PEAR1. *Blood* 2012;**119**:4056-4065.
15. Kauskot A, Vandenbriele C, Louwette S, Gijsbers R, Tousseyn T, Freson K, Verhamme P, Hoylaerts MF. PEAR1 attenuates megakaryopoiesis via control of the PI3K/PTEN pathway. *Blood* 2013;**121**:5208-5217.
16. Jiang BH, Liu LZ. AKT signaling in regulating angiogenesis. *Curr Cancer Drug Targets* 2008;**8**:19-26.
17. Hayashi T, Yano K, Matsui-Hirai H, Yokoo H, Hattori Y, Iguchi A. Nitric oxide and endothelial cellular senescence. *Pharmacol Ther* 2008;**120**:333-339.
18. Jaffe EA, Nachman RL, Becker CG, Minick CR. Culture of human endothelial cells derived from umbilical veins. Identification by morphologic and immunologic criteria. *J Clin Invest* 1973;**52**:2745-2756.
19. van Beem RT, Verloop RE, Kleijer M, Noort WA, Loof N, Koolwijk P, van der Schoot CE, van Hinsbergh VW, Zwaginga JJ. Blood outgrowth endothelial cells from cord blood and peripheral blood: angiogenesis-related characteristics in vitro. *J Thromb Haemost* 2009;**7**:217-226.
20. Thomas S, Robinson CJ, Gray E. Responses of HUVEC and EAhy926 to heparin and fibroblast growth factors. *In Vitro Cell Dev Biol Anim* 1997;**33**:492-494.
21. Coppiello G, Collantes M, Sirerol-Piquer MS, Vandenwijngaert S, Schoors S, Swinnen M, Vandersmissen I, Herijgers P, Topal B, van Loon J, Goffin J, Prosper F, Carmeliet P, Garcia-Verdugo JM,

Janssens S, Penuelas I, Aranguren XL, Luttun A. Meox2/Tcf15 Heterodimers Program the Heart Capillary Endothelium for Cardiac Fatty Acid Uptake. *Circulation* 2015.

22. Ingram DA, Mead LE, Tanaka H, Meade V, Fenoglio A, Mortell K, Pollok K, Ferkowicz MJ, Gilley D, Yoder MC. Identification of a novel hierarchy of endothelial progenitor cells using human peripheral and umbilical cord blood. *Blood* 2004;**104**:2752-2760.
23. Sieveking DP, Buckle A, Celermajer DS, Ng MK. Strikingly different angiogenic properties of endothelial progenitor cell subpopulations: insights from a novel human angiogenesis assay. *J Am Coll Cardiol* 2008;**51**:660-668.
24. Yoon CH, Hur J, Park KW, Kim JH, Lee CS, Oh IY, Kim TY, Cho HJ, Kang HJ, Chae IH, Yang HK, Oh BH, Park YB, Kim HS. Synergistic neovascularization by mixed transplantation of early endothelial progenitor cells and late outgrowth endothelial cells: the role of angiogenic cytokines and matrix metalloproteinases. *Circulation* 2005;**112**:1618-1627.
25. Livak KJ, Schmittgen TD. Analysis of relative gene expression data using real-time quantitative PCR and the 2(-Delta Delta C(T)) Method. *Methods* 2001;**25**:402-408.
26. Zhou X, He P. Improved measurements of intracellular nitric oxide in intact microvessels using 4,5-diaminofluorescein diacetate. *Am J Physiol Heart Circ Physiol* 2011;**301**:H108-114.
27. Fransen P, Van Assche T, Guns PJ, Van Hove CE, De Keulenaer GW, Herman AG, Bult H. Endothelial function in aorta segments of apolipoprotein E-deficient mice before development of atherosclerotic lesions. *Pflugers Arch* 2008;**455**:811-818.
28. Hazarika S, Dokun AO, Li Y, Popel AS, Kontos CD, Annex BH. Impaired angiogenesis after hindlimb ischemia in type 2 diabetes mellitus: differential regulation of vascular endothelial growth factor receptor 1 and soluble vascular endothelial growth factor receptor 1. *Circ Res* 2007;**101**:948-956.
29. Cherwek DH, Hopkins MB, Thompson MJ, Annex BH, Taylor DA. Fiber type-specific differential expression of angiogenic factors in response to chronic hindlimb ischemia. *Am J Physiol Heart Circ Physiol* 2000;**279**:H932-938.
30. Lamalice L, Le Boeuf F, Huot J. Endothelial cell migration during angiogenesis. *Circ Res* 2007;**100**:782-794.
31. Scholz D, Ziegelhoeffer T, Helisch A, Wagner S, Friedrich C, Podzuweit T, Schaper W. Contribution of arteriogenesis and angiogenesis to postocclusive hindlimb perfusion in mice. *J Mol Cell Cardiol* 2002;**34**:775-787.
32. Arbiser JL, Moses MA, Fernandez CA, Ghiso N, Cao Y, Klauber N, Frank D, Brownlee M, Flynn E, Parangi S, Byers HR, Folkman J. Oncogenic H-ras stimulates tumor angiogenesis by two distinct pathways. *Proc Natl Acad Sci U S A* 1997;**94**:861-866.
33. Jiang BH, Jiang G, Zheng JZ, Lu Z, Hunter T, Vogt PK. Phosphatidylinositol 3-kinase signaling controls levels of hypoxia-inducible factor 1. *Cell Growth Differ* 2001;**12**:363-369.
34. Mazure NM, Chen EY, Laderoute KR, Giaccia AJ. Induction of vascular endothelial growth factor by hypoxia is modulated by a phosphatidylinositol 3-kinase/Akt signaling pathway in Ha-ras-transformed cells through a hypoxia inducible factor-1 transcriptional element. *Blood* 1997;**90**:3322-3331.
35. Zundel W, Schindler C, Haas-Kogan D, Koong A, Kaper F, Chen E, Gottschalk AR, Ryan HE, Johnson RS, Jefferson AB, Stokoe D, Giaccia AJ. Loss of PTEN facilitates HIF-1-mediated gene expression. *Genes Dev* 2000;**14**:391-396.
36. Hamada K, Sasaki T, Koni PA, Natsui M, Kishimoto H, Sasaki J, Yajima N, Horie Y, Hasegawa G, Naito M, Miyazaki J, Suda T, Itoh H, Nakao K, Mak TW, Nakano T, Suzuki A. The PTEN/PI3K pathway governs normal vascular development and tumor angiogenesis. *Genes Dev* 2005;**19**:2054-2065.
37. Ma J, Sawai H, Ochi N, Matsuo Y, Xu D, Yasuda A, Takahashi H, Wakasugi T, Takeyama H. PTEN regulates angiogenesis through PI3K/Akt/VEGF signaling pathway in human pancreatic cancer cells. *Mol Cell Biochem* 2009;**331**:161-171.
38. Huang J, Kontos CD. PTEN modulates vascular endothelial growth factor-mediated signaling and angiogenic effects. *J Biol Chem* 2002;**277**:10760-10766.
39. Kroll J, Waltenberger J. The vascular endothelial growth factor receptor KDR activates multiple signal transduction pathways in porcine aortic endothelial cells. *J Biol Chem* 1997;**272**:32521-32527.
40. Veeranki S, Givvimani S, Pushpakumar S, Tyagi SC. Hyperhomocysteinemia attenuates angiogenesis through reduction of HIF-1alpha and PGC-1alpha levels in muscle fibers during hindlimb ischemia. *Am J Physiol Heart Circ Physiol* 2014;**306**:H1116-1127.
41. Lee MJ, Thangada S, Paik JH, Sapkota GP, Ancellin N, Chae SS, Wu M, Morales-Ruiz M, Sessa WC, Alessi DR, Hla T. Akt-mediated phosphorylation of the G protein-coupled receptor EDG-1 is required for endothelial cell chemotaxis. *Mol Cell* 2001;**8**:693-704.

42. Kim KY, Ahn JH, Cheon HG. Anti-angiogenic action of PPARgamma ligand in human umbilical vein endothelial cells is mediated by PTEN upregulation and VEGFR-2 downregulation. *Mol Cell Biochem* 2011;**358**:375-385.
43. Song R, Tian K, Wang W, Wang L. P53 suppresses cell proliferation, metastasis, and angiogenesis of osteosarcoma through inhibition of the PI3K/AKT/mTOR pathway. *Int J Surg* 2015.
44. Tonnesen MG, Feng X, Clark RA. Angiogenesis in wound healing. *J Investig Dermatol Symp Proc* 2000;**5**:40-46.
45. Werner S, Grose R. Regulation of wound healing by growth factors and cytokines. *Physiol Rev* 2003;**83**:835-870.
46. Osterholzer JJ, Chen GH, Olszewski MA, Curtis JL, Huffnagle GB, Toews GB. Accumulation of CD11b+ lung dendritic cells in response to fungal infection results from the CCR2-mediated recruitment and differentiation of Ly-6Chigh monocytes. *J Immunol* 2009;**183**:8044-8053.
47. Vivanco I, Sawyers CL. The phosphatidylinositol 3-Kinase AKT pathway in human cancer. *Nat Rev Cancer* 2002;**2**:489-501.
48. Datta SR, Dudek H, Tao X, Masters S, Fu H, Gotoh Y, Greenberg ME. Akt phosphorylation of BAD couples survival signals to the cell-intrinsic death machinery. *Cell* 1997;**91**:231-241.
49. Cully M, You H, Levine AJ, Mak TW. Beyond PTEN mutations: the PI3K pathway as an integrator of multiple inputs during tumorigenesis. *Nat Rev Cancer* 2006;**6**:184-192.
50. Harper JW, Adami GR, Wei N, Keyomarsi K, Elledge SJ. The p21 Cdk-interacting protein Cip1 is a potent inhibitor of G1 cyclin-dependent kinases. *Cell* 1993;**75**:805-816.
51. Zhou BP, Liao Y, Xia W, Spohn B, Lee MH, Hung MC. Cytoplasmic localization of p21Cip1/WAF1 by Akt-induced phosphorylation in HER-2/neu-overexpressing cells. *Nat Cell Biol* 2001;**3**:245-252.
52. Dong Y, Chi SL, Borowsky AD, Fan Y, Weiss RH. Cytosolic p21Waf1/Cip1 increases cell cycle transit in vascular smooth muscle cells. *Cell Signal* 2004;**16**:263-269.
53. Zhang W, Liu HT. MAPK signal pathways in the regulation of cell proliferation in mammalian cells. *Cell Res* 2002;**12**:9-18.
54. Arnaoutova I, George J, Kleinman HK, Benton G. The endothelial cell tube formation assay on basement membrane turns 20: state of the science and the art. *Angiogenesis* 2009;**12**:267-274.
55. Akhtar N, Dickerson EB, Auerbach R. The sponge/Matrigel angiogenesis assay. *Angiogenesis* 2002;**5**:75-80.
56. Ackah E, Yu J, Zoellner S, Iwakiri Y, Skurk C, Shibata R, Ouchi N, Easton RM, Galasso G, Birnbaum MJ, Walsh K, Sessa WC. Akt1/protein kinase Balpha is critical for ischemic and VEGF-mediated angiogenesis. *J Clin Invest* 2005;**115**:2119-2127.
57. Zachary I, Gliki G. Signaling transduction mechanisms mediating biological actions of the vascular endothelial growth factor family. *Cardiovasc Res* 2001;**49**:568-581.
58. Oudit GY, Penninger JM. Cardiac regulation by phosphoinositide 3-kinases and PTEN. *Cardiovasc Res* 2009;**82**:250-260.
59. Kuo HM, Lin CY, Lam HC, Lin PR, Chan HH, Tseng JC, Sun CK, Hsu TF, Wu CC, Yang CY, Hsu CM, Tai MH. PTEN overexpression attenuates angiogenic processes of endothelial cells by blockade of endothelin-1/endothelin B receptor signaling. *Atherosclerosis* 2012;**221**:341-349.
60. Lee MY, Luciano AK, Ackah E, Rodriguez-Vita J, Bancroft TA, Eichmann A, Simons M, Kyriakides TR, Morales-Ruiz M, Sessa WC. Endothelial Akt1 mediates angiogenesis by phosphorylating multiple angiogenic substrates. *Proc Natl Acad Sci U S A* 2014;**111**:12865-12870.
61. Partovian C, Zhuang Z, Moodie K, Lin M, Ouchi N, Sessa WC, Walsh K, Simons M. PKCalpha activates eNOS and increases arterial blood flow in vivo. *Circ Res* 2005;**97**:482-487.
62. Morales-Ruiz M, Fulton D, Sowa G, Languino LR, Fujio Y, Walsh K, Sessa WC. Vascular endothelial growth factor-stimulated actin reorganization and migration of endothelial cells is regulated via the serine/threonine kinase Akt. *Circ Res* 2000;**86**:892-896.
63. Liu YW, Zuo PY, Zha XN, Chen XL, Zhang R, He XX, Liu CY. Octacosanol Enhances the Proliferation and Migration of Human Umbilical Vein Endothelial Cells via Activation of the PI3K/Akt and MAPK/Erk Pathways. *Lipids* 2015;**50**:241-251.
64. Helisch A, Wagner S, Khan N, Drinane M, Wolfram S, Heil M, Ziegelhoeffer T, Brandt U, Pearlman JD, Swartz HM, Schaper W. Impact of mouse strain differences in innate hindlimb collateral vasculature. *Arterioscler Thromb Vasc Biol* 2006;**26**:520-526.
65. Carmeliet P. Mechanisms of angiogenesis and arteriogenesis. *Nat Med* 2000;**6**:389-395.

66. Hendrickx B, Verdonck K, Van den Berge S, Dickens S, Eriksson E, Vranckx JJ, Luttun A. Integration of blood outgrowth endothelial cells in dermal fibroblast sheets promotes full thickness wound healing. *Stem Cells* 2010;**28**:1165-1177.
67. Somanath PR, Razorenova OV, Chen J, Byzova TV. Akt1 in endothelial cell and angiogenesis. *Cell Cycle* 2006;**5**:512-518.
68. Phung TL, Ziv K, Dabydeen D, Eyiah-Mensah G, Riveros M, Perruzzi C, Sun J, Monahan-Earley RA, Shiojima I, Nagy JA, Lin MI, Walsh K, Dvorak AM, Briscoe DM, Neeman M, Sessa WC, Dvorak HF, Benjamin LE. Pathological angiogenesis is induced by sustained Akt signaling and inhibited by rapamycin. *Cancer Cell* 2006;**10**:159-170.
69. Liu ZJ, Xiao M, Balint K, Soma A, Pinnix CC, Capobianco AJ, Velazquez OC, Herlyn M. Inhibition of endothelial cell proliferation by Notch1 signaling is mediated by repressing MAPK and PI3K/Akt pathways and requires MAML1. *FASEB J* 2006;**20**:1009-1011.
70. Phng LK, Gerhardt H. Angiogenesis: a team effort coordinated by notch. *Dev Cell* 2009;**16**:196-208.
71. Wang S, Amato KR, Song W, Youngblood V, Lee K, Boothby M, Brantley-Sieders DM, Chen J. Regulation of Endothelial Cell Proliferation and Vascular Assembly through Distinct mTORC2 Signaling Pathways. *Mol Cell Biol* 2015.
72. Tan C, Cruet-Hennequart S, Troussard A, Fazli L, Costello P, Sutton K, Wheeler J, Gleave M, Sanghera J, Dedhar S. Regulation of tumor angiogenesis by integrin-linked kinase (ILK). *Cancer Cell* 2004;**5**:79-90.
73. Sun Y, Vandenbriele C, Kauskot A, Verhamme P, Hoylaerts MF, Wright GJ. A human platelet receptor protein microarray identifies FcepsilonR1alpha as an activating PEAR1 ligand. *Mol Cell Proteomics* 2015.
74. Bejarano J. The cutting balloon for in-stent restenosis: a review. *J Interv Cardiol* 2004;**17**:203-209.
75. Farber HW, Loscalzo J. Pulmonary arterial hypertension. *N Engl J Med* 2004;**351**:1655-1665.

General Discussion
Future Perspectives

General Discussion

Introduction

Platelet Endothelial Aggregation Receptor 1 (PEAR1) was first described by Nanda *et al.* in 2005.[1] They identified PEAR1 as a platelet-platelet contact receptor, responsible for the stabilisation of both platelet aggregates and fully-formed thrombi. Our group has previously studied the underlying PEAR1 signalling pathway and described a role for PEAR1 in the sustained activation of $\alpha_{IIb}\beta_3$, hence a role in stabilising platelet aggregates.[5] The principal aim of this thesis was to further elucidate the role of PEAR1 in platelet signalling and megakaryopoiesis in addition to studying the expression profile and function of PEAR1 in ECs, a so far untouched field in EC biology.

In the previous four chapters I provided answers to some important questions regarding this novel receptor. We have identified a physiological and non-physiological ligand for PEAR1, described a role for PEAR1 in haematopoiesis and discovered PEAR1 as a novel modifier of neo-angiogenesis. This section of the thesis will go into more detail on some interesting overarching topics concerning PEAR1.

PEAR1: A Controller of Cell Quiescence

In 2007 Krivtsov et *al.* described a role for PEAR1 in hematopoietic cell regulation. They reported that the overexpression of *PEAR1* in murine bone marrow cells led to a decrease in the total number of progenitor cells[6] and thus suggested that PEAR1 negatively regulates hematopoietic cell proliferation and differentiation in the early stages. These preliminary findings prompted us to study whether PEAR1 was also a regulator of platelet production and EC proliferation.

As discussed in Chapter I and compatible with the data provided by Krivtsov *et al.* in murine bone marrow cells, we found the expression of *PEAR1* to be very low at day 0 in cultured human CD34(+) cells and found that *PEAR1* expression is progressively upregulated during the process of megakaryopoiesis up to day 12.[4] Indeed, *PEAR1* knockdown in CD34(+) cells via lentiviral transduction of a short hairpin PEAR1 construct (*shPEAR1*) strongly enhanced megakaryocyte progenitor proliferation and thrombopoiesis *in vitro*. These observations were confirmed in an *in vivo* zebrafish model where again *Pear1* mRNA was low at 24 hours post-fertilisation and progressively increased up to day 4. Early knockdown of *Pear1* (via a morpholino knockdown strategy) enhanced thrombopoiesis in zebrafish at day 2.[4]

Both of these approaches demonstrated that PEAR1 negatively regulates the early stages of megakaryopoiesis and thrombopoiesis.

Similar to these findings of enhanced proliferation in *shPEAR1*-transduced CD34(+) cells (Chapter I), comparable results were seen in ECs (Chapter IV). Knockdown of *PEAR1* in cultured ECs (*shPEAR1* ECs) also resulted in a proliferative phenotype and, in line with our findings in megakaryocytes (MKs), we observed low *PEAR1* expression in rapidly-proliferating cultured ECs (BOECs, HUVECs and HUAECs) compared to a higher level of expression in the slowly-

proliferating microvascular ECs of the heart and liver.[7] This was also the case in the rapidly-proliferating ECs of pyogenic granuloma, a hypervascularised skin tumour where an inverse association between PEAR1 expression and EC proliferation was observed.[7] All of these results suggested that PEAR1 can modify endothelial angiogenic behaviour leading to an increased proliferation rate and tube-forming capacity in its absence (Chapter IV).[7]

Our results also show that specific triggers such as hypoxia or skin injury resulted in enhanced neo-angiogenesis in a *Pear1*$^{-/-}$ mouse model, although *Pear1*$^{-/-}$ pups showed no overt vascular phenotype at birth and detailed IHC and angiographic analyses of various murine tissues at the age of 13 weeks did not detect abnormalities in blood vessels in the absence of Pear1.[7] We therefore concluded that knocking out *Pear1* does not affect embryological angiogenesis but does affect sprouting from mature ECs (neo-angiogenesis). This hypothesis was supported by our findings in the ECs of zebrafish. Similar to human ECs, very low *Pear1* expression was found in the zebrafish ECs during embryonic development (Figure 1), in agreement with the low PEAR1 expression that was observed in ECs with a highly proliferative and migratory state. Knockdown of *Pear1* in zebrafish using a morpholino strategy did not affect vasculogenesis in the early stages of development (Figure 2), further suggesting that PEAR1 does not play an important role during early vascular development and supporting a selective role for it in mature blood vessels. To further establish this hypothesis, in a future research project it would be of great value to study the expression of Pear1 during the different stages of murine embryogenesis to verify whether Pear1 expression rises during murine development at well-defined stages.

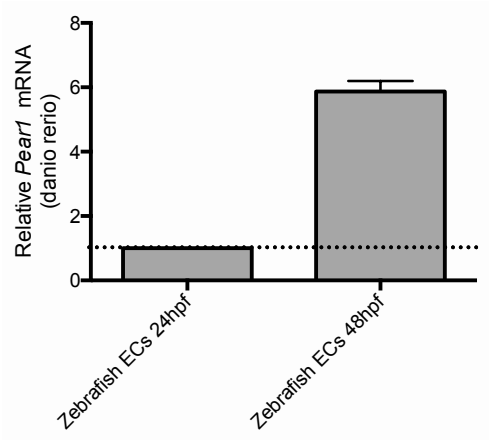

Figure 1 - Relative *Pear1* expression in isolated Fli1:eGFP zebrafish ECs at 24 and 48 hours post-fertilisation (hpf) was extremely low (Ct values ≈ 33; ΔΔCt normalised to the *Elfa* housekeeping gene ≈ 6; values were comparable to *PEAR1* mRNA levels in human BOECs). Total *Pear1* expression in the zebrafish progressively rose up to day 4, as previously shown by our group.[4]

Through these results we have identified that PEAR1 controls the proliferation of MKs and ECs and modifies neo-angiogenesis. These findings could form a basis for further (clinical) research seeking to clarify a potential role for PEAR1 in platelet disorders (e.g. congenital platelet production disorders, leukaemia, essential thrombocytosis, etc), in diseases associated with enhanced or diminished neo-angiogenesis (haemangiomata, tumour angiogenesis, collateral vessel formation, etc) or in diseases where platelets and ECs meet (e.g. pulmonary hypertension, stent re-endothelialisation, vasculitis, etc). Some of these topics will be more thoroughly discussed in the section entitled "Future Perspectives".

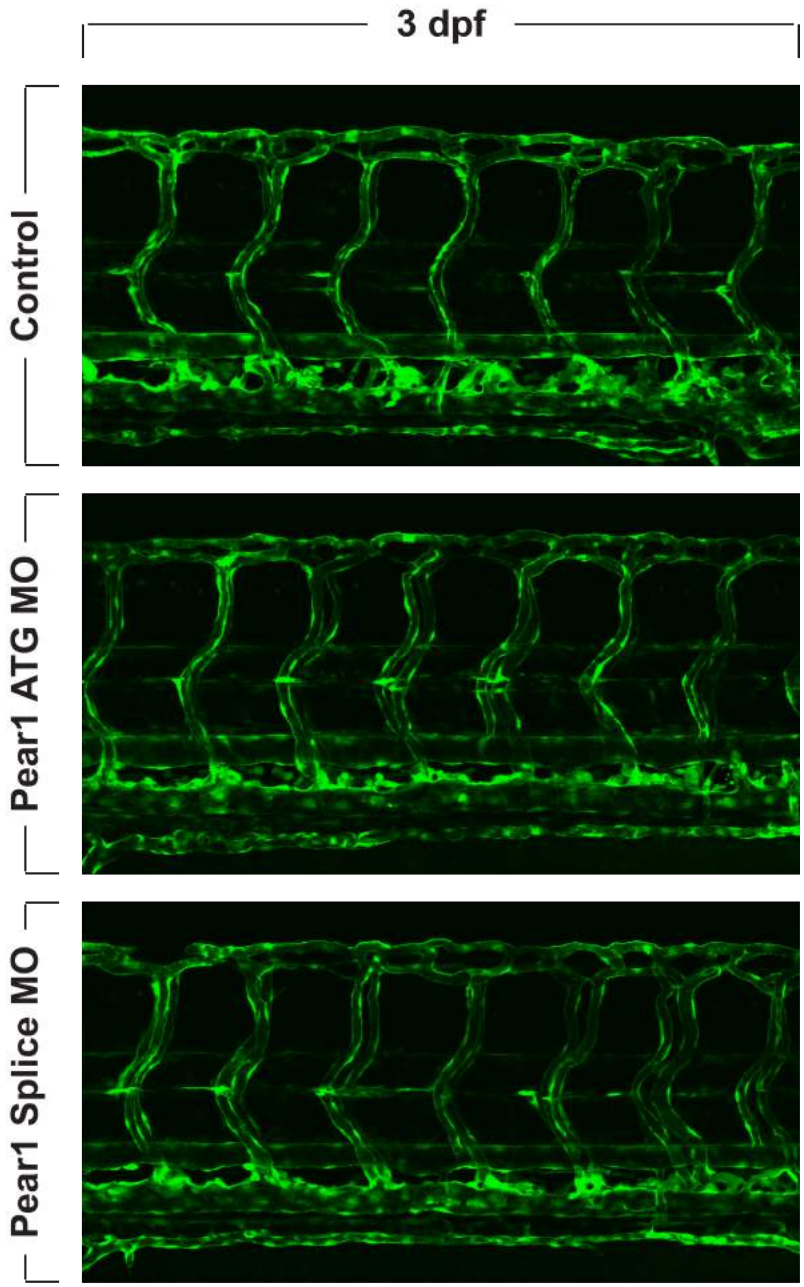

Figure 2 - Confocal microscopy analyses of Fli1:eGFP zebrafish embryos, injected with control MO (upper panel), PEAR1-ATG MO (middle panel) and PEAR1-splice MO (lower panel). Embryos were screened at 1, 2, 3 and 5 days post-fertilisation. No changes in early vasculogenesis were observed, compared to control embryos. MO = morpholino.

PEAR1 AND THE PTEN/PI3K/AKT AXIS

In both platelets and ECs we identified the PTEN/PI3K/Akt pathway as a crucial axis downstream of PEAR1. Moreover, we were able to restore the hyperproliferative phenotype in *shPEAR1* ECs via restoring the PEAR1-driven imbalance between PTEN and PI3K activity. Our results highlight a role for PEAR1 in modifying the expression levels of PTEN, resulting in enhanced activity of PI3K and enhanced phosphorylation levels of Akt, highlighting PEAR1 as a central orchestrator of important cell functions in both platelets and ECs. The mechanism by which PEAR1 regulates the PTEN/PI3K/Akt pathway in ECs is still unknown. In *shPEAR1* CD34(+) cells, however, we found that HES1, a direct target of the Notch receptor pathway, was upregulated without any modification of expression of the Notch receptors. As discussed in Chapter I, HES1 is reported to be a negative regulator of *PTEN* transcription during megakaryopoiesis.[8, 9] Therefore we concluded that PEAR1 signalling in CD34(+) cells controls PTEN expression via the NOTCH pathway, although other signalling pathways might also be involved. The role of integrins in platelet PEAR1 signalling is a topic of ongoing research in our laboratory.

In ECs, the mechanism of PEAR1-mediated regulation of the PTEN/PI3K/Akt pathway is less clear. As discussed in Chapter IV, The PTEN/PI3K/Akt pathway is a central player in EC biology in normal vascular development and tumour angiogenesis through regulation of EC migration, proliferation, cell survival and vascular tone[10]. Given that *PEAR1* deletion did not affect embryogenesis, we then focussed our investigations on post-natal neovascularisation. Post-natal neovascularisation is a complex process that depends on the coordinated interactions between endothelial shear stress, endothelial vascular growth factors (VGFs; e.g. VEGF, Ang-1, Ang-2, bFGF [basic fibroblast growth factor], PDGF-B [platelet-derived growth factor-B], Ephrins, and TGF-β [transforming growth factor β] superfamily members), intracellular signalling proteins (e.g. Notch signalling) and cell-cell adhesion molecules (e.g. connexions and VCAM-1 [vascular cell adhesion molecule-1]). All of these activate or modulate the PI3K/Akt pathway, highlighting the importance of this axis.[10, 11]

PTEN regulates EC function at various levels and many signalling pathways in turn regulate the expression and function of this tumour suppressor gene.[12] PTEN is important for the homeostasis of the cardiovascular system and it is well known that *Pten*/*PTEN* overexpression or the administration of PI3K inhibitors blocks vascular sprouting and EC tube formation *in vitro* and blocks tumour angiogenesis and tumour growth *in vivo.*[12] This is probably mediated via hypersensitisation to VGFs upon the loss of *Pten* and via dysregulation of the downstream mediators of PI3K/Akt signalling.[12-14] In parallel, heterozygous knockout mutations of *PTEN* in ECs have been shown to promote post-natal tumour angiogenesis and neovascularisation whereas (floxed) homozygous deletion of *Pten* in murine ECs was shown to impair cardiovascular morphogenesis.[11]

Homozygous null mutations for *Pten* in mice are embryonic lethal.[11] However, zebrafish embryos lacking *Pten* show an enhanced EC proliferation and hyperbranching of blood vessels.[15] This is in sharp contrast with the normal embryogenic (vascular) development of *Pear1*$^{-/-}$ mice, as discussed in Chapter IV, again underpinning the fact that PEAR1 does not play a role in embryological biology and again suggesting that PEAR1 expression is low/absent during embryological development.

In the next part of the discussion I will further review the known roles of some of the PTEN/PI3K-modulating players in post-natal angiogenesis and put them into perspective relative to PEAR1.

I. HIF1A AND VEGF

It has been thoroughly established that high levels of PTEN inhibit VEGF-induced sprouting and capillary formation. Impaired PTEN levels led to an increase in EC proliferation, migration and vascular sprouting.[12, 14] Moreover, it was shown that PTEN deficiency directly leads to an altered VGF profile (decreased expression of Ang-1, EphrinB2 and VCAM, and increased levels of Ang-2, VEGF-A, VEGFR 1 and 2)[11, 14], which likely explains the changes induced in cardiovascular development in *Pten*$^{-/-}$ mice. However, as was discussed in Chapter IV, a lack of PEAR1 did not affect any of the important players in the p53-Hif1α-VEGF-VEGFR2 pathway.

II. ANGIOPOIETINS

Ang-1 (angiopoietin 1) and its receptor Tie2 are important in PI3K-mediated EC survival and migration as well as in vessel permeability and in the recruitment of smooth muscle cells.[16] Tie2 is mainly expressed on ECs and its ligand (Ang-1) is antagonised by Ang-2.[17] Hamada *et al.* showed that heterozygous *Pten*-floxed ECs have a more proliferative and faster migratory phenotype and an altered Ang-1/Ang-2 ratio.[11] Since angiopoietins regulate both EC proliferation and migration, it will be of interest to unravel their involvement in PEAR1 signalling.

III. NOTCH SIGNALLING

HES1 is a negative regulator of *PTEN* transcription during megakaryopoiesis.[8, 9] As previously discussed, we found an upregulation of HES1 expression in *shPEAR1* CD34(+) cells, linking the decreased PTEN expression in *shPEAR1* CD34(+) cells with the NOTCH pathway. In ECs however, a link between HES1 and PTEN has not been clearly established. As explained in the Introduction chapter of this thesis, NOTCH plays an important role in blood vessel growth. Briefly, guiding tip cells are associated with high levels of Dll4, which activates the NOTCH pathway in neighbouring stalk cells, preventing them from becoming a tip cell. Dll4-induced activation of NOTCH in ECs leads to cell cycle arrest and thus the arrest of EC proliferation both *in vitro*[18] and *in vivo*[19]. Very recently, it was found that NOTCH exerts its negative effects on EC proliferation via PTEN.[2] Sera *et al.* reported that NOTCH signalling fails to arrest early stalk cell proliferation upon *PTEN* deletion (or that PTEN negatively regulates stalk cell proliferation), resulting in defective sprout length and patterning.[2] They showed that NOTCH regulates stalk cell proliferation via stimulation of *PTEN* transcription. This is summarised in Figure 3.

Although endothelial PTEN is essential for regulating NOTCH-induced stalk cell proliferation and thus sprouting, it is dispensable for the regulation of the sprouting activity of tip cells.[2] This is illustrated well by the fact that *NOTCH* mutants show both proliferative and (VEGFR3-driven) sprouting defects,[20, 21] whereas *PTEN* mutants only show proliferative effects. Although we found an enhanced proliferation of ECs and

increased vessel formation in our *Pear1*$^{-/-}$ hindlimb ischemia model, these newly formed vessels were apparently functional since they resulted in a faster blood flow recovery. Therefore, we argue that they cannot be compared with the dysfunctional vascular density defects reported in *PTEN* mutants (Figure 3B). This inconsistency might be explained by the fact that knockdown of *PEAR1* reduced but did not completely abrogate *PTEN* expression in ECs (Chapter IV). These findings suggest that PEAR1 might help to regulate NOTCH-driven sprouting and neo-angiogenesis, via the modulation of PTEN in stalk cells and via the control of tip cell formation and EC migration. This should be a topic for further investigation.

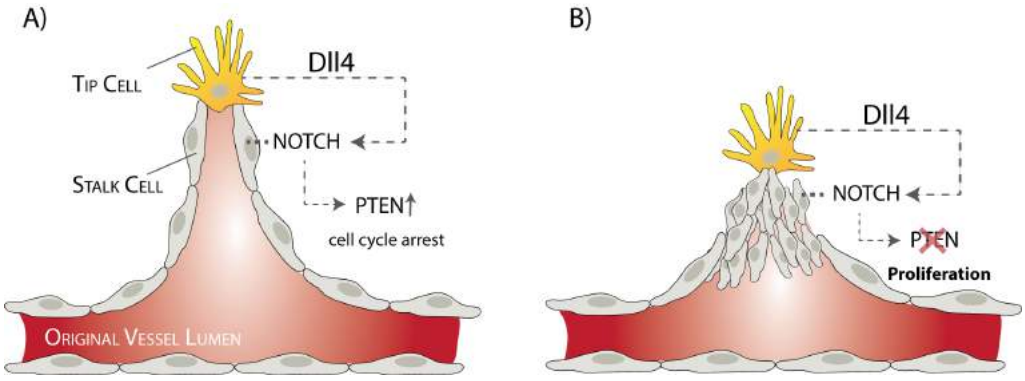

Figure 3 – A) Activation of NOTCH by Dll4 induces the expression of PTEN, which blocks stalk cell proliferation. B) Upon a loss of PTEN, NOTCH signalling fails to arrest stalk cells resulting in defective sprout length and patterning. – adapted from Serra *et al.*[2]

IV. Shear Stress

Shear stress is a complex, haemodynamic force that is applied across the endothelial surface and modulates essential EC functions such as vascular tone, inflammatory processes, EC remodelling and angiogenesis[22-24], and activates a broad variety of important EC signalling pathways such as those involving MAPK, protein kinase C (PKC), c-Src, Rho family GTPases and PTEN/PI3K/Akt.[25, 26] An important mediator in shear stress-induced angiogenesis is nitric oxide (NO), whose production via the subcellular localisation of endothelial NO synthase (eNOS) is mainly orchestrated via KLF-2 (Krüppel-like factor 2), protein kinase A (PKA) and the PI3K/Akt pathway.[27] NO modulates essential EC processes such as EC survival, proliferation, migration and interaction with the ECM. VEGF-induced angiogenesis is blocked in the presence of an NO inhibitor (L-NAME)[28] and NO production is impaired in a variety of pathophysiological conditions such as atherosclerosis, smoking, hypercholesterolemia, etc.[29] Although NO is essential for shear stress-induced angiogenesis, the mechanistic link between shear stress, NO production and angiogenesis is poorly understood.

In Chapter IV we showed that knockdown of PEAR1 in ECs did not result in enhanced NO production. Nevertheless, additional research has shown (unpublished results; Figure 4) that the incubation of ECs with an anti-PEAR1 antibody results in the transient phosphorylation of PEAR1 and Akt (as seen in platelets)[5] and the transient

(peaking at 15 minutes) phosphorylation of eNOS (at activation site S1177), leading to a transient rise in NO production *in vitro* (see Chapter IV).

Based on these findings, ongoing research will try to elucidate whether shear stress can induce PEAR1 phosphorylation *in vitro* and *in vivo* and whether PEAR1 might function as a mechanoreceptor on ECs, ultimately inducing shear stress-mediated NO production and Akt/NO-induced angiogenesis (Figure 5 shows a hypothetical scheme; further discussed in the Future Perspectives paragraph). These findings have very recently been further supported by Adam *et al.*, who showed that the minor allele of the rs12041331 SNP in *PEAR1* is significantly associated with a greater brachial artery flow-mediated dilatation (FMD),[30] a test previously shown to be largely dependent on NO.[31]

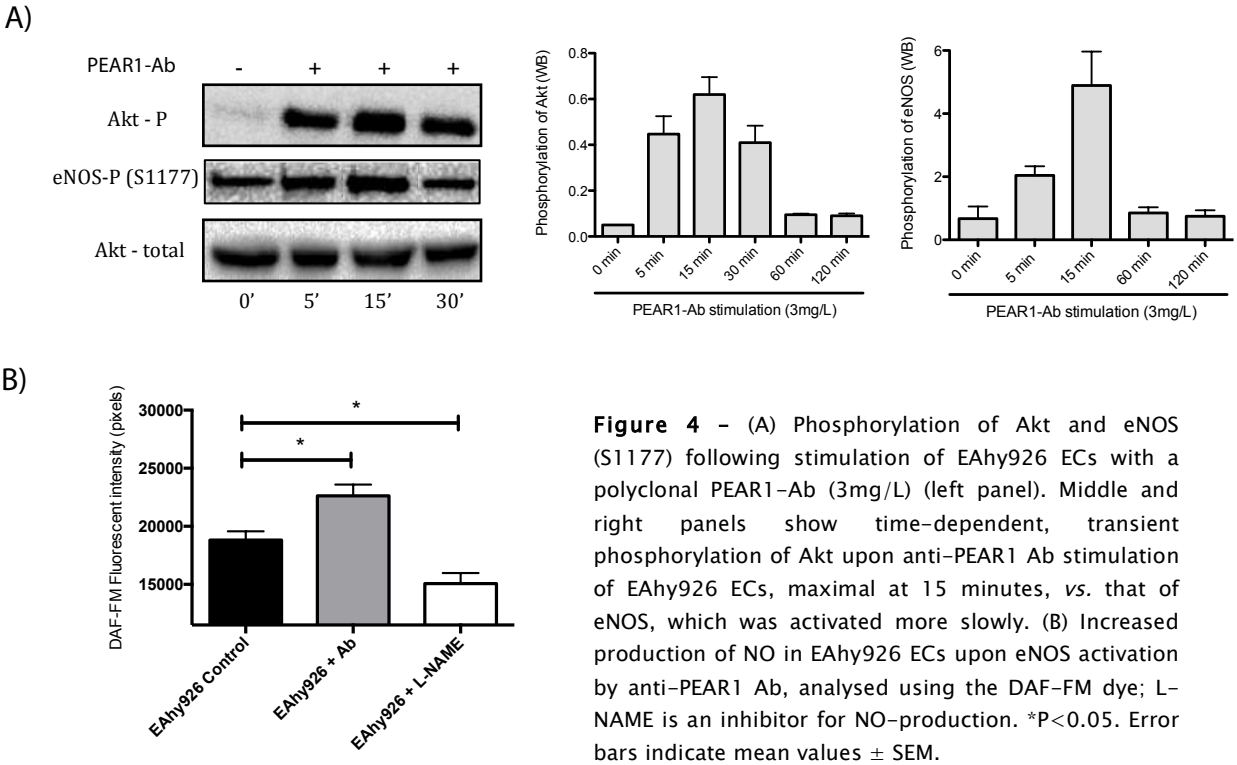

Figure 4 - (A) Phosphorylation of Akt and eNOS (S1177) following stimulation of EAhy926 ECs with a polyclonal PEAR1-Ab (3mg/L) (left panel). Middle and right panels show time-dependent, transient phosphorylation of Akt upon anti-PEAR1 Ab stimulation of EAhy926 ECs, maximal at 15 minutes, *vs.* that of eNOS, which was activated more slowly. (B) Increased production of NO in EAhy926 ECs upon eNOS activation by anti-PEAR1 Ab, analysed using the DAF-FM dye; L-NAME is an inhibitor for NO-production. *P<0.05. Error bars indicate mean values ± SEM.

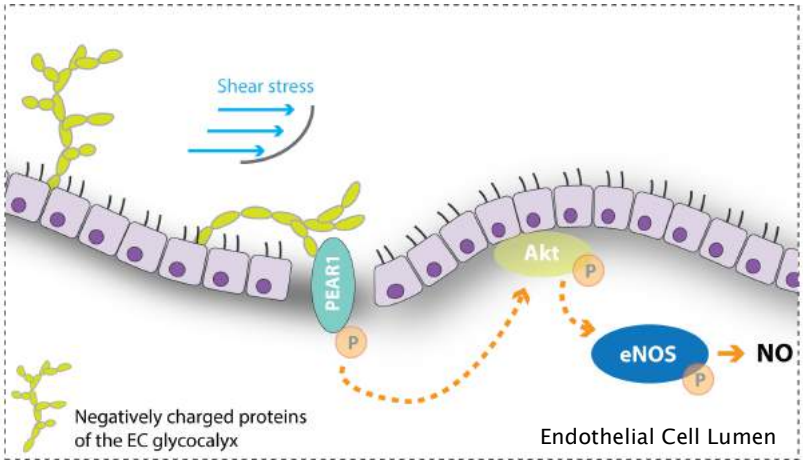

Figure 5 - Hypothetical scheme for PEAR1 as a mechanoreceptor for EC shear stress. Undefined negatively charged proteins of the glycocalyx (e.g. chondroitin sulphate, heparan sulphate, etc), lead to shear stress-mediated PEAR1 activation and subsequent Akt and eNOS phosphorylation.

V. uPAR Signalling

The urokinase receptor (uPAR, CD87) has been shown to play an essential role in growth factor-induced EC activation and EC migration/invasion. In a very recent report, Unseld *et al.* reported an inverse correlation between uPAR and PTEN expression.[32] They showed that overexpression of uPAR downregulated *PTEN* transcription, leading to enhanced Akt-driven EC motility and EC survival *in vitro* and the promotion of Akt-driven EC invasion *in vivo*. Although uPAR deficiency in ECs led to a remarkable enhanced migratory phenotype and survival rate, EC proliferation was not affected.[32] In future research it will be of interest to measure the uPAR expression profile in *PEAR1* knockdown ECs as a possible explanation for the enhanced migratory phenotype seen in these cells.

VI. Integrins

Angiogenesis is a complex process, not only necessitating EC migration and proliferation but also their attachment to the extracellular matrix (ECM) and proteolysis of this ECM via the activation of specific matrix metalloproteases (see next paragraph).[33] In order to cross tissue boundaries during EC migration, various adhesion receptors (integrins) play a crucial role.[34] Integrins are characterised by their bidirectional signalling and PI3K plays an important role in both of these processes[35]. Firstly, "inside-out signalling" causes integrins to adopt an active conformation and organise adhesion to ECM molecules, a process which is required for adequate cell movement.[35] Then, through "outside-in signalling" they regulate intracellular signalling pathways that control the organisation of the cytoskeleton and mediate cell survival. Various integrins play a role in angiogenesis, for example, the deletion of α_5 reduces capillary plexus formation[36], and $\alpha_v\beta_3$ integrins are known to be upregulated during angiogenesis[37]. However, β_1 integrins are reported to be particularly important during vasculogenesis.[38, 39] *In vitro*, β_1*-integrin*$^{-/-}$ ECs show reduced migration and elongation despite an increase in proliferation and apoptosis, ultimately leading to a reduced cell number. These effects are also observed *in vivo*, where a reduction in EC maturation, migration and sprouting has been reported.[38, 39] Interestingly, the enhanced EC proliferative phenotype observed in β_1*-integrin*$^{-/-}$ ECs was found to be mediated via the PI3K/Akt pathway.[38]

We previously reported (Chapter IV) a high expression of human PEAR1 in EC ruffles and lamellipodia, suggesting a role for PEAR1 in EC migration and the involvement of PEAR1 in the bidirectional cell-ECM contacts, as seen for integrins. We confirmed an enhanced migratory phenotype in *shPEAR1* ECs and confirmed an enhanced neo-angiogenesis in *Pear1*$^{-/-}$ models of hypoxia. Therefore it will be of interest to investigate whether the integrin expression profile in *shPEAR1* ECs becomes altered (e.g. to a more "metastatic" profile) or whether *PEAR1* knockdown affects the affinity of certain integrins for their ligands.

VII. Modulators of the ECM

The ECM is an important source of angiogenic signals. It is not only an important extracellular source of VGFs, such as VEGF, but degradation of ECM compounds also

leads to the production of strong pro- or anti-angiogenic factors. The most relevant proteases involved in this process are matrix metalloproteases (MMPs), with MMP-2 and MMP-9 being the key players.[40, 41] MMPs are reported to be primarily involved in EC migration by interference with EC-EC and EC-ECM interactions.[19] PTEN overexpression in a multiple myeloma cell line results in decreased protein levels of MMP-2 and MMP-9[42], illustrating a negative correlation between PTEN and MMP expression.[19] Interestingly, this decreased MMP expression in PTEN-overexpressing cells was reversed by the addition of a PI3K inhibitor.[43] Therefore, it would be interesting to correlate the enhanced migratory phenotype of *shPEAR1* ECs with MMP expression.

VIII. EPH/EPHRINS

Eph-receptors belong to the receptor tyrosine kinase (RTK) superfamily and are known to play a role in embryogenesis, angiogenesis and axonal guidance.[44-46] They are divided in the A and B subfamilies and their respective ligands are ephrin A and ephrin B. Eph-receptors and ephrins are frequently overexpressed by tumours and tumour ECs, leading to the promotion of tumour angiogenesis.[19] Various groups have reported that Eph-receptors activate PI3K and are regulated via the PTEN/PI3K pathway.[47-49] Eph-receptor/ephrin interactions are crucial for a broad spectrum of cell regulatory processes such as the modulation of cell adhesion, cell repulsion, cell motility and cell positioning.[47] Since ephrins are particularly crucial for embryological vascular development, it is less likely that they are coupled to PEAR1 signalling.

IX. TGFβ

TGFβ is an important signalling molecule in the complex process of angiogenesis, and is involved mainly in EC proliferation and migration.[50-52] The crucial roles for TGFβ were elucidated using human and murine genetic studies, where mutations in important TGFβ signalling pathway components (e.g. endoglin [ENG], Alk1, Smad4) were found to result in diseases such as pulmonary arterial hypertension, hereditary haemorrhagic telangiectasias (HHT) and vascular malformations (see below).[52] It has also been reported that the TGFβ/Smad4 complex regulates angiogenesis via regulation of the expression of certain pro-angiogenic micro RNAs (miRNAs) such as miR-21 and miR-29a, which exercise their effects via the direct downregulation of PTEN (miR-29a)[50] or upregulation of Akt activity (miR-21)[53], promoting EC migration, proliferation and ultimately tube formation.[50] Interestingly, the effect of miR-29a in stimulating tube formation via TGFβ was completely blocked by an PI3K inhibitor (LY294002).[50] The link between TGFβ and PTEN has been well-established (PTEN is also known as TEP1: TGFβ-regulated and epithelial cell-enriched phosphatase) and very recently, Adam *et al.* conducted meta-analyses of 75000 publicly available microarrays which revealed that *PEAR1* expression is highly correlated with the expression of *ANG-2*, *ACVRL1/ALK1* and *ENG*, which are important genes in the TGFβ signalling cascade.[30] This makes TGFβ and its associated genes (*ENG*, *ALK1*, etc) of particular interest when further investigating the effect of *PEAR1* knockdown on this important signalling pathway.

Further studies investigating the expression and signalling of these important players in blood vessel formation will be needed to find out the underlying mechanisms of the enhanced neo-angiogenesis observed upon *PEAR1*-knockdown/*Pear1*-knockout. Since ECs lacking *PEAR1* showed both a proliferative and migratory phenotype, it would not be surprising to find that PEAR1 affects both tip and stalk cell formation and/or ECM modification during neo-angiogenesis and modulates several of the previously discussed crucial signalling pathways. It will be of particular interest to investigate the involvement of PEAR1 in PTEN-modulated tumour angiogenesis (which is discussed below) and to analyse patients with *PEAR1* mutations to see if they result in, e.g. Cowden-like disease (Cowden disease is a disorder in which hereditary *PTEN* mutations lead to tumour susceptibility disorders[54]). This will be discussed in more detail in the Future Perspectives section below.

PEAR1 AND ITS LIGANDS

I. THE IGE-RECEPTOR FCεR1α, A PHYSIOLOGICAL LIGAND FOR PEAR1 ON PLATELETS

As discussed in Chapter II, we identified human FcεR1α as a physiological ligand for PEAR1 in platelets. PEAR1 is in competition (albeit with a lower affinity) with IgE for FcεR1α, suggesting a interaction between IgE-mediated diseases and platelet aggregate stability (Figure 6). This interaction was surprising to us, even though we found there to be a high affinity between PEAR1 and FcεR1α and we confirmed, in line with previous reports[55, 56], the expression of FcεR1α on the platelet surface. Various reports have suggested that patients with an atopic constitution have decreased platelet aggregate responses to various classical platelet agonists.[57, 58] These responses are even cyclic, depending on the allergy season.[59] Nevertheless, the underlying signalling mechanisms remained to be unravelled.

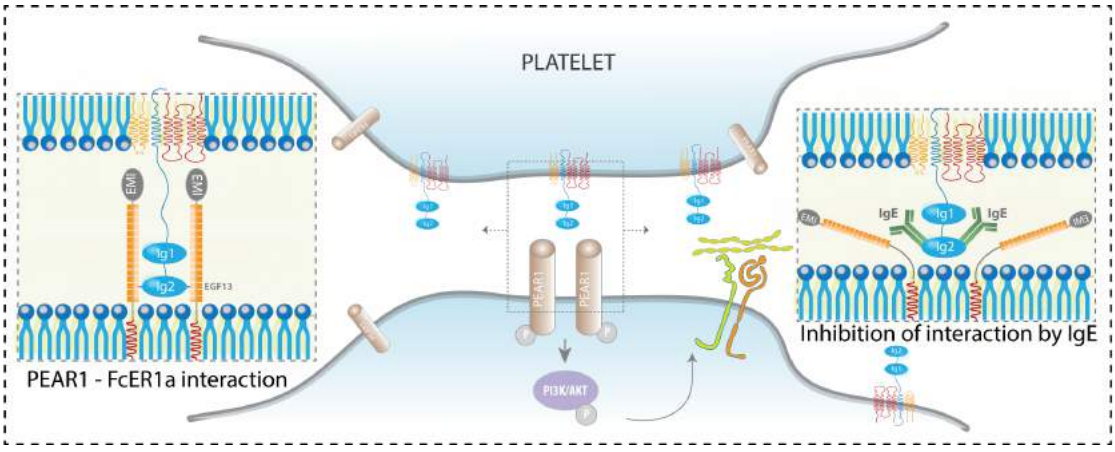

Figure 6 – Schematic reproduction of platelet-platelet contact between PEAR1 and FcεR1α (left and middle part). PEAR1 and IgE are in competition for FcεR1α, the latter having the highest affinity for FcεR1α (right part).

In healthy individuals, the concentration of circulating IgE is very low, at approximately 0.5 nM.[60] Where circulating levels of IgE are increased, for example in atopic patients,[60] this would significantly decrease the amount of IgE-free FcεR1α on the platelet surface that is available for PEAR1 binding, reducing PEAR1-induced platelet-platelet activation. This is consistent with reports of a systemic lack of secondary platelet responsiveness in atopic patients, an observation

that has also been correlated with elevated IgE levels.[59, 61-63]

To further investigate the FcεR1α-PEAR1-mediated link between platelet function and allergy, we added exogenous IgE to collagen-induced platelet aggregation assays using multiple atopic donors, and observed a consistent inhibition of platelet aggregation (Figure 7, unpublished results). These results might open the door for a prospective randomised trial, linking atopic patients to decreased platelet responsiveness, and eventually revealing allergy to be a (minor) protective phenotype for cardiovascular disease. In addition, this would further underpin the importance of the impact of the environment on the heart and blood vessels.

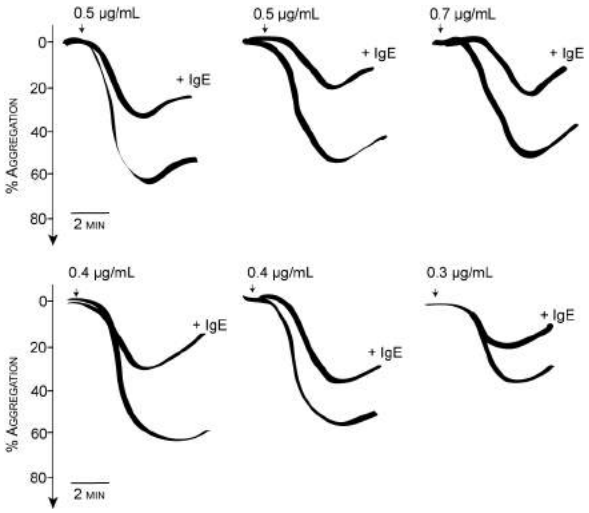

Figure 7 - Exogenously added IgE inhibited platelet aggregation triggered by donor-specific concentrations of collagen that elicited 40-70% aggregation. Aggregation traces from six representative atopic donors are shown.

FcεR1α is reported to be expressed on mast cells, eosinophils, basophils, monocytes, epidermal Langerhans cells and dendritic cells.[55] In addition to this, I also confirmed the presence of FcεR1α on the membrane of human ECs (through immunofluorescence and western blotting - unpublished results) and that sFcεR1α activates the PEAR1/Akt pathway in ECs, identifying FcεR1α as a ligand for PEAR1 in ECs as well as platelets (unpublished results).

The presence of PEAR1 on both platelets and ECs and the expression of FcεR1α on the surface of platelets, ECs and eosinophils raises the question of whether the PEAR1- FcεR1α interaction could play a role in the broad disease spectrum of **vasculitis**. The spectrum of this disease, in which inflammation and eosinophilia meet each other, is broad and ranges from granulomatosis with polyangiitis (GPA; Wegener's disease), microscopic polyangiitis (MPA) and rheumatoid arthritis to systemic sclerosis and systemic lupus erythematosus (SLE).[64] Although inflammation and eosinophilia are central to all of these disease entities, the most typical one that brings hypereosinophilia and inflammation/vasculitis together is eosinophilic granulomatosis with polyangiitis (EGPA; Churg-Strauss syndrome).[64]

Churg-Straus has a broad variety of symptoms. Briefly, it is associated with asthma, parenchymal lung disease, vasculitis (most commonly involving the peripheral nerves or skin, leading to purpura, nodules, ulcerating lesions, livedo reticularis), renal failure (glomerulonephritis), gastrointestinal disease (related to eosinophilic infiltration and/or vasculitis) and cardiac involvement (cardiomyopathy from myocarditis, pericarditis, endocarditis, valvulitis, coronary vasculitis).[65, 66] It is well known that eosinophils, activated platelets and activated ECs play a central role in the pathogenesis of Churg-Strauss.[67] Nevertheless, the underlying mechanism of

this disease remains unknown. Therefore, it might be interesting to study whether the FcεR1α–PEAR1 interaction in platelet–platelet, platelet–EC, eosinophil–platelet and/or eosinophil–EC contacts contributes to this disease spectrum since it is characterised by vascular occlusion.

II. Dextran Sulphate: a Non-Physiological ligand for PEAR1 in Platelets

In Chapter III we identified PEAR1 as the major platelet receptor responsible for the dextran sulphate (DxS)–induced platelet aggregation that was recently reported by Getz *et al.*[68] Although oral administration of (high molecular weight) DxS is a well–established model for the induction of murine colitis,[69] its physiological role in platelet activation and aggregation remains unclear.

In addition to its activation of PEAR1 in platelets, we also found that DxS is able to induce the phosphorylation of PEAR1 in ECs (unpublished results), leading to the phosphorylation of both Akt and downstream eNOS. Based on our knowledge, discussed previously in the paragraph on *shear stress*, this is a very interesting finding. It was surprising that a very negatively–charged molecule such as DxS was able to bind to an EC surface receptor in the environment of the negatively–charged glycocalyx, but we think that this is due to the well–described fast degeneration of the EC glycocalyx in cultured ECs.[70] DxS shows strong structural similarities with heparan sulphate (HS), a major component of the EC glycocalyx, therefore we hypothesised that DxS is a non–physiological ligand for PEAR1 and is involved in EC mechanotransduction.

The main components of the EC glycocalyx are hyaluronic acid, heparan sulphate (HS) and chondroitin sulphate. Excellent work from the group of Tarbell *et al.* has shown that during the first 30 minutes of shear stress, HS (and its anchoring protein glypican–1) shifts to align with the direction of the flow, whereas other components of the glycocalyx do not move.[71] In addition, dissolving HS on the EC surface using heparanase completely blocks shear stress–induced phosphorylation of eNOS and NO production.[72] These results demonstrate that HS proteoglycans play a role in the mechanotransduction of fluid shear stress in ECs. This has led to the HS–glypican–eNOS hypothesis: that the HS–glypican complex transmits mechanical forces to the caveolae of ECs, where eNOS is phosphorylated, leading to NO production.[73] Although it has been established that this involves intermediate signalling through c–Src and its downstream signalling cascades, the underlying mechanoreceptors responsible for this c–Src–mediated eNOS phosphorylation are poorly understood.[74]

Many components of the glycocalyx disappear from ECs in culture, although immunohistology has demonstrated the sustained presence of HS, the main constituent of the glycocalyx, both *ex vivo* and *in vitro.*[70] The presence of HSs on cultured cells may explain why mechanotransduction phenomena can be observed *in vitro*, even with an immature glycocalyx.[70]

Therefore, we now know that PEAR1 phosphorylation is mediated via c–Src and activates Akt–eNOS pathways in ECs, and that HS resembles DxS structurally. Since DxS is a ligand for PEAR1 on both platelets and ECs, our future work will use an *in vitro* shear stress technique to investigate whether PEAR1 acts as a mechanoreceptor on ECs, ultimately leading to shear stress–induced NO production (see Figure 5). This might create new insights into the described intervariability in responses to stent endothelialisation where an inverse correlation exists between shear stress and neo–intimal hyperplasia, a process that is mainly driven by EC migration and the proliferation of stent–adjacent ECs.[75]

FUTURE PERSPECTIVES

In the following paragraphs I will give an overview of some important planned experiments for the future, which concern the mechanism of PEAR1 signalling. I will also discuss some important clinical pathologies in which I hypothesize PEAR1 might be involved.

OVEREXPRESSION STUDIES OF PEAR1

So far I discussed: the effect of lentiviral-mediated *PEAR1* knockdown in CD34(+) cells (Chapter I) and ECs *in vitro* (Chapter IV); the effect of morpholino-driven *Pear1* knockdown in zebrafish *in vivo* (Chapter I); the effect of *Pear1* knockout in murine platelets *ex vivo* (Chapter III); and the effect of (non-conditional) *Pear1* knockout in murine ECs *in vivo* (Chapter IV).

A burning question concerns the effect of PEAR1 overexpression on the phenotype of platelet production and neo-angiogenesis. Of particular interest will be whether the overexpression of PEAR1 in megakaryocytes and ECs results in enhanced levels of *PTEN* expression, leading to a decreased activity of the PI3K/Akt axis. Several studies have shown that PTEN overexpression, or gain-of-function mutations in *PTEN*, significantly inhibit Akt-driven cell proliferation and/or enhanced cell apoptosis.[76–79] Interestingly, constitutively active forms of PI3K and Akt can rescue PTEN-induced suppression of cell proliferation.[80] In megakaryopoiesis, *Pten* overexpression inhibits megakaryocyte development *in vivo* and *ex vivo,*[8] and in angiogenesis it was recently shown that overexpression of *PTEN* in stalk cells reduces vascular density and abrogates the increased EC proliferation induced by blocking NOTCH (as described above).[2]

To address this, our group recently designed a floxed PEAR1-GFP cassette-based *PEAR1* overexpression vector (CMV-eGFP ON-PEAR1 OFF IRES BSdR) which can be transduced into CD34(+) cells or ECs to induce *PEAR1* overexpression at certain time points by adding lentiviral-transduced Cre (Virus Like Particle Carrying Cre (VLP-Cre). This will flox the cassette to a CMV-PEAR1 ON-eGFP OFF IRES BsdR PEAR1 overexpressing vector and will allow us to study the effect of *PEAR1* overexpression on the phenotype of both megakaryocytes (for example, will it reduce platelet production and megakaryocyte proliferation?) and ECs (will they have reduced proliferation and increased apoptosis?) and will allow us to study the downstream cellular signalling effects of *PEAR1* overexpression.

PEAR1 AND PULMONARY ARTERIAL HYPERTENSION

Pulmonary arterial hypertension (PAHT) is a complex disease. It comprises a collective group of pathophysiological processes that lead to similar symptoms but result from a variety of underlying causes. The main entities in the PAHT disease spectrum are vasoconstriction, smooth muscle cell and EC proliferation, and thrombosis. PAHT arises due to imbalances in the homeostasis of these entities, probably due to pulmonary EC dysfunction or injury.[3]

An overview of the most important mediators of pulmonary vascular responses in PATH is given in Table 1 An imbalance between those mediators is believed to be the main reason for impaired

vasoconstriction, EC proliferation and thrombosis in PAHT, forming the basis for the development of a whole range of medicines for the treatment of PAHT.[81-85]

VASOCONSTRICTION	CELL PROLIFERATION	THROMBOSIS
Increased TXA_2	Increased VEGF	Increased TXA_2
Decreased PGI_2	Decreased PGI_2	Decreased PGI_2
Decreased NO	Decreased NO	Decreased NO
Increased ET-1	Increased ET-1	
Increased 5-HT	Increased 5-HT	Increased 5-HT
Decreased VIP	Decreased VIP	Decreased VIP

Table 1 - Mediators of pulmonary vascular responses in pulmonary arterial hypertension. TxA_2, thromboxane A2; PGI_2, prostaglandin I2 (prostacyclin); NO, nitric oxide; ET-1, endothelin-1; 5-HT, 5-hydroxytryptamine (serotonin); VEGF, vascular endothelial growth factor; VIP, vasoactive intestinal peptide. Adapted from Farber *et al.*[3]

Interestingly, the VEGF-driven disordered angiogenic responses in ECs in PAHT have been shown to be c-Src/PI3K/Akt-driven.[86, 87] Our interest is mainly focussed on the familial and idiopathic (primary) form of PAHT. The familial form of PAHT accounts for 6% of all cases of PAHT and can be related to mutations in *Ang-1/Tie 2*, to mutations in the TGFβ-receptor pathway or the serotoninergic pathway.[88] Two genes that have been strongly linked to familial PAHT are the bone morphogenetic protein receptor type 2 (*BMPR2*: controlling EC proliferation via Smad) and the TGFβ-receptor *ALK1* (Activin receptor-like kinase 1; also known as *ACVRL1*; controlling Smad-mediated EC proliferation).[88] Interestingly, in approximately 15% of patients with hereditary haemorrhagic telangiectasia (HHT; The Rendu-Osler-Weber syndrome), patients also present with an idiopathic form of PAHT.[89] HHT is a rare genetic disorder that is characterised by mucocutaneous telangiectasia and recurrent bleeding due to nasal, cerebral, pulmonary and gastro-intestinal arteriovenous malformations. HHT is caused by mutations in the *ENG* gene (HHT type 1) or by mutations in the *ALK1/ACVRL1*-gene (HHT type 2) and it has been shown that the association of HHT with PAHT is also related to mutations in these genes.[90] Because clinically-apparent disease occurs only in a small percentage of *BMPR2*, *ALK1* and/or *ENG* mutations and because not all patients with *ENG*- and/or *ALK1*-induced HHT also present with PAHT, it is believed that there must exist some modifier genes and/or environmental triggers being important to the pathogenesis of PAHT. Therefore, a multiple-hit theory has been suggested.[3, 88]

It was of particular interest to us to translate these data to our PEAR1 results. Indeed, we showed that PEAR1 is involved in the NO metabolism of ECs and that *PEAR1* knockdown results in an enhanced EC proliferation and increased platelet formation; three cornerstones of idiopathic PAHT.[91] We also showed that PEAR1 expression is low in rapidly-proliferating vascular abnormalities (pyogenic granuloma; see Chapter IV), suggesting that it might be involved in the discontinuation of the angiogenic control, as is also seen in HHT. We have previously suggested that it would be of high interest to investigate the gene profile for the angiopoietins *Ang1* and *Ang2* as well as for the TGFβ receptor pathway in *shPEAR1* ECs, since these genes appear to be central to the disease mechanism of both PAHT and HHT. Some very preliminary (unpublished) results from our group have indeed shown that the knockdown of *PEAR1* in ECs affects the expression profile of *ENG* and *ALK1,* results that are in line with the recent publication of Adam *et al.*[30] Therefore, we believe that patients with PAHT/HHT should be analysed for the occurrence of certain single nucleotide polymorphisms (SNPs) in *PEAR1* and that a possible role for *PEAR1* as a modifier gene in the development of PAHT/HHT should be investigated.

PEAR1: A ROLE IN TUMOUR ANGIOGENESIS?

As I discussed in Chapter IV, *PEAR1* knockdown and murine *Pear1* knockout resulted in enhanced tube formation *in vitro,* and enhanced vascular density *in vivo*.[92] This raises the question as to whether PEAR1 could also be a player in tumour angiogenesis. Since PEAR1 has been linked to PTEN, I would like to start this part of the discussion by an explanation of the autosomal dominant Cowden syndrome, which is associated with *PTEN* mutations, as briefly mentioned before.

Patients with Cowden disease (≈ 1/200,000) carry hereditary mutations of *PTEN* and as a result are at high risk for the development of a broad spectrum of benign and malignant tumours. They may also experience accelerated tumour growth due to the loss of *PTEN* in ECs, resulting in enhanced angiogenesis.[11, 93] Excellent work by Suzuki *et al.* showed that the loss of *PTEN* in murine ECs makes these cells hypersensitive to VGFs, resulting in enhanced angiogenesis and accelerated tumour growth.[11] Although the loss of *PTEN* results in a very strong phenotype, an important question is whether loss-of-function mutations in *PEAR1* could contribute to an imbalance of the PTEN/PI3K/Alt pathway, thus resulting in a Cowden-like syndrome, or whether *PEAR1* might function as a modifier gene in patients with Cowden syndrome, explaining the phenotypic heterogeneity in these patients.

A possible role for PEAR1 in benign vascular malformations (e.g. as seen in HHT, pyogenic granuloma, PHT) has been discussed above. A major question of interest is whether PEAR1 is also involved in the angiogenesis of malignant tumours and/or in tumour metastasis. Tumour vessels are structurally and functionally different from normal vessels.[94, 95] They are characterised by chaotic, heterogeneous and tortuous vessels, most of which do not succeed in delivering sufficient oxygen (or drugs) to the organising tumour,[95, 96] resulting in the overproduction of pro-angiogenic factors and creating a self-reinforcing vicious circle. Tumour ECs are no longer quiescent, instead they are organised in a non-polarised way and lack proper tight junctions, making them leaky and fenestrated which forms an ideal substrate for bleeding and tumour metastasis.[95, 97, 98] Their EC gene expression profile is also very heterogeneous, resulting in a chaotic underlying signalling substrate.[99]

Various antibodies against VEGF (bevacizumab, Avastin®) or against the VEGFR tyrosine kinases (sorafenib, Nexavar®; sunitinib, Sutent®; pazopanib, Votrient® and vandetanib, Zactima®) have been developed for clinical use. Although initially they provided promising results, their success was limited and often the problem of tumour resistance arose, resulting in the promotion of metastasis.[100] Therefore, increasing evidence indicates that shifting anti-tumour therapy targets from anti-angiogenic towards vessel normalisation should be considered.[100] Recent murine genetic and pharmacological studies have identified some groups of molecules that directly induce vessel normalisation.[100] In tumours, there is a persistant imbalance between angiogenic activators and inhibitors, in favour of the activators. Therefore it is reasonable to suggest that removing the excess pro-angiogenic signals (e.g. via VEGF inhibitors, upregulating ANG-1, blocking ANG-2, enhancing eNOS-activity or blocking the oxygen sensor prolyl hydroxylase domain-containing protein 2 [PHD2 or EGLN1]) could result in a shift of tumour vessel disorganisation towards vessel normalisation, an important step in blocking the previously discussed vicious circle. This type of therapy could result in less aggressive and less

malignant/metastatic tumours and might increase the responsiveness to chemotherapy and immunotherapy. Although highly speculative, it would be of great interest to study the contribution of PEAR1 to tumour vessel growth. As previously discussed, the knockdown of *PEAR1* resulted in enhanced tubulogenesis, but the maturation of ECs by *PEAR1* knockdown was not affected (Chapter IV). This was also true for the maturation of CD34(+) cells after *PEAR1* knockdown (Chapter I), indicating that PEAR1 affects proliferation but not maturation. In addition, PEAR1 expression is low or non-existing in rapidly-proliferating ECs, as seen in pyogenic granuloma or in cells with a high proliferating phenotype (e.g. BOECs). Based on these findings, we assume that PEAR1 expression is also low in the ECs of tumour vessels and probably stays low during the process of tumour angiogenesis since this process is characterised by immaturity. Therefore, in line with the hypothesis discussed above, the induction of PEAR1 overexpression in the ECs of invading tumour vessels might be a target for restoring ECs to a more quiescent, normalised state.

GENETIC VARIATION IN PEAR1

As discussed in the Introduction chapter, genetic variants in both the coding and non-coding regions of *PEAR1* are associated with increased or impaired responses to various platelet agonists and are associated with inter-individual variability to antiplatelet drugs. Williams *et al.* identified *PEAR1* as a candidate gene that may be linked to kidney injury in the salt-sensitive Dahl rat[101] (see Introduction), suggesting a possible link between PEAR1 and the development of hypertension. Taken together with our previously discussed findings on NO metabolism, our group therefore looked for associations between changes in blood pressure and the incidence of hypertension and genetic variation in *PEAR1*. We measured blood pressure at baseline and followed up on 1973 randomly recruited people, all genotyped for *PEAR1*. All associations of systolic and diastolic blood pressure changes with nine SNPs in *PEAR1* were found to be non-significant ($p \geq 0.059$), suggesting that *PEAR1* is not a hypertension susceptibly gene in humans.[102] Although this was the first study focussing on a role for PEAR1 in EC function, it must be noted that the most discussed SNP that gives the greatest phenotype (rs12041331; Figure 8) was not included in our analyses. This should be considered as a major shortcoming in this study. Recently it was reported that HUVECs homozygous for the A-allele of *PEAR1* rs12041331 have approximately 117% better wound healing capabilities compared to cells homozygous for the major G-allele.[30] I believe that additional research on the effect of gain-of-function or loss-of-function SNPs in *PEAR1* on certain diseases (e.g. PAHT, HHT, hypertension, tumour angiogenesis, etc) or other effects of genetic variability (e.g. methylation in epigenetics) in *PEAR1* should be encouraged.

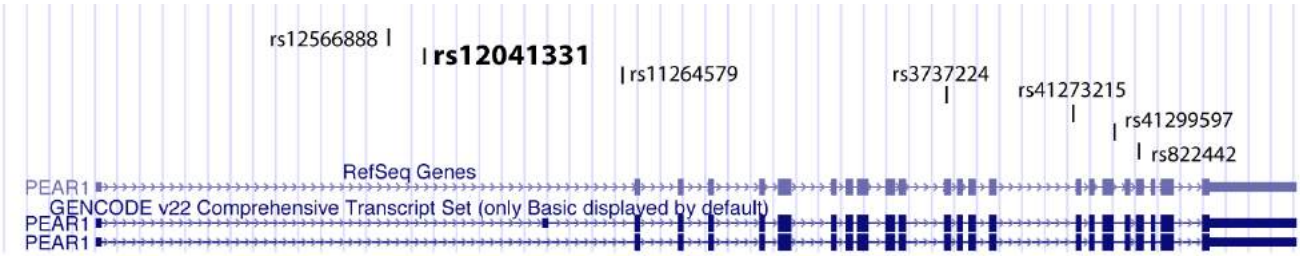

Figure 8 - Overview of reported SNPs in human *PEAR1* (chromosome 1) as summarised in Table 1 of the Introduction Chapter. Nucleotide positions are according to the December 2013 human reference sequence (NCBI Build 38.3), produced by the International Human Genome Sequencing Consortium).

REFERENCES

1. Nanda N, Bao M, Lin H, Clauser K, Komuves L, Quertermous T, Conley PB, Phillips DR, Hart MJ. Platelet endothelial aggregation receptor 1 (PEAR1), a novel epidermal growth factor repeat-containing transmembrane receptor, participates in platelet contact-induced activation. *J Biol Chem* 2005;**280**:24680-24689.
2. Serra H, Chivite I, Angulo-Urarte A, Soler A, Sutherland JD, Arruabarrena-Aristorena A, Ragab A, Lim R, Malumbres M, Fruttiger M, Potente M, Serrano M, Fabra A, Vinals F, Casanovas O, Pandolfi PP, Bigas A, Carracedo A, Gerhardt H, Graupera M. PTEN mediates Notch-dependent stalk cell arrest in angiogenesis. *Nat Commun* 2015;**6**:7935.
3. Farber HW, Loscalzo J. Mechanisms of disease: Pulmonary arterial hypertension. *New England Journal of Medicine* 2004;**351**:1655-1665.
4. Kauskot A, Vandenbriele C, Louwette S, Gijsbers R, Tousseyn T, Freson K, Verhamme P, Hoylaerts MF. PEAR1 attenuates megakaryopoiesis via control of the PI3K/PTEN pathway. *Blood* 2013;**121**:5208-5217.
5. Kauskot A, Di Michele M, Loyen S, Freson K, Verhamme P, Hoylaerts MF. A novel mechanism of sustained platelet alphaIIbbeta3 activation via PEAR1. *Blood* 2012;**119**:4056-4065.
6. Krivtsov AV, Rozov FN, Zinovyeva MV, Hendrikx PJ, Jiang Y, Visser JW, Belyavsky AV. Jedi--a novel transmembrane protein expressed in early hematopoietic cells. *J Cell Biochem* 2007;**101**:767-784.
7. Vandenbriele C, Kauskot A, Vandersmissen I, Criel M, Geenens R, Craps S, Luttun A, Janssens S, Hoylaerts MF, Verhamme P. Platelet Endothelial Aggregation Receptor -1: A novel modifier of neoangiogenesis. *Cardiovasc Res* 2015.
8. Cornejo MG, Mabialah V, Sykes SM, Khandan T, Lo Celso C, Lopez CK, Rivera-Munoz P, Rameau P, Tothova Z, Aster JC, DePinho RA, Scadden DT, Gilliland DG, Mercher T. Crosstalk between NOTCH and AKT signaling during murine megakaryocyte lineage specification. *Blood* 2011;**118**:1264-1273.
9. Wong GW, Knowles GC, Mak TW, Ferrando AA, Zuniga-Pflucker JC. HES1 opposes a PTEN-dependent check on survival, differentiation and proliferation of TCRbeta-selected mouse thymocytes. *Blood* 2012.
10. Lee MY, Luciano AK, Ackah E, Rodriguez-Vita J, Bancroft TA, Eichmann A, Simons M, Kyriakides TR, Morales-Ruiz M, Sessa WC. Endothelial Akt1 mediates angiogenesis by phosphorylating multiple angiogenic substrates. *Proc Natl Acad Sci U S A* 2014;**111**:12865-12870.
11. Suzuki A, Hamada K, Sasaki T, Mak TW, Nakano T. Role of PTEN/PI3K pathway in endothelial cells. *Biochem Soc Trans* 2007;**35**:172-176.
12. Huang J, Kontos CD. PTEN modulates vascular endothelial growth factor-mediated signaling and angiogenic effects. *J Biol Chem* 2002;**277**:10760-10766.
13. Su JD, Mayo LD, Donner DB, Durden DL. PTEN and phosphatidylinositol 3'-kinase inhibitors up-regulate p53 and block tumor-induced angiogenesis: evidence for an effect on the tumor and endothelial compartment. *Cancer Res* 2003;**63**:3585-3592.
14. Hamada K, Sasaki T, Koni PA, Natsui M, Kishimoto H, Sasaki J, Yajima N, Horie Y, Hasegawa G, Naito M, Miyazaki J, Suda T, Itoh H, Nakao K, Mak TW, Nakano T, Suzuki A. The PTEN/PI3K pathway governs normal vascular development and tumor angiogenesis. *Genes Dev* 2005;**19**:2054-2065.
15. Stumpf M, Choorapoikayil S, den Hertog J. Pten function in zebrafish: anything but a fish story. *Methods* 2015;**77-78**:191-196.
16. DeBusk LM, Hallahan DE, Lin PC. Akt is a major angiogenic mediator downstream of the Ang1/Tie2 signaling pathway. *Exp Cell Res* 2004;**298**:167-177.
17. Daly C, Wong V, Burova E, Wei Y, Zabski S, Griffiths J, Lai KM, Lin HC, Ioffe E, Yancopoulos GD, Rudge JS. Angiopoietin-1 modulates endothelial cell function and gene expression via the transcription factor FKHR (FOXO1). *Genes Dev* 2004;**18**:1060-1071.
18. Noseda M, Chang L, McLean G, Grim JE, Clurman BE, Smith LL, Karsan A. Notch activation induces endothelial cell cycle arrest and participates in contact inhibition: role of p21Cip1 repression. *Mol Cell Biol* 2004;**24**:8813-8822.
19. Rodriguez S, Huynh-Do U. The Role of PTEN in Tumor Angiogenesis. *J Oncol* 2012;**2012**:141236.
20. Benedito R, Roca C, Sorensen I, Adams S, Gossler A, Fruttiger M, Adams RH. The notch ligands Dll4 and Jagged1 have opposing effects on angiogenesis. *Cell* 2009;**137**:1124-1135.

21. Hellstrom M, Phng LK, Hofmann JJ, Wallgard E, Coultas L, Lindblom P, Alva J, Nilsson AK, Karlsson L, Gaiano N, Yoon K, Rossant J, Iruela-Arispe ML, Kalen M, Gerhardt H, Betsholtz C. Dll4 signalling through Notch1 regulates formation of tip cells during angiogenesis. *Nature* 2007;**445**:776-780.
22. Davies PF. Flow-mediated endothelial mechanotransduction. *Physiol Rev* 1995;**75**:519-560.
23. Ueda A, Koga M, Ikeda M, Kudo S, Tanishita K. Effect of shear stress on microvessel network formation of endothelial cells with in vitro three-dimensional model. *Am J Physiol Heart Circ Physiol* 2004;**287**:H994-1002.
24. Kolluru GK, Sinha S, Majumder S, Muley A, Siamwala JH, Gupta R, Chatterjee S. Shear stress promotes nitric oxide production in endothelial cells by sub-cellular delocalization of eNOS: A basis for shear stress mediated angiogenesis. *Nitric Oxide* 2010;**22**:304-315.
25. Lehoux S, Castier Y, Tedgui A. Molecular mechanisms of the vascular responses to haemodynamic forces. *J Intern Med* 2006;**259**:381-392.
26. Li YS, Haga JH, Chien S. Molecular basis of the effects of shear stress on vascular endothelial cells. *J Biomech* 2005;**38**:1949-1971.
27. Boo YC, Sorescu G, Boyd N, Shiojima I, Walsh K, Du J, Jo H. Shear stress stimulates phosphorylation of endothelial nitric-oxide synthase at Ser1179 by Akt-independent mechanisms: role of protein kinase A. *J Biol Chem* 2002;**277**:3388-3396.
28. Ziche M, Morbidelli L, Choudhuri R, Zhang HT, Donnini S, Granger HJ, Bicknell R. Nitric oxide synthase lies downstream from vascular endothelial growth factor-induced but not basic fibroblast growth factor-induced angiogenesis. *J Clin Invest* 1997;**99**:2625-2634.
29. Cooke JP, Losordo DW. Nitric oxide and angiogenesis. *Circulation* 2002;**105**:2133-2135.
30. Adam S. Fisch LMY-A, Joshua D. Backman, Hong Wang, Patrick Donnelly, Kathleen A. Ryan, Ankita Parihar, Mary A. Pavlovich, Braxton D. Mitchell, Jeffrey R. O'Connell, William Herzog, Christopher R. Harman, Jonathan D. Wren, Joshua P. Lewis. Genetic Variation in the Platelet Endothelial Aggregation Receptor 1 Gene Results in Endothelial Dysfunction. *Plos One, in press* 2015.
31. Green DJ, Dawson EA, Groenewoud HM, Jones H, Thijssen DH. Is flow-mediated dilation nitric oxide mediated?: A meta-analysis. *Hypertension* 2014;**63**:376-382.
32. Unseld M, Chilla A, Pausz C, Mawas R, Breuss J, Zielinski C, Schabbauer G, Prager GW. PTEN expression in endothelial cells is down-regulated by uPAR to promote angiogenesis. *Thromb Haemost* 2015;**114**:379-389.
33. Mignatti P, Rifkin DB. Biology and biochemistry of proteinases in tumor invasion. *Physiol Rev* 1993;**73**:161-195.
34. Cheresh DA, Stupack DG. Regulation of angiogenesis: apoptotic cues from the ECM. *Oncogene* 2008;**27**:6285-6298.
35. Hood JD, Cheresh DA. Role of integrins in cell invasion and migration. *Nat Rev Cancer* 2002;**2**:91-100.
36. Francis SE, Goh KL, Hodivala-Dilke K, Bader BL, Stark M, Davidson D, Hynes RO. Central roles of alpha5beta1 integrin and fibronectin in vascular development in mouse embryos and embryoid bodies. *Arterioscler Thromb Vasc Biol* 2002;**22**:927-933.
37. Brooks PC, Clark RA, Cheresh DA. Requirement of vascular integrin alpha v beta 3 for angiogenesis. *Science* 1994;**264**:569-571.
38. Malan D, Wenzel D, Schmidt A, Geisen C, Raible A, Bolck B, Fleischmann BK, Bloch W. Endothelial beta1 integrins regulate sprouting and network formation during vascular development. *Development* 2010;**137**:993-1002.
39. Qiu J, Wang G, Peng Q, Hu J, Luo X, Zheng Y, Teng Y, Tang C. Id1 induces tubulogenesis by regulating endothelial cell adhesion and cytoskeletal organization through beta1-integrin and Rho-kinase signalling. *Int J Mol Med* 2011;**28**:543-548.
40. Whitelock JM, Murdoch AD, Iozzo RV, Underwood PA. The degradation of human endothelial cell-derived perlecan and release of bound basic fibroblast growth factor by stromelysin, collagenase, plasmin, and heparanases. *J Biol Chem* 1996;**271**:10079-10086.
41. Xu J, Rodriguez D, Petitclerc E, Kim JJ, Hangai M, Moon YS, Davis GE, Brooks PC. Proteolytic exposure of a cryptic site within collagen type IV is required for angiogenesis and tumor growth in vivo. *J Cell Biol* 2001;**154**:1069-1079.
42. Wang S, Cheng Z, Yang X, Deng K, Cao Y, Chen H, Pan L. Effect of wild type PTEN gene on proliferation and invasion of multiple myeloma. *Int J Hematol* 2010;**92**:83-94.
43. Giovannetti E, Funel N, Peters GJ, Del Chiaro M, Erozenci LA, Vasile E, Leon LG, Pollina LE, Groen A, Falcone A, Danesi R, Campani D, Verheul HM, Boggi U. MicroRNA-21 in pancreatic cancer: correlation

with clinical outcome and pharmacologic aspects underlying its role in the modulation of gemcitabine activity. *Cancer Res* 2010;**70**:4528-4538.
44. Kuijper S, Turner CJ, Adams RH. Regulation of angiogenesis by Eph-ephrin interactions. *Trends Cardiovasc Med* 2007;**17**:145-151.
45. Stephen LJ, Fawkes AL, Verhoeve A, Lemke G, Brown A. A critical role for the EphA3 receptor tyrosine kinase in heart development. *Dev Biol* 2007;**302**:66-79.
46. Wilkinson DG. Multiple roles of EPH receptors and ephrins in neural development. *Nat Rev Neurosci* 2001;**2**:155-164.
47. Steinle JJ, Meininger CJ, Forough R, Wu G, Wu MH, Granger HJ. Eph B4 receptor signaling mediates endothelial cell migration and proliferation via the phosphatidylinositol 3-kinase pathway. *J Biol Chem* 2002;**277**:43830-43835.
48. Wong EV, Kerner JA, Jay DG. Convergent and divergent signaling mechanisms of growth cone collapse by ephrinA5 and slit2. *J Neurobiol* 2004;**59**:66-81.
49. Rodriguez S, Huynh-Do U. Phosphatase and tensin homolog regulates stability and activity of EphB1 receptor. *FASEB J* 2013;**27**:632-644.
50. Wang J, Wang Y, Wang Y, Ma Y, Lan Y, Yang X. Transforming growth factor beta-regulated microRNA-29a promotes angiogenesis through targeting the phosphatase and tensin homolog in endothelium. *J Biol Chem* 2013;**288**:10418-10426.
51. Weis SM, Cheresh DA. Tumor angiogenesis: molecular pathways and therapeutic targets. *Nat Med* 2011;**17**:1359-1370.
52. Carmeliet P, Jain RK. Molecular mechanisms and clinical applications of angiogenesis. *Nature* 2011;**473**:298-307.
53. Liu LZ, Li C, Chen Q, Jing Y, Carpenter R, Jiang Y, Kung HF, Lai L, Jiang BH. MiR-21 induced angiogenesis through AKT and ERK activation and HIF-1alpha expression. *PLoS One* 2011;**6**:e19139.
54. Liaw D, Marsh DJ, Li J, Dahia PL, Wang SI, Zheng Z, Bose S, Call KM, Tsou HC, Peacocke M, Eng C, Parsons R. Germline mutations of the PTEN gene in Cowden disease, an inherited breast and thyroid cancer syndrome. *Nat Genet* 1997;**16**:64-67.
55. Hasegawa S, Pawankar R, Suzuki K, Nakahata T, Furukawa S, Okumura K, Ra C. Functional expression of the high affinity receptor for IgE (FcepsilonRI) in human platelets and its' intracellular expression in human megakaryocytes. *Blood* 1999;**93**:2543-2551.
56. Joseph M, Gounni AS, Kusnierz JP, Vorng H, Sarfati M, Kinet JP, Tonnel AB, Capron A, Capron M. Expression and functions of the high-affinity IgE receptor on human platelets and megakaryocyte precursors. *Eur J Immunol* 1997;**27**:2212-2218.
57. McDonald JR, Tan EM, Stevenson DD, Vaughan JH. Platelet aggregation in asthmatic and normal subjects. *J Allergy Clin Immunol* 1974;**54**:200-208.
58. Harwell WB, Patterson JT, Lieberman P, Beachey E. Platelet aggregation in atopic and normal patients. *J Allergy Clin Immunol* 1973;**51**:274-284.
59. Gallagher JS, Bernstein IL, Maccia CA, Splansky GL, Glueck HI. Cyclic platelet dysfunction in IgE-mediated allergy. *J Allergy Clin Immunol* 1978;**62**:229-235.
60. Gould HJ, Sutton BJ. IgE in allergy and asthma today. *Nat Rev Immunol* 2008;**8**:205-217.
61. Ind PW. Platelet and clotting abnormalities in asthma. *Clin Exp Allergy* 1991;**21**:395-398.
62. Maccia CA, Gallagher JS, Ataman G, Glueck HI, Brooks SM, Bernstein IL. Platelet thrombopathy in asthmatic patients with elevated immunoglobulin e. *J Allergy Clin Immunol* 1977;**59**:101-108.
63. Palma-Carlos AG, Palma-Carlos ML, Santos MC, de Sousa JR. Platelet aggregation in allergic reactions. *Int Arch Allergy Appl Immunol* 1991;**94**:251-253.
64. Tamaki H, Chatterjee S, Langford CA. Eosinophilia in Rheumatologic/Vascular Disorders. *Immunol Allergy Clin North Am* 2015;**35**:453-476.
65. Guillevin L, Cohen P, Gayraud M, Lhote F, Jarrousse B, Casassus P. Churg-Strauss syndrome. Clinical study and long-term follow-up of 96 patients. *Medicine (Baltimore)* 1999;**78**:26-37.
66. Lanham JG, Elkon KB, Pusey CD, Hughes GR. Systemic vasculitis with asthma and eosinophilia: a clinical approach to the Churg-Strauss syndrome. *Medicine (Baltimore)* 1984;**63**:65-81.
67. Ames PR, Margaglione M, Mackie S, Alves JD. Eosinophilia and thrombophilia in churg strauss syndrome: a clinical and pathogenetic overview. *Clin Appl Thromb Hemost* 2010;**16**:628-636.
68. Getz TM, Manne BK, Buitrago L, Mao Y, Kunapuli SP. Dextran sulphate induces fibrinogen receptor activation through a novel Syk-independent PI-3 kinase-mediated tyrosine kinase pathway in platelets. *Thromb Haemost* 2013;**109**:1131-1140.

69. Perse M, Cerar A. Dextran sodium sulphate colitis mouse model: traps and tricks. *J Biomed Biotechnol* 2012;**2012**:718617.
70. Chappell D, Jacob M, Paul O, Rehm M, Welsch U, Stoeckelhuber M, Conzen P, Becker BF. The glycocalyx of the human umbilical vein endothelial cell: an impressive structure ex vivo but not in culture. *Circ Res* 2009;**104**:1313-1317.
71. Zeng Y, Waters M, Andrews A, Honarmandi P, Ebong EE, Rizzo V, Tarbell JM. Fluid shear stress induces the clustering of heparan sulfate via mobility of glypican-1 in lipid rafts. *Am J Physiol Heart Circ Physiol* 2013;**305**:H811-820.
72. Florian JA, Kosky JR, Ainslie K, Pang Z, Dull RO, Tarbell JM. Heparan sulfate proteoglycan is a mechanosensor on endothelial cells. *Circ Res* 2003;**93**:e136-142.
73. Harrison DG, Widder J, Grumbach I, Chen W, Weber M, Searles C. Endothelial mechanotransduction, nitric oxide and vascular inflammation. *J Intern Med* 2006;**259**:351-363.
74. Tarbell JM, Ebong EE. The endothelial glycocalyx: a mechano-sensor and -transducer. *Sci Signal* 2008;**1**:pt8.
75. Van der Heiden K, Gijsen FJ, Narracott A, Hsiao S, Halliday I, Gunn J, Wentzel JJ, Evans PC. The effects of stenting on shear stress: relevance to endothelial injury and repair. *Cardiovasc Res* 2013;**99**:269-275.
76. Maehama T, Taylor GS, Dixon JE. PTEN and myotubularin: novel phosphoinositide phosphatases. *Annu Rev Biochem* 2001;**70**:247-279.
77. Ma J, Sawai H, Ochi N, Matsuo Y, Xu D, Yasuda A, Takahashi H, Wakasugi T, Takeyama H. PTEN regulates angiogenesis through PI3K/Akt/VEGF signaling pathway in human pancreatic cancer cells. *Mol Cell Biochem* 2009;**331**:161-171.
78. Tian T, Nan KJ, Wang SH, Liang X, Lu CX, Guo H, Wang WJ, Ruan ZP. PTEN regulates angiogenesis and VEGF expression through phosphatase-dependent and -independent mechanisms in HepG2 cells. *Carcinogenesis* 2010;**31**:1211-1219.
79. Wang X, He H, Lu Y, Ren W, Teng KY, Chiang CL, Yang Z, Yu B, Hsu S, Jacob ST, Ghoshal K, Lee LJ. Indole-3-carbinol inhibits tumorigenicity of hepatocellular carcinoma cells via suppression of microRNA-21 and upregulation of phosphatase and tensin homolog. *Biochim Biophys Acta* 2015;**1853**:244-253.
80. Paramio JM, Navarro M, Segrelles C, Gomez-Casero E, Jorcano JL. PTEN tumour suppressor is linked to the cell cycle control through the retinoblastoma protein. *Oncogene* 1999;**18**:7462-7468.
81. Christman BW, McPherson CD, Newman JH, King GA, Bernard GR, Groves BM, Loyd JE. An imbalance between the excretion of thromboxane and prostacyclin metabolites in pulmonary hypertension. *N Engl J Med* 1992;**327**:70-75.
82. Giaid A, Saleh D. Reduced expression of endothelial nitric oxide synthase in the lungs of patients with pulmonary hypertension. *N Engl J Med* 1995;**333**:214-221.
83. Hassoun PM, Thappa V, Landman MJ, Fanburg BL. Endothelin 1: mitogenic activity on pulmonary artery smooth muscle cells and release from hypoxic endothelial cells. *Proc Soc Exp Biol Med* 1992;**199**:165-170.
84. Herve P, Launay JM, Scrobohaci ML, Brenot F, Simonneau G, Petitpretz P, Poubeau P, Cerrina J, Duroux P, Drouet L. Increased plasma serotonin in primary pulmonary hypertension. *Am J Med* 1995;**99**:249-254.
85. Petkov V, Mosgoeller W, Ziesche R, Raderer M, Stiebellehner L, Vonbank K, Funk GC, Hamilton G, Novotny C, Burian B, Block LH. Vasoactive intestinal peptide as a new drug for treatment of primary pulmonary hypertension. *J Clin Invest* 2003;**111**:1339-1346.
86. Tuder RM, Chacon M, Alger L, Wang J, Taraseviciene-Stewart L, Kasahara Y, Cool CD, Bishop AE, Geraci M, Semenza GL, Yacoub M, Polak JM, Voelkel NF. Expression of angiogenesis-related molecules in plexiform lesions in severe pulmonary hypertension: evidence for a process of disordered angiogenesis. *Journal of Pathology* 2001;**195**:367-374.
87. Tuder RM, Flook BE, Voelkel NF. Increased Gene-Expression for Vegf and the Vegf Receptors Kdr/Flk and Flt in Lungs Exposed to Acute or to Chronic Hypoxia - Modulation of Gene-Expression by Nitric-Oxide. *Journal of Clinical Investigation* 1995;**95**:1798-1807.
88. Galie N, Humbert M, Vachiery JL, Gibbs S, Lang I, Torbicki A, Simonneau G, Peacock A, Vonk Noordegraaf A, Beghetti M, Ghofrani A, Gomez Sanchez MA, Hansmann G, Klepetko W, Lancellotti P, Matucci M, McDonagh T, Pierard LA, Trindade PT, Zompatori M, Hoeper M. 2015 ESC/ERS Guidelines for the diagnosis and treatment of pulmonary hypertension: The Joint Task Force for the Diagnosis and Treatment of Pulmonary Hypertension of the European Society of Cardiology (ESC) and the European

Respiratory Society (ERS): Endorsed by: Association for European Paediatric and Congenital Cardiology (AEPC), International Society for Heart and Lung Transplantation (ISHLT). *Eur Respir J* 2015;**46**:903-975.
89. Trembath RC, Thomson JR, Machado RD, Morgan NV, Atkinson C, Winship I, Simonneau G, Galie N, Loyd JE, Humbert M, Nichols WC, Morrell NW, Berg J, Manes A, McGaughran J, Pauciulo M, Wheeler L. Clinical and molecular genetic features of pulmonary hypertension in patients with hereditary hemorrhagic telangiectasia. *N Engl J Med* 2001;**345**:325-334.
90. Vandenbriele C, Peerlinck K, de Ravel T, Verhamme P, Vanassche T. Pulmonary arterio-venous malformations in a patient with a novel mutation in exon 10 of the ACVRL1 gene. *Acta Clin Belg* 2014;**69**:139-141.
91. McQuillan LP, Leung GK, Marsden PA, Kostyk SK, Kourembanas S. Hypoxia inhibits expression of eNOS via transcriptional and posttranscriptional mechanisms. *Am J Physiol* 1994;**267**:H1921-1927.
92. Vandenbriele C, Kauskot A, Vandersmissen I, Criel M, Geenens R, Craps S, Luttun A, Janssens S, Hoylaerts MF, Verhamme P. Platelet endothelial aggregation receptor-1: a novel modifier of neoangiogenesis. *Cardiovasc Res* 2015.
93. Ngeow J, Eng C. PTEN hamartoma tumor syndrome: clinical risk assessment and management protocol. *Methods* 2015;**77-78**:11-19.
94. Jain RK. Normalizing tumor vasculature with anti-angiogenic therapy: a new paradigm for combination therapy. *Nat Med* 2001;**7**:987-989.
95. Jain RK. Normalization of tumor vasculature: an emerging concept in antiangiogenic therapy. *Science* 2005;**307**:58-62.
96. Jain RK, Stylianopoulos T. Delivering nanomedicine to solid tumors. *Nat Rev Clin Oncol* 2010;**7**:653-664.
97. Baluk P, Hashizume H, McDonald DM. Cellular abnormalities of blood vessels as targets in cancer. *Curr Opin Genet Dev* 2005;**15**:102-111.
98. Jain RK. Determinants of tumor blood flow: a review. *Cancer Res* 1988;**48**:2641-2658.
99. Langenkamp E, Molema G. Microvascular endothelial cell heterogeneity: general concepts and pharmacological consequences for anti-angiogenic therapy of cancer. *Cell Tissue Res* 2009;**335**:205-222.
100. Carmeliet P, Jain RK. Principles and mechanisms of vessel normalization for cancer and other angiogenic diseases. *Nat Rev Drug Discov* 2011;**10**:417-427.
101. Williams JM, Johnson AC, Stelloh C, Dreisbach AW, Franceschini N, Regner KR, Townsend RR, Roman RJ, Garrett MR. Genetic variants in Arhgef11 are associated with kidney injury in the Dahl salt-sensitive rat. *Hypertension* 2012;**60**:1157-1168.
102. Olivi L, Vandenbriele C, Gu YM, Salvi E, Carpini SD, Liu YP, Jacobs L, Jin Y, Thijs L, Citterio L, Cusi D, Verhamme P, Staessen JA. PEAR1 is not a human hypertension-susceptibility gene. *Blood Press* 2015;**24**:61-64.

Concluding Remarks

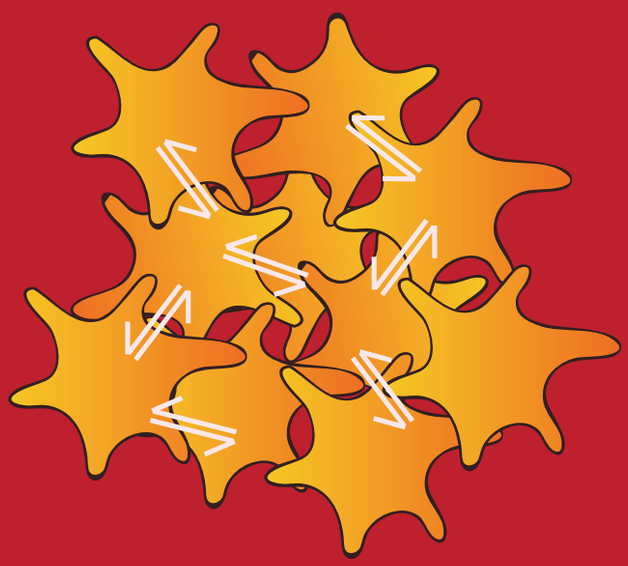

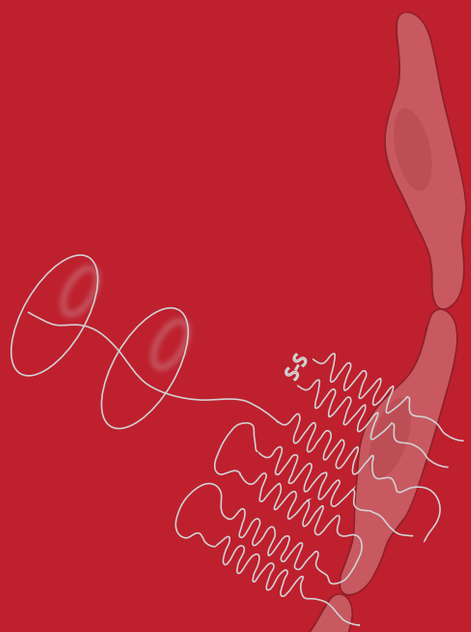

Curriculum Vitae & Publications

CONCLUDING REMARKS

In this thesis, I investigated the contribution of PEAR1-signalling to the (patho)physiologic role of megakaryocytes/platelets and endothelial cells. In addition to opening up the way for further studies that unravel more into detail the underlying signalling pathways, downstream of PEAR1, these findings also hold the potential for further research concerning a potential role for PEAR1 in various diseases. I believe that our findings delivered a significant contribution to the unexplored field of PEAR1.

1 IDENTIFICATION OF A ROLE FOR PEAR1 IN ATTENUATING MEGAKARYOPOIESIS - *CHAPTER I*

We showed that a reduced *PEAR1* expression in MK progenitors lowers Akt dephosphorylation, secondarily to transcriptional downregulation of *PTEN*. PEAR1-knockdown promoted MK progenitor proliferation, indirectly enhancing megakaryopoiesis and thrombopoiesis. This was validated in human MK progenitors *in vitro* and in a *Pear1*-morpholino based knockdown model in zebrafish *in vivo*.

2 IDENTIFICATION OF FCεR1A AS A PHYSIOLOGICAL LIGAND FOR PEAR1 ON HUMAN PLATELETS - *CHAPTER II*

A protein library was created, representing the cell surface receptor repertoire and secretome of the human platelet. We postulated that this library will be a valuable tool in cardiovascular disease research and identified the high affinity IgE-receptor (FcεR1α) as a platelet ligand for PEAR1, making an important contribution towards understanding the mechanistic role of this receptor in platelet function and linking IgE-mediated allergy to cardiovascular disease.

3 IDENTIFICATION OF DXS AS A NON-PHYSIOLOGICAL LIGAND FOR PEAR1 ON HUMAN AND MURINE PLATELETS - *CHAPTER III*

We identified high molecular DxS as a non-physiological ligand for human and murine platelet PEAR1 and showed that DxS-mediated platelet aggregation is induced through parallel signalling via PEAR1 and CLEC2. This hypothesis was validated via aggregation experiments using *Pear1*$^{-/-}$ platelets.

4 IDENTIFICATION OF PEAR1 AS A NOVEL MODIFIER OF NEO-ANGIOGENESIS - *CHAPTER IV*

We identified PEAR1 as a controller of EC proliferation, migration and tube formation *in vitro* and as a modifier of neo-angiogenesis *in vivo* in two murine *Pear1*$^{-/-}$ revascularization models. We could link these findings to the sustained phosphorylation status of Akt, a central player in vessel assembly.

CURRICULUM VITAE

Vandenbriele Christophe
Tweekleinewegenstraat 38, 3001 Leuven (Belgium)
+32(0)474/65.79.62
Christophe.vandenbriele@med.kuleuven.be; Vandenbriele@hotmail.com

PERSONAL INFORMATION

Full name: Christophe Roger Honoré Vandenbriele
Date of birth: September, 11, 1984 – Lier – Belgium
Nationality: Belgian

EDUCATION

1997 – 2002 SECONDARY EDUCATION
Latin – Mathematics, St. Romboutscollege, Mechelen

2002 – 2009 MEDICAL DOCTOR, UNIVERSITY OF LEUVEN,
2009, MAGNA CUM LAUDE

1st bachelor – *cum laude*
2nd bachelor – *magna cum laude*
3rd bachelor – *magna cum laude*
1st master – *magna cum laude*
2nd master – *magna cum laude*
3rd master – *summa cum laude*
4th master – magna cum laude
pre-specialisation internal medicine (UZ Leuven)
master thesis: the treatment of hematologic malignancies in pregnancy

SPECIALIST TRAINING

2009 – 2013 INTERNSHIP INTERNAL MEDICINE
Internal medicine, University Hospitals Leuven, Belgium
Internal medicine, St-Maarten Hospital, Mechelen, Belgium
Medical Intensive Care Unit, University Hospitals Leuven, Belgium

2013 – present INTERNSHIP CARDIOLOGY
Cardiology, University Hospitals Leuven, Belgium (Prof. dr. S. Janssens)
Cardiology, AZ Imelda, Bonheiden, Belgium (Dr. L. Janssens)

DOCTORAL RESEARCH

2005 – 2006 Statute *Student Investigator*, KU Leuven (Prof. dr. G. Opdenakker)
The role of urinary MMP-2/9 in patients with lymphangioleiomyomatosis

2011 – present Research grant of the Research Foundation Flanders (FWO) – 2011-2015
PhD-project: The role of PEAR1 in platelets and endothelial cell biology
Center for Molecular and Vascular Biology
Department of Cardiovascular Sciences, University of Leuven, Belgium
Promotor: Prof. dr. P. Verhamme
Co-promotors: Prof. dr. MF. Hoylaerts, Prof. dr. S. Janssens

KU Leuven OCCUPATIONS

2003 – 2012 PROTOCOL MEMBER, CONFERENCE AND EVENTS OFFICE, KU LEUVEN

2013 – 2015 ELECTED ABAP-REPRESENTATIVE, GROUP BIOMEDICAL SCIENCES, KU LEUVEN:
2015 – 2017 ELECTED ABAP-REPRESENTATIVE, GROUP BIOMEDICAL SCIENCES, KU LEUVEN:

University Council, KU Leuven (em. Prof. dr. H. Daems)
Academic Council, KU Leuven (Prof. dr. R. Torfs)
Executive Committee, Biomedical Sciences Group (Prof. dr. W. Robberecht)
Research Council (Prof. dr. L. Schoofs)
POC Doctoral School, Biomedical Sciences (Prof. dr. J. Creemers)
Vereniging Academisch Personeel Leuven (VAPL; Prof. dr. C. Waelkens)
Library Council, Biomedical Sciences group (Prof. dr. J. Arnout)
Election committee honorary doctorates, KU Leuven (em. Prof. dr. A. Van de Putte)

ADDITIONAL TRAINING

2007 Animator Course
Scouts en Gidsen Vlaanderen, Belgium
2011 Advanced Life Support Provider Course
European Resuscitation Council (ERC), Malle, Antwerpen
2012 Laboratory Animal Science Training Certificate, KU Leuven
2014 Training course 'Radiation protection'
2015 Course transthoracic echocardiography
(Hamer en Pieper – AMC Amsterdam)

CLINICAL TRIAL EXPERIENCE

2011 – 2013 Participant in the medical support team of **HOKUSAI** clinical trial
Edoxaban versus Warfarin for the Treatment of Symptomatic VTE
Clinicaltrials.gov NCT00986154; **N Eng J Med.** 2013, Oct 10;369(15):1406-15.

2012 – 2013 Participant in the medical support team of **TB-402** clinical trial
TB-402 or rivaroxaban after total hip replacement
Clinicaltrials.gov NCT01344954; **Thromb Haemost.** 2013 Jun;109(6):1091-8.

2012 – 2014 Participant in the medical support team of **ISIS-FXIRx** clinical trial
Active Comparator-Controlled Study to assess Safety and Efficacy of ISIS-FXIRx in Total Knee Arthroplasty;
Clinicaltrials.gov NCT01713361; **N Eng J Med.** 2015, Jan 15;372(3):232-40.

2015 – … Participant in the medical support team of **HOKUSAI VTE Cancer** clinical trial
Edoxaban versus dalteparin for treatment of VTE in cancer patients
Clinicaltrials.gov NCT02073682

INTERNATIONAL EXPERIENCE

2008 – 2009 CHU de Grenoble, France
Surgery internship

2012 – 2015 International Research Collaborations as part of Doctoral Research:
Cell Surface Signalling Laboratory, Wellcome Trust Sanger Institute, Cambridge, UK

OTHER ACTIVITIES

1990 – 2011 Member and Leader, Scouts en Gidsen Vlaanderen, Heist o/d Berg, Belgium
2012 – … Flemish Cross – festival doctor (Tomorrowland, Pukkelpop, Werchter)

Publications

PEER REVIEWED PUBLICATIONS

a) Publications as part of doctoral thesis

DEXTRAN SULPHATE TRIGGERS PLATELET ACTIVATION VIA DIRECT ACTIVATION OF PEAR1

Vandenbriele C, Sun Y, Criel M, Cludts K, Izzi B, Verhamme P, Hoylaerts MF

Platelets. Accepted for publication. 2015 October

PEAR1: A NOVEL MODIFIER OF ANGIOGENESIS

Vandenbriele C, Kauskot A, Criel M, Vandersmissen I, Geenens R, Craps S, Luttun A, Janssens S, Hoylaerts MF, Verhamme P

Cardiovasc Res. 2015 Oct 1;108(1):124-38.

A HUMAN PLATELET RECEPTOR PROTEIN MICROARRAY IDENTIFIES THE HIGH AFFINITY IMMUNOGLOBULIN-E RECEPTOR SUBUNIT A (FCER1A) AS AN ACTIVATING PLATELET ENDOTHELIUM AGGREGATION RECEPTOR 1 (PEAR1) LIGAND.

Sun Y, ***Vandenbriele C***, Kauskot A, Verhamme P, Hoylaerts MF, Wright GJ

Mol Cell Proteomics. 2015 May; 14(5):1265-74.

PEAR1 IS NOT A HUMAN HYPERTENSION-SUSCEPTIBILITY GENE

Olivi L, ***Vandenbriele C***, Gu Y, Salvi E, Delli Carpini S, Liu YP, Jacobs L, Jin Y, Thijs L, Citterio L, Cusi D, Verhamme P, Staessen J

Blood pressure. 2015 Feb; 24(1):61-4.

PEAR1 ATTENUATES MEGAKARYOPOIESIS VIA CONTROL OF THE PI3K/PTEN PATHWAY.

Kauskot A(*), ***Vandenbriele C(*),*** Louwette S, Gijsbers R, Tousseyn T, Freson K, Verhamme P, Hoylaerts MF

Blood. 2013 Jun 27;121(26):5208-17.

* : Both authors contributed equally

b) Clinical Trials

SINGLE-DOSE TB-402 OR RIVAROXABAN FOR THE PREVENTION OF VENOUS THROMBOEMBOLISM AFTER TOTAL HIP REPLACEMENT. A RANDOMISED, CONTROLLED TRIAL.

Verhamme P, Gunn S, Sonesson E, Peerlinck K, Vanassche T, ***Vandenbriele C***, Ageno W, Glazer S, Prins M, Buller H, Tangelder M

Thromb Haemost. 2013 Jun;109(6):1091-8.

FACTOR XI ANTISENSE OLIGONUCLEOTIDE FOR PREVENTION OF VENOUS THROMBOSIS

Büller HR, Bethune C, Bhanot S, Gailani D, Monia BP, Raskob GE, Segers A, Verhamme P, Weitz JI; ***FXI-ASO TKA Investigators***

N Eng J Med. 2015, Jan 15;372(3):232-40 (*Pubmed registered study investigator*).

EDOXABAN VERSUS WARFARIN FOR THE TREATMENT OF SYMPTOMATIC VENOUS THROMBOEMBOLISM

Hokusai-VTE Investigators, Büller HR, Décousus H, Grosso MA, Mercuri M, Middeldorp S, Prins MH, Raskob GE, Schellong SM, Schwocho L, Segers A, Shi M, Verhamme P, Wells P.

N Eng J Med. 2013, Oct 10;369(15):1406-15 (*Pubmed registered study collaborator*).

c) Other Publications

PHARMACOTHERAPY WITH ORAL XA INHIBITORS FOR VENOUS THROMBOEMBOLISM

Vanassche T, ***Vandenbriele C***, Peerlinck K, Verhamme P
Expert Opin. Pharmacother. 2015 Apr:16(5):645-58

VENOUS THROMBOEMBOLISM IN THE ELDERLY: EFFICACY AND SAFETY OF NON-VKA ORAL ANTICOAGULANTS

Geldhof V, ***Vandenbriele C***, Verhamme P, Vanassche T
Thromb J. 2014 Oct 13;12:21

ADHESION OF STAPHYLOCOCCUS AUREUS TO THE VESSEL WALL UNDER FLOW IS MEDIATED BY ON WILLEBRAND FACTOR-BINDING PROTEIN

Claes J, Vanassche T, Peetermans M, Liesenborghs L, ***Vandenbriele C***, Vanhoorelbeke K, Missiakas D, Schneewind O, Hoylaerts MF, Heying R, Verhamme P
Blood. 2014 Sep 4;124(10):1669-76

RENAL INFARCTIONS CAUSED BY DISSECTIONS OF SURNUMERARY RENAL ARTERIES

Vandenbriele C, van Cann T, Dejagere T, Verhamme P
Acta Cardiol. 2014, Apr; 69(2):203-5

PULMONARY ARTERIO-VENOUS MALFORMATIONS IN A PATIENT WITH A NOVEL MUTATION IN EXON 10 OF THE ACVRL1 GENE

Vandenbriele C, Peerlinck K, de Ravel T, Verhamme P, Vanassche T
Acta Clin Belg. 2014 Apr;69(2):139-41

RIVAROXABAN FOR THE TREATMENT OF CONSUMPTIVE COAGULOPATHY ASSOCIATED WITH A VASCULAR MALFORMATION

Vandenbriele C, Vanassche T, Peetermans M, Verhamme P, Peerlinck K
J Thromb Thrombolysis. 2014 Jul;38(1):121-3

THE TREATMENT OF HEMATOLOGIC MALIGNANCIES IN PREGNANCY

Vandenbriele C, Dierickx D, Amant F, Delforge M
Facts Views Vis Obgyn. 2010;2(2):74-87

CHAPTERS IN BOOKS

HEMATOLOGIC MALIGNANCIES IN PREGNANCY

C. Vandenbriele, A. Vassou, G. Pentheroudakis, K. Van Calsteren and F. Amant
Acute Leukemia, the scientist's perspective and challenge (Red. M. Antica)
Intech, ISBN 978-953-307-553-2

ORAL PRESENTATIONS AT (INTER)NATIONAL CONFERENCES

PEAR1: A NOVEL MODIFIER OF NEO-ANGIOGENESIS

25th Congress of the International Society for Thrombosis and Hemostasis (ISTH); Toronto, Canada, 2015
J Thromb Haemost. 2015, ISTH congress abstracts, ISTH congress abstracts, Volume 13, Issue suppl 2

PEAR1: A NOVEL LINK BETWEEN IgE-MEDIATED ALLERGY AND CARDIOVASCULAR DISEASE

25th Congress of the International Society for Thrombosis and Hemostasis (ISTH); Toronto, Canada, 2015

J Thromb Haemost. 2015, ISTH congress abstracts, Volume 13, Issue suppl 2, 12993

PEAR1: A NOVEL LINK BETWEEN IgE-MEDIATED ALLERGY AND CARDIOVASCULAR DISEASE

Congress of the Belgian Society of Cardiology (BSC); Brussels, Belgium, 2015

RIVAROXABAN FOR THE TREATMENT OF CONSUMPTIVE COAGULOPATHY ASSOCIATED WITH VASCULAR MALFORMATIONS

Annual congress of the Belgian Society on Thrombosis and Haemostasis (BSTH);
Mechelen, Belgium, 2014

PEAR1: A NOVEL LINK BETWEEN IgE-MEDIATED ALLERGY AND CARDIOVASCULAR DISEASE

Annual congress of the Belgian Society on Thrombosis and Haemostasis (BSTH);
Mechelen, Belgium, 2014

PLATELET ENDOTHELIAL AGGREGATION RECEPTOR-1 IS A CRITICAL DETERMINANT OF ENDOTHELIAL CELL FUNCTION – STATE OF THE ART LECTURE – ANGIOGENESIS

Congress of the European Society of Cardiology (ESC); Amsterdam, The Netherlands, 2013

Eur Heart J. 2013, Volume 34, Issue suppl 1, 3676

PLATELET ENDOTHELIAL AGGREGATION RECEPTOR-1 IS A CRITICAL DETERMINANT OF ENDOTHELIAL CELL FUNCTION

24th Congress of the International Society for Thrombosis and Hemostasis; Amsterdam, The Netherlands, 2013

J Thromb Haemost. 2013, (11); 203-204

THE ROLE OF PEAR1 IN ENDOTHELIAL CELL BIOLOGY

Princess Lilian Visiting Professorship; Prof. J. Loscalzo (Editor Circulation)

2013 – Leuven, Belgium

KNOCKDOWN OF PEAR1 BY SHORT HAIRPIN BASED miRNA LENTIVIRAL VECTORS

Viral vector core user days 2013

2013 – Leuven, Belgium

PEAR1 AS A NOVEL HYPERTENSION SUSCEPTIBILITY LOCUS

4th European Study on Genes in Hypertension (EPOGH)-meeting

2013 – Leuven, Belgium

POSTER PRESENTATIONS AT (INTER)NATIONAL CONFERENCES

PEAR1: A NOVEL MODIFIER OF NEO-ANGIOGENESIS

ESC-congress 2015, London, UK

Eur Heart J. 2015, Volume 36, Issue suppl 1, 163-508

PEAR1: A NOVEL LINK BETWEEN IgE-MEDIATED ALLERGY AND CARDIOVASCULAR DISEASE

ESC-congress 2015, London, UK

Eur Heart J. 2015, Volume 36, Issue suppl 1, 849-1187

THE SYK-INDEPENDENT ARM OF PLATELET AGGREGATION BY DEXTRAN SULPHATE RESULTS FROM PEAR1-PHOSPHORYLATION

ISTH-congress 2015, Toronto, Canada

J Thromb Haemost. 2015, ISTH congress abstracts, Volume 13, Issue suppl 2

RIVAROXABAN FOR THE TREATMENT OF CONSUMPTIVE COAGULOPATHY ASSOCIATED WITH VASCULAR MALFORMATIONS

BSC-congress 2015, Brussels, Belgium

PEAR1 TEMPERS TUBULOGENESIS VIA THE AKT-PATHWAY

ATVB-congress 2014, Toronto, Canada

Arterioscl Thromb Vasc Biol. 2014; 34:A333

PLATELET ENDOTHELIAL AGGREGATION RECEPTOR-1 IS A CRITICAL DETERMINANT OF EC FUNCTION

Congress of the American Heart Association (AHA) 2012, Los Angeles, USA

Circulation. 2013, 2013, (126); A11115

AWARDS and NOMINATIONS

2015 – International congress of the European Society of Cardiology (*ESC; London*)

Congress highlights basic research

PEAR1: a novel link between IgE-mediated allergy and cardiovascular disease

2015 – Congress of the International Society for Thrombosis and Hemostasis (*ISTH; Toronto*)

Congress highlights basic research

PEAR1: a novel link between IgE-mediated allergy and cardiovascular disease

2015 – Congress of the International Society for Thrombosis and Hemostasis (*ISTH; Toronto*)

Young Investigator Award (YIA)

PEAR1: a novel modifier of neo-angiogenesis

2015 – Belgian Society for Cardiology (*BSC, Brussels*)

Top Five Abstracts Award

PEAR1: a novel link between IgE-mediated allergy and cardiovascular disease

2014 – Belgian Society on Thrombosis and Haemostasis (*BSTH, Mechelen*)

Paul Capel Price for Clinical and Laboratory Research

Rivaroxaban for the treatment of consumptive coagulopathy associated with vascular malformations.

ALGEMENE SAMENVATTING

Het cardiovasculair systeem is cruciaal voor het transport van zuurstofrijk bloed, hormonen en voedingsstoffen naar de verschillende organen en voor de afvoer van afvalstoffen zoals koolstofdioxide (CO_2) uit het lichaam. Binnen de systeemcirculatie kunnen we een opdeling maken in het arterieel netwerk (slagaders, hoge druk, transport van zuurstofrijk bloed), het veneus netwerk (aders, lage druk, transport van zuurstofarm bloed) en het lymfatisch netwerk, met het hart als drijvende pomp voor het bloedtransport doorheen dit complexe systeem (Figuur 1). De helft van dit circulerend bloedvolume bestaat uit plasma en de andere helft bestaat uit circulerende bloedcellen: a) rode bloedcellen voor het transport van zuurstof, b) witte bloedcellen voor de strijd tegen infecties en c) bloedplaatjes, cruciaal voor de bloedstolling (Figuur 1 van de Introductie).

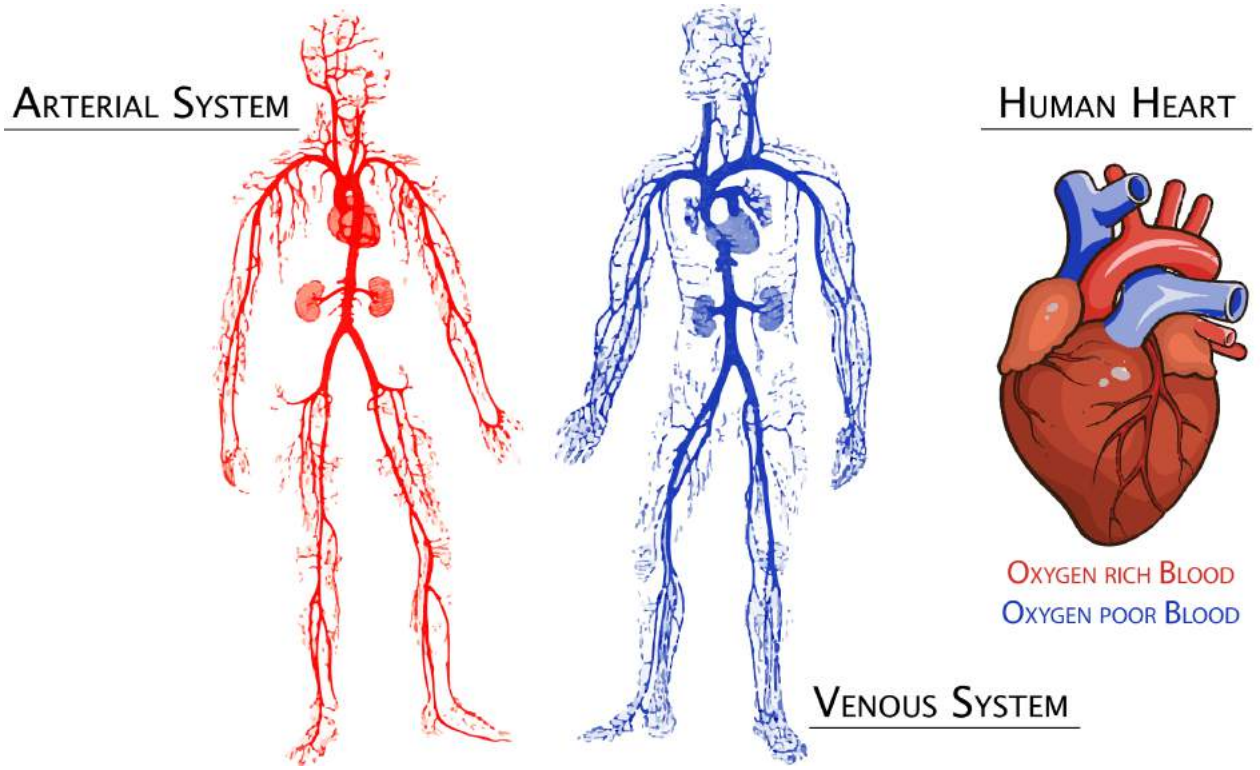

Figure 1 – Arterial blood vessels transport plasma and blood cells from the heart to the tissues/organs of the body whereas the venous system transports blood from the organs back to the heart.

"*Cardiovascular disease*" (verzamelnaam voor aandoeningen van het cardiovasculair systeem) vormen heden ten dage nog steeds de grootste doodsoorzaak wereldwijd. In 2012 stierven naar schatting 16,7 miljoen mensen (of 29% van het wereldwijde jaarlijkse sterftecijfer) ten gevolge van aandoeningen zoals atheromatose (aderverkalking), arteriële hypertensie en/of diabetes, in de hand gewerkt door onder meer obesitas, roken en hypercholesterolemie. Atheromatose is een langzaam en complex proces waarbij vetten in de slagaderwand worden afgezet en zich in een later stadium gaan organiseren tot een cholesterolplaque in het lumen van het bloedvat (zie Figuur 2 van de Introductie, pagina **5**). Enerzijds kan dergelijke plaque zo sterk aangroeien dat dit leidt tot het afsluiten van het

bloedvatlumen. Frequenter echter zal een scheur van een plaque in de bloedvatwand optreden; Hierbij komt de inhoud van de plaque vrij wat ogenblikkelijk resulteert in een activatie van circulerende bloedplaatjes, vorming van een bloedplaatjesprop (trombus) en een acuut afsluiten van de bloedvatflow met zuurstoftekort (ischemie) en infarcering van het achterliggende weefsel tot gevolg. Dit proces leidt – afhankelijk van het bloedvat dat afgesloten wordt – tot een acuut myocard infarct (AMI), herseninfarct (stroke), acuut darminfarct etc. Een gevreesd bijkomend probleem is dat dergelijke trombus kan losraken van de vaatwand en door het stromende bloed meegevoerd wordt tot deze vast komt te zitten in een kleiner bloedvat met volledig afsluiten tot gevolg (embolie).

De vorming van een trombus bij een plaqueruptuur (maar even goed bij het afsluiten van een wonde bij een trauma) is een complex proces, bestaande uit verschillende interacties tussen eiwitten op het oppervlak van bloedplaatjes (receptoren) onderling en verschillende interacties tussen plaatjesreceptoren en circulerende stoffen in het plasma. *Grosso modo* kunnen we de vorming van een trombus opdelen in vier verschillende fasen (zie Figuur 4 van de Introductie, pagina 11). Bij plaqueruptuur komen zogenaamde "pro-trombogene" stoffen vrij, dewelke zorgen voor activatie van circulerende bloedplaatjes in de bloedstroom (fase van de activatie). Dit zal er voor zorgen dat bepaalde bloedplaatjesreceptoren geactiveerd zullen worden, wat zal leiden tot verdere activatie van bloedplaatjes en aangroei van de initiële (kleine) trombus (amplificatie fase). Uiteindelijk zal dit leiden tot een reeks van complexe interacties tussen een heel aantal oppervlaktereceptoren waarbij de gevormde trombus zal evolueren naar een stabiele "klonter" (stabilisatie fase). In een laatste fase zal ervoor gezorgd worden dat de stabiliteit van de klonter zal verminderen en uiteindelijk de trombus uit elkaar zal vallen (desintegratie fase).

Hoewel de meeste receptoren op bloedplaatjes heden ten dage gekarakteriseerd zijn en hun onderliggende werking in de fysiologie van het bloedplaatje goed gekend is, zijn lang niet alle receptoren reeds geïdentificeerd. In 2005 werd door de groep van Nanda *et al.* (Stanford, California, USA) een nieuwe bloedplaatjesreceptor beschreven, die PEAR1 (Platelet Endothelial Aggregation Receptor 1) genoemd werd. Nanda *et al.* rapporteerden dat PEAR1 tussenkwam in de stabilisatie fase van de trombus en dat PEAR1 niet alleen op het oppervlak van bloedplaatjes tot expressie kwam maar ook op het oppervlak van endotheelcellen (die cellen die de binnenkant van bloedvaten aflijnen). Onze groep (Kauskot *et al.*) toonde in 2012 aan dat er meer PEAR1 tot expressie komt aan het oppervlak van een bloedplaatje wanneer dit geactiveerd wordt en dat activatie van PEAR1 in bloedplaatjes leidt tot activatie van de $\alpha_{IIb}\beta_3$-receptor (een belangrijke receptor voor trombusvorming en stabiliteit van de gevormde trombus) via Akt (een centrale speler in activatie en regulatie van bloedplaatjesfunctie). Desondanks bleven vele vragen omtrent deze "nieuwe" receptor nog onopgelost.

Daarom hebben we als doel gesteld in dit thesis manuscript (zie ook Aims, pagina 21) om de bijdrage van PEAR1 aan megakaryopoïese (het vormen van nieuwe bloedplaatjes uit megakaryocyten) te bestuderen, het onderwerp van Hoofdstuk I. Vermits onze groep reeds aangetoond had dat PEAR1 een rol speelt in het stabiliseren van trombi, hebben we verder onderzocht welke partner hiertoe bijdraagt. In hoofdstuk II beschrijven we hoe PEAR1 geactiveerd wordt door een PEAR1-activerend eiwit (ligand), gelegen op een naburig bloedplaatje in de gevormde trombus. Tot op heden is het in dit hoofdstuk beschreven ligand voor PEAR1 het enige gekende ligand, op bloedplaatjes en op andere

cellen. Zoals beschreven in Hoofdstuk III, hebben we echter ook een niet-fysiologisch experimenteel ligand geïdentificeerd, dat in staat is om bloedplaatjes krachtig te activeren via het induceren van PEAR1-activering. PEAR1 komt niet alleen tot expressie aan het oppervlak van bloedplaatjes maar ook aan het oppervlak van humane endotheelcellen (cellen die de binnenkant van het hart, bloedvaten en lymfevaten bekleden). Tot dusver was de rol van PEAR1 in endotheelcellen niet gekend. In **Hoofdstuk IV** wordt de bijdrage van PEAR1 aan de functie van endotheelcellen en nieuwe bloedvatvorming (angiogenese) uitvoerig besproken.

Hoofdstuk I – De rol van PEAR1 in bloedplaatjesvorming

In Hoofdstuk I hebben we aangetoond dat, naast de aanwezigheid van PEAR1 op het oppervlak van (mature) bloedplaatjes, PEAR1 ook aanwezig is aan op het oppervlak van megakaryocyten, cellen in het beenmerg die instaan voor de productie van circulerende bloedplaatjes in het bloed. We stelden vast dat de expressie van PEAR1 stijgt naarmate de megakaryocyt progenitorcel (in celkweek; *in vitro*) meer uitrijpt. Dit bracht er ons toe te onderzoeken wat het effect is op de uitrijping en bloedplaatjesproductie van de progenitorcel (voorlopercel) wanneer de PEAR1 expressie fors onderdrukt wordt (*PEAR1 knockdown*) tijdens dit proces. Knockdown van PEAR1 resulteerde in een verdubbeling van het aantal progenitoren *in vitro* (en dus uiteindelijk ook van het aantal bloedplaatjes), zonder effect op de maturatie van de megakaryocyt. Zoals eerder verteld is het eiwit Akt één van de belangrijkste regulatoren van cel functies (onder andere celgroei) in bloedplaatjes en ook in mekaryocyten. Akt wordt geactiveerd door het eiwit PI3K en wordt geïnactiveerd door het eiwit PTEN. Binnen de megakaryocyt wordt de balans tussen PI3K en PTEN strikt gereguleerd om een goede controle te kunnen uitvoeren op de groei van de megakaryocyt progenitoren. Ons onderzoek toonde aan dat knockdown van PEAR1 resulteerde in een overhand van Akt-activiteit door een verminderde expressie van PTEN (hoewel de directe link tussen PTEN-daling en knockdown van PEAR1 tot op heden nog ongekend is) en dus resulteerde in verhoogde megakaryocytproliferatie. Dit werd aangetoond *in vitro* met humane megakaryocyten ($CD34^+$ cellen), maar werd ook bevestigd in een levend organisme (*in vivo*) door het uitschakelen van *Pear1* in embryo's van zebravissen. Ook hier zagen we dat *Pear1*-afwezigheid resulteert in een Pten-afhankelijke verhoging van het bloedplaatjesaantal in zebravissen.

Hoofdstuk II en III – De liganden van bloedplaatjes PEAR1

Zoals eerder vermeld toonde onze groep aan dat activatie van PEAR1 in bloedplaatjes leidt tot activatie van de $\alpha_{IIb}\beta_3$-receptor via Akt en dus zorgt voor stabilisatie van de gevormde trombus. Dit impliceert dat een bepaald (ongekend) eiwit op het oppervlak van het ene plaatje zorgt voor activatie van PEAR1 op een naburig gelegen bloedplaatje binnen de zich vormende trombus. Een cruciale vraag die zich stelde, was de identificatie van dit PEAR1 activerende eiwit (het PEAR1 ligand). Hiertoe werd – in samenwerking met dr. Y. Sun en dr. G. Wright van het Sanger Institute te Cambridge – een "bibliotheek" ontworpen waarbinnen elk eiwit dat aan het oppervlak van een bloedplaatje tot expressie komt, kunstmatig nagemaakt werd. Door de bindingen van elk van deze 173 eiwitten onderling te verifiëren (in totaal werden meer dan 13.000 interacties gecontroleerd) kon het fysiologische ligand voor PEAR1 geïdentificeerd worden, zoals beschreven in Hoofdstuk II: de Immuunglobuline E (IgE)-receptor FcεR1α. Dit was erg verrassend voor ons, sinds deze receptor

vooral gekend is bij IgE gemedieerde processen in het lichaam zoals astma, allergie en chronisch obstructief longlijden. Bovendien konden wij aantonen dat er een competitie optreedt tussen IgE en PEAR1 voor de bindingsplaats op FcεR1α. Inderdaad, in een *in vitro* model voor trombusvorming, toonden wij aan dat PEAR1 gemedieerde trombusvorming verminderd kon worden in de aanwezigheid van hoge dosissen IgE; of anders gezegd: hoge dosissen IgE verhinderen de activatie van PEAR1 door FcεR1α en verhinderen bijgevolg de Akt-gemedieerde $\alpha_{IIb}\beta_3$- activatie en dus de vorming van trombose. Dit is de eerste keer dat er een verband aangetoond wordt tussen IgE-gemedieerde allergie en bloedplaatjesactiviteit. Naast het fysiologische ligand voor PEAR1, identificeerden wij ook – in aansluiting op een recent manuscript door Getz *et al.* – een niet-fysiologisch ligand voor PEAR1, namelijk dextraan sulfaat (DxS). Het werkingsmechanisme van DxS wordt in detail besproken in Hoofdstuk III. Deze studie levert een bruikbaar pseudo-ligand op, dat kan ingezet worden in verdere PEAR1 studies.

Hoofdstuk IV - PEAR1 en Endotheelcellen

PEAR1 komt niet alleen tot expressie aan het oppervlak van bloedplaatjes, maar ook op het membraanoppervlak van endotheelcellen zoals eerder vermeld. In een eerste reeks van resultaten, beschreven in Hoofdstuk IV, bevestigden wij inderdaad de aanwezigheid van PEAR1 in endotheelcellen van tal van (humane) weefsels. Tot dusver bleef de functie van PEAR1 in endotheelcelbiologie ongekend. Parallel aan onze bevindingen in megakaryocyten, toonden wij aan dat *PEAR1* knockdown in humane endotheelcellen (*in vitro*) tevens resulteerde in een verdubbeling van de endotheelcelgroei. In lijn met onze bevindingen in megakaryocyten, konden wij aantonen dat knockdown van *PEAR1* in endotheelcellen gepaard ging met verhoogde activiteit van Akt, wederom een belangrijke regulator van proliferatie maar ook van migratie van het endotheel. Inderdaad, knockdown van PEAR1 in endotheelcellen, resulteerde eveneens in een versnelde migratie van het endotheel. Gezien endotheelcelproliferatie en -migratie de hoeksteen vormen van nieuwe bloedvatvorming (neo-angiogenese), trachtten wij onze bevindingen te valideren in twee gevestigde modellen van angiogenese in een *Pear1* knockout muis (*Pear1*$^{-/-}$) *in vivo*. Na het afbinden van de slagader die het onderbeen van de muis bevloeit, bemerkten we (met behulp van Doppler analyse) een significant sneller herstel van de bloedflow in het afgebonden been van de knockout muis vergeleken met de wildtype muis. Dit kon verklaard worden door snellere vorming van nieuwe bloedvaten in de afgebonden poot om de bloedflow te herstellen. Tevens, bij het aanleggen van een gestandaardiseerde wonde op de rug van de muis, zien we een dubbel zo snel toegroeien van de wonde in de knockout muis vergeleken met wildtype muizen, opnieuw door versnelde bloedvatvorming in het ingroeiend weefsel van de wonde en dus versnelde wondsluiting. Ook hier konden we aantonen dat dit te verklaren is door verhoogde activiteit van Akt, de regulator van endotheelcel proliferatie, migratie en finaal bloedvatvorming. Deze bevindingen identificeerden PEAR1 als een nieuwe regulator van neoangiogenese.

Dit thesismanuscript heeft een functionele en mechanistische basis gelegd voor de rol die PEAR1 speelt tijdens bloedplaatjesvorming en tijdens bloedplaatjesactivering. Bovendien werd een cruciale functie voor PEAR1 in endotheelcelbiologie aangetoond, hetgeen verder aan de basis kan liggen voor meer uitgebreide populatiestudies en verder cardiovasculair onderzoek.

DANKWOORD

BESTE ALLEN,

Dit is het dan, dàt moment waarnaar elke PhD'er uitkijkt. Dàt moment waarop net dat toch gelukt is waarvan zij/hij nooit gedacht had dat het zou lukken. Dàt moment waarop je vol trots je eigen bijgedragen steentje aan "de wetenschap" kan voorstellen. Het waren vier intense jaren; vier jaren van vreugde, plezier en vriendschap maar tegelijk ook vier jaren van volharding, vallen en opstaan en blijven werken voor iets waar het succes lang niet vanzelfsprekend verzekerd is. En toch, toch is het net dat ongekende, de passie om te weten én nieuwe dingen te ontdekken die je elke dag weer verder drijft. Velen onder ons zullen dat beamen. Het kan denk ik niet mooier verwoord worden dan in het lievelingscitaat van mijn promotor.

"SUCCES IS THE ABILITY TO GO FROM FAILURE TO FAILURE WITHOUT LOSING YOUR ENTHUSIASM"
Peter Verhamme (and Winston Churchill)

Dit brengt mij naadloos bij mijn twee promotoren en copromotor. Hoewel het doctoraatsreglement van de KU Leuven oplegt dat het "*doctoraat gebeurt onder begeleiding van een promotor en eventueel één of meerdere copromotoren (Art. 3)*", kan ik vol overtuiging zeggen, Peter en Marc – Marc en Peter, dat jullie er beiden meer dan 100% voor mij geweest zijn. Ik was zodanig verwend dat ik vaak een half uur na het verzenden van een e-mail al zenuwachtig op mijn stoel zat te draaien omdat het antwoord op zich liet wachten. Marc, de luxe dat je gewoon het bureau naast mij zat en élk moment van de dag voor ons tijd kon en wou vrijmaken is iets wat elke PhD benijdt. Je brede kennis omtrent de fundamentele wetenschap en je drijfveer om te blijven zoeken (hoewel we moeten toegeven dat het soms ook wel flirtte met de grenzen van het begrijpbare) is in mijn ogen uniek. Zelfs wanneer ik op een vrijdagnamiddag kwam aandraven met versie 14.a.II.bis van één of andere tekst, liet je toch weer alles vallen en had ik binnen het uur een gecorrigeerde versie. We hebben heel wat (lange) gesprekken gehad over wetenschap maar ook vele andere topics. Wat me telkens weer opviel is dat je oor had voor de mening van anderen en hoewel dit soms niet strookte met je eigen visie, gaf je ons toch de ruimte om datgene te doen waarin we zelf het meest in geloofden. Ik zou je vandaag dan ook oprecht hiervoor willen bedanken. Peter, wat heb ik immens veel van je geleerd. Ik sta hier vandaag met heel wat resultaten die ik enkel kan voorleggen omdat je altijd die mensen met wie je nauw samenwerkt, betrekt in je eigen succes. Je doorzettingsvermogen is fenomenaal, of het nu gaat om een giga clinical trial, dan wel om een schijnbaar minder belangrijk iets. Je grootste belang was dat we konden (mee)werken aan dat waarin we zelf geloofden en je spaarde daarvoor kosten noch moeite. Je bent niet alleen een steun voor je eigen PhD's maar voor velen van ons binnen de groep van cardiologie. We hebben samen een heel deel van de wereld gezien en ook heel wat "feestjes" voor het labo georganiseerd doch wat ik bovenal geleerd heb is dat je àltijd het aangename aan het nuttige moet koppelen. Peter, een érg oprechte merci hiervoor !! Prof. Janssens, ik zou u graag willen bedanken voor het enthousiasme waarmee u altijd luisterde naar een update van mijn data. Ik bewonder u omdat u telkens na één blik op een figuur of een tabel een nieuwe richting kon aansturen waarin we verder moesten zoeken, ideeën die vaak een extra dimensie aan het project hebben gegeven. Daarnaast wil ik u ook bedanken voor de mogelijkheden die u aan ons "de klinische PhD'ers" verschaft om op een evenwichtige manier onderzoek en kliniek met elkaar te combineren. Uw passie ligt zowel 100% in de kliniek als 100% in het onderzoek en dat is – naar mijn mening – uniek.

I would also like to express my gratitude towards the international jury members, Prof. Harrisson and Prof. Chiche, for reading the manuscript and for their valuable input and also for coming to Leuven.

Hoewel mijn naam op de voorkant van dit manuscript staat, is dit geheel het resultaat van het werk van velen. Op het einde van dit traject begrijp ik waarom deze zin vrijwel in elk dankwoord van een thesis terug te vinden is.

In de eerste plaats zou ik de mensen van het labo willen bedanken. Hartelijke dank aan Prof. Herijgers om binnen het departement cardiovasculaire wetenschappen mijn doctoraat te kunnen volbrengen en om vandaag de verdediging voor te zitten en dank aan Prof. Lijnen en zijn voorgangers em. Prof. Verstraeten, Vermylen en Collen om te kunnen werken in "*het wereldvermaarde stollingsinstituut van Leuven"*. Ook een bijzonder woord van dank aan Prof. Van Geet, Prof. Freson, Prof. Peerlinck, Prof. Luttun, Prof. Jones, Prof. Heying en Prof. Jacquemin voor de bijzondere bijdragen tijdens de labmeetings, de gesprekken in de gang en de sfeer bij onze talkrijke labo-etentjes. Zeker en vast een welgemeende dank aan Diane, Roos, Karen en Gabriela voor de leuke babbels en jullie uitmuntendheid in het "regelen".

In de tweede plaats zou ik – naast aan mijn collega's – een bijzonder woord van dank willen uiten aan "onze laboranten". Katrien, Soetkin, Serena, Chantal, Christine, Marleen en Hilde, jullie hulp en bijdrage was – zoals Alex zou zeggen – impeccable. Katrien, duizendmaal dank voor al het werk dat je voor mij gedaan hebt, telkens met de grootste precisie en gemiddeld tweemaal sneller dan ik dacht dat het zou gaan. Ik heb het even opgeteld en we hebben samen niet minder dan 400 western blots gedaan! Ik hoop dat we in de toekomst nog vaak met elkaar kunnen samenwerken. Soetkin, bedankt voor al die kleuringen waar ik je maar mee lastig bleef vallen. Marleen, een topper in dierwerk was ik niet en zal ik ook nooit zijn, jouw precies werk was onmisbaar!

Cher Alex, je voudrais te remercier pour tes idées, pour me confier le projet sur PEAR1 et surtout pour ton amitié et gaieté et pour tout ce que t'as fait pour moi et le labo. Dommage que tu ne puisses pas être ici aujourd'hui mais on se revoit certainement à Paris.

I'm also very greatfull to Prof. Wright and dr. Sun of the University of Cambridge, for the tremendous efforts made to the "PEAR1 ligand-manuscript" and for the friendly welcome at Cambridge. Also special thanks to the team of Prof. Staessen, for their great interest in the PEAR1 project.

Ook een enorme bedankt aan de collega's PhDs en postdocs van het CMVB. Marijke, Jorien, Anouck en Anne: ik voelde me vaak in ons bureau als een haan in een kippenhok maar ik keek elke avond opnieuw uit naar de terugkeer naar dat kippenhok. Benedetta en Maarten, veel succes met het verderzetten van het PEAR1-project! Laurens, Elise, Dries, Lotte, Thibault, Maarten, Dieter, Sander, Peter, Ine, Sander, Bianca, Ilse, Manisha, Rachel, Lucas en Ward. Bedankt allemaal voor de vele leuke momenten, het delen van leuke en minder leuke momenten en de super toffe sfeer. Ik wens jullie allemaal nog enorm veel succes toe met jullie lopende projecten en weet zeker dat jullie één voor één zullen uitblinken.

Thomas, zoals je zelf schreef in je thesisdankwoord, waren we "helplijn-partners-in-crime". Wat hebben we achteraf toch gelachen om die onverstaanbare Indische oproepen en Canadezen in het holst van de nacht. Je bent altijd mijn grote voorbeeld geweest en ik kijk enorm naar je op ! Bedankt voor de leuke momenten tijdens congressen, in Leuven bij onze befaamde Harvard-pump, in Canada en eender waar. Cheers mate !

Graag wil ik ook via deze weg het Fonds voor Wetenschappelijk Onderzoek (FWO) bedanken voor de financiële steun aan dit project.

Ik ben blij dat ik tijdens mijn PhD-traject ook nog tijd heb gehad voor enkele zijsporen:

Mijnheer de rector, geachte vice-rectoren, decanen en leden van de Academische Raad. Geachte leden van de raad van bestuur van de KU Leuven en UZ Leuven. Geachte leden van het groepsbestuur Biomedische Wetenschappen. Het was mij een zeer groot genoegen en een hele eer de voorbije jaren deel te mogen uitmaken – als ABAP-vertegenwoordiger van de groep biomedische wetenschappen – van de beleidsorganen van deze universiteit. Ik heb veel geleerd uit de verschillende projecten die we gestart zijn en uit de talrijk gevoerde discussies en was erg aangenaam verrast hoezeer met onze mening als vertegenwoordiger rekening gehouden werd. Ik ben trots dat ik deel heb mogen uitmaken van dit goed geolied team. Mijnheer de rector, ik dank u voor de immer grappige gesprekken, de enorme rekening die ik u gekost heb aan de Faculty Club (☺) en voor het vertrouwen. Ik zou hierbij ook een bijzonder woord van dank willen richten aan Dhr. J. Vaesen.

Geachte ererector Vervenne en ererector Waer. Graag had ik u – als lid van de hostgroup van de KU Leuven – willen bedanken voor de fijne samenwerking tijdens uw rectorschap. Veel succes met uw verder lopende projecten waarover u beiden met een aanstekelijke passie kan vertellen. Graag wil ik in één adem een dankwoord hieraan koppelen voor mevr. Demin. Beste Katrijn, je hebt me acht jaar lang geleerd wat protocol is. We hebben samen heel wat kleine brandjes geblust. Mijn oprechte dank hiervoor !

Een speciale *merci* aan de "dames (en heer) van het rectoraat" en uiteraard ook aan Iris en Margot van de dienst communicatie. Beste Iris, Margot, Anne-Mie, Inge, Katrien en Jos. We hebben samen heel wat plezier beleefd en menig receptie afgeschuimd, tot gauw ! Beste Rob, bedankt voor de leuke babbels en om vandaag ook paraat te willen zijn voor de fotografie.

Een ander zijspoor was het verzorgen – binnen de dienst bloedings- en vaatziekten – van de telefonische hulplijn voor enkele multi-center trials. Ik zou hiervoor dan ook graag mijn dank willen betuigen aan Prof. H. Büller, Annelise Segers en het ganse ITREAS-team. Dank voor het vertrouwen dat u in ons stelde en de opportuniteit om ons te laten proeven van het wel en wee achter dergelijke trials.

Naast "doctoreren" was het natuurlijk ook nog "specialiseren". Bedankt aan Prof. Peetermans om mij toe te laten tot de grote groep van de inwendige geneeskunde en bedankt aan de geweldige teams van bloedings- en vaatziekten, MIG-A onder leiding van Prof. Wilmer en van de CCU onder leiding van Prof. Desmet. De nachten/dagen waren pittig, de pathologie was uitdagend en het geheel functioneerde als een team ! Ook een heel speciaal woord van dank aan de verpleging van spoedgevallen en INZO van het AZ St. Maarten in Mechelen en aan het artsencorps inwendige geneeskunde en cardiologie. Ik zou mij heel speciaal willen richten tot dr. C. Libeer. Beste Christophe, wat je mij geleerd hebt omtrent interne geneeskunde en intensieve zorgen had ik nergens zo goed onderricht kunnen krijgen. Je geduld was eindeloos en je hebt de kunst om overal rust te brengen, zowel bij de verpleging als bij je patiënten. Je hebt mij de smaak doen pakken van de intensieve zorgen en ik hoop dat we in de toekomst nog vaak kunnen samenwerken. Uiteraard ook een welgemeende bedankt voor de artsen en verpleging van de dienst cardiologie onder leiding van dr. L. Janssens in het Imeldaziekenhuis (Bonheiden) waar ik nu sinds een zestal weken mijn aanvullende opleiding cardiologie volbreng. Ik heb me hier vanaf de eerste dag thuis gevoeld en heb zelden zo'n warm onthaal ergens gekregen. Hoewel ik hier als "cardiologie-dummie" binnen gekomen ben, ben ik ervan overtuigd dat het een boeiend en leerrijk jaar gaat worden.

Graag had ik via deze weg ook de mensen van Daiichi Sankyo, Boehringer Ingelheim en Bayer willen bedanken. Guy, Katrien, Frederik, Sophie, Dirk en Lieselot bedankt voor jullie aanwezigheid en de interesse in het werk dat we als groep geleverd hebben.

Last but not least zou ik graag mijn vrienden en familie willen danken voor de onvoorwaardelijke steun en vriendschap. Ik prijs me elke dag weer gelukkig dat ik omringd ben met een buitengewoon geweldige groep van mensen en dat geluk kan ik alleen maar koesteren. Ik hoop dat jullie nu toch eindelijk een beetje begrepen heb wat ik al die jaren in dat labo met die muizen en cellen heb zitten uitsteken.

Laura, Bert, An, Lien, Joost, Vincent G en Anka: sommigen waren er sinds de eerste dag in Leuven bij en sindsdien zijn we alleen maar betere vrienden geworden. Ik kan jullie niet genoeg bedanken voor de ongelooflijk mooie momenten die we samen beleefd hebben en voor de steun die ik kreeg van jullie tijdens moeilijke momenten. Woorden schieten mij hierbij te kort. BEDANKT! Mathias, Joachim, Katrien, Jan, Vincent P, Bart, Wim, Jeroen, Jonas, Peter, Kevin, Bram, Anzor, Ward, Caroline, Beatrijs, Machteld, Geertrui, thanks voor de geweldige momenten samen ! Jullie betekenen enorm veel voor mij. Ik hoop dat ik nu terug wat meer tijd ga hebben om met jullie op te trekken.

Een welgemeend dikke merci aan mijn scoutsmaten. Sinds onze 6-7 jaar vormen we een onafscheidelijke groep waar niets of niemand tussen kan komen. Wat ons bindt is dat we allemaal weten wat we willen en we er dan ook resoluut voor gaan. Bert, Hans, Jo, Kristof, Tom, Maarten, Willem T, Willem VDH; ik kon me geen betere maten indenken. BEDANKT !

Mijn allergrootste dank gaat uit naar jullie: mama, papa, Pieter, Frederik, Valerie en mémé. Mama en papa, jullie hebben mij altijd alle kansen gegeven die ik me maar kon dromen. Nooit was iets te veel om voor ons te doen. Pieter en Frederik, ik beloof dat ik vanaf nu terug wat meer tijd zal hebben. Frederik, je bent de beste broer die ik me kon inbeelden, bedankt ! Jammer genoeg is mijn grootmoeder tijdens mijn thesisjaren overleden. Ik zou dan ook graag dit werk aan haar willen opdragen !

Tot slot zou ik graag iedereen willen bedanken die de tijd heeft vrijgemaakt om vandaag hier aanwezig te kunnen zijn. Hoewel het onderwerp waarschijnlijk niet iedereen even hard kan boeien hoop ik dat ik het doch deels goed gemaakt heb door een lang dankwoord te schrijven ☺. Tot gauw,

Christophe VANDENBRIELE
Leuven, 08/11/2015